Fishery Bulletin 105(3) Contents

Click on page numbers to go to PDF version of article.

Articles

313–326
Auth, Toby D., Richard D. Brodeur, and Kathleen M. Fisher
Diel variation in vertical distribution of an offshore ichthyoplankton community off the Oregon coast

327–336
Curtis, Janelle M. R.
Validation of a method for estimating realized annual fecundity in a multiple spawner, the long-snouted seahorse (*Hippocampus guttulatus*), using underwater visual census

337–347
Benson, Scott R., Karin A. Forney, James T. Harvey, James V. Carretta, and Peter H. Dutton
Abundance, distribution, and habitat of leatherback turtles (*Dermochelys coriacea*) off California, 1990–2003

348–355
Bengtson, John L., Alana V. Phillips, Elizabeth A. Mathews, and Michael A. Simpkins
Comparison of survey methods for estimating abundance of harbor seals (*Phoca vitulina*) in glacial fjords

356–367
DeMartini, Edward E., James H. Uchiyama, Robert L. Humphreys Jr., Jeffrey D. Sampaga, and Happy A. Williams
Age and growth of swordfish (*Xiphias gladius*) caught by the Hawaii-based pelagic longline fishery

368–378
Anderson, Joel D.
Systematics of the North American menhadens: molecular evolutionary reconstructions in the genus Brevoortia (Clupeiformes: Clupeidae)

379–389
Schaefer, Kurt M., and Daniel W. Fuller
Vertical movement patterns of skipjack tuna (*Katsuwonus pelamis*) in the eastern equatorial Pacific Ocean, as revealed with archival tags

390–395
Golet, Walter J., Andrew B. Cooper, Robert Campbell, and Molly Lutcavage
Decline in condition of northern bluefin tuna (*Thunnus thynnus*) in the Gulf of Maine

396–407
Stark, James W.

Geographic and seasonal variations in maturation and growth of female Pacific cod (*Gadus macrocephalus*) in the Gulf of Alaska and Bering Sea

408–417
Garrison, Lance P.
Interactions between marine mammals and pelagic longline fishing gear in the U.S. Atlantic Ocean between 1992 and 2004

418–425
Melville-Smith, Roy, and Simon de Lestang
Changes in egg production of the western rock lobster (*Panulirus cygnus*) associated with appendage damage

426–435
Able, Kenneth W., and Thomas M. Grothues
Diversity of estuarine movements of striped bass (*Morone saxatilis*): a synoptic examination of an estuarine system in southern New Jersey

Notes

436–439
Renshaw, Mark A., Eric Saillant, Siya Lem, Philip Berry, and John R. Gold
Microsatellite multiplex panels for genetic studies of gray snapper (*Lutjanus griseus*) and lane snapper (*Lutjanus synagris*)

440–444
Kane, Joseph, and Jacquelyn L. Anderson
Effect of towing speed on retention of zooplankton in bongo nets

445-446
Guidelines for authors

Subscription form

U.S. Department of Commerce

Carlos M. Gutierrez
Secretary

National Oceanic and Atmospheric Administration

Vice Admiral
Conrad C. Lautenbacher Jr., USN (ret.)
Under Secretary for
Oceans and Atmosphere

National Marine Fisheries Service

William T. Hogarth
Assistant Administrator
for Fisheries

Scientific Editor
Adam Moles, Ph.D.

Associate Editor
Elizabeth Siddon

Ted Stevens Marine Research Institute
Auke Bay Laboratories
Alaska Fisheries Science Center
17109 Pt. Lena Loop Road
Juneau, Alaska 99801

Managing Editor
Sharyn Matriotti

National Marine Fisheries Service
Scientific Publications Office
7600 Sand Point Way NE, BIN C1570
Seattle, Washington 98115-0070

Editorial Committee

Jeffrey M. Leis	Australian Museum,
Thomas Shirley	Texas A&M Universit
David Somerton	National Marine Fish
Mark Terceiro	National Marine Fish

Diel variation in vertical distribution of an offshore ichthyoplankton community off the Oregon coast

Toby D. Auth (contact author)[1]

Richard D. Brodeur[2]

Kathleen M. Fisher[3]

Email address for T. D. Auth: toby.auth@noaa.gov

[1] Cooperative Institute for Marine Resources Studies
Oregon State University, Hatfield Marine Science Center
2030 Marine Science Drive
Newport, Oregon 97365

[2] Northwest Fisheries Science Center
NOAA Fisheries, Hatfield Marine Science Center
2030 Marine Science Drive
Newport, Oregon 97365

[3] National Ocean Service
NOAA, The Center for Operational Oceanographic Products and Services
1305 East-West Highway
Silver Spring, Maryland 20910

Abstract—We examined the diel vertical distribution, concentration, and community structure of ichthyoplankton from a single station 69 km off the central Oregon coast in the northeast Pacific Ocean. The 74 depth-stratified samples yielded 1571 fish larvae from 20 taxa, representing 11 families, and 128 fish eggs from 11 taxa within nine families. Dominant larval taxa were *Sebastes* spp. (rockfishes), *Stenobrachius leucopsarus* (northern lampfish), *Tarletonbeania crenularis* (blue lanternfish), and *Lyopsetta exilis* (slender sole), and the dominant egg taxa were *Sardinops sagax* (Pacific sardine), *Icichthys lockingtoni* (medusafish), and *Chauliodus macouni* (Pacific viperfish). Larval concentrations generally increased from the surface to 50 m, then decreased with depth. Larval concentrations were higher at night than during the day, and there was evidence of larval diel vertical migration. Depth stratum was the most important factor explaining variability in larval and egg concentrations.

Early life stages of fishes have long been studied to gain insight into adult spawning locations and biomass (Hunter et al., 1993), trophic interactions between fish larvae and their surrounding zooplankton and piscivore communities (Hunter and Kimbrell, 1980), and the relationship between early life processes and subsequent recruitment success (Bradford, 1992; Houde, 1997). Knowledge of the diel vertical distribution of fish eggs and larvae is critical to understanding the structure and ecological interactions of ichthyoplankton communities, and for the development of appropriate sampling strategies (Gray, 1998). Furthermore, variation in the diel vertical distributions of different larval fish taxa and their associated predator and prey fields may influence the occurrence, degree, and timing of competitive, trophic, and environmental interactions (Neilson and Perry, 1990). In addition, an understanding of the differences in ichthyoplankton depth distribution and concentration is essential for accurate quantitative estimates of whole water-column abundance when the depth to be sampled is limited (Ahlstrom, 1959; Comyns and Lyczkowski-Shultz, 2004). Also, because in many surveys sampling is conducted during both night and day, it is often necessary to separate diel (e.g., visual net avoidance by larvae during daylight conditions) and depth effects when analyzing variable ichthyoplankton distributions (Ahlstrom, 1959; Boehlert et al., 1985).

Larvae of many fish species are known to perform diel vertical migrations (Ahlstrom, 1959; Neilson and Perry, 1990). These migrations can follow several different patterns; the most common is movement into the upper water column during night and into deeper water during the day (Shoji et al., 1999; Tsukamoto et al., 2001). However, the reverse pattern has also been observed (Lyczkowski-Shultz and Steen, 1991; Brodeur and Rugen, 1994). In addition, some fish larvae have been found to disperse during the night and aggregate during the day (Brewer and Kleppel, 1986; Munk et al., 1989).

In the present study the diel variation in vertical distributions and concentrations of fish eggs and larvae was examined by repeatedly sampling fish eggs and larvae from a single offshore station off the central Oregon coast in the northeast Pacific Ocean. We used univariate and multivariate statistical techniques such as ANO-

Manuscript submitted 15 August 2006 to the Scientific Editor's Office.

Manuscript approved for publication 25 October 2006 by the Scientific Editor.

Fish. Bull. 105:313–326 (2007)

Table 1

Date, time (Pacific daylight-savings time [PDT]), and number of depth-stratified samples collected during each sampling period. All hauls were conducted at the same station (HH-05), located at 44°00′N, 125°00′W at a station depth of 950 m.

Haul	Date	Time	Day or night	Number of depth-stratified samples
HH-05A	3 Aug 2000	1600	Day	8
HH-05B	5 Aug 2000	2356	Night	8
HH-05C	6 Aug 2000	0330	Night	8
HH-05D	6 Aug 2000	0630	Day	8
HH-05E	6 Aug 2000	1623	Day	9
HH-05F	7 Aug 2000	0343	Night	9
HH-05G	7 Aug 2000	0633	Day	7
HH-05B	11 Aug 2002	0350	Night	9
HH-05C	11 Aug 2002	0722	Day	8

VA, diversity and evenness indices, multidimensional scaling, and cluster analyses to assess the influence of water depth, diel migration, temperature, and salinity on the occurrence and concentration of dominant ichthyoplankton taxa and assemblages. This is the first examination of diel variation in the vertical distributions of ichthyoplankton in the northern California Current since Boehlert et al. (1985), and the only work of its kind for an offshore assemblage. In addition, no similar study has been conducted examining fish egg diel vertical distributions and assemblages in this region. Results from this study are intended to supplement previous spatial and temporal analyses of Oregon coast ichthyoplankton (Richardson and Pearcy, 1977; Auth and Brodeur, 2006)–analyses that were based on samples collected along the Newport Hydrographic (NH) line (44°39′N) over many years.

Materials and methods

Sampling procedures

Ichthyoplankton samples were collected from a single station (HH-05) approximately 69 km off of Heceta Head (44°00′N, 125°00′W) along the central Oregon coast in 950 m of water. Sampling cruises in August 2000 and 2002 resulted in the collection of 74 depth-stratified samples from nine diel hauls: five during the day and four at night (Table 1). Samples collected after the beginning of civil twilight (~0445 Pacific daylight-savings time [PDT]) were considered day samples, whereas those collected after the end of civil twilight (~2006 PDT) were considered night samples. A multiple opening and closing net and environmental sensing system (MOCNESS; Wiebe et al., 1976) with a 1.2-m^2 mouth opening and 333-µm mesh nets was used to collect ichthyoplankton at 7–9 discrete depths. The MOCNESS was fished as a continuous oblique tow from a depth of 350 m to the surface at a retrieval rate of 20–30 m/min and a ship speed of 1.0–1.5 m/s. Ship and retrieval speeds were continually adjusted during each tow so as to maintain the mouth opening at a 45° angle for an effective mouth opening of 1 m^2 at all times. Mean water volume filtered by each net was 210 m^3 (standard error [SE]=18.0), but was always greater in nets from deeper strata and less in nets fished in the upper 50 m. Because strata had unequal depth ranges, towing times were different for each stratum. Throughout the water column during each tow, we recorded volume of water filtered, temperature, salinity, depth of the net, length of wire out, and angle of the net mouth relative to the geoid.

Ichthyoplankton samples were preserved at sea in a 10% buffered-formalin seawater solution. Fish eggs and larvae from each sample were completely sorted, counted, and identified to the lowest taxonomic level possible in the laboratory with a dissecting microscope. The lesser of either all larvae or a random subsample of 50 individuals from each species in each sample was measured to the nearest 0.1 mm standard length (SL) (or notochord length for preflexon larvae) using an ocular micrometer mounted on the sorting microscope.

It should also be noted that *Sebastes* spp. were not identifiable below the generic level based on meristics and pigmentation patterns (see Richardson and Pearcy [1977] and Matarese et al. [1989] for a more complete discussion of this problem); therefore no species-specific inferences are intended for this taxon in this study. Recent work has allowed the identification of rockfishes to species level based on mitochondrial markers (Gray et al., 2006), and this identification should enable future researchers to discern specific patterns in larval rockfish distribution and abundance.

Data analyses

Fish egg and larval concentrations for each depth-stratified sample (D_i) were expressed as the number of individuals per 1000 m^3. Weighted mean water-column densities for each haul (D_{Haul}) were calculated according to the following equation:

$$D_{Haul} = \sum D_i r_i / \sum r_i, \qquad (1)$$

where r_i = the depth range (m) of each depth-stratified sample.

Weighted mean depths (*WMD*s) of dominant larval taxa were calculated according to the following equation (Pearre, 1973):

$$WMD = \sum n_i d_i / \sum n_i, \qquad (2)$$

where n_i = the number of individuals in each depth-stratified sample; and
d_i = the mean depth (m) of each sample.

To facilitate vertical distribution analyses, the water column was divided into seven depth strata: 0–10, 10–20, 20–50, 50–100, 100–150, 150–200, and 200–350 m. The weighted mean density of eggs and larvae in all samples collected in each depth stratum per haul were calculated as the strata densities for each haul. A type-II ANOVA model was used to test the null hypothesis that egg and larval densities did not differ between day and night periods or between depth strata, and that there was no interaction among these factors (Dunn and Clark, 1974; Lough and Potter, 1993). ANOVA and a Tukey's multiple range test were applied to the $\log_e(n+0.1)$-transformed haul and depth-strata densities to test for significant differences between day and night periods and depth strata. Weighted mean (based on density) larval lengths of important species were also calculated for each haul and depth stratum, and were similarly tested for significant differences between day and night periods and depth strata.

Taxa diversity and evenness for day and night and total diversity and evenness for each depth stratum were analyzed for all identifiable egg (n=11) and larval (n=20) taxa. The Shannon-Wiener diversity index (H') was used to measure egg and larval diversity, where higher H' values denote greater diversity. Taxa evenness was assessed by using Pielou's evenness index (J'), which ranges from zero to one, with the maximum J' value indicating that all taxa are represented in the same relative concentrations. Both H' and J' were calculated according to the formulas of Shannon and Weaver (1949) and Krebs (1989).

On Field et al.'s (1982) recommendation, we performed a hierarchical cluster analyses in conjunction with nonmetric multidimensional scaling (MDS) ordinations to identify assemblages by potential taxa, depth-strata, and diel egg and larval concentrations. For analyses of taxa assemblages, only those egg (n=4) and larval (n=12) taxa found during more than 5% of the sampling events were included, whereas all identifiable egg (n=10) and larval (n=19) taxa were included in the other assemblage analyses. Concentrations for each egg and larval taxon were averaged for each diel tow (eggs: n=8; larvae: n=9) and each depth stratum from all tows (eggs: n=22; larvae: n=53), which constituted the sampling units in the respective multivariate matrices. Sampling units for which no taxa were found were excluded from the analyses.

Dendrograms of egg and larval taxa, depth strata, and diel presence were created using hierarchical, group-averaged clustering from Bray-Curtis ranked similarities on standardized, fourth root-transformed egg and larval concentrations (Clarke and Warwick, 2001). Dendrograms were cut to produce ecologically interpretable clusters when they were apparent. In order to verify our interpretations of the dendrograms, we performed nonmetric MDS ordinations using similarity matrices from the cluster analyses, with 20 random restarts each to minimize stress levels. A two-dimensional ordination approach was adopted because stress levels were sufficiently low (≤0.08) in all cases and were not appreciably reduced by the addition of a third dimension, and the results were sufficiently interpretable ecologically in two-dimensional space (Clarke and Warwick, 2001).

A nonparametric, multivariate procedure (BIO-ENV) was used to analyze the relationship between select environmental variables and egg and larval community structures. The details of the BIO-ENV algorithm and its suitability for use in analyzing the interactions of biological and environmental data are described by Clarke and Gorley (2001) and Clarke and Warwick (2001). Two separate analyses were performed: one with a similarity matrix of depth-stratified samples by egg taxa (24 samples × 9 taxa), and the other with a similarity matrix of depth-stratified samples by larval taxa (61 samples × 19 taxa). These matrices were analyzed in association with three environmental variables: mean depth (m), mean temperature (°C), and mean salinity of each depth-stratified sample. Both BIO-ENV analyses were performed by using the Spearman rank correlation method on the normalized Euclidean distance similarity matrices of the $\log_e(n+0.1)$-transformed, nonstandardized environmental variables by depth-stratified samples (Clarke and Gorley, 2001). All diversity, evenness, cluster, MDS, and BIO-ENV analyses were performed by using PRIMER statistical software (PRIMER, vers. 5.2.9, PRIMER-E Ltd, Plymouth, UK).

Pairwise correlation analyses were also conducted to assess the relationship between concentrations of several prominent egg (*Sardinops sagax* [Pacific sardine], *Icichthys lockingtoni* [medusafish], and *Chauliodus macouni* [Pacific viperfish]) and larval (*Sebastes* spp. [rockfishes], *Stenobrachius leucopsarus* [northern lampfish], *Tarletonbeania crenularis* [blue lanternfish], and *Lyopsetta exilis* [slender sole]) taxa as well as total eggs and larvae and the environmental variables salinity and temperature. Mean egg and larval densities, salinity, and temperature per depth-stratified sample were used as variable measures. Before inclusion in the analyses, egg and larval concentrations were $\log_e(n+0.1)$-transformed to normalize the data and homogenize residual variances. Statistical significance was determined at α = 0.05. All ANOVA and correlation analyses were performed using the statistical software JMP (JMP, vers. 5.1., SAS Inst., Inc., Cary, NC).

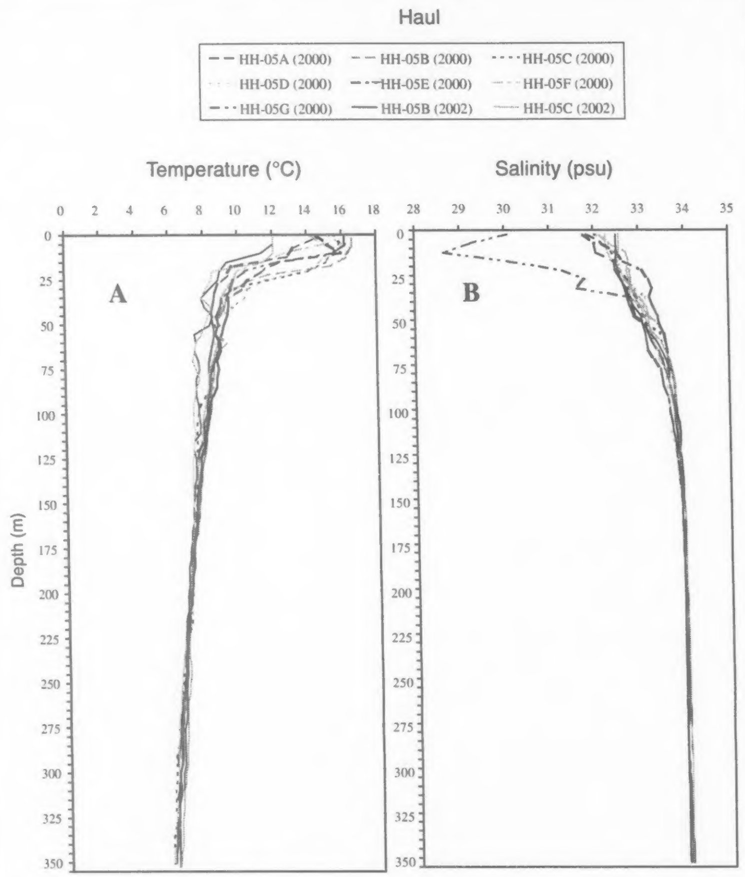

Figure 1

Temperature (**A**) and salinity (**B**) water-column profiles from a single offshore station (HH-05 [44°00′N, 125°00′W]) sampled repeatedly off the central Oregon coast during August in 2000 and 2002.

Results

Hydrography

The water column at the sampling station was similarly stratified for each of the nine diel hauls, and a thermocline was centered approximately at 20 m (Fig. 1, A and B). Mean water temperature was 14.7°C (standard deviation [SD]=1.6) at the surface, and decreased to 6.2°C (SD=0.2) at 350 m. Salinity increased from a mean of 31.9 psu (SD=0.7) at the surface to 34.0 psu (SD=0.03) at 350 m. The unusually low salinities recorded in the upper 35 m of the water column during the last haul in 2000 (HH-05G) may have resulted from an infusion of low-salinity Columbia River plume water from the north.

Egg concentrations and distributions

A surprisingly small sum of 128 fish eggs representing 11 taxa from nine families was collected throughout the study. Three taxa were dominant according to total mean concentration and frequency of occurrence from all depth-stratified samples: *S. sagax* (3.42/1000 m^3; 0.07), *I. lockingtoni* (2.00/1000 m^3; 0.14), and *C. macouni* (1.07/1000 m^3; 0.12). Together these three taxa accounted for over 71% of the total mean egg concentration. *Trachurus symmetricus* (jack mackerel) eggs were found at a high concentration (241.29/1000 m^3) in a single daytime surface (0–10 m) sample in 2000 but were found in only two other samples and at much lower densities (6.80 and 17.54/1000 m^3). These two samples were collected from two depths

Table 2

Day, night, and total mean densities (number/1000 m^3) of fish eggs collected at all different depth strata from a single offshore station off the central Oregon coast in 2000 and 2002 (1 standard error in parentheses). For between-stratum comparisons of each taxon within each diel category, different superscripts indicate significant differences (ANOVA, $P<0.05$).

	Depth (m)							
Taxa	0–10	10–20	20–50	50–100	100–150	150–200	200–350	Total
Day								
Total eggs	159.90 (79.0)^{a}	31.01 (14.1)^{ab}	18.60 (4.1)^{a}	0.70 (0.7)^{b}	0 (0)^{b}	0 (0)^{b}	1.30 (1.3)^{b}	13.43 (5.8)
Sardinops sagax	84.11 (78.9)	6.26 (6.3)	1.36 (1.4)	0 (0)	0 (0)	0 (0)	0 (0)	5.99 (5.6)
Lipolagus ochotensis	2.10 (2.1)	0 (0)	0 (0)	0 (0)	0 (0)	0 (0)	0 (0)	0.14 (0.1)
Chauliodus macouni	2.14 (2.1)^{ab}	9.39 (6.3)^{ab}	8.70 (2.5)^{a}	0 (0)^{b}	0 (0)^{b}	0 (0)^{b}	0 (0)^{b}	1.74 (0.8)
Merluccius productus	0 (0)	0 (0)	0 (0)	0 (0)	0 (0)	0 (0)	0 (0)	0 (0)
Trachipterus altivelus	0 (0)	2.09 (2.1)	4.45 (4.4)	0 (0)	0 (0)	0 (0)	0.43 (0.4)	0.75 (0.4)
Trachurus symmetricus	50.36 (47.8)	3.51 (3.5)	1.36 (1.4)	0 (0)	0 (0)	0 (0)	0 (0)	2.10 (1.9)
Icichthys lockingtoni	14.76 (7.9)	6.26 (6.3)	1.37 (1.4)	0.70 (0.7)	0 (0)	0 (0)	0 (0)	1.83 (0.7)
Tetragonurus cuvieri	0 (0)	0 (0)	1.37 (1.4)	0 (0)	0 (0)	0 (0)	0 (0)	0.14 (0.1)
Lyopsetta exilis	0 (0)	0 (0)	0 (0)	0 (0)	0 (0)	0 (0)	0 (0)	0 (0)
Microstomus pacificus	0 (0)	0 (0)	0 (0)	0 (0)	0 (0)	0 (0)	0.87 (0.9)	0.28 (0.3)
Undetermined spp.	6.42 (6.4)	3.51 (3.5)	0 (0)	0 (0)	0 (0)	0 (0)	0 (0)	0.44 (0.3)
Night								
Total eggs	42.42 (40.2)	26.66 (11.2)	1.02 (1.0)	0.95 (1.0)	0 (0)	0.67 (0.7)	0.58 (0.6)	3.65 (2.2)
Sardinops sagax	0 (0)	7.28 (7.3)	0 (0)	0 (0)	0 (0)	0 (0)	0 (0)	0.21 (0.2)
Lipolagus ochotensis	0 (0)	0 (0)	0 (0)	0 (0)	0 (0)	0 (0)	0 (0)	0 (0)
Chauliodus macouni	0 (0)	3.64 (3.6)	1.02 (1.0)	0 (0)	0 (0)	0 (0)	0 (0)	0.24 (0.1)
Merluccius productus	0 (0)	3.88 (3.9)	0 (0)	0 (0)	0 (0)	0 (0)	0 (0)	0.14 (0.1)
Trachipterus altivelus	0 (0)	0 (0)	0 (0)	0 (0)	0 (0)	0 (0)	0 (0)	0 (0)
Trachurus symmetricus	0 (0)	0 (0)	0 (0)	0 (0)	0 (0)	0 (0)	0 (0)	0 (0)
Icichthys lockingtoni	34.28 (32.0)	11.87 (7.5)	0 (0)	0 (0)	0 (0)	0 (0)	0 (0)	2.21 (1.9)
Tetragonurus cuvieri	2.71 (2.7)	0 (0)	0 (0)	0 (0)	0 (0)	0 (0)	0 (0)	0.14 (0.1)
Lyopsetta exilis	0 (0)	0 (0)	0 (0)	0.95 (1.0)	0 (0)	0 (0)	0 (0)	0.13 (0.1)
Microstomus pacificus	0 (0)	0 (0)	0 (0)	0 (0)	0 (0)	0.67 (0.7)	0.58 (0.6)	0.31 (0.3)
Undetermined spp.	5.43 (5.4)	0 (0)	0 (0)	0 (0)	0 (0)	0 (0)	0 (0)	0.28 (0.3)
Total								
Total eggs	107.69 (49.3)^{a}	29.08 (8.7)^{ab}	10.78 (3.8)^{abc}	0.81 (0.5)^{bc}	0 (0)^{c}	0.33 (0.3)^{c}	0.98 (0.7)^{bc}	9.08 (3.6)
Sardinops sagax	46.73 (44.1)	6.71 (4.4)	0.76 (0.8)	0 (0)	0 (0)	0 (0)	0 (0)	3.42 (3.1)
Lipolagus ochotensis	1.17 (1.2)	0 (0)	0 (0)	0 (0)	0 (0)	0 (0)	0 (0)	0.08 (0.08)
Chauliodus macouni	1.19 (1.2)^{ab}	6.83 (3.8)^{ab}	5.28 (1.9)^{a}	0 (0)^{b}	0 (0)^{b}	0 (0)^{b}	0 (0)^{b}	1.07 (0.5)
Merluccius productus	0 (0)	1.72 (1.7)	0 (0)	0 (0)	0 (0)	0 (0)	0 (0)	0.06 (0.06)
Trachipterus altivelus	0 (0)	1.16 (1.2)	2.47 (2.5)	0 (0)	0 (0)	0 (0)	0.24 (0.2)	0.42 (0.2)
Trachurus symmetricus	27.98 (26.7)	1.95 (1.9)	0.76 (0.8)	0 (0)	0 (0)	0 (0)	0 (0)	1.17 (1.1)
Icichthys lockingtoni	23.43 (14.1)^{a}	8.75 (4.6)^{ab}	0.76 (0.8)^{b}	0.39 (0.4)^{b}	0 (0)^{b}	0 (0)^{b}	0 (0)^{b}	2.00 (0.8)
Tetragonurus cuvieri	1.21 (1.2)	0 (0)	0.76 (0.8)	0 (0)	0 (0)	0 (0)	0 (0)	0.14 (0.1)
Lyopsetta exilis	0 (0)	0 (0)	0 (0)	0.42 (0.4)	0 (0)	0 (0)	0 (0)	0.06 (0.06)
Microstomus pacificus	0 (0)	0 (0)	0 (0)	0 (0)	0 (0)	0.33 (0.3)	0.74 (0.5)	0.30 (0.2)
Undetermined spp.	5.98 (4.1)	1.95 (1.9)	0 (0)	0 (0)	0 (0)	0 (0)	0 (0)	0.37 (0.2)

(10–20 and 20–50 m, respectively) in the same haul (HH-05A).

Fish egg concentrations varied across depth-stratified and diel scales (Table 2). However, depth stratum was the only significant factor explaining variation in *C. macouni*, *I. lockingtoni*, and total egg densities in the type-II ANOVA model ($P<0.05$). Almost 91% of the total egg abundance was found in the upper 100 m of the water column. Egg densities were generally highest near the surface and decreased with depth. There were no *S. sagax*, *C. macouni*, or *I. lockingtoni* eggs found at depths >100 m.

Mean total water-column concentrations were greater during the day than at night for *S. sagax* (5.99/1000 m^3

[day]; 0.21/1000 m^3 [night]), *C. macouni* (1.74/1000 m^3 [day]; 1.07/1000 m^3 [night]), and total eggs (13.43/1000 m^3 [day]; 3.65/1000 m^3 [night]), although differences were not significant (ANOVA, $P>0.05$). However, *I. lockingtoni* eggs occurred in slightly higher concentrations in the water column at night (2.21/1000 m^3) than during the day (1.83/1000 m^3). Egg concentrations were generally higher during the day than at night at each depth stratum for most taxa (Table 2).

Larval concentrations and distributions

A total of 1571 fish larvae representing 20 taxa from 11 families were collected throughout the study. Three families accounted for 97.4% of the total standardized larval concentration: Scorpaenidae (55.6%), Myctophidae (35.6%), and Pleuronectidae (6.2%). Within these families, four taxa were dominant based on total mean concentration and frequency of occurrence from all depth-stratified samples: *Sebastes* spp. (57.75/1000 m^3; 0.42), *S. leucopsarus* (25.23/1000 m^3; 0.45), *T. crenularis* (8.81/1000 m^3; 0.35), and *L. exilis* (3.78/1000 m^3; 0.15). Several other taxa were documented at relatively high frequencies but at lower mean concentrations: *Glyptocephalus zachirus* (rex sole) (2.10/1000 m^3; 0.18), *Protomyctophum thompsoni* (northern flashlightfish) (1.17/1000 m^3; 0.16), *I. lockingtoni* (1.01/1000 m^3; 0.11), *Diaphus theta* (California headlightfish) (0.91/1000 m^3; 0.11), and *Liparis fucensis* (slipskin snailfish) (0.66/1000 m^3; 0.11).

Larval concentrations varied across depth-stratified and diel scales (Table 3). For *S. leucopsarus* larvae, both factors and their interaction term (depth, diel presence, and depth×diel presence) in the type-II ANOVA model were significant ($P<0.05$). However, depth stratum was the only significant factor explaining variation in *L. exilis*, *Sebastes* spp., *T. crenularis*, and total larval densities in the model. More than 96% of the total larval abundance was distributed in the upper 100 m of the water column. Mean concentrations of *Sebastes* spp., *S. leucopsarus*, *T. crenularis*, and total larvae generally increased from the surface to the 20–50 m depth, then declined steadily as depth increased. No *Sebastes* spp. larvae were collected below 100 m. In addition, *L. exilis* larvae were found only in the 20–100 m depth range, where concentrations were greater than 3× higher in the 20–50 than in the 50–100 m depth stratum.

Mean larval densities were generally greater at night than during the day at all but one depth stratum for *Sebastes* spp., *S. leucopsarus*, *T. crenularis*, and total larvae (Table 3). These differences were significant for *S. leucopsarus* and total larvae at the 0–10 and 10–20 m depth strata (ANOVA, $P<0.05$). However, higher larval densities were found during the day than at night for *Sebastes* spp., *S. leucopsarus*, and total larvae at the 50–100 m depth stratum. In addition, *L. exilis* larvae were found at higher densities during the day than at night at all depths at which they were collected.

Analysis of the dominant larval taxa depth distributions over a 16-h period revealed evidence of diel vertical migration (Fig. 2). Weighted mean depth (WMD) of *L. exilis* and *Sebastes* spp. larvae increased from 2324 to 1550 PDT, whereas larval *S. leucopsarus* WMD decreased slightly between 2324 and 0303 PDT before increasing as the day progressed. In contrast, *T. crenularis* larvae appeared to move up in the water column from 2324 to 0604 PDT but were not found in any sample from the haul conducted at 1550 PDT.

Weighted mean standard lengths (SL) of *L. exilis*, *Sebastes* spp., *S. leucopsarus*, and *T. crenularis* larvae generally increased with depth (Table 4). Mean SL for *S. leucopsarus* larvae collected during night and during both day and night combined was significantly greater at the 20–100 m than at the 10–20 m depth stratum (ANOVA, $P<0.05$). *Lyopsetta exilis*, *Sebastes* spp., and *T. crenularis* larvae collected at night were generally the same size or larger than those collected during the day at each depth stratum, although these differences were not significant (ANOVA, $P>0.05$).

Diversity and evenness

Larval and egg diversity and evenness varied across depth strata. Larval diversity generally increased with depth. Egg diversity increased from the surface to 20 m then declined with increasing depth. Egg and larval evenness generally increased with depth before declining slightly at the 200–350 m depth stratum. Egg diversity and evenness could not be assessed at the 100–150 and 150–200 m depth strata because no eggs were found between 100 and 150 m, and only one egg (*Microstomus pacificus* [Dover sole]) was found at the 150–200 m depth stratum. There was no appreciable difference in egg and larval diversity and evenness between day and night samples.

Assemblages

Several taxa and depth assemblages were identified on the basis of cluster analyses and MDS, although no diel assemblages were apparent (Fig. 3, A–C). Larval taxa separated out into four assemblages (Fig. 3A). In more than 5% of the samples too few egg taxa ($n=4$) were present to permit identification of any assemblages. Cluster analyses and MDS also indicated the presence of two egg and larval depth assemblages: <100 m and >100 m (Fig. 3, B and C).

Environmental relationships

BIO-ENV and correlation analyses revealed significant relationships between several environmental factors and egg and larval mean concentrations. A depth-stratified BIO-ENV analysis, which included mean depth (m), mean temperature (°C), and mean salinity of each depth-stratified sample, showed that depth alone explained 46% of the variability in mean egg concentrations and 44% in larval concentrations. No multiple-factor combination explained more variability in egg or larval concentration data. Pairwise correlation analyses revealed significant

Table 3

Day, night, and total mean densities (number/1000 m^3) of fish larvae collected at different depth strata from a single offshore station off the central Oregon coast in 2000 and 2002 (1 SE in parentheses). For between stratum comparisons of each taxon within each diel category, different alphabetic supercripts indicate significant differences (ANOVA, $P<0.05$). For diel comparisions of each taxon within each depth stratum, different numeric superscripts indicate significant differences (ANOVA, $P<0.05$).

Taxa	Depth (m)							Total
	0–10	10–20	20–50	50–100	100–150	150–200	200–350	
Day								
Total larvae	^{2}47.47 (22.6)^{abc}	^{2}130.11 (71.3)^{ab}	324.49 (104.4)^{a}	150.55 (59.3)^{a}	6.27 (2.6)^{bcd}	1.93 (1.3)^{d}	2.97 (0.8)^{cd}	75.05 (20.1)
Sardinops sagax	0 (0)	0 (0)	0 (0)	0 (0)	0 (0)	0 (0)	0 (0)	0 (0)
Pseudobathylagus milleri	0 (0)	0 (0)	0 (0)	0 (0)	0 (0)	0 (0)	0.43 (0.4)	0.19 (0.2)
Chauliodus macouni	0 (0)	0 (0)	0 (0)	0 (0)	1.59 (1.6)	0 (0)	0 (0)	0.11 (0.1)
Tactostoma macropus	2.09 (2.1)	0 (0)	0 (0)	0 (0)	0 (0)	0 (0)	0 (0)	0.14 (0.1)
Lestidiops ringens	0 (0)	0 (0)	0 (0)	0 (0)	0 (0)	0 (0)	0 (0)	0 (0)
Myctophidae spp.	0 (0)	0 (0)	0 (0)	0 (0)	0 (0)	0 (0)	0 (0)	0 (0)
Protomyctophum thompsoni	0 (0)	0 (0)	0 (0)	1.70 (1.1)	3.92 (1.5)	0 (0)	0.62 (0.4)	0.88 (0.3)
Tarletonbeania crenularis	0 (0)^{c}	12.98 (9.6)^{abc}	26.69 (13.8)^{a}	18.63 (13.9)^{ab}	0.76 (0.8)^{abc}	0 (0)^{bc}	0.26 (0.3)^{bc}	8.40 (5.1)
Nannobrachium regale	0 (0)	2.46 (2.5)	0 (0)	0 (0)	0 (0)	0 (0)	0 (0)	0.14 (0.1)
Stenobrachius leucopsarus	^{2}0 (0)^{b}	^{2}3.13 (3.1)^{b}	55.79 (34.4)^{a}	46.50 (16.4)^{a}	0 (0)^{b}	0 (0)^{b}	0.79 (0.5)^{b}	15.42 (5.3)
Diaphus theta	0 (0)	2.46 (2.5)	0 (0)	0 (0)	0 (0)	0 (0)	0 (0)	0.14 (0.1)
Brosmophycis marginata	0 (0)	3.13 (3.1)	0 (0)	0 (0)	0 (0)	0 (0)	0 (0)	0.14 (0.1)
Sebastes spp.	33.45 (26.0)^{ab}	85.61 (51.0)^{ab}	190.12 (54.4)^{a}	64.04 (38.6)^{a}	0 (0)^{b}	0 (0)^{b}	0 (0)^{b}	38.73 (8.9)
Liparis fucensis	0 (0)	0 (0)	2.69 (1.6)	2.60 (1.7)	0 (0)	0.53 (0.5)	0 (0)	0.81 (0.4)
Icichthys lockingtoni	8.47 (5.2)	10.94 (5.1)	0 (0)	0 (0)	0 (0)	0 (0)	0 (0)	1.28 (0.6)
Citharichthys sordidus	0 (0)	0 (0)	0 (0)	0 (0)	0 (0)	0 (0)	0 (0)	0 (0)
Glyptocephalus zachirus	0 (0)	9.39 (9.4)	8.43 (5.2)	4.65 (4.7)	0 (0)	0 (0)	0 (0)	2.21 (0.7)
Lyopsetta exilis	0 (0)^{b}	0 (0)^{b}	40.77 (25.7)^{a}	11.72 (5.1)^{a}	0 (0)^{b}	0 (0)^{b}	0 (0)^{b}	5.60 (2.7)
Microstomus pacificus	0 (0)	0 (0)	0 (0)	0.70 (0.7)	0 (0)	1.40 (1.4)	0.87 (0.5)	0.66 (0.3)
Undetermined spp.	3.45 (3.5)	0 (0)	0 (0)	0 (0)	0 (0)	0 (0)	0 (0)	0.19 (0.2)
Night								
Total larvae	^{1}293.20 (131.3)^{a}	^{1}667.70 (153.9)^{a}	630.54 (281.2)^{a}	84.33 (41.4)^{ab}	13.21 (7.8)^{b}	3.66 (1.2)^{b}	2.68 (1.0)^{b}	139.73 (42.4)
Sardinops sagax	4.42 (2.7)	0 (0)	0 (0)	0 (0)	0 (0)	0 (0)	0 (0)	0.27 (0.2)
Pseudobathylagus milleri	0 (0)	0 (0)	0 (0)	0 (0)	0 (0)	0 (0)	0 (0)	0 (0)
Chauliodus macouni	0 (0)	0 (0)	0 (0)	3.26 (1.1)	0.94 (0.9)	0 (0)	0 (0)	0.58 (0.3)
Tactostoma macropus	0 (0)	0 (0)	0 (0)	0 (0)	0 (0)	0 (0)	0 (0)	0 (0)
Lestidiops ringens	0 (0)	0 (0)	0 (0)	1.45 (1.4)	0 (0)	0 (0)	0 (0)	0.14 (0.1)
Myctophidae spp.	0 (0)	0 (0)	3.05 (3.1)	1.90 (1.9)	0 (0)	0 (0)	0 (0)	0.68 (0.4)
Protomyctophum thompsoni	0 (0)	0 (0)	0 (0)	3.61 (2.5)	8.30 (4.8)	1.29 (1.3)	0 (0)	1.52 (0.7)
Tarletonbeania crenularis	1.34 (1.3)^{ab}	27.65 (19.4)^{ab}	38.98 (27.9)^{a}	19.26 (10.7)^{a}	3.02 (3.0)^{ab}	0.67 (0.7)^{ab}	0 (0)^{b}	9.34 (5.5)
Nannobrachium regale	5.43 (5.4)	12.36 (12.4)	2.03 (1.2)	0 (0)	0 (0)	0 (0)	0 (0)	0.94 (0.4)
Stenobrachius leucopsarus	^{1}5.09 (2.2)^{abc}	^{1}248.31 (170.3)^{a}	175.64 (61.7)^{a}	34.70 (19.4)^{ab}	0 (0)^{c}	1.71 (1.0)^{bc}	1.59 (0.6)^{bc}	37.50 (13.3)

continued

Table 3 (continued)

Taxa	Depth (m) 0–10	10–20	20–50	50–100	100–150	150–200	200–350	Total
Night (continued)								
Diaphus theta	3.05 (1.8)	11.52 (3.9)	9.20 (6.7)	0 (0)	0 (0)	0 (0)	0 (0)	1.88 (1.0)
Brosmophycis marginata	0 (0)	0 (0)	0 (0)	0 (0)	0 (0)	0 (0)	0 (0)	0 (0)
Sebastes spp.	263.65 (124.1)^{a}	356.70 (176.9)^{a}	379.92 (209.6)^{a}	14.96 (12.0)^{ab}	0 (0)^{b}	0 (0)^{b}	0 (0)^{b}	81.52 (25.7)
Liparis fucensis	0 (0)	0 (0)	0 (0)	3.23 (1.9)	0 (0)	0 (0)	0 (0)	0.47 (0.3)
Icichthys lockingtoni	6.45 (4.8)	0 (0)	1.02 (1.0)	0 (0)	0 (0)	0 (0)	0 (0)	0.67 (0.5)
Citharichthys sordidus	1.70 (1.7)	0 (0)	0 (0)	0 (0)	0 (0)	0 (0)	0 (0)	0.13 (0.1)
Glyptocephalus zachirus	2.07 (2.1)	11.17 (6.9)	7.15 (4.5)	0 (0)	0.94 (0.9)	0 (0)	0.81 (0.8)	1.96 (1.0)
Lyopsetta exilis	0 (0)^{b}	0 (0)^{b}	9.23 (3.5)^{a}	1.95 (2.0)^{ab}	0 (0)^{b}	0 (0)^{b}	0 (0)^{b}	1.50 (0.5)
Microstomus pacificus	0 (0)	0 (0)	2.28 (1.3)	0 (0)	0 (0)	0 (0)	0.29 (0.3)	0.34 (0.2)
Undetermined spp.	0 (0)	0 (0)	2.04 (2.0)	0 (0)	0 (0)	0 (0)	0 (0)	0.28 (0.3)
Total mean								
Total larvae	156.68 (69.8)^{a}	369.04 (119.5)^{a}	460.51 (138.2)^{a}	121.11 (37.4)^{a}	9.74 (4.0)^{b}	2.80 (0.9)^{b}	2.84 (0.6)^{b}	103.80 (23.3)
Sardinops sagax	1.96 (1.3)	0 (0)	0 (0)	0 (0)	0 (0)	0 (0)	0 (0)	0.12 (0.1)
Pseudobathylagus milleri	0 (0)	0 (0)	0 (0)	0 (0)	0 (0)	0 (0)	0.24 (0.2)	0.11 (0.1)
Chauliodus macouni	0 (0)	0 (0)	0 (0)	1.45 (0.7)	1.26 (0.9)	0 (0)	0 (0)	0.32 (0.1)
Tactostoma macropus	1.16 (1.2)	0 (0)	0 (0)	0 (0)	0 (0)	0 (0)	0 (0)	0.08 (0.08)
Lestidiops ringens	0 (0)	0 (0)	0 (0)	0.64 (0.6)	0 (0)	0 (0)	0 (0)	0.06 (0.06)
Myctophidae spp.	0 (0)	0 (0)	1.36 (1.4)	0.85 (0.8)	0 (0)	0 (0)	0 (0)	0.30 (0.2)
Protomyctophum thompsoni	0 (0)	0 (0)	0 (0)	2.55 (1.2)	6.11 (2.5)	0.64 (0.6)	0.34 (0.2)	1.17 (0.3)
Tarletonbeania crenularis	0.60 (0.6)^{c}	19.50 (9.7)^{abc}	32.15 (13.7)^{a}	18.91 (8.6)^{ab}	1.89 (1.5)^{bc}	0.33 (0.3)^{c}	0.15 (0.1)^{c}	8.81 (3.5)
Nannobrachium regale	2.41 (2.4)	6.86 (5.5)	0.90 (0.6)	0 (0)	0 (0)	0 (0)	0 (0)	0.50 (0.2)
Stenobrachius leucopsarus	2.26 (1.3)^{bc}	112.1 (81.8)^{ab}	109.06 (37.5)^{a}	41.25 (11.9)^{a}	0 (0)^{c}	0.85 (0.6)^{bc}	1.14 (0.4)^{bc}	25.23 (7.2)
Diaphus theta	1.35 (0.9)	6.49 (2.6)	4.09 (3.2)	0 (0)	0 (0)	0 (0)	0 (0)	0.91 (0.5)
Brosmophycis marginata	0 (0)	1.74 (1.7)	0 (0)	0 (0)	0 (0)	0 (0)	0 (0)	0.08 (0.08)
Sebastes spp.	135.76 (66.3)^{ab}	206.09 (90.6)^{ab}	274.47 (96.2)^{a}	42.22 (22.6)^{b}	0 (0)^{c}	0 (0)^{c}	0 (0)^{c}	57.75 (13.7)
Liparis fucensis	0 (0)	0 (0)	1.50 (1.0)	2.88 (1.2)	0 (0)	0.27 (0.3)	0 (0)	0.66 (0.2)
Icichthys lockingtoni	7.57 (3.4)	6.08 (3.3)	0.45 (0.5)	0 (0)	0 (0)	0 (0)	0 (0)	1.01 (0.4)
Citharichthys sordidus	0.76 (0.8)	0 (0)	0 (0)	0 (0)	0 (0)	0 (0)	0 (0)	0.06 (0.06)
Glyptocephalus zachirus	0.92 (0.9)	10.18 (5.7)	7.86 (3.3)	2.58 (2.6)	0.47 (0.5)	0 (0)	0.36 (0.4)	2.10 (0.5)
Lyopsetta exilis	0 (0)^{b}	0 (0)^{b}	26.75 (14.7)^{a}	7.38 (3.3)^{a}	0 (0)^{b}	0 (0)^{b}	0 (0)^{b}	3.78 (1.6)
Microstomus pacificus	0 (0)	0 (0)	1.02 (0.7)	0.39 (0.4)	0 (0)	0.70 (0.7)	0.61 (0.3)	0.52 (0.2)
Undetermined spp.	1.92 (1.9)	0 (0)	0.91 (0.9)	0 (0)	0 (0)	0 (0)	0 (0)	0.23 (0.2)

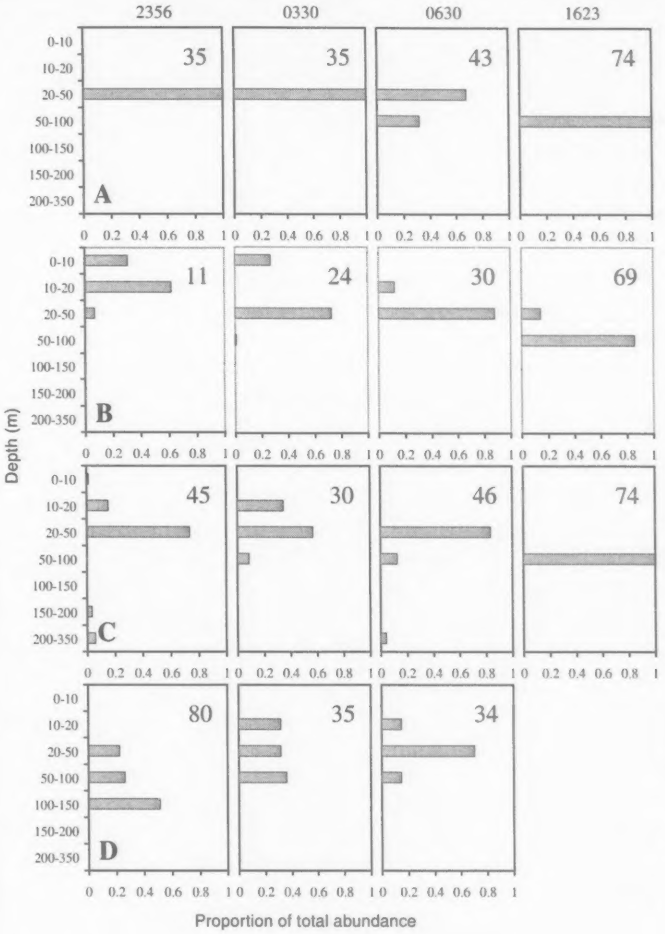

Figure 2

Diel differences in the proportion of total abundances for (**A**) *Lyopsetta exilis*, (**B**) *Sebastes* spp., (C) *Stenobrachius leucopsarus*, and (D) *Tarletonbeania crenularis* larvae collected at different depth strata during a 16-h period at a single offshore station off the central Oregon coast on 5–6 August 2000. No *T. crenularis* larvae were collected in the 1623 PDT haul. The times at which the first MOCNESS net of each haul was opened are given above the panels. Numbers in the upper right corner of each panel represent the weighted mean depth (m) of larvae collected in each haul. During the sampling period, sunset occurred at 2033 and sunrise at 0610 PDT.

correlations between temperature and mean concentrations of *Sebastes* spp. and total larvae, *C. macouni*, *I. lockingtoni*, and total eggs. Significant negative correlations were seen between these same taxa and salinity, and temperature and salinity were negatively correlated with each other ($P<0.05$) (Table 5). Mean concentrations of *L. exilis*, *S. leucopsarus*, and *T. crenularis* larvae, and *S. sagax* eggs were also positively correlated with temperature and negatively correlated with salinity, although the correlations were not significant ($P>0.05$).

Discussion

The species composition, assemblages, and dominant taxa identified in this study were similar to those found

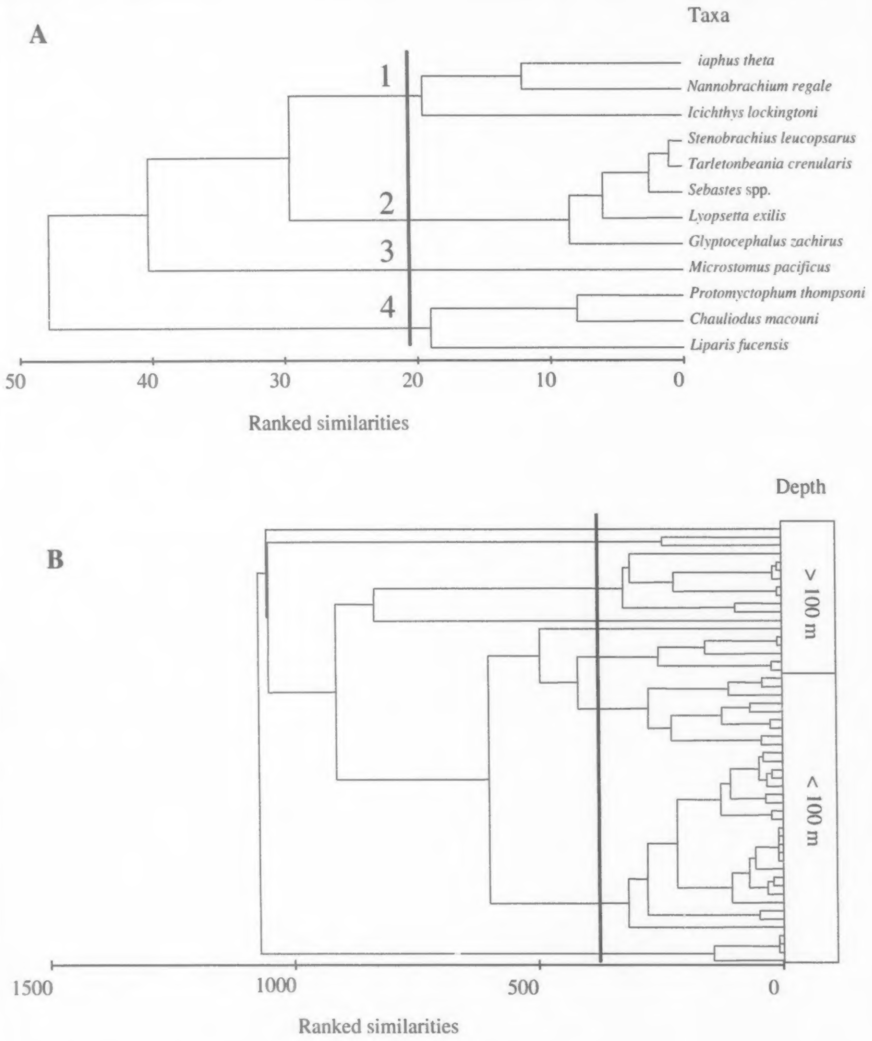

Figure 3

Dendrograms of (**A**) larval taxa, (**B**) larval depth, and (**C**) egg depth. Cluster and multidimensional scaling analyses were performed on fish larvae and eggs collected from a single offshore station off the central Oregon coast in 2000 and 2002. Taxon (A) and depth (B and C) cluster identifications are indicated on each figure. Numbers in figure 3A refer to the four identifiable larval taxa assemblages. Depth strata 1 = 0–10 m, 2 = 10–20 m, 3 = 20–50 m, 4 = 50–100 m, 5 = 100–150 m, 6 = 150–200 m, and 7 = 200–350 m.

in other studies conducted during the summer in offshore waters off the central Oregon coast (Richardson, 1973; Richardson and Pearcy, 1977; Brodeur et al., 1985; Auth and Brodeur, 2006). This similarity may indicate that the composition of dominant larval fishes in this area is resilient to dramatic environmental fluctuations such as those observed during the last 35 years in the northern California Current (Schwing and Moore, 2000; Grantham et al., 2004). It also provides evidence in support of the hypothesis of Auth and Brodeur (2006) that past sampling of ichthyoplankton along the NH line during the summer is indeed representative of summer ichthyoplankton assemblages elsewhere along the Oregon coast.

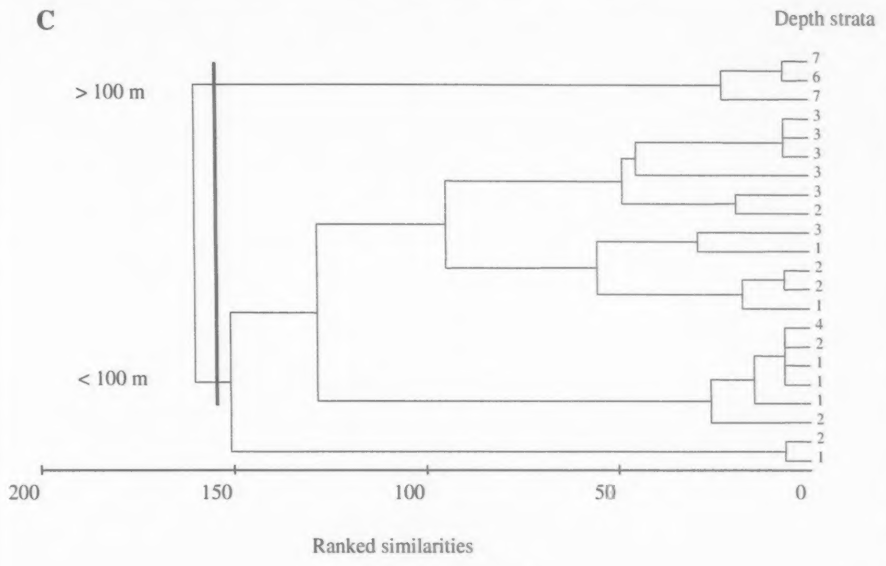

Figure 3 (continued)

Table 4

Day, night, and total mean standard lengths (mm) of fish larvae collected at different depth strata from a single offshore station off the central Oregon coast in 2000 and 2002 (1 SE in parentheses). For between stratum comparisons of each taxon within each diel category, different superscripts indicate significant differences (ANOVA, $P<0.05$).

	Depth (m)							
Taxa	0–10	10–20	20–50	50–100	100–150	150–200	200–350	Total
Day								
Lyopsetta exilis	—	—	8.7 (0.6)	10.3 (0.5)	—	—	—	9.1 (0.4)
Sebastes spp.	4.1 (1.4)	5.1 (0.2)	6.6 (0.7)	7.4 (1.4)	—	—	—	6.2 (0.5)
Stenobrachius leucopsarus	—	13.6	9.3 (0.9)	9.5 (0.6)	—	—	14.7 (0.3)	9.5 (0.5)
Tarletonbeania crenularis	—	9.2 (2.2)	8.9 (1.1)	10.7 (1.4)	14.3	—	16.3	9.6 (0.7)
Night								
Lyopsetta exilis	—	—	9.6 (0.4)	8.6	—	—	—	9.4 (0.4)
Sebastes spp.	6.4 (0.2)	6.2 (0.5)	7.9 (0.5)	10.0 (2.3)	—	—	—	6.9 (0.3)
Stenobrachius leucopsarus	5.6 (0.7)^{ab}	7.6 (0.2)^{b}	9.7 (0.8)^{a}	11.4 (0.3)^{a}	—	14.8 (0.0)^{ab}	15.4 (0.9)^{ab}	8.8 (0.4)
Tarletonbeania crenularis	8.7	7.7 (0.3)	9.4 (0.5)	12.1 (0.9)	13.4	16.0	—	9.6 (0.6)
Total mean								
Lyopsetta exilis	—	—	8.8 (0.4)	10.1 (0.5)	—	—	—	9.1 (0.3)
Sebastes spp.	6.1 (0.5)	6.0 (0.4)	7.4 (0.4)	7.5 (1.1)	—	—	—	6.7 (0.3)
Stenobrachius leucopsarus	5.6 (0.7)^{ab}	7.7 (0.4)^{b}	9.6 (0.5)^{a}	10.2 (0.5)^{a}	—	14.8 (0.0)^{ab}	15.1 (0.6)^{ab}	8.9 (0.3)
Tarletonbeania crenularis	8.7	8.3 (0.9)	9.2 (0.6)	11.3 (0.8)	13.5 (0.4)	16.0	16.3	9.6 (0.4)

However, in our study we collected no *Engraulis mordax* (northern anchovy) eggs or larvae, which usually comprise a significant portion of the offshore ichthyoplankton in August (Richardson and Pearcy, 1977). *Engraulis mordax* larvae have been associated with warmer, less saline, offshore surface waters from the Columbia River (Richardson, 1973; Auth and Brodeur, 2006). This warmer surface water did not appear to have occurred as far south as our sampling station, except perhaps during the last haul in 2000 (HH-05G) (Fig. 2).

Table 5

Correlation coefficients for the depth-stratified sample means ($n=74$) of eleven variables sampled during the day and night from a single station (HH-05) off the Oregon coast in August 2000 and 2002: water temperature (°C), salinity (kg/m^3), and $\log_e$-transformed densities (number/1000 m^3) of *Lyopsetta exilis*, *Sebastes* spp., *Stenobrachius leucpsarus*, *Tarletonbeania crenularis*, and total fish larvae, and *Chauliodus macouni*, *Icichthys lockingtoni*, *Sardinops sagax*, and total fish eggs. *=$P<0.05$, *=$P<0.001$, ***=$P<0.0001$.

	Temperature	Salinity
Salinity	–0.82***	
Lyopsetta exilis	0.03	–0.09
Sebastes spp.	0.48***	–0.51***
Stenobrachius leucopsarus	0.16	–0.18
Tarletonbeania crenularis	0.15	–0.14
Total larvae	0.57***	–0.53***
Chauliodus macouni	0.24*	–0.40**
Icichthys lockingtoni	0.63***	–0.47***
Sardinops sagax	0.20	–0.23
Total eggs	0.55***	–0.51***

In addition, we found evidence that *S. sagax* spawn in this region, as documented since the 1990s (Emmett et al., 2005; Auth and Brodeur, 2006). Similarly, we collected *T. symmetricus* eggs, which are normally found off southern California but which have been reported off southern Oregon by Kendall and Clark[1], off Washington by Ahlstrom (1956), and most recently in the Columbia River plume by Parnel et al.[2]

Our finding that the vast majority (96%) of fish larvae were present in the upper 100 m of the water column has been supported by several other studies (Brodeur and Rugen, 1994; Suntsov, 2002; Sabatés, 2004; Auth and Brodeur, 2006). This finding has significant implications for strategies to sample ichthyoplankton off Oregon and potentially throughout the California Current. *Sebastes* spp. primarily occurred in the 10–50 m depth range, as previously reported (Ahlstrom, 1961; Boehlert et al., 1985; Sakuma et al., 1999; Auth and Brodeur, 2006), whereas *L. exilis* larvae were found between 20 and 100 m as observed by Auth and Brodeur (2006) and during daytime collections made by Boehlert et al. (1985). Also, myctophid larvae within the subfamily Myctophinae (*T. crenularis*) were found at greater depths than those within the subfamily Lampanyctinae (*S. leucopsarus*) as reported by Sassa et al. (2002), although the vast majority was still found above 100 m.

One implication from these findings is that sampling in the upper 100 m of the water column should be sufficient to characterize pelagic summer ichthyoplankton abundances and distributions of the majority of fish taxa along the northeastern Pacific coast (Brodeur and Rugen, 1994; Auth and Brodeur, 2006). A further implication is that sampling strategies without discrete vertical strata, which expend additional effort collecting ichthyoplankton below 100 m, may underestimate larval fish abundances by using samples from largely uninhabited portions of the water column.

Differences in the abundance and size of fish larvae collected in diel samples have often led researchers to suspect bias due to net avoidance, resulting in underestimation of larvae (especially larger larvae) collected during the day (Richardson and Pearcy, 1977; Boehlert et al., 1985). These differences can vary depending on such factors as gear type, size, and tow speed. The present study supports this contention, particularly for the upper 20 m of the water column, where light penetration is of greatest concern. Sakuma et al. (1999) found that total adjusted catches of *Sebastes* spp. larvae off the central California coast were significantly greater at night than during the day. Richardson and Pearcy (1977) observed that large *Sebastes* spp. larvae (9–11 mm) were collected exclusively during the night, while smaller larvae (3–4 mm) were collected during both day and night at the 0–50 m depth off the central Oregon coast. However, they did not find evidence of daytime net avoidance for *S. leucopsarus* (5–11 mm) or *Isopsetta isolepis* (butter sole) (14–23 mm) larvae collected during the same study. In addition, Laroche and Richardson (1979) found no evidence of increased net avoidance by larger *Parophrys vetulus* (English sole) larvae collected during the day versus night off the Oregon coast. However, considering results from the present and similar studies on differences in diel ichthyoplankton abundance (Ahlstrom, 1959), we believe that ichthyoplankton sampling should be conducted primarily at night if at all possible to eliminate any potential bias due to net avoidance. Net avoidance should at least be factored into any model estimating abundances and depth distributions of larvae collected during both day and night.

As noted earlier, diel vertical migration (DVM) has been well documented for larvae of many marine fish species. A variety of theories have been put forth to explain DVM in larval fish, including predator avoidance (Hunter and Sanchez, 1976; Yamashita et al., 1985), the pursuit of zooplankton prey (Fortier and Leggett, 1983; Munk et al., 1989), facilitated larval transport in varying tidal currents (Norcross and Shaw, 1984; Hare and Govoni, 2005), optimization of the energetic advantage gained by larvae at certain depths in thermally stratified water (Wurtsbaugh and Neverman, 1988; Neilson and Perry, 1990), and the pursuit of optimum light conditions for larval survival (Heath et al., 1988). Although this study was not designed to determine the underlying causes of the DVM of larval fish, it does provide some evidence for type-I DVM (up at night, down during the day) for *S. leucopsarus* and *Sebastes* spp. larvae (and to a lesser extent for *L. exilis* larvae), and type-II DVM (down at night, up during the day) for *T. crenularis* larvae (Fig. 3). Evidence for either type of DVM for larval *Sebastes* spp. has not been found in previous studies (Sakuma et al., 1999; Bjorkstedt et al., 2002). This new type-I DVM could help explain the retention of *Sebastes* spp. larvae close to settlement areas along and inshore from the shelf as observed by Auth and Brodeur (2006)—a retention that is due to the ability of larvae to regulate their position in the water column and to take advantage of selective Ekman transport (Sakuma and Larson, 1995).

---

[1] Kendall, A. W., Jr., and J. Clark. 1982. Ichthyoplankton off Washington, Oregon, and northern California April–May 1980. AFSC Proc. Rep. 82-11, 44 p. National Oceanic and Atmospheric Administration, Alaska Fisheries Science Center, 7600 Sand Point Way NE, Seattle, WA 98115.

[2] Parnel, M. M., R. L. Emmett, and R. D. Brodeur. 2006. Interannual and seasonal variation in ichthyoplankton collected off the Columbia River. Unpubl. manuscr., 20 p. Oregon State Univ., Hatfield Marine Science Center, 2030 SE Marine Sci. Dr., Newport, OR 97365.

Acknowledgments

We thank the captains and crews of all research vessels participating in this study for their cooperation and assistance in the sampling. Collection of all MOCNESS tows discussed in this paper was made possible through two grants to W. Peterson from the U. S. GLOBEC program (NA 67RJ10151 and NA 86OP0589). We are indebted to the Peterson Zooplankton Group for their efforts in collecting data at sea and for archiving the samples. In this regard, special thanks to J. Keister, M. Vance, L. Feinberg, T. Shaw, J. Lamb, A. Røestad, and D. Swenson. We also thank M. Busby, D. Blood, and A. Matarese of the Alaska Fisheries Science Center Recruitment Studies Program for their help in identifying eggs and larvae. We thank G. Boehlert, B. Mundy, A. Moles, and three anonymous reviewers for critical reviews of the manuscript. Funding was provided by NOAA's Stock Assessment Improvement Program, Fisheries and the Environment Initiative, and the Northeast Pacific GLOBEC Program. This is contribution number 512 of the U.S. GLOBEC Program.

Literature cited

Ahlstrom, E. H.
1956. Eggs and larvae of anchovy, jack mackerel, and Pacific mackerel. Fish. Bull. 5:33–42.
1959. Vertical distribution of pelagic fish eggs and larvae off California and Baja California. Fish. Bull. 60:107–46.
1961. Distribution and relative abundance of rockfish (*Sebastodes* spp.) larvae off California and Baja California. ICNAF Spec. Pub. 3:169–176.

Auth, T. D., and R. D. Brodeur.
2006. Distribution and community structure of ichthyoplankton off the coast of Oregon, USA, in 2000 and 2002. Mar. Ecol. Prog. Ser. 319:199–213.

Bjorkstedt, E. P., L. K. Rosenfeld, B. A. Grantham, Y. Shkedy, and J. Roughgarden.
2002. Distributions of larval rockfishes *Sebastes* spp. across nearshore fronts in a coastal upwelling region. Mar. Ecol. Prog. Ser. 242:215–228.

Boehlert, G. W., D. M. Gadomski, and B. C. Mundy.
1985. Vertical distribution of ichthyoplankton off the Oregon coast in spring and summer months. Fish. Bull. 83:611–621.

Bradford, M. J.
1992. Precision of recruitment predictions from early life stages of marine fishes. Fish. Bull. 90:439–453.

Brewer, G. D., and G. S. Kleppel.
1986. Diel vertical distribution of fish larvae and their prey in nearshore waters of southern California. Mar. Ecol. Prog. Ser. 27:217–226.

Brodeur, R. D., D. M. Gadomski, W. G. Pearcy, H. P. Batchelder, and C. B. Miller.
1985. Abundance and distribution of ichthyoplankton in the upwelling zone off Oregon during anomalous El Niño conditions. Estuarine Coastal Shelf Sci. 21: 365–378.

Brodeur, R. D., and W. C. Rugen.
1994. Diel vertical distribution of ichthyoplankton in the northern Gulf of Alaska. Fish. Bull. 92:223–235.

Clarke, K. R., and R. N. Gorley.
2001. Primer v5: user manual/tutorial, 91 p. PRIMER-E Ltd., Plymouth, UK.

Clarke, K. R., and R. M. Warwick.
2001. Change in marine communities: an approach to statistical analysis and interpretation, 2nd ed., 172 p. PRIMER-E Ltd., Plymouth, UK.

Comyns, B. H., and J. Lyczkowski-Shultz.
2004. Diel vertical distribution of Atlantic croaker, *Micropogonias undulatus*, larvae in the northcentral Gulf of Mexico with comparisons to red drum, *Sciaenops ocellatus*. Bull. Mar. Sci. 74:69–80.

Dunn, O. J., and V. A. Clark.
1974. Applied statistics: Analysis of variance and regression, 387 p. John Wiley, New York, NY.

Emmett, R. L., R. D. Brodeur, T. W. Miller, S. S. Pool, P. J. Bentley, G. K. Krutzikowsky, and J. McCrae.
2005. Pacific sardine (*Sardinops sagax)* abundance, distribution and ecological relationships in the Pacific Northwest. Calif. Coop. Oceanic Fish. Invest. Rep. 46:122–143.

Field, J. G., K. R. Clarke, and R. M. Warwick.
1982. A practical strategy for analyzing multispecies distribution patterns. Mar. Ecol. Prog. Ser. 8:37–52.

Fortier, L., and W. C. Leggett.
1983. Vertical migrations and transport of larval fish in a partially mixed estuary. Can. J. Fish. Aquat. Sci. 40:1543–1555.

Grantham, B. A., F. Chan, K. J. Nielsen, D. S. Fox, J. A. Barth, J. Huyer, J. Lubchenco, and B. A. Menge.
2004. Upwelling-driven nearshore hypoxia signals ecosystem and oceanographic changes in the northeast Pacific. Nature 429:749–754.

Gray, C. A.
1998. Diel changes in vertical distributions of larval fishes in unstratified coastal waters off southeastern Australia. J. Plankton Res. 20:1539–1552.

Gray, A. K., A. W. Kendall Jr., B. L. Wing, M. G. Carls, J. Heifetz, Z. Li, and A. J. Gharrett.
2006. Identification and first documentation of larval rockfishes in southeast Alaskan waters was possible using mitochondrial markers but not pigmentation patterns. Trans. Am. Fish. Soc. 135:1–11.

Hare, J. A., and J. J. Govoni.
2005. Comparison of average larval fish vertical distributions among species exhibiting different transport

pathways on the southeast United States continental shelf. Fish. Bull. 103:728–736.

Heath, M. R., E. W. Henderson, and D. L. Baird.
1988. Vertical distribution of herring larvae in relation to physical mixing and illumination. Mar. Ecol. Prog. Ser. 47:211–228.

Houde, E. D.
1997. Patterns and consequences of selective processes in teleost early life histories. *In* Early life history and recruitment in fish populations (R. C. Chambers, and E. A. Trippel, eds.), p. 172–196. Chapman and Hall, London.

Hunter, J. R., and C. Kimbrell.
1980. Egg cannibalism in the northern anchovy, *Engraulis mordax*. Fish. Bull. 78:811–816.

Hunter, J. R., and C. Sanchez.
1976. Diel changes in swim bladder inflation of the larvae of the northern anchovy *Engraulis mordax*. Fish. Bull. 74:847–855.

Hunter, J. R., N. C.-H. Lo, and L. A. Fuiman..
1993. Advances in the early fife history of fishes; Part 2, Ichthyoplankton methods for estimating fish biomass. Bull. Mar. Sci. 53:723–935.

Krebs, C. J.
1989. Ecological methodology, 654 p. Harper Collins Publishers, New York, NY.

Laroche, J. L., and S. L. Richardson.
1979. Winter-spring abundance of larval English sole, *Parophrys vetulus*, between the Columbia River and Cape Blanco, Oregon during 1972–1975 with notes on occurrences of three other pleuronectids. Estuarine Coastal Mar. Sci. 8:455–476.

Lough, R. G., and D. C. Potter.
1993. Vertical distribution patterns and diel migrations of larval and juvenile haddock *Melanogrammus aeglefinus* and Atlantic cod *Gadus morhua* on Georges Bank. Fish. Bull. 91:281–303.

Lyczkowski-Shultz, J., and J. P. Steen Jr.
1991. Diel vertical patterns in abundance and distribution of red drum (*Sciaenops ocellatus*) larvae in the northcentral Gulf of Mexico. Fish. Bull. 89:631–641.

Matarese, A. C., A. W. Kendall Jr., D. M. Blood, and B. M. Vinter.
1989. Laboratory guide to early life history stages of northeast Pacific fishes. NOAA Tech. Rep. NMFS 80, 652 p.

Munk, P., T. Kiørboe, and V. Christensen.
1989. Vertical migrations of herring, *Clupea harengus*, larvae in relation to light and prey distribution. Environ. Biol. Fishes. 26:87–96.

Neilson, J. D., and R. I. Perry.
1990. Diel vertical migrations of marine fishes: an obligate or facultative process? Adv. Mar. Bio. 26:115–168.

Norcross, B. L., and R. F. Shaw.
1984. Oceanic and estuarine transport of fish eggs and larvae: a review. Trans. Am. Fish. Soc. 113:153–165.

Pearre, S., Jr.
1973. Vertical migration and feeding in *Sagitta elegans*. Ecology 54:300–314.

Richardson, S. L.
1973. Abundance and distribution of larval fishes in waters off Oregon, May–October 1969, with special emphasis on the northern anchovy, *Engraulis mordax*. Fish. Bull. 71:697–711.

Richardson, S. L., and W. G. Pearcy.
1977. Coastal and oceanic larvae in an area of upwelling off Yaquina Bay, Oregon. Fish. Bull. 75:125–145.

Sabatés, A.
2004. Diel vertical distribution of fish larvae during the winter-mixing period in the Northwestern Mediterranean. ICES J. Mar. Sci. 61:1243–1252.

Sakuma, K. M., and R. J. Larson.
1995. Distribution of pelagic metamorphic-stage sanddabs *Citharichthys sordidus* and *C. stigmaeus* within areas of upwelling off central California. Fish. Bull. 93:516–529.

Sakuma, K. M., S. Ralston, and D. A. Roberts.
1999. Diel vertical distribution of postflexion larval *Citharichthys* spp. and *Sebastes* spp. off central California. Fish. Oceanogr. 8:68–76.

Sassa, C., H. G. Moser, and K. Kawaguchi.
2002. Horizontal and vertical distribution patterns of larval myctophid fishes in the Kuroshio Current region. Fish. Oceanogr. 11(1):1–10.

Schwing, F. B., and C. Moore.
2000. 1999—A year without summer for California or a harbinger of a climate shift? Eos Trans. AGU 81:301, 304–305.

Shannon, C. E., and W. Weaver.
1949. The mathematical theory of communication, 543 p. Univ. Illinois Press, Urbana, IL.

Shoji, J., T. Maehara, and M. Tanaka.
1999. Diel vertical movement and feeding rhythm of Japanese Spanish mackerel larvae in the Central Seto Inland Sea. Fish. Sci. 65:726–730.

Suntsov, A. V.
2002. Vertical and horizontal distribution of ichthyoplankton off Peru in February 1982. J. Ichthyol. 42(5): 391–399.

Tsukamoto, Y., H. Zenitani, R. Kimura, Y. Watanabe, and Y. Oozeki.
2001. Vertical distribution of fish larvae in the Kuroshio and Kuroshio-Oyashio transition region in early summer. Bull. Natl. Res. Inst. Fish. Sci. 16:39–56.

Wiebe, P. H., K. H. Burt, S. H. Boyd, and A. W. Morton.
1976. A multiple opening/closing net and environmental sampling system for sampling zooplankton. J. Mar. Res. 34:313–326.

Wurtsbaugh, W. A., and D. Neverman.
1988. Post-feeding thermotaxis and daily vertical migration in a larval fish. Nature 333:846–848.

Yamashita, Y., D. Kitagawa, and T. Aoyama.
1985. Diel vertical migration and feeding rhythm of the larvae of the Japanese sand-eel *Ammodytes personatus*. Bull. Jap. Soc. Sci. Fish. 51:1–5.

Validation of a method for estimating realized annual fecundity in a multiple spawner, the long-snouted seahorse (*Hippocampus guttulatus*), using underwater visual census

Janelle M. R. Curtis

Email address: j.curtis@fisheries.ubc.ca
Department of Biology
McGill University
1205 Dr. Penfield Avenue, Montréal
Québec, Canada H3A 1B1
Present address: Project Seahorse
Fisheries Centre
University of British Columbia
2202 Main Mall, Vancouver
British Columbia, Canada V6T 1Z4

Abstract—The long-snouted seahorse (*Hippocampus guttulatus*) (Cuvier, 1829), was used to validate the predictive accuracy of three progressively realistic models for estimating the realized annual fecundity of asynchronous, indeterminate, multiple spawners. Underwater surveys and catch data were used to estimate the duration of the reproductive season, female spawning frequency, male brooding frequency, and batch fecundity. The most realistic model, a generalization of the spawning fraction method, produced unbiased estimates of male brooding frequency (mean ±standard deviation [SD]=4.2 ±1.6 broods/year). Mean batch fecundity and realized annual fecundity were 213.9 (±110.9) and 903.6 (±522.4), respectively. However, females prepared significantly more clutches than the number of broods produced by males. Thus, methods that infer spawning frequency from patterns in female egg production may lead to significant overestimates of realized annual fecundity. The spawning fraction method is broadly applicable to many taxa that exhibit parental care and can be applied nondestructively to species for which conservation is a concern.

Manuscipt submitted: 27 April 2006
to the Scientific Editor's Office.

Manuscript approved for publication
25 October 2006 by the Scientific Editor.

Fish. Bull. 105:327–336 (2007).

Reliable estimates of fecundity for multiple spawning fishes are difficult to obtain because of the logistic challenges associated with monitoring the reproductive activity of mature individuals over extended periods of time (Parrish et al., 1986). Fecundity estimates require knowing the number of young produced per spawning event (batch fecundity), as well as the number of batches of young produced per year (annual spawning frequency) (Hunter et al., 1986; Lowerre-Barbieri et al., 1996). Consequently, estimates of annual fecundity for multiple spawners often are derived from the sampling of ovaries to evaluate temporal patterns in the development and maturation of oocytes (Hunter and Leong, 1981; Murua and Saborido-Rey, 2003). However, the reliability of histological assessments is limited for estimating the annual fecundity of fishes with asynchronous oocyte development and indeterminate recruitment (e.g., anchovies, *Engraulis* spp.) (Brown-Peterson et al., 1988, Murua and Saborido-Rey, 2003). In these fishes, no one cohort of oocytes is dominant, and yolked oocytes forming new clutches are recruited from previtellogenic stages on a continual basis throughout the reproductive season (Wallace and Selman, 1981). To obtain estimates of annual fecundity in asynchronous, indeterminate spawners, batch fecundity and spawning frequency are estimated by using different approaches. Batch fecundity can be obtained directly from the number of eggs released per spawning event or from the number of hydrated eggs present in the ovary immediately before spawning. Spawning frequency can be obtained indirectly by using a plot of the fraction of females spawning (indicated by the presence of hydrated eggs or new postovulatory follicles in the ovaries) over time (spawning fraction method, Hunter and Leong, 1981; Murua and Saborido-Rey, 2003).

Estimates of annual fecundity based on the number of eggs produced per year are reliable provided populations are sampled adequately and appropriately (DeMartini and Fountain, 1981; Hunter and Leong, 1981), and egg production is an unbiased proxy for the actual number of offspring produced. Histological methods for estimating annual fecundity may overestimate the actual number of young produced, or realized annual fecundity, if estimates do not correct for losses due to atresia, inability of females to secure mates, low fertilization efficiency, or clutch predation (Weddle and Burr, 1991; Cole and Sadovy, 1995). Such estimates of "potential" annual fecundity are usually difficult to validate because of the challenges of monitoring early life history stages (e.g., eggs, embryos, larvae) over time and space. In many species that provide parental care, however, both mating and brooding may be directly observed (e.g., Vincent and Giles, 2003). Such species provide an opportunity to validate indirect inferences based on egg production and to obtain more accurate estimates of the actual number of young produced (e.g., Cole and Sadovy, 1995). Seahorses are asynchronous, indeterminate multiple spawners that provide obligate paternal care in a sealed brood pouch (Boisseau, 1967; Wallace and Selman, 1981). Although numerous studies have investigated aspects of seahorse reproductive behavior (e.g., Vincent and Sadler, 1995; Perante et al., 2002), annual fecundity has been estimated for only one wild seahorse population (White's seahorse, *Hippocampus whitei*, Vincent and Giles, 2003) by dividing the duration of the reproductive season by the brooding period (time required for a male to brood a clutch of eggs), and multiplying this estimate of spawning frequency by the average brood size (i.e., batch fecundity). Implicit in this method are three assumptions: 1) the time between release of young and remating is negligible, an assumption that was supported by observations of rapid remating in *H. whitei* (Vincent and Sadler, 1995), 2) individuals reproduce continuously from the beginning until the end of the reproductive season, and 3) there is no variation in brood size (a potentially unrealistic assumption, Vincent and Giles [2003]). If validated, this method could be used to estimate the realized annual fecundity of several *Hippocampus* spp. (IUCN[1]) with data that already exist (Foster and Vincent, 2004).

In this article, I used European long-snouted seahorses (*Hippocampus guttulatus*) (Cuvier, 1829), to validate three progressively realistic models for estimating spawning frequency and realized annual fecundity. The objectives of this study were 1) to estimate the batch fecundity and spawning frequency of *H. guttulatus*, 2) to identify correlates of fecundity, and 3) to evaluate the predictive accuracy of the three models. The simplest model is the calculation employed by Vincent and Giles (2003). The second model includes an estimate of interbrood interval. The most realistic model is a generalization of the "spawning fraction" method (Hunter and Leong, 1981) that could be applied nondestructively to estimate realized annual fecundity in species of conservation concern. The study objectives were addressed by using fishery-independent sampling and underwater visual census in a locally abundant and unexploited population of *H. guttulatus*.

Materials And Methods

Species description

The life history and ecology of seahorses has been reviewed by Foster and Vincent (2004). *Hippocampus guttulatus* inhabits seagrass- and macroalgae-dominated communities in the Mediterranean Sea and the northeastern Atlantic Ocean (Lourie et al., 1999). Individuals begin reproducing at approximately 1 year of age and live 4 to 5.5 years (Boisseau, 1967; Curtis and Vincent, 2006). Adults range in size from 110 to 210 mm standard length (sum of head, trunk, and tail lengths, Lourie et al., 1999) and from 2.4 to 22.5 g wet mass (Curtis and Vincent, 2006). Male and female seahorses mate monogamously within reproductive cycles: the female deposits an entire clutch of eggs into the male's brood pouch (Jones et al., 1998). Brooding male *H. guttulatus* (i.e., with full pouches) have been captured from March to October (Boisseau, 1967; Reina-Hervás, 1989) and in January (Lo Bianco, 1888). The ovarian structure of *H. guttulatus* indicates that females produce multiple clutches per year (Boisseau, 1967).

Sampling

This study was carried out in the Ria Formosa lagoon in southern Portugal (36°59′N, 7°51′W). The Ria Formosa is a shallow, productive coastal lagoon characterized by high water turnover rates, seagrass beds, sand flats, salt marshes, and a network of channels and tidal creeks (Machás and Santos, 1999; Curtis and Vincent, 2005). Data employed in this study were derived from fisheries-independent samples of fish community structure (Erzini et al.[2]) and from underwater visual censuses of tagged *H. guttulatus* on a small focal study site (Curtis and Vincent, 2006). Seahorses captured during fisheries-independent sampling were collected monthly from September 2000 to July 2002 (except January 2002) at 53 stations throughout the western part of the Ria Formosa lagoon by using small beach seines, push nets, or beam trawls (Erzini et al.[2]), and then frozen. Data from all the captured seahorses were opportunistically recorded and included the standard length, life history stage, sex, reproductive state, wet mass, and brood size of males with full pouches (details provided in Curtis, 2004; Curtis and Vincent, 2006). Brood sizes were obtained by dissecting the full pouches of captured males and counting all of the developing embryos. Broods with embryos captured during the earliest stages of development (<stage 10, *sensu* Boisseau, 1967) were

---

[1] IUCN (World Conservation Union). 2006. 2006 IUCN Red List of Threatened Species. IUCN Species Survivial Commission, 219c Huntingdon Road, Cambridge CB3 0DL, United Kingdom. Website: http://www.redlist.org (accessed 31 May 2006).

[2] Erzini, K., L. Bentes, R. Coelho, C. Correia, P. G. Lino, P. Monteiro, J. Ribeiro, and J. M. S. Gonçalves. 2002. Recruitment of sea breams (Sparidae) and other commercially important species in the Algarve (southern Portugal). Final Report, 178 p. Commission of the European Communities DG XIV/C/1. Directorate-General for Fisheries and Maritime Affairs, Unit for Information and Communication, European Commission, B-1049, Brussels, Belgium.

excluded from the analyses because eggs and small embryos were in poor condition due to freezing and were therefore difficult to count. For the same reason, it was not possible to estimate clutch sizes by examining the ovaries of captured adult females. Data were recorded from a total of 1264 adult males and 1211 adult females captured with the fishing gears (Erzini et al.[2]).

Underwater visual censuses of tagged *H. guttulatus* were also carried out on a 10 m × 10 m focal study grid established in June 2001. The grid was located 5 m from the intertidal zone next to a permanent pier located within the Ria Formosa Natural Park at a depth of 1.3 to 6.1 m (additional details provided in Curtis, 2006; Curtis and Vincent, 2006). Tagged seahorses exhibited high site fidelity to small home ranges averaging 20 m^2 during multiple years (Curtis and Vincent, 2006). The juveniles released by eight tagged males on the grid were also counted and used to estimate brood size as in Vincent and Giles (2003). The eight brooding males were placed in cages (0.3 m high × 0.45 m wide, 0.5 mm mesh) *in situ* for a maximum of 48 h each between 18 July and 16 August 2002 (Curtis and Vincent, 2006). The mesh allowed water and small zooplankton to flow through the cages, while retaining newborn juveniles. After juveniles were born, the cages were slowly brought to the surface and emptied into large tanks filled with seawater where the total number of juveniles was counted. Males and their juveniles were released at their original capture site within 12 hours of birth.

Three models for estimating annual fecundity

The assumptions of rapid remating and continuous reproduction during the reproductive season were examined by using three progressively realistic models to estimate realized annual fecundity: the continuous reproduction (CR) model, the intermittent reproduction (IR) model, and the intermittent and seasonal reproduction (ISR) model.

Continuous reproduction (CR) model

In the simplest model, individuals were assumed to reproduce continuously from the beginning to the end of the reproductive season, from March to October (Boisseau, 1967; Reina-Hervás, 1989). Annual fecundity, $f_{b\cdot yr}$, was estimated by using mean estimates of the brooding period, t_b, and brood size, f_b:

$$f_{b\cdot yr} = f_b \times t_s / t_b \,, \tag{1}$$

where $f_{b\cdot yr}$ = the total number of young produced per male per year; and

t_s = the duration of the reproductive season.

In the CR model, f_b and t_b were assumed to be constant throughout t_s, and the interbrood interval, t_{ib}, was 0. The brooding period, t_b, was estimated by monitoring changes in the reproductive state of tagged adult males on the grid using underwater visual census. In 2001 and 2002, 553 *H. guttulatus* (264 males, 254 females, 35 juveniles) were individually tagged with visible implanted fluorescent elastomer (VIE tags, Northwest Marine Technologies, Inc., Shaw Island, WA) (Curtis, 2006; Curtis and Vincent, 2006). A total of 163 underwater visual censuses (2–5 person-hours/dive) were carried out with SCUBA on the grid during two census periods: from 17 July to 26 October 2001 and from 23 May to 12 September 2002. On average, one underwater visual census was carried out every 1 to 2 days during each of these census periods. During underwater visual censuses, observers swam ~1 m above the substrate and searched for tagged seahorses. The date, tag, life history stage, sex, size (trunk length, converted to standard length by using equations developed for *H. guttulatus*, Curtis and Vincent 2005, 2006), and reproductive state of all tagged seahorses were noted. The reproductive state of adult males (full or empty brood pouch) was determined by visual (and in ambiguous cases, manual) inspection.

Changes in reproductive state were plotted as a function of census date for each tagged male. Because of high seahorse density on the grid (1.5/m^2; Curtis and Vincent, 2006), it was not feasible to verify the status of all individuals during each dive; therefore, t_b was estimated by recording the minimum and maximum possible durations of each brooding period, as graphically depicted in Figure 1. Unmated male *H. guttulatus* occasionally mimic males that are close to releasing juveniles by temporarily and completely filling their pouches with water during reproductive displays to females (J. Curtis, personal observ.). Reproductive interactions between male and female *H. guttulatus* generally occurred within two hours of sunrise and lasted on average 4.8 min ±3.3 SD (standard deviation) (J. Curtis, unpubl. data). Therefore putative brooding periods were included in the analysis only when a male was observed ≥3 times with a full pouch during a period bracketed by observations of an empty pouch. The minimum and maximum possible brooding periods were averaged within and among all males.

Intermittent reproduction (IR) model

This model expanded the continuous reproduction model by incorporating a mean estimate of the interbrood interval, t_{ib}, which was assumed to be constant throughout the reproductive season:

$$f_{b\cdot yr} = f_b \cdot t_s \;/\; (t_b + t_{ib}), \tag{2}$$

where t_{ib} = the time elapsed between release of young and deposition of a new clutch of eggs into the male's brood pouch.

The interbrood interval was estimated by using a similar approach to that employed to estimate the brooding period (Fig. 1): the maximum and minimum possible durations of each interbrood interval were recorded and averaged within and among tagged males observed on the grid in 2001 and 2002.

For comparison, the annual frequency of clutches prepared by tagged females was also estimated by monitoring the time required to prepare eggs, t_c, and the interval between inferred clutches, t_{ic} (Fig. 1). Female trunk girth was used as an indicator of reproductive status (Vincent and Sadler, 1995; Perante et al., 2002). Females whose trunks were bulging between trunk rings (occasionally with visible eggs) were assumed to be preparing a clutch of eggs for mating. Within monogamous pairs of *H. comes* (Perante et al., 2002) and *H. whitei* (Vincent and Sadler, 1995), changes in female trunk girth were significantly correlated with changes in the reproductive state of their male partner. Therefore trunk girth was assumed to be a reliable proxy for clutch preparation in *H. guttulatus*. Because female sea pony (*Hippocampus fuscus*), prepared and released their eggs within approximately three days (Vincent, 1990), t_{ic} was estimated only during periods when female *H. guttulatus* were observed on average at least once every two to three days.

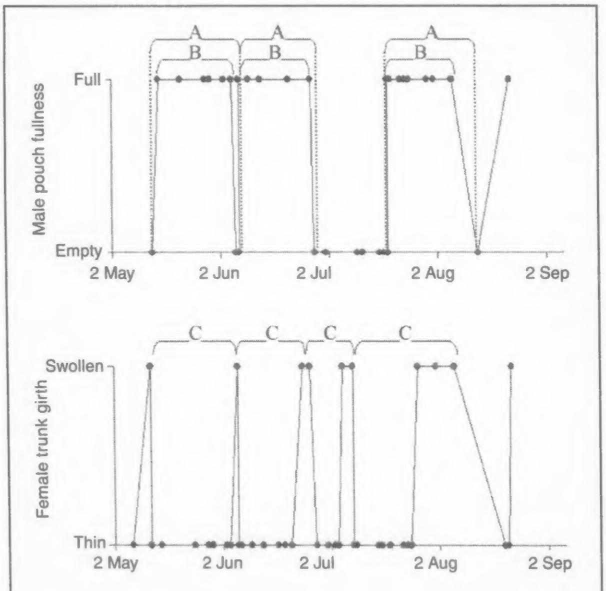

Examples of the changes in reproductive state from May to September 2002 in one marked male (**top**) and one marked female (**bottom**) *Hippocampus guttulatus* (long-snouted seahorse) during the census period in 2002. Males have full pouches when brooding eggs and embryos. Females whose trunks were bulging between trunk rings (i.e., swollen) were assumed to be preparing a clutch of eggs. Brackets marked with an A indicate the maximum duration of three brooding periods, and brackets marked with a B indicate minimum durations. One brief and one lengthy interbrood interval are evident. The interclutch intervals, inferred from changes in female trunk girth are also denoted with brackets marked with a C.

Intermittent and seasonal reproduction (ISR) model

This model is more realistic than the two previous models because information about seasonal trends in reproductive activity is incorporated, rather than the assumption that there is constant reproduction throughout the reproductive season. This model was adapted from the spawning fraction method used to estimate the average number of spawnings per year among female northern anchovy (Hunter and Leong, 1981). A Gaussian curve was fitted to the fraction of mature males with full pouches in the catch data plotted against sampling month by using nonlinear regression, as in Curtis and Vincent (2006). The area beneath this curve corresponds to an estimate of the total number of days the average adult male brooded embryos per year, $t_{b\cdot yr}$. The mean number of broods produced per male each year (i.e., annual spawning frequency), $s_{b\cdot yr}$, was estimated as $t_{b\cdot yr}/t_b$. Annual fecundity was then calculated as $f_b s_{b\cdot yr}$. Similarly, the ISR model was applied to the proportion of adult females preparing eggs, where the number of clutches produced by females each year, $s_{c\cdot yr}$, was estimated as the total time spent preparing clutches of eggs, $t_{c\cdot yr}$, divided by the time required to prepare a single clutch, t_c. In order to characterize among-population differences in *H. guttulatus* spawning frequency, this method was also applied to male catch data reported from the Arcachon Basin, France (Boisseau, 1967).

Model validation

An independent estimate of the brooding period (21 days; Boisseau, 1967) was used to evaluate the predictive accuracy of the CR and ISR models. The CR model was used to predict the expected number of broods produced by males, $s_{b\cdot cen}$, during the census periods from 18 July to 26 October (2001, 112 days) and 23 May to 12 September (2002, 108 days). Similarly, the curve fitted to the male catch data using the ISR model was used to calculate the predicted number of broods produced by males during these two census periods. Because the only estimate of the time females take to prepare eggs, t_c (used to estimate the number of clutches produced by females in the ISR model) was based on the underwater visual census data, the ISR model could not be used to predict the total expected number of clutches produced by females during the census periods. Therefore, the ISR model was used to predict the total number of days females spent preparing eggs during the census periods, $t_{c\cdot cen}$. Expected values of $s_{b\cdot cen}$ and $t_{c\cdot cen}$ based on the CR and ISR models were compared to the mean values of $s_{b\cdot cen}$ and $t_{c\cdot cen}$ directly observed on the grid during the corresponding census periods. The IR model could not be validated because there was no independent estimate of interbrood interval, t_{ib}, for *H. guttulatus*.

Correlates of fecundity

The influences of body size, water temperature, season, and lunar phase on batch fecundity and reproductive activity (i.e., the proportion of spawning males and females) were investigated. Daily and mean monthly water temperatures in the Ria Formosa were recorded with an Onset HOBO Temperature logger (Onset Computer, Bourne, MA) placed 0.3 m above the substrate on the grid from June 2001 to September 2002. All means are reported with one standard deviation or 95% confidence intervals (95% CI). Statistical procedures were carried out with SPSS 10.0.7 (SPSS Inc., Chicago, IL).

Results

Continuous reproduction (CR) model

Nonlinear regression indicated that the size of male *H. guttulatus* was a significant predictor of brood size, f_b, which varied from 10 to 567 embryos or juveniles, with a mean of 213.9 ±110.9 (n=117, caged and dissected males pooled). Both standard length (r^2=0.29, P<0.0001, n=117) and wet mass (r^2=0.20, P<0.003, n=39) significantly predicted f_b (Fig. 2). Brood size was not correlated with mean monthly temperature (r^2=0.00, P=0.90, n=117) but was weakly correlated with Julian day in 2001 (r^2=0.06, P=0.015, n=106).

A total of 4550 records were collected from the 553 individually tagged *H. guttulatus* in 2001 and 2002 for an average of 8.2 records per individual (maximum 87). On the grid, 94% of resighted, mature males mated at least once within a census period. The mean brooding period, t_b, was 21.4 (±5.5) days (n=80 intervals from 73 males, median=20.0 days). Temperature was not a significant predictor of t_b (r^2=0.004, $F_{[1,55]}$ =0.22, P>0.05), despite reports of an inverse relationship between temperature and brooding period in other seahorse species (Vincent and Sadler, 1995; Foster and Vincent, 2004).

The CR model produced the highest estimates of annual spawning frequency, $s_{b\text{-}yr}$, and realized annual fecundity, $f_{b\text{-}yr}$. Assuming continuous reproduction from March to October (245 days), male *H. guttulatus* was predicted to produce 11.5 broods annually. Mean annual fecundity was estimated as approximately 2450 young per year (Table 1).

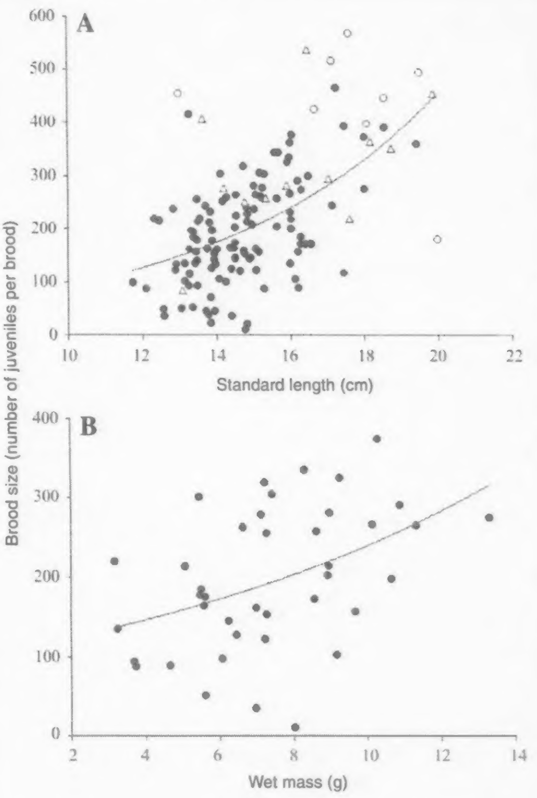

Figure 2

Relationship between *Hippocampus guttulatus* (long-snouted seahorse) male size and brood size (solid circles represent embryos dissected from brood pouches, open circles represent live juveniles born in cages): (**A**) standard length (n=117), and (**B**) wet mass (n=40). Equations of the fitted line in (A) and (B) are $y=18.7e^{0.16x}$ and $y=104.3e^{0.08x}$, respectively. Open triangles in (A) represent mean clutch sizes of female *Hippocampus guttulatus* in 12 length classes (Americano, D. 2004. Aspects of the reproductive biology of *Hippocampus guttulatus* (Cuvier, 1829) [In Portuguese], Undergraduate thesis, 51 p. Universidade do Algarve, Faro, Portugal.)

Intermittent reproduction (IR) model

The interbrood interval, t_{ib}, ranged from 0 to 61 days and had a mean of 12.9 (±8.2) days (n=98 intervals from 58 males; median=10.5 days) (Table 1). Size did not influence the number of broods produced by males during the census periods (Kruskal-Wallis test, χ^2=3.0, n=73, df=5, P=0.7) and temperature was not a significant predictor of t_{ib} (r^2=0.001, $F_{[1,97]}$=0.07, P=0.79). Incorporating t_{ib} into the IR model led to substantially lower estimates of spawning frequency and annual fecundity than predicted by the CR model: 7.14 (±4.89) broods per year and 1527 (±1309) young per year, respectively (Table 1).

All resighted, mature females prepared at least one clutch of eggs within a census period on the grid. The mean number of days females had hydrated eggs, t_c, was 2.58 (±2.66) days (n=72 inferred clutches), indicating that females required at least 2.5 days to prepare

Table 1

Parameter values (± standard deviation) and model predictions from three progressively realistic models for the Ria Formosa population of *Hippocampus guttulatus* (long-snouted seahorse). Estimates are also given for the Arcachon Basin population by using the intermittent and seasonal reproduction model.

Model	Continous reproduction (CR)	Intermittent reproduction (IR)	Intermittent and seasonal reproduction (ISR)	Intermittent and seasonal reproduction (ISR)
Population	Ria Formosa	Ria Formosa	Ria Formosa	Arcachon Basin
Parameters				
Reproductive season t_s (days)	245[1]	245[1]	250[2]	102[2]
Brooding period t_b (days)	21.4 (±5.6)	21.4 (±5.6)	21.4 (±5.6)	21[3]
Interbrood interval t_{ib} (days)	0	12.9 (±8.2)		
Time spent brooding $t_{b \cdot yr}$ (days)			90.4	20.7
Brood size (batch fecundity) f_b	213.9 (±110.9)	213.9 (±110.9)	213.9 (±110.9)	232 (±82.8)[3]
Predictions				
Spawning frequency $s_{b \cdot yr}$	11.5 (±2.9)	7.14 (±4.89)	4.22 (±1.09)	0.98
Annual fecundity $f_{b \cdot yr}$	2449.2 (±1415.9)	1527.2 (±1309.8)	903.6 (±522.4)	227.4 (±81.6)

[1] Assuming 8 months from March through October (Reina-Hervás, 1989).

[2] Period when ≥1% of mature males were predicted to have full pouches.

[3] Values reported in Boisseau (1967).

eggs for mating. Although there was no significant difference between the brooding period, t_b, of males and female interclutch interval, t_{ic} (21.06 6.6 days, n=102 intervals from 26 females; median=20 days) (t-test, df=180, t=−0.36, P=0.72), females produced significantly more clutches than males brooded during both underwater visual census periods (2001: df=37, t=3.32, P=0.002; 2002: df=62, t=7.16, P<0.0001, Table 2). Assuming that the duration of the reproductive season is the same for both sexes and that the IR model is correct, the estimate of the interclutch interval indicates that the average female prepared 11.63 (±3.65) clutches per year. Temperature was not a significant predictor of t_{ic} (r^2= 0.02, $F_{[1,101]}$=1.66, P=0.2).

Intermittent and seasonal reproduction (ISR) model

The reproductive activity of males varied significantly within years (r^2=0.78, $F_{[2,19]}$=39.28, P<0.0001, Fig. 3A). *Hippocampus guttulatus* males reproduced during most of the year and peaked in reproductive activity from June through August. No reproductively active males were captured from December 2000 to March 2001, or in February 2002. Male reproductive activity was also significantly and positively correlated with water temperature (r^2=0.55, $F_{[1,12]}$ = 13.32, P=0.004), which varied seasonally from 10– 28°C (mean annual temperature=18.2°C). There was no effect of lunar phase on male reproductive activity (r^2=0.01, $F_{[2,50]}$=0.26, P=0.78), as inferred by Boisseau (1967). The fraction of mature females that were preparing eggs also varied seasonally (r^2=0.21, $F_{[2,17]}$=3.59, P=0.05, Fig. 3B). Temperature was weakly correlated with female reproductive activity (r^2=0.30, $F_{[1,12]}$=4.80, P=0.05), but lunar phase was not (r^2=0.04, $F_{[2,50]}$=1.15, P=0.33).

Incorporation of seasonal variation in reproductive activity into the ISR model resulted in estimates of $s_{b \cdot yr}$ and $f_{b \cdot yr}$ that were 63.1% smaller than those predicted by the CR model. The ISR model predicted that the total time an average male *H. guttulatus* spent brooding embryos per year in the Ria Formosa was 90.4 days, giving an estimate of male annual spawning frequency, $s_{b \cdot yr}$, of 4.22 broods per year (Table 1). Similarly, the total time females spent preparing eggs per year was 13.51 days, giving an estimate of female annual spawning frequency, $s_{c \cdot yr}$, equal to 5.23 clutches per year. These estimates of annual spawning frequency were at least four times greater than estimates from the Arcachon Basin population. During the reproductive season, which lasted 3.5 months (Fig. 4), the average male had a full pouch for 20.7 days, indicating that, on average, males in the Arcachon Basin population bred only once a year (Table 1).

Model validation

The number of broods predicted by the CR model for the 2001 and 2002 census periods, $s_{b \cdot cen}$, was significantly greater than observed directly with underwater visual census (Table 2), indicating that this model produces upwardly biased estimates of spawning frequency for *H. guttulatus*. By contrast, the more realistic ISR model produced expected values of $s_{b \cdot cen}$ and the total number of days female spent with hydrated eggs, $t_{c \cdot cen}$, which were within 95% confidence intervals for the observed mean values on the grid in both 2001 and 2002. This latter inference is supported by close correspondence between observed male and female reproductive activity observed over time on the grid and the values predicted by the ISR model (Fig. 3).

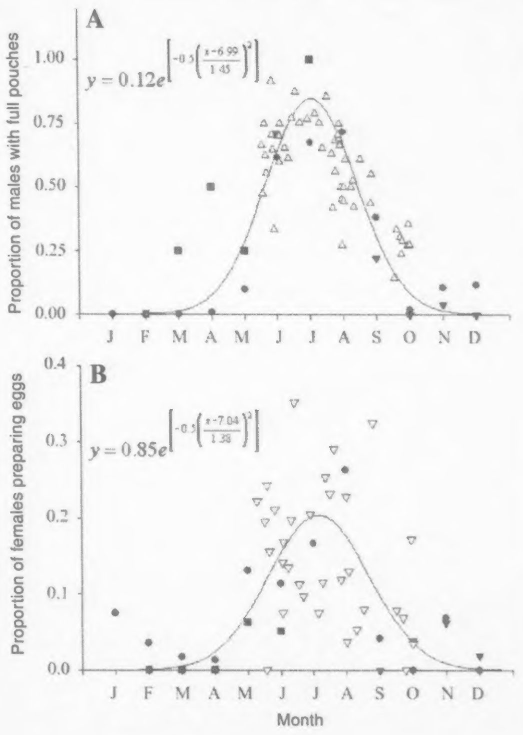

Figure 3

Within-year variation in the reproductive activity of *Hippocampus guttulatus* (long-snouted seahorse) in the Ria Formosa: (**A**) the proportion of males with full pouches, and (**B**) the proportion of females preparing eggs for mating. The curves (equations given) were fitted to catch data from 2000 (solid squares), 2001 (solid circles), and 2002 (solid triangles). The reproductive activity of males (open, upward-pointing triangles) and females (open, downward-pointing triangles) observed during underwater visual censuses of the grid (2001–2002) are plotted against census date for comparison.

Discussion

This article presents the first estimates of realized annual fecundity in a population of wild European long-snouted seahorses (*H. guttulatus*) and validates a potentially nondestructive application of the spawning fraction method (Hunter and Leong, 1981) for estimating spawning frequency. Results indicate that estimates of spawning frequency and annual fecundity based on egg production alone may lead to significant overestimates of realized annual fecundity and thus underscore the importance of testing assumptions when using proxies for estimating fecundity in multiple spawning fishes.

Batch fecundity

A significant relationship between male size and brood size of *H. guttulatus* means that size-specific realized annual fecundities can be calculated and converted to age-specific fecundities (e.g., Curtis, 2004) by using a length-at-age model developed for *H. guttulatus* (Curtis and Vincent, 2006). Among fishes, fecundity is strongly size-dependent (Davis and West, 1993; Lowerre-Barbieri et al., 1996). Female size is typically used to predict clutch size in fishes (Bagenal, 1978), including syngnathids (Teixeira and Musick, 2001; Vincent and Giles, 2003), but male dimensions can be also be used to predict brood size in fishes that provide paternal care, such as syngnathids (Strawn, 1958; Teixeira and Musick, 2001) and mouthbrooding cardinalfishes (Okuda et al., 1998; Kolm, 2002). Because both the volume of the female's abdominal cavity and volume of the male's sealed brood pouch potentially limit the number or size (or both) of embryos that can be successfully produced by seahorses (Boisseau, 1967), correlations between the dimensions of both parents and brood size likely reflect mutual mate selection for size (Vincent and Sadler, 1995; Teixeira and Musick, 2001; Vincent and Giles, 2003). A positive correlation between the standard lengths of *H. guttulatus* males and females engaged in courtship behavior on the grid (J. Curtis, unpubl. data), indicates that mating is size-assortative in this population.

Annual spawning frequency

The underwater visual census data indicate that on average, female *H. guttulatus* prepared significantly more clutches of eggs (1.2–1.7 times as many) than males brooded in the Ria Formosa in 2001 and 2002 (Table 2). This means that estimates of spawning frequency and annual fecundity based on female egg production (e.g., histological assessments) may significantly overestimate the actual number of young produced. Brood production by males was probably not limited by the availability of mature females because sex ratios were slightly biased in favor of females (Curtis and Vincent, 2006), and the interclutch intervals of females were equal to the brooding periods of males. Significantly longer interbrood intervals for the population of male *H. guttulatus* in the present study may have derived in part from depredation by other fishes during egg transfer to male brood pouches. This depredation occurred during one of three matings witnessed on the grid. Approximately 1% of male *H. guttulatus* in the Ria Formosa had holes in their pouch. Such injuries indicate that other predators

Table 2

Predicted and observed number of broods (males) and clutches (females) produced during underwater visual census periods in 2001 and 2002. Expected values were calculated by estimating the area beneath fitted curves in Figure 3 that corresponded to census periods in 2001 and 2002. Observed values (mean ± standard deviation) were taken from *n* males and females that were tagged and monitored throughout the entire census period. * =greater than upper 95% confidence limit of mean observed value.

	2001		2002	
	17 Jul–26 Oct	*n*	23 May–12 Sept	*n*
Males				
Observed number of broods	2.07 ±1.10	28	2.72 ±0.86	45
(95% confidence interval)	(0–4.22)		(1.03–4.40)	
Continuous reproduction (CR) model				
Predicted number of broods	5.33*		5.14*	
Intermittent and seasonal reproduction (ISR) model				
Predicted days with full pouch	56.65		71.59	
Predicted number of broods	2.69		3.40	
Females				
Observed number of clutches	3.40 ±1.07	10	4.66 ±1.23	18
(95% confidence interval)	(1.30–5.49)		(2.24–7.07)	
Observed days with prepared eggs	8.51 ±3.37		11.58 ±5.13	
(95% confidence interval)	(1.88–15.11)		(1.52–21.65)	
Intermittent and seasonal reproduction (ISR) model				
Predicted days with prepared eggs	8.14		10.46	

may also depredate eggs or developing embryos directly from the pouch (Curtis, 2004). A wounded wild *H. whitei* male had a hole in his pouch that precluded mating for nearly three reproductive cycles (~60 days, Vincent and Sadler, 1995). The degree to which predation affects reproductive success in *H. guttulatus* is unknown, but reproductive success in other fishes that provide male parental care is strongly affected by interspecific predation (e.g., Cole and Sadovy, 1995).

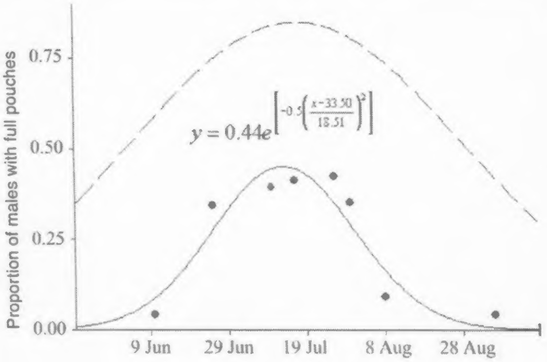

Figure 4

Within-year variation in the reproductive activity of *Hippocampus guttulatus* (long-snouted seahorse) in the Arcachon Basin from June to September 1952. The equation for the solid line fitted to the data from Boisseau (1967) is given. The dashed line is fitted to catch data from the Ria Formosa lagoon (see Fig. 3A).

A fourfold difference in estimated spawning frequency between the Arcachon Basin (one brood per year) and the Ria Formosa (4.2 broods per year) indicates that realized annual fecundity varies among *H. guttulatus* populations. Spawning frequencies are positively correlated with temperature in many marine fishes (Bone et al., 1995), including darters (Gale and Deutsch, 1985). Variation in spawning frequency among northern anchovy populations was also linked to energetic constraints (4–20 spawnings per year, Hunter and Leong, 1981). With an estimated mean spawning frequency of once per year and a shorter reproductive season, *H. guttulatus* in the Arcachon Basin may be more vulnerable to environmental stochasticity than the Ria Formosa population. Spawning that occurs multiple times within a reproductive season confers fitness benefits, particularly for small-bodied fishes inhabiting variable environments. By spawning fewer times in variable environments, the risk of catastrophic losses of eggs and larvae due to temporarily poor environmental conditions are increased (Nikolsky, 1963; McEvoy and McEvoy, 1992).

Trends in reproductive activity

Peaks in the reproductive activity of male and female *H. guttulatus* in the Ria Formosa lagoon corresponded to months with warmer water temperatures and higher primary and secondary production (Sprung, 1994a, 1994b), as observed in other fishes (Bye, 1984; Milton and Blaber, 1990). The duration of the reproductive season in the Ria Formosa lagoon (March–November) was similar to that reported for populations in southern Spain at a similar latitude (March–October, 36.7°N; Reina-Hervás, 1989) but was almost twice as long as in the higher latitude Arcachon Basin population (May–September, 44.7°N; Boisseau, 1967). Among-population differences in the duration of the reproductive season may be attributable to differences in temperature regimes (Robert et al., 1993) and photoperiod. Although Boisseau (1967) suggested that peaks in *H. guttulatus* reproductive activity occurred during full moons in the Arcachon Basin, there was no evidence of a correlation between lunar phase and reproduction in the Ria Formosa.

Models for estimating realized annual fecundity

Neither assumption of the CR model (rapid remating and continuous reproduction) was met empirically for *H. guttulatus* (Table 1, Fig. 3). This means that accurate estimates of realized annual fecundity in other seahorse species of conservation concern (Foster and Vincent 2004; IUCN[1]) may require further biological research. Annual spawning frequency and realized annual fecundity may be overestimated by as much as 270% when the assumptions of rapid remating or continuous reproduction have not been met (Table 1). Assumptions inherent in the CR model may be more likely to hold for monogamous species with short interbrood intervals (e.g., *H. whitei*; Vincent and Sadler, 1995) that breed year round in tropical environments (e.g., *H. comes*; Perante et al., 2002). Incorporating an estimate of interbrood interval into the IR model produced intermediate estimates of annual spawning frequency. However, estimates of interbrood intervals required considerable effort because of the need to monitor changes in the reproductive activity of individually tagged seahorses. Use of the ISR model circumvented the need to directly estimate interbrood intervals (see "Material and methods" section) and led to unbiased estimates of spawning frequency for both males and females.

The success of the ISR model in predicting observed estimates of male spawning frequency and the number of days females spent preparing eggs indicates that this model, based on the spawning fraction method developed by Hunter and Leong (1981), may be broadly applicable to all organisms for which batch fecundity and the time to prepare or brood a clutch of eggs are known. This model is suitable for species with broods that can be readily and periodically surveyed by using either fisheries-independent catches or underwater visual census techniques. Although fisheries-independent collections were opportunistically used in this study to estimate brood sizes and the fraction of spawning males and females, reliable estimates of these values were also obtained nondestructively by caging brooding males to count batch fecundity directly, and by monitoring changes in the fraction of spawning males and females over time with underwater visual censuses (Fig. 3). For species at risk that can be surveyed periodically during the reproductive season with nondestructive fisheries-independent sampling (e.g., underwater visual census), the generalized spawning fraction method becomes a potentially effective and appropriate means of estimating spawning frequency and realized annual fecundity.

Acknowledgments

This is a contribution from Project Seahorse. I thank K. Erzini and J. Ribeiro for providing their seahorse catches, the Parque Natural da Ria Formosa for logistic support, and R. Adams, H. Balasubramanian, K. Bigney, J. d'Entremont, B. Gunn, S. Lemieux, C.-M. Lesage, E. Murray, J. Nadeau, S. Overington, M. Veillette, K. Wieckowski, and S. V. Santos for excellent assistance. C Hall, D. O'Brien, and A. Vincent provided valuable comments on this manuscript. Funding was provided by Guylian, Natural Science and Engineering Research Council, Fonds Québécois de la Recherche sur la Nature et les Technologies, and McGill University.

Literature Cited

Bagenal, T. B.
1978. Aspects of fish fecundity. *In* Ecology of freshwater fish production (S. D. Gerking, ed.), p. 75–101. Blackwell Scientific Publications, Oxford, UK.
Boisseau, J.
1967. Hormonal regulation of incubation in a male vertebrate: research on seahorse reproduction. [In French]. Ph. D. diss., 379 p. Univ. Bordeaux, Bordeaux, France.
Bone, Q., N. B. Marshall, and J. S. H. Blaxter (eds.).
1995. Biology of fishes, 2nd ed., 288 p. Blackie Academic and Professional, London.
Brown-Peterson, N., P. Thomas, and C. R. Arnold.
1988. Reproductive biology of the spotted seatrout, *Cynoscion nebulosus*, in south Texas. Fish. Bull. 86: 373–388.
Bye, V. J.
1984. The role of environmental factors in the timing of reproductive cycles. *In* Fish reproduction: strategies and tactics (G. W. Potts, and R. J. Wooton, eds), p. 188–205. Academic Press, London.
Cole, K. S., and Y. Sadovy.
1995. Evaluating the use of spawning success to estimate reproductive success in a Caribbean reef fish. J. Fish Biol. 47:181–191
Curtis, J. M. R.
2004. Life history, ecology and conservation of European seahorses. Ph. D. thesis, 213 p. McGill Univ., Montreal, Canada.
2006. Visible implant elastomer color determination, tag visibility, and tag loss: Potential sources of error for mark-recapture studies. N. Am. J. Fish. Manage. 26:327–337.

Curtis, J. M. R., and A. C. J. Vincent.
2005. Distribution of sympatric seahorse species along a gradient of habitat complexity in a seagrass-dominated community. Mar. Ecol. Prog. Ser. 291:81–91.
2006. Life history of an unusual marine fish: survival, growth and movement patterns of the European long-snouted seahorse, *Hippocampus guttulatus* (Cuvier 1829). J. Fish Biol. 68:707–733.

Davis, T. L. O., and G. J. West.
1993. Maturation, reproductive seasonality, fecundity, and spawning frequency in *Lutjanus vittus* (Quoy and Gaimard) from the North West shelf of Australia. Fish. Bull. 91:224–236.

DeMartini, E. E., and R. K. Fountain.
1981. Ovarian cycling frequency and batch fecundity in the queenfish, *Seriphus politus*—attributes representative of serial spawning fishes. Fish. Bull. 79: 547–560.

Foster S, and A. C. J. Vincent.
2004. The life history and ecology of seahorses, *Hippocampus* spp.: implications for conservation and management. J. Fish Biol. 65:1–61.

Gale, W., and W. Deutsch.
1985. Fecundity and spawning frequency of captive tessellated darters—fractional spawners. Trans. Am. Fish. Soc. 111:35–40.

Hunter, J. R., and R. Leong.
1981. The spawning energetics of female northern anchovy, *Engraulis mordax*. Fish. Bull. 79: 215–230.

Hunter, J. R., B. J. Macewicz, and J. R. Sibert.
1986. The spawning frequency of skipjack tuna, *Katsuwonus pelamis*, from the south Pacific. Fish. Bull 84:895–903.

Jones, A. G., C. Kvarnemo, G. I. Moore, L. W. Simmons, and J. C. Avise.
1998. Microsatellite evidence for monogamy and sex-biased recombination in the Western Australian seahorse *Hippocampus angustus*. Mol. Ecol. 7:1497–1505.

Kolm, N.
2002. Male size determines reproductive output in a paternal mouthbrooding fish. Anim. Behav. 63:727–733.

Lo Bianco, S.
1888. Biological note on the period of sexual maturity of animals in the Gulf of Napoli [In Italian]. Mitte. Zool. Stat. Neapel. 8:385–440.

Lourie, S. A., A. C. J. Vincent, and H. J. Hall.
1999. Seahorses: An identification guide to the world's species and their conservation, 214 p. Project Seahorse, London.

Lowerre-Barbieri, S. K., M. E. Chittenden Jr., and L. R. Barbieri.
1996. Variable spawning activity and annual fecundity of weakfish in Chesapeake Bay. Trans. Am. Fish. Soc. 125:532–545.

Machás, R., and R. Santos.
1999. Sources of organic matter in Ria Formosa revealed by stable isotope analysis. Acta. Oecol. Int. J. Ecol. 20:463–469.

McEvoy, L. A., and J. McEvoy.
1992. Multiple spawning in several commercial fish species and its consequences for fisheries management, cultivation and experimentation. J. Fish Biol. 41(Suppl. B):125–136.

Milton, D. A., and M. Blaber.
1990. Maturation, spawning seasonality, and proximate spawning stimuli of six species of tuna baitfish in the Solomon Islands. Fish. Bull. 89:221–237.

Murua, H., and F. Saborido-Rey.
2003. Female reproductive strategies of marine fish species of the north Atlantic. J. Northw. Atl. Fish. Sci.33: 23–31.

Nikolsky, G. V.
1963. The ecology of fishes, 353 p. Academic Press, New York, NY.

Okuda, N., I. Tayasu, and Y. Yanagisawa.
1998. Determinate growth in a paternal mouthbrooding fish whose reproductive success is limited by buccal capacity. Evol. Ecol. 12:681–699.

Parrish, R. H., D. L. Mallicoate, and R. A. Klingbeil.
1986. Age dependent fecundity, number of spawnings per year, sex ratio, and maturation stages in northern anchovy, *Engraulis mordax*. Fish. Bull. 84:503–517.

Perante, N. C., M. G. Pajaro, J. J. Meeuwig, and A. C. J. Vincent.
2002. Biology of a seahorse species *Hippocampus comes* in the central Philippines. J. Fish Biol. 60:821–837.

Reina-Hervás, J. A.
1989. Contribution to the study of the family Syngnathidae (Pisces) along the southeast coast of Spain [In Spanish]. Arq. Mus. Bocage 1:325–334.

Robert, R., G. Trut, and J. L. Laborde.
1993. Growth, reproduction and gross biochemical composition of the Manila clam *Ruditapes philippinarum* in the Bay of Arcachon, France. Mar. Biol. 116:291–299.

Sprung, M.
1994a. High larval abundances in the Ria Formosa (Southern Portugal)—methodological or local effect? J. Plankton Res. 16:151–160.
1994b. Macrobenthic secondary production in the intertidal zone of the Ria Formosa—a lagoon in Southern Portugal. Est. Marine Coastal Shelf. Sci. 38:539–558.

Strawn, K.
1958. Life history of the pigmy seahorse, *Hippocampus zosterae* Jordan and Gilbert, at Cedar Key, Florida. Copeia 1:16–22.

Teixeira, R. L., and J. A. Musick.
2001. Reproduction and food habits of the lined seahorse, *Hippocampus erectus* (Teleostei: Syngnathidae) of Chesapeake Bay, Virginia. Brazil. J. Biol. 61:79–90.

Vincent, A. C. J.
1990. Reproductive ecology of seahorses. Ph. D. diss., 101 p. Cambridge Univ., Cambridge, UK.

Vincent, A. C. J., and B. Giles.
2003. Correlates of reproductive success in a wild population of *Hippocampus whitei*. J. Fish. Biol. 63:344–355.

Vincent, A. C. J., and L. M. Sadler.
1995. Faithful pair bonds in wild seahorses, *Hippocampus whitei*. Anim. Behav. 50: 1557–1569.

Wallace, R. A., and K. Selman.
1981. Cellular and dynamic aspects of oocyte growth in teleosts. Am. Zool. 21:325–343.

Weddle, G. K., and B. M. Burr.
1991. Fecundity and the dynamics of multiple spawning in darters: an in-stream study of *Etheostoma rafinesquei*. Copeia 1991:419–433.

Abundance, distribution, and habitat of leatherback turtles (*Dermochelys coriacea*) off California, 1990–2003

Scott R. Benson (contact author)[1]
Karin A. Forney[2]
James T. Harvey[3]
James V. Carretta[4]
Peter H. Dutton[4]
Email address for S. R. Benson: Scott.Benson@noaa.gov
[1] Protected Resources Division
Southwest Fisheries Science Center, NMFS, NOAA
c/o MLML Norte
7544 Sandholdt Rd.
Moss Landing, California 95039
[2] Protected Resources Division
Southwest Fisheries Science Center, NMFS, NOAA
110 Shaffer Road
Santa Cruz, California 95060
[3] Moss Landing Marine Laboratories
8272 Moss Landing Road
Moss Landing, California 95039
[4] Protected Resources Division
Southwest Fisheries Science Center, NMFS, NOAA
8604 La Jolla Shores Drive
La Jolla, California 92037

Abstract—Leatherback turtles (*Dermochelys coriacea*) are regularly seen off the U.S. West Coast, where they forage on jellyfish (Scyphomedusae) during summer and fall. Aerial line-transect surveys were conducted in neritic waters (<92 m depth) off central and northern California during 1990–2003, providing the first foraging population estimates for Pacific leatherback turtles. Males and females of about 1.1 to 2.1 m length were observed. Estimated abundance was linked to the Northern Oscillation Index and ranged from 12 (coefficient of variation [CV]=0.75) in 1995 to 379 (CV=0.23) in 1990, averaging 178 (CV=0.15). Greatest densities were found off central California, where oceanographic retention areas or upwelling shadows created favorable habitat for leatherback turtle prey. Results from independent telemetry studies have linked leatherback turtles off the U.S. West Coast to one of the two largest remaining Pacific breeding populations, at Jamursba Medi, Indonesia. Nearshore waters off California thus represent an important foraging region for the critically endangered Pacific leatherback turtle.

Manuscript submitted 21 August 2006 to the Scientific Editor's Office.

Manuscript approved for publication 29 November 2006 by the Scientific Editor.

Fish. Bull. 105:337–347 (2007).

The leatherback turtle (*Dermochelys coriacea*) is listed as a critically endangered species on the World Conservation Union Red List 2006 (IUCN[1]). The Pacific population is at risk of extirpation because of over-harvest of eggs, commercial and residential development on nesting beaches, and incidental bycatch in fisheries (Spotila et al., 2000). Declines have been documented at nesting beaches in the eastern Pacific and throughout the Indo-Pacific region, where there has been a complete loss of the Malaysian nesting population (Chan and Liew, 1996), severe declines at nesting beaches in Costa Rica (Spotila et al., 2000) and Mexico (Sarti et al., 1996), and lesser declines at western Pacific nesting beaches (Hitipeuw et al., 2007).

Research on leatherback turtles in the Pacific has typically been limited to nesting beaches and few studies have been conducted in foraging areas. In the eastern North Pacific, the leatherback turtle is the most common sea turtle sighted north of Mexico (Stinson, 1984), although no nesting occurs at these latitudes. Sightings and incidental capture data indicate that this species is found as far north as Alaska but has been most frequently encountered off the coast of central California (Stinson, 1984; Starbird et al., 1993). Genetic analyses of tissues from leatherback turtles stranded on California beaches or caught incidentally in the California-Oregon drift gillnet fishery indicate that these turtles originate from nesting beaches in the western Pacific (Dutton et al., 2000, 2007). Thus, leatherback turtles travel thousands of kilometers from western Pacific beaches to forage on seasonally abundant jellyfish (Scyphomedusae) along the West Coast of North America (Eisenberg and Frazier, 1983; Shenker, 1984), where coastal upwelling creates a dynamic and highly productive ecosystem.

---

[1] IUCN (World Conservation Union). 2006. Species Survival Commission. Red List database 2006. Website: http://www.iucnredlist.org/ (accessed 19 November 2006).

The California Current ecosystem is dominated by seasonal upwelling that is most intense between Pt. Conception and Cape Mendocino and gradually abates between July and October (Bakun et al., 1974). Previous studies of sighting patterns have linked leatherback turtle distribution and occurrence off the West Coast of North America to sea surface temperatures of 15–16°C during late summer and early fall (Stinson, 1984; Starbird et al., 1993). In particular, Monterey Bay, California, was identified as an area where leatherback turtles can be found during August, according to incidental sighting information collected by recreational boaters, researchers, and whale-watching operators. The spatially biased nature of these observations, however, precluded the estimation of overall leatherback turtle density and abundance.

In this study, we report the results of systematic aerial surveys conducted over coastal California waters between 1990 and 2003 and provide the first estimates of abundance for foraging leatherback turtles along the California coast. We also describe the density, distribution, and interannual variability of leatherback turtles off California during the peak period of occurrence in late summer and fall, examine oceanographic factors related to their occurrence in this region, and evaluate the potential significance of this foraging area to the western Pacific stock. Knowledge of leatherback foraging habitats is essential for the recovery of this critically endangered species, and the results of this study provide a basis for identifying and examining other potential foraging regions in the northeastern Pacific.

Materials and methods

Field methods

Aerial line-transect surveys for marine mammals and sea turtles were conducted between 15 August and 15 November in 10 of 14 years between 1990 and 2003. The primary objective of these surveys was to estimate abundance and trends of harbor porpoise (*Phocoena phocoena*), a small, cryptic nearshore cetacean; however, turtle sightings were also recorded systematically. Surveys were restricted to good weather days, defined as days with clear to partly cloudy skies and winds of less than about 12 kt (Beaufort sea states of 0–3). The transects followed a zigzag pattern designed to survey systematically between the coast and the 92-m (50-fathom) isobath, located less than 30 km offshore, and covering the primary habitat for harbor porpoise (Fig. 1). During each survey year, 26 transects between Pt. Conception and the Russian River (38°27′N) were replicated 4–8 times, depending on weather conditions. An additional 17 transects were surveyed 1–3 times a year off northern California between the Russian River and the California-Oregon border. Total transect length was 916 km, and under good weather conditions all transects were surveyed in two days. The full set of 43 transects was surveyed during the years 1990, 1991, 1993, 1995, 1997, 1999, and 2002. A subset of the transect lines (between Pt. Sur and Pt. Arena) was surveyed during 2000, 2001, and 2003 to provide further information on leatherback turtle occurrence off central California during these years.

Details of the survey methods have been reported elsewhere (Forney et al., 1991), and only a summary of key methods is provided here. The survey platform was a high-wing, twin-engine Partenavia P-68 aircraft, with two bubble windows for lateral viewing and a belly port for downward viewing. The survey team consisted of three observers (one on the left, right, and belly) and one data recorder. Distances to sighted animals were calculated from the declination angle to the sighting when abeam of the aircraft (obtained with a hand-held clinometer) and the aircraft's altitude. Surveys were flown at 167–185 km/h (90–100 kt) airspeed and 213 m (700 ft) altitude. Sighting information and environmental conditions, including Beaufort sea state, percentage cloud cover, and horizontal sun position (to measure glare direction) were recorded and updated throughout the survey by using a laptop computer connected to the aircraft's LORAN or GPS navigation system.

Visibility of submerged leatherback turtles is dependent upon water clarity and color contrast of the animals. When viewed from the air, this species generally exhibits considerable contrast to the surrounding waters within the California study area. To approximate the visibility of turtles at varying depths below the surface, a calibration experiment was conducted by using a set of multiple light-colored Secchi disks submerged at 1 m, 2 m, 3 m, and 4 m depth. During overflights, observers recorded the maximum visible Secchi disk depth. The proportion of time leatherback turtles spent within the visible depth range was estimated from dive data obtained during 2005 on free-swimming turtles, using a suction cup apparatus containing a VHF transmitter and a Lotek LTD 1110 time-depth-recorder (TDR) (Lotek, St. John's, Newfoundland, Canada). The suction cup apparatus (280 g weight in air) was attached to the dorsal surface of three leatherback turtles by using a pole from a small vessel, without capturing or handling the animal. The TDRs recorded depth every 5 sec at a resolution of 0.5 m and with an accuracy of ±1%. Tagged turtles were tracked for several hours until the tag disengaged from the animal or was actively removed with the pole, creating little or no disturbance to the animal. Potential posttagging effects were examined by visually inspecting the full dive profile, and by analysis of variance to test for differences in the time spent within the estimated visual depth range between the first 30 minutes and subsequent 30-minute periods. All deployments occurred during daylight hours between 12:00 and 16:30 local time.

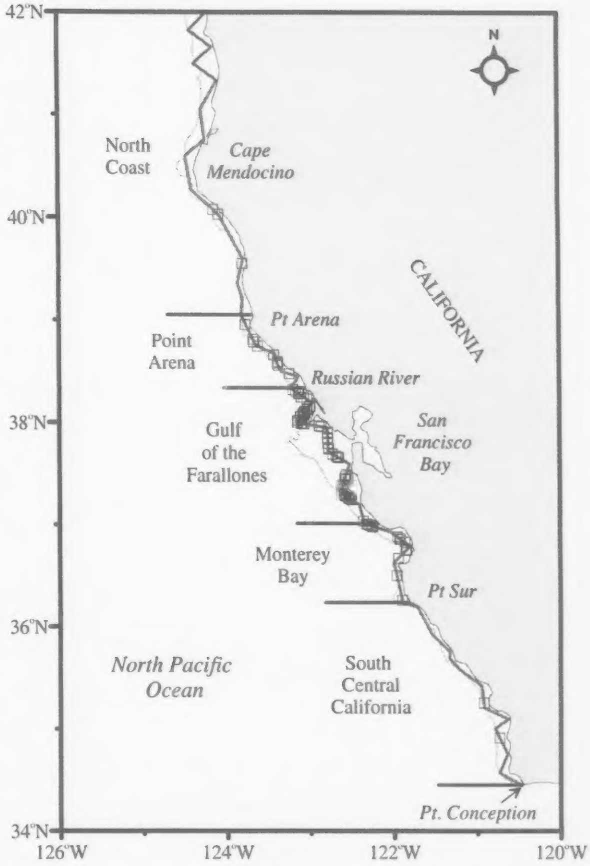

Figure 1

California study area with survey transects and geographic strata. Open squares represent locations of leatherback turtle (*Dermochelys coriacea*) sightings during systematic surveys. Thin gray line denotes the 90-m isobath.

Analytical methods

For analysis of regional patterns of leatherback turtle density and distribution, the study area was divided into five geographic strata, near prominent features of the coastline, to capture variation in bathymetric and oceanographic characteristics (Fig. 1): north coast (3765 km^2), Pt. Arena (772 km^2), Gulf of the Farallones (4189 km^2), Monterey Bay (908 km^2), and south central California (1849 km^2).

Leatherback turtle sighting rates were evaluated for potential effects of sea state, glare, and cloud cover, by using a two-way extension of the Kruskal-Wallis nonparametric analysis of variance (Scheirer et al., 1976), because these factors can influence one's ability to detect marine animals. Glare conditions were categorized as either optimal, when the sun position was behind the aircraft or directly ahead and did not affect the primary field of view, or marginal, when the sun position was just ahead of or perpendicular to the aircraft's travel direction. Cloud cover was divided into four categories: clear (<25% cloud cover), partly cloudy (26–50%), mostly cloudy (51–75%), and overcast (76–100%). Data collected in sea states greater than Beaufort 3 were excluded from the analysis; cloud cover and glare did not appear to exhibit any effect (see "Results" section) and were not considered further.

The detection function of leatherback turtles was estimated from the pooled perpendicular distances by using DISTANCE software (Thomas et al.[2]). Truncation of the 5–10% most distant sightings was investigated but it did not improve precision or model fit, and the final models included all data without truncation. Hazard, half-normal, and uniform models with and without cosine adjustment terms were fit to the ungrouped perpendicular distance data. The best model was selected according to Akaike's information criterion, AIC (Akaike, 1973), and visual inspection of goodness-of-fit.

The density (D) and abundance (N) of leatherback turtles within each geographic stratum, j, were estimated by using standard line-transect formulae (Buckland et al., 2001):

$$D_j = \frac{n_j f(0)}{2L_j g(0)}, \tag{1}$$

$$N_j = D_j A_j, \tag{2}$$

where n_j = the total number of turtles seen during systematic surveys;
$f(0)$ = the probability density function evaluated at zero perpendicular distance;
L_j = the linear distance surveyed in km;
$g(0)$ = the probability of detection at zero perpendicular distance, estimated from leatherback turtle dive data (see below); and
A_j = the area size in km^2.

Although we attempted to complete each transect the same number of times, weather conditions often resulted in uneven coverage. To avoid this potential within-stratum source of bias, encounter rates (n_j/L_j) for each geographic stratum were calculated from the individual transect encounter rates, weighted according to the proportional contribution of each transect:

---

[2] Thomas, L., J. L. Laake, S. Strindberg, F. F. C. Marques, S. T. Buckland, D. L. Borchers, D. R. Anderson, K. P. Burnham, S. L. Hedley, J. H. Pollard, and J. R. B. Bishop. 2004. Distance 4.1. Release 2. Research Unit for Wildlife Population Assessment, University of St. Andrews, UK. Website: http://www.ruwpa.st-and.ac.uk/distance/ (accessed 19 November 2006).

Table 1

Number of leatherback turtle (*Dermochelys coriacea*) sightings and kilometers of trackline surveyed by geographic stratum, 1990–2003 (SC=South Central California, MB=Monterey Bay, GF=Gulf of the Farallones, PA=Pt. Arena, NC=North Coast).

	1990	1991	1993	1995	1997	1999	2000	2001	2002	2003
No. of leatherback turtles										
SC	0	0	0	1	0	0	0	0	1	0
MB	4	0	0	1	0	1	2	0	8	0
GF	21	1	5	0	11	12	1	3	11	4
PA	3	0	0	0	2	5	0	0	0	0
NC	0	2	1	0	0	0	0	0	0	0
Total	28	3	6	2	13	18	3	3	20	4
Km surveyed										
SC	1605	922	1643	1197	1492	1317	0	0	1652	0
MB	655	509	860	730	860	585	74	368	812	334
GF	1316	293	1273	1030	1343	1026	197	482	1664	668
PA	343	107	287	192	328	327	12	179	475	27
NC	806	517	762	477	814	777	0	0	549	0
Total	4724	2347	4826	3626	4837	4032	283	1030	5151	1030

$$\frac{n_j}{L_j}=\sum_{i=1}^{k}\frac{t_{ij}}{T_{ij}}\frac{n_{ij}}{L_{ij}}, \qquad (3)$$

where k = the total number of transects within geographic stratum j;
t_{ij} = the length (in km) of the ith transect in stratum j;
T_{ij} = the total length of all transects in stratum j;
n_{ij} = the number of turtles seen on transect i in stratum j; and
L_{ij} = the actual distance flown on transect i within stratum j.

The probability of detecting a leatherback turtle at zero perpendicular distance, $g(0)$, is primarily influenced by the proportion of time a turtle is unavailable to be seen by the aerial survey team because it is diving (availability bias; Marsh and Sinclair, 1989). In other cases, animals may be present at or near the surface, but missed by observers for other reasons, such as fatigue or poor viewing conditions (perception bias). In this study, no correction was available for perception bias. Availability bias was estimated from leatherback turtle dive data and the estimated visible depth range from the visibility calibration experiment. Variances for D and N were calculated on basis of the variances of n, $f(0)$, and $g(0)$, according to the method of Buckland et al. (2001). The variance in number of sightings, n, was expected to differ by year and stratum because of differences in mean turtle density; however, it was not possible to calculate stratum-specific and year-specific variances empirically because not all transects were replicated in all years. The variance of leatherback turtle detections, therefore, was assumed to follow a Poisson distribution, with $\hat{var}(n) = n$. The variance of $f(0)$ was estimated analytically with DISTANCE software, and the variance of $g(0)$ was estimated from the individual $g(0)$ estimates for the three tagged turtles.

Overall abundance estimates for the entire study area were calculated as the sum of the stratum-specific abundance estimates for the seven full survey years: 1990, 1991, 1993, 1995, 1997, 1999, and 2002. During the three years when surveys were flown only off central California (2000, 2001, and 2003), coastwide abundance of leatherback turtles was estimated as the sum of the abundances for the Monterey Bay and Gulf of the Farallones strata, divided by the mean proportion of the total abundance found in these two strata during full survey years. The variance in this proportion was estimated across years (n=7) and incorporated into the variance of N and D by using standard formulae. Abundance estimates were examined for trends and potential large-scale environmental influences by linear least squares regression that included year and the 12-month average Northern Oscillation Index (NOI; Schwing et al., 2002) as predictor variables. Regressions were performed for all years, and for the subset of seven full survey years, because there was greater uncertainty in the abundance estimates for 2000, 2001, and 2003.

Results

Survey summary

A total of 31,885 km were surveyed in Beaufort sea states of 0–3 during 1990–2003 (Table 1), and annual totals ranged from 2347 to 5151 km during the full survey years when all strata were surveyed, and from 283 to 1030 km during the partial survey years, when only waters between Pt. Sur and Pt. Arena were surveyed. Weather conditions varied by year and were the primary determinant of the level of survey coverage achieved. Leatherback turtle encounter rates were identical for Beaufort sea states 0–1, 2, and 3 (0.003 turtles/km). Cloud cover and glare categories did not have a significant effect on encounter rates (P=0.08 and P=0.23, respectively).

The number of leatherback turtles seen per year ranged from 2 to 28, and totaled 100 individuals for all years (Table 1). The majority of turtles were subjectively estimated to be 5–7 ft (1.5–2.1 m) in total length, but only three smaller individuals (3.5–4.5 ft; 1.1–1.4 m) and one very large individual, estimated to be about 7.5 ft (2.3 m), were also recorded. Whenever possible, the presence of a long tail (indicating an adult male) was noted; however, this feature was often difficult to determine from the aircraft. In particular, males with tails of intermediate length may have had a greater likelihood of being recorded as "tail length undetermined." The proportion of identified males, 6 of 44 (14%), therefore, is a minimum proportion of males in the study area. Greatest concentrations of leatherback turtles were observed in the Gulf of the Farallones stratum, but turtles were observed in all geographic strata (Fig. 1).

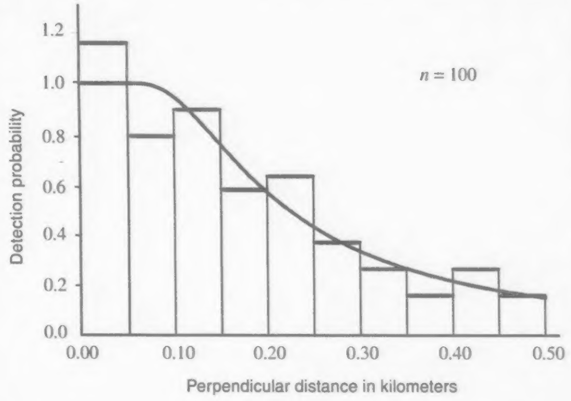

Figure 2

Detection probability function (Hazard rate model) and distribution of perpendicular distances for 100 leatherback turtle (*Dermochelys coriacea*) sightings.

Estimation of line-transect parameters

All three detection function models yielded similar estimates of $f(0)$, and AIC values were within one point. The Hazard rate model (Buckland et al., 2001) was selected because it provided the best fit, especially near the transect line (Fig. 2), yielding an estimated $f(0)$=4.465 (coefficient of variation, CV=0.136).

During the visibility calibration experiment, only the Secchi disk at 1 m depth was visible to the aerial observers; therefore, the depth at which leatherback turtles were detected was estimated to be about 1 m. Time-depth recorders (TDRs) were attached to three turtles (1 male, 2 females) on 29 September (for 153 minutes), 30 September (167 minutes), and 13 October, 2005 (229 minutes). There was no visible reaction by the turtles to the application of the tag, and the proportion of time spent within 1 m of the surface did not differ between the first 30 minutes and subsequent 30-minute periods of tag deployment (P=0.08). The parameter $g(0)$ was, therefore, estimated from the complete TDR dive record as the average proportion of time leatherbacks spent at or above 1 m depth. The three individuals exhibited a remarkably similar proportion of time spent within the upper meter of the sea surface (Table 2), and $g(0)$ was estimated as 0.471 (CV=0.029). Corrected estimates of abundance thus are about twice the uncorrected values (Fig. 3).

Abundance and density

Estimated leatherback turtle abundance was variable among years (Fig. 3; Table 3), ranging from 12 (CV=0.74) during 1995 to 379 (CV=0.23) during 1990. The greatest proportion of turtles was encountered within the two central California strata (Monterey Bay and Gulf of the Farallones), accounting for an average of 72% (range 31–97%, CV=0.37) of the total abundance. In partial survey years, when only these two strata were surveyed, total abundance within the study area was estimated as the central California abundance divided by the mean percentage (72%). For all years combined, estimated leatherback turtle abundance averaged 140 (CV=0.17) within the central California strata and 178 (CV=0.15) for the entire study area (Table 3). Although the Gulf of the Farallones stratum contributed the most to overall abundance because of its larger size, turtle densities were only slightly less for the Monterey Bay and Pt. Arena strata (Table 3). The South Central California and North Coast strata had the lowest densities. Monthly encounter rates of leatherback turtles by stratum (Fig. 4) were consistent with past reports of frequent sightings in Monterey Bay during August (Starbird et al., 1993); however, in our study, encounter rates were also high during September in the Monterey Bay and Gulf of the Farallones strata, and during October within the Gulf of the Farallones. Encounter rates decreased markedly throughout the study area during November. Interannual variability was least during September, and regionally within the Gulf of the Farallones stratum.

The estimates of abundance of leatherback turtles off California (Fig. 3) did not exhibit a trend between 1990 and 2003 (P=0.19 when data for all ten survey years were used, P=0.41 including only the seven coastwide survey years) but appeared to be related to the average annual NOI (Schwing et al., 2002), i.e, there were positive index values associated with greater leatherback turtle abundance and vice versa (Fig. 5; P=0.03 when

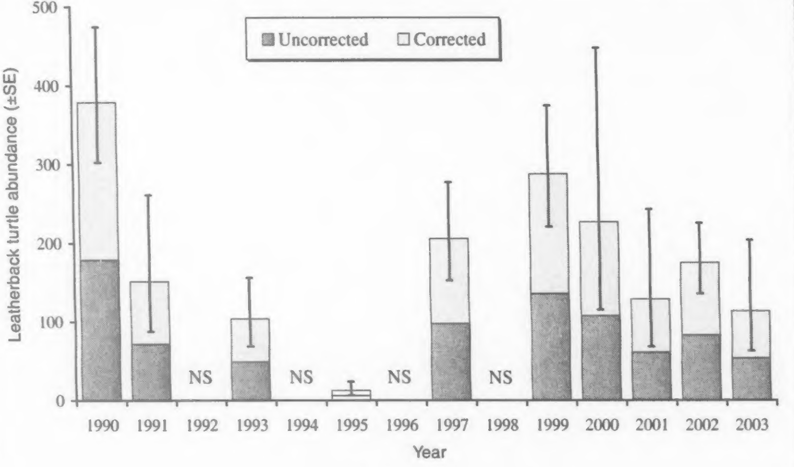

Figure 3

Estimated leatherback turtle (*Dermochelys coriacea*) abundance within the California study area, with and without $g(0)$ correction for diving behavior. Error bars indicate one standard error (SE); NS indicates no surveys were conducted during that year.

Table 2

Proportion of time spent in upper 5 meters of the water column by three foraging leatherback turtles (*Dermochelys coriacea*) tagged with time-depth recorders off central California during 2005. Dates and deployment times are provided for each turtle. "No. of intervals" represents the number of samples recorded by the depth logger (every 5 sec) within each depth category. The proportion of intervals within the upper 1 m was used for $g(0)$ estimation. CV = coefficient of variation.

	29 Sep 2005 (12:20–14:53)		30 Sep 2005 (13:28–16:16)		13 Oct 2005 (12:06–15:54)		Average	
Depth (m)	No. of intervals	Proportion of intervals	No. of intervals	Proportion of intervals	No. of intervals	Proportion of intervals	Porportion of intervals	CV
At surface	804	0.437	876	0.436	1099	0.400	0.425	0.029
≤1	35	0.456	124	0.498	164	0.460	0.471	0.029
≤2	104	0.513	260	0.628	219	0.540	0.560	0.062
≤3	63	0.547	123	0.689	150	0.595	0.610	0.069
≤4	220	0.666	229	0.803	287	0.699	0.723	0.057
≤5	76	0.708	92	0.849	91	0.732	0.763	0.057
>5	538	1.000	303	1.000	735	1.000	1.000	—

including all ten survey years; $P=0.04$ for only the seven coastwide survey years).

Discussion

The results of this study demonstrate the importance of neritic waters off California to foraging leatherback turtles and provide the first estimates of abundance for a Pacific foraging population of this critically endangered species. The aerial line-transect surveys, although not originally designed to census this species, provided quantitative data during the summer and fall peak season of occurrence (Starbird et al., 1993). Absolute abundances of foraging Pacific leatherback turtles were estimated for the first time by applying a new telemetry-based correction factor to account for submerged animals. Corrected densities in this study were 2.1 times greater than uncorrected densities. This contrasts markedly with the correction factor of 7.6 derived from dive data for a single leatherback turtle off St. Croix, U.S. Virgin Islands

Table 3

Estimated density and abundance of leatherback turtles (*Dermochelys coriacea*) by year and geographic stratum (SC=South Central California, MB = Monterey Bay, GF=Gulf of the Farallones, PA=Pt. Arena, NC=North Coast. Central CA includes MB and GF). CV = Coefficient of variation.

	1990	1991	1993	1995	1997	1999	2000[1]	2001[1]	2002	2003[1]	Mean	CV
Density (no./100 km^2)												
SC	0.0	0.0	0.0	0.4	0.0	0.0	—	—	0.3	—	0.1	0.72
MB	2.8	0.0	0.0	0.5	0.0	1.0	7.2	0.0	4.9	0.0	1.3	0.29
GF	7.7	1.1	1.9	0.0	4.3	5.4	2.3	2.2	3.0	1.9	3.6	0.18
PA	4.1	0.0	0.0	0.0	3.5	6.6	0.0	0.0	0.0	0.0	2.3	0.35
NC	0.0	2.8	0.6	0.0	0.0	0.0	—	—	0.0	—	0.3	0.59
Total area	3.3	1.3	0.9	0.1	1.8	2.5	2.0	1.1	1.5	1.0	1.6	0.15
Abundance												
SC	0	0	0	8	0	0	—	—	6	—	2	0.72
MB	25	0	0	4	0	9	66	0	45	0	15	0.29
GF	321	47	80	0	179	227	97	92	124	81	125	0.18
PA	32	0	0	0	27	51	0	0	0	0	14	0.35
NC	0	105	23	0	0	0	—	—	0	—	18	0.59
Total area	379	151	104	12	205	287	226	129	175	113	178	0.15
CV	0.23	0.59	0.43	0.74	0.30	0.27	0.77	0.70	0.26	0.64		
Central CA	347	47	80	4	179	236	162	92	169	81	140	0.17
CV	0.24	1.01	0.47	1.01	0.33	0.31	0.67	0.59	0.26	0.52		
% of total	92%	31%	78%	36%	87%	82%	—	—	97%	—	72%	0.37

[1] In these years, only central California was surveyed. Abundance estimates for the total area were extrapolated from central CA estimates based on the mean proportion of leatherbacks in central California during full survey years.

(Keinath and Musick, 1993) and applied to aerial survey density estimates for Atlantic leatherback turtles (Keinath et al., 1996). The correction used in the Keinath and Musick study, however, was based on the proportion of time the transmitter was above the water surface (and wave action), not the estimated proportion of time a turtle would have been visible to an aerial survey team (to about 1 m depth), as in this study. Furthermore, St. Croix represents a nesting area, and leatherback diving behavior may differ between nesting and foraging areas.

Average uncorrected densities of leatherback turtles off California during our study (0.75 turtles/100 km^2) are within the range of 0.21 to 2.2 leatherback turtles/100 km^2 reported during 1978–82 along the U.S. Atlantic coast (Shoop and Kenney, 1992), although the Atlantic study reported monthly estimates, not a seasonal average, and encompassed a larger study area. Average uncorrected densities in a smaller foraging area off North Carolina during August–November 1986–91 (0.80 leatherback turtles/100 km^2; Keinath et al., 1996), were similar to those observed in this study.

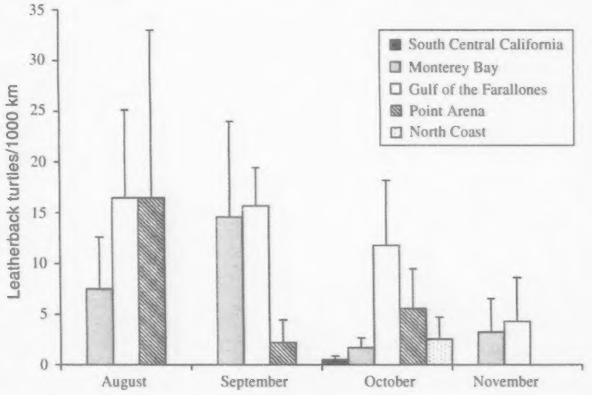

Figure 4

Average monthly leatherback turtle (*Dermochelys coriacea*) encounter rates (turtles / 1000 km surveyed) by geographic stratum, 1990–2003. Error bars indicate one standard error.

Leatherback turtles along the U.S. West Coast are part of the western Pacific genetic stock (Dutton et al., 2000, 2007), which is known to nest in Papua (Indonesia), Papua New Guinea, Solomon Islands, and on other western Pacific islands (Dutton et al., 2007). The western Pacific metapopulation was estimated to contain roughly 1800 nesting females in 1995 (Spotila et al., 1996); however, a more comprehensive evaluation indicates that the total western Pacific metapopulation may contain 2700–4500 breeding females (Dutton et al., 2007). Satellite telemetry studies have linked leatherback turtles foraging along the U.S. West Coast with one of the two largest remaining nesting beaches, Jamursba Medi (Papua, Indonesia) (Benson et al., 2007a), which experiences peak nesting activity during the austral winter. No links to the U.S. West Coast have been identified for animals nesting during the austral summer at nearby Wermon, Papua, Indonesia (S. Benson and P. Dutton, unpubl. data) or in Papua New Guinea (Benson et al., 2007b).

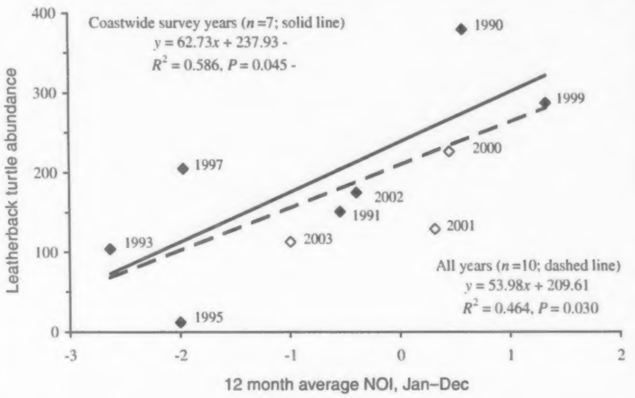

Figure 5

Regression of estimated leatherback turtle (*Dermochelys coriacea*) abundance versus 12 month average Northern Oscillation Index (NOI; Schwing et al., 2002) for the period January–December of each survey year (indicated next to the points). Filled symbols represent years in which surveys were conducted coastwide; open symbols represent years in which estimates of coastwide abundance were based on central California abundance (see "Materials and methods" section).

In a recent analysis of nest counts at Jamursba Medi, an average of about 750 females were estimated to nest annually between 1993 and 2004 (Hitipeuw et al., 2007). Efforts are underway to determine the relationship between the number of females nesting annually and the total number of females in the Jamursba-Medi nesting population; however, it is thought that this population currently has at least 1000–2000 nesting females (Spotila et al., 1996; Dutton et al., 2007). Capture studies off central California during 2000–2005 documented that about 67.5% (27 of 40) of foraging leatherback turtles were female (S. Benson and P. Dutton, unpubl. data). Our average annual estimate of 178 leatherback turtles along the California coast, therefore, should correspond to approximately 120 females. It is difficult, however, to evaluate this number in relation to the total Jamursba-Medi nesting population, because insufficient data are available on migration intervals between nesting beaches and foraging grounds. If each nesting year corresponds to one year at the California foraging grounds, then an average of about 16% of Jamursba-Medi females (120 divided by 750) potentially use the California foraging area; however there is evidence that leatherback turtles do not alternate nesting and foraging at such regular intervals. Remigration intervals to nesting beaches can range up to seven years (Price et al., 2004; Dutton et al., 2005), and some turtles have returned to forage off the U.S. West Coast during consecutive years without nesting (S. Benson and P. Dutton, unpubl. data). Further studies of remigration patterns and foraging site fidelity of western Pacific leatherback turtles will be required to resolve the proportion of these turtles that forage off California.

Estimates of foraging abundance in this study vary markedly among years (Fig. 3) and have a number of known sources of downward bias. First, the California study area includes only the nearshore environment to a water depth of about 92 m (50 fm), but leatherback turtles also have been captured incidentally in drift gill nets set in deeper waters (Julian and Beeson, 1998; Carretta et al., 2005). Second, the estimate calculated in this article represents an average snapshot abundance, and will be an underestimate of the true number of individuals using the area to the extent that residence times in the study area are less than our three-month study season. For example, if leatherback turtles forage within the study area for two months, then turtles observed in August would likely be different individuals from those observed during October or November, but average line-transect densities would only reflect the presence of a single turtle. Similarly, if leatherback turtle density is not constant throughout the three-month study period, the pooled estimate presented in this study will be lower than the peak seasonal abundance. Lastly, no estimate of perception bias was available for leatherback turtles in this study; however, small groups of small dolphins and porpoises are missed about 33% of the time (Forney et al., 1995). Therefore, it is likely that the detection of available turtles along the transect line is less than 100%.

The estimate of $g(0)$ developed in this study is the first to be based on dive records of leatherback turtles within a foraging region. Although the three turtles exhibited remarkably similar proportions of time within near-surface waters (Table 2), there is some uncertainty in the estimate because it is based on limited afternoon deployments (n=3) within a single year (2005). Furthermore, the depth to which turtles are visible to aerial observers may vary in space and time, as turbidity changes. The estimated $g(0)$ =0.471 should, therefore,

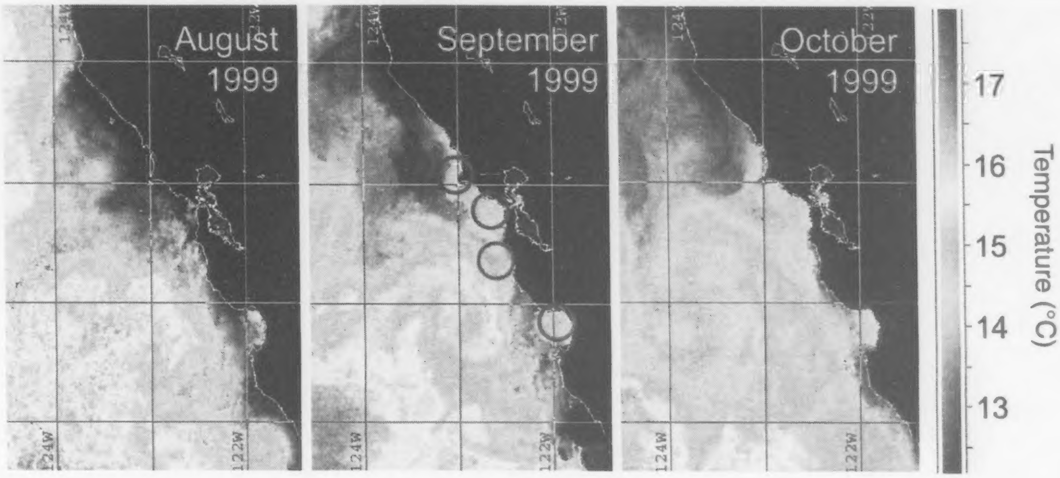

Figure 6

Pattern of upwelling and retention along the central California coast, illustrated with monthly satellite-derived sea surface temperature images for August, September, and October 1999. Leatherback turtles (*Dermochelys coriacea*) and Scyphomedusae were primarily found in areas of retention (circled in middle panel). High resolution monthly composite satellite images courtesy of NOAA CoastWatch, West Coast Node.

be considered provisional, pending further TDR deployments and calibration experiments.

Leatherback turtle populations at many Pacific nesting beaches have decreased dramatically during the last decade (Spotila et al., 2000), but decreases at Jamursba-Medi have been less pronounced (Hitipeuw et al., 2007), and the abundance of turtles foraging off California does not exhibit a trend between 1990 and 2003 (Fig. 3). The California study area is a dynamic upwelling environment that exhibits great interannual variability in oceanographic conditions (Chelton et al., 1982; McGowan et al., 1998) and distribution of marine vertebrates (e.g., Ainley et al., 1993; Benson et al., 2002). Links have been proposed elsewhere between large-scale environmental indices, such as the Southern Oscillation Index and the North Atlantic Oscillation, and sea turtles (Limpus and Nicholls, 1988; Rivalan, 2004) or their prey (Lynam et al., 2004). In this study, leatherback turtle abundance off California exhibited a positive relationship with the average annual NOI (Fig. 5). Positive NOI values correspond with conditions favorable to upwelling along the California coast, leading to increased zooplankton production (Schwing et al., 2002) and the development of large aggregations of gelatinous zooplankton (Graham, 1994), which are known to be the primary prey of leatherback turtles (Eisenberg and Frazier, 1983).

Although we did not measure underlying physical and biological processes, central California has been the focus of numerous oceanographic studies that shed light on potential trophic links between physical processes and leatherback turtles. Strong northwest winds during late spring and early summer lead to wind-driven upwelling (Bakun et al., 1974), particularly near points and headlands. These prominences can interact with local hydrographic features to create localized retention areas (upwelling shadows; Graham, 1994), where nutrient-rich, upwelling-modified water is entrained nearshore, particularly during wind relaxation. This process creates favorable conditions for phytoplankton growth and increases retention of zooplankton, larval fish, crabs, and gelatinous organisms (Wing et al., 1995; Graham et al., 2001). Dense aggregations of jellyfish (Scyphomedusae), primarily *Chrysaora fuscescens*, *C. colorata*, and *Aurelia* spp., have been observed regularly in these nearshore regions (Graham, 1994; this study). Similar processes have been reported off Oregon, where Scyphomedusae become denser and larger in size during summer, when the movement of surface and near-surface waters concentrates plankton in nearshore retention areas (Shenker, 1984). During our surveys, Scyphomedusae were common in retention areas between Pt. Reyes and Monterey Bay (Fig. 6), where leatherback turtles were most frequently encountered and observed feeding on *C. fuscescens*, *C. colorata*, and *Aurelia* spp. (Starbird et al., 1993; this study). We hypothesize that variability in the expression of these physical and trophic processes leads to interannual and seasonal variability in observed leatherback turtle abundance off central California, with densities greatest during periods of significant upwelling and subsequent relaxation events.

Previous researchers have linked leatherback turtle occurrence at high latitudes to the 15–16°C isotherm (Stinson, 1984; McMahon and Hays, 2006). Off central California, this reported pattern may reflect the presence of >15°C waters during summer and fall relaxation events and in upwelling shadows where jellyfish aggregations are found (Graham, 1994; Graham and Largier, 1997), rather than a physiological limitation of leatherback turtles. The broad shallow area of retention in the Gulf of the Farallones consistently exhibited greater abundances of leatherback turtles during our study. In contrast, few turtles were observed south of Pt. Sur, where the shelf is extremely narrow and cooler waters dominate along a nearly straight coastline where there are limited retention zones.

Many questions remain unanswered regarding the role of physical and biological factors and their influence on leatherback turtle abundance and distribution along the U.S. West Coast. Upwelling shadows and relaxation events probably affect leatherback turtle occurrence, but directed studies are needed to establish trophic links. Furthermore, the potential influence and role of the San Francisco Bay outflow on this nearshore foraging area is unknown. Results of this study provide a means for designing finer-scale surveys in key index areas of reliable leatherback turtle occurrence, such as the Gulf of the Farallones and Monterey Bay. Aerial surveys of these index areas should be coupled with telemetry studies and investigations of environmental variables that affect leatherback turtle foraging behavior to provide insights into the relevant trophic processes.

Ultimately, successful conservation efforts for leatherback turtles must include both protection of nesting beaches and mitigation of at-sea threats in foraging areas and along migratory routes. This study has demonstrated that waters off central California are a critical foraging area for one of the largest remaining Pacific nesting populations. Fortunately, threats such as coastal gillnet and longline fisheries that may incidentally catch leatherback turtles have largely been eliminated within our nearshore study area although pelagic driftnet and longline fisheries remain along the migratory pathways to and from the coast (e.g., Spotila et al., 1996; Carretta et al., 2005). Continued efforts to identify and characterize Pacific foraging areas are critical for mitigating at-sea threats, monitoring population trends, and, ultimately, for the successful recovery of Pacific leatherback turtle populations.

Acknowledgments

This study could not have been completed without the dedicated support of many aerial observers, whom we thank sincerely. S. Eckert originally noted the significance of leatherback turtle sighting data collected during these nearshore surveys and encouraged us to initiate the analyses presented here. Aspen Helicopters, Inc. provided aircraft and pilots, and Moss Landing Marine Laboratories Marine Operations provided small boat support. Captain J. Douglas' exceptional boat handling skills were key to the success of the telemetry studies. Suction-cup telemetry was conducted under ESA permit no. 1227. Surveys were conducted under National Marine Fisheries Service permit nos. 748 and 773-1437, and National Marine Sanctuary permit nos. GFNMS / MBNMS-03-93, MBNMS-11-93, GFNMS / MBNMS / CINMS-09-94, GFNMS / MBNMS / CINMS-04-98-A1, and MULTI-2002-003. Financial support and personnel were provided by the National Marine Fisheries Service (Southwest Fisheries Science Center, Southwest Region, and Office of Protected Resources), Monterey Bay National Marine Sanctuary, and the California Department of Fish and Game. We thank J. Barlow, E. Calvert, A. Moles, J. Musick, F. Schwing, J. Seminoff, and three anonymous reviewers for their helpful reviews of this manuscript.

Literature cited

Ainley, D. G., W. J. Sydeman, R. H. Parrish, and W. H. Lenarz.
1993. Oceanic factors influencing distribution of young rockfish (*Sebastes*) in central California: a predator's perspective. CalCOFI Rep. 34:133–139.

Akaike, H.
1973. Information theory and an extension of the maximum likelihood principle. *In* Second international symposium on information theory (B. N. Petran and F. Csàaki, eds.), p. 267–281. Akadèemiai Kiadi, Budapest, Hungary.

Bakun, A., D. R. McLain, and F. V. Mayo.
1974. The mean annual cycle of coastal upwelling off western North America as observed from surface measurements. Fish. Bull. 72:843–844.

Benson, S. R., D. A. Croll, B. Marinovic, F. P. Chavez, and J. T. Harvey.
2002. Changes in the cetacean assemblage of a coastal upwelling ecosystem during El Niño 1997–98 and La Niña 1999. Prog. Oceanogr. 54:279–291.

Benson, S. R., P. H. Dutton, C. Hitipeuw, B. Samber, J. Bakarbessy, and D. Parker.
2007a. Post-nesting migrations of leatherback turtles (*Dermochelys coriacea*) from Jamursba-Medi, Bird's Head Peninsula, Indonesia. Chelonian Conserv. Biol. 6(1):150–154.

Benson, S. R., K. M. Kisokau, L. Ambio, V. Rei, P. H. Dutton, and D. Parker.
2007b. Beach use, internesting movement, and migration of leatherback turtles, *Dermochelys coriacea*, nesting on the north coast of Papua New Guinea. Chelonian Conserv. Biol. 6(1):7–14.

Buckland, S. T., D. R. Anderson, K. P. Burnham, J. L. Laake, D. L. Borchers, and L. Thomas.
2001. Introduction to distance sampling: estimating abundance of biological populations, 432 p. Oxford Univ. Press, Inc., New York, NY.

Carretta, J. V., T. Price, D. Petersen, and R. Read.
2005. Estimates of marine mammal, sea turtle, and seabird mortality in the California drift gillnet fishery for swordfish and thresher shark, 1996–2002. Mar. Fish. Rev. 66(2):21–30.

Chan, E. H., and H. C. Liew.
1996. Decline of the leatherback population in Tereng-

ganu, Malaysia, 1956–1995. Chelonian Conserv. Biol. 2(2):196–203.

Chelton, D. B., P. A. Bernal, and J. A. McGowan.
1982. Large-scale interannual physical and biological interaction in the California Current. J. Mar. Res. 40:1095–1125.

Dutton, D. L., P. H. Dutton, M. Chaloupka, and R. H. Boulon.
2005. Increase of a Caribbean leatherback turtle *Dermochelys coriacea* nesting population linked to long-term nest protection. Biol. Conserv. 126(2):186–194.

Dutton, P. H., A. Frey, R. LeRoux, and G. Balazs.
2000. Molecular ecology of leatherbacks in the Pacific. *In* Sea turtles of the Indo-Pacific. Research, management and conservation (N. Pilcher, and G. Ismael, eds.), p. 248–253. Asean Academic Press Ltd, London, UK.

Dutton, P. H., C. Hitipeuw, M. Zein, S. R. Benson, G. Petro, J. Pita, V. Rei, L. Ambio, and J. Bakarbessy.
2007. Status and genetic structure of nesting populations of leatherback turtles (*Dermochelys coriacea*) in the western Pacific. Chelonian Conserv. Biol. 6(1):47–53.

Eisenberg, J. F., and J. Frazier.
1983. A leatherback turtle (*Dermochelys coriacea*) feeding in the wild. J. Herpetol. 17:81–82.

Forney, K. A., J. Barlow, and J. V. Carretta.
1995. The abundance of cetaceans in California coastal waters. Part II: Aerial surveys in winter and spring of 1991 and 1992. Fish. Bull. 93:15–26.

Forney, K. A., D. A. Hanan, and J. Barlow.
1991. Detecting trends in harbor porpoise abundance from aerial surveys using analysis of covariance. Fish. Bull. 89:367–377.

Graham, W. M.
1994. The physical oceanography and ecology of upwelling shadows. Ph.D. diss., 205 p. Univ. California, Santa Cruz, CA.

Graham, W. M., and J. L. Largier.
1997. Upwelling shadows as nearshore retention sites: the example of northern Monterey Bay. Cont. Shelf Res. 17(5):509–532.

Graham, W. M, F. Pagès, and W. M. Hamner.
2001. A physical context for gelatinous zooplankton aggregations: a review. Hydrobiologia 451:199–212.

Hitipeuw, C., P. H. Dutton, S. R. Benson, J. Thebu, and J. Bakarbessy.
2007. Population status and internesting movement of leatherback turtles (*Dermochelys coriacea*) nesting on the northwest coast of Papua, Indonesia. Chelonian Conserv. Biol. 6(1):28–36.

Julian, F., and M. Beeson.
1998. Estimates of marine mammal, turtle and bird mortality for two California gillnet fisheries: 1990–1995. Fish. Bull. 96:271–284.

Keinath, J. A, and J. A. Musick.
1993. Movements and diving behavior of a leatherback turtle, *Dermochelys coriacea*. Copeia 1993: 1010–1017.

Keinath, J. A, J. A. Musick, and D. E. Barnard.
1996. Abundance and distribution of sea turtles off North Carolina. OCS Study/MMS 95-0024, 156 p. U. S. Department of the Interior, Minerals Management Service, Gulf of Mexico OCS Region, 1201 Elmwood Park Boulevard, New Orleans, LA 70123-2394.

Limpus, C. J., and N. Nicholls.
1988. The Southern Oscillation regulates the annual numbers of green turtles (*Chelonia mydas*) breeding around northern Australia. Austral. J. Wildl. Res. 15(2):157–161.

Lynam, C. P., S. J. Hay, and A. S. Brierley.
2004. Interannual variability in abundance of North Sea jellyfish and links to the North Atlantic Oscillation. Limnol. Oceanogr. 49:637–643.

Marsh, H., and D. F. Sinclair.
1989. Correcting for visibility bias in strip transect aerial surveys of aquatic fauna. J. Wildl. Manage. 53:1017–1024.

McGowan, J. A., D. R. Cayan, and L. M. Dorman.
1998. Climate-ocean variability and ecosystem response in the Northeast Pacific. Science 281:210–217.

McMahon, C. R., and G. C. Hays.
2006. Thermal niche, large-scale movements and implications of climate change for a critically endangered marine vertebrate. Global Change Biol. 12:1–9.

Price, E. R., B. P. Wallace, R. D. Reina, J. R. Spotila, F. V. Paladino, R. Piedra, and E. Vélez.
2004. Size, growth, and reproductive output of adult female leatherback turtles *Dermochelys coriacea*. Endang. Species Res. 5:1–8.

Rivalan, P.
2004. Population dynamics of leatherback turtles in French Guiana: Research on relevant factors and application to the establishment of conservation strategies. [In French.] Ph.D. diss., 249 p. Univ. Paris XI Orsay, Paris.

Sarti, L., S. A. Eckert, N. García, and A. R. Barragan.
1996. Decline of the world's largest nesting assemblage of leatherback turtles. Mar. Turtle Newsl. 74:2–5.

Scheirer, C. J., W. S. Ray, and N. Hare.
1976. The analysis of ranked data derived from completely randomized factorial designs. Biometrics 32:429–434.

Schwing, F. B., T. Murphree, and P. M. Green.
2002. The Northern Oscillation Index (NOI): a new climate index for the northeast Pacific. Prog. Oceanogr. 53(2):115–139.

Shenker, J. M.
1984. Scyphomedusae in surface waters near the Oregon coast, May–August, 1981. Estuar. Coastal Shelf Sci. 19:619–632.

Shoop, C. R., and R. D. Kenney.
1992. Seasonal distributions and abundances of loggerhead and leatherback sea turtles in waters of the northeastern United States. Herpetol. Monogr. 6:43–67.

Spotila, J. R, A. E. Dunham, A. J. Leslie, A. C. Steyermark, P. T. Plotkin, and F. V. Paladino.
1996. Worldwide population decline of *Dermochelys coriacea*: Are leatherback turtles going extinct? Chelonian Conserv. Biol. 2(2):209–222.

Spotila, J. R., R. D. Reina, A. C. Steyermark, P. T. Plotkin, and F. V. Paladino.
2000. Pacific leatherback turtles face extinction. Nature 405:529–530.

Starbird, C. H., A. Baldridge, and J. T. Harvey.
1993. Seasonal occurrence of leatherback sea turtles (*Dermochelys coriacea*) in the Monterey Bay region, with notes on other sea turtles, 1986–1991. Calif. Fish Game 79(2):54–62.

Stinson, M. L.
1984. Biology of sea turtles in San Diego Bay, California, and the north eastern Pacific Ocean. M.S. thesis, 578 p. San Diego State Univ., San Diego, CA.

Wing, S. R., J. L. Largier, L. W. Botsford, and J. F. Quinn.
1995. Settlement and transport of benthic invertebrates in an intermittent upwelling system. Limnol. Oceanogr. 40:316–329.

Comparison of survey methods for estimating abundance of harbor seals (*Phoca vitulina*) in glacial fjords

John L. Bengtson (contact author)[1]
Alana V. Phillips[1]
Elizabeth A. Mathews[2]
Michael A. Simpkins[1,3]

E-mail: John.Bengtson@noaa.gov

[1] National Marine Mammal Laboratory
Alaska Fisheries Science Center
National Marine Fisheries Service, NOAA
7600 Sand Point Way NE
Seattle, Washington 98115

[2] University of Alaska Southeast
Department of Natural Sciences
11120 Glacier Highway
Juneau, Alaska 99801

[3] Marine Mammal Commission
4340 East-West Highway, Rm. 905
Bethesda, Maryland 20814

Abstract—The importance of glacial ice habitats to harbor seals (*Phoca vitulina*) in Alaska has become increasingly apparent. However, enumerating harbor seals hauled out on ice in glacial fjords has been difficult. At Johns Hopkins Inlet in Glacier Bay, Alaska, we compared a shore-based counting method to a large-format aerial photography method to estimate seal abundance. During each aerial survey, shore-based observers simultaneously counted seals from an observation post. Both survey methods incurred errors in double-counting and missing seals, especially when ice movements caused seals to drift between survey zones. Advantages of shore-based counts included the ability to obtain multiple counts for relatively little cost, distinguish pups from adults, and to distinguish mobile seals from shadows or glacial debris of similar size. Aerial photography provided a permanent record of each survey, allowing both a reconciliation of counts in overlapping zones and the documentation of the spatial distribution of seals and ice within the fjord.

Manuscript submitted 2 December 2005 to the Scientific Editor's Office.

Manuscript approved for publication 20 December 2006 by the Scientific Editor.

Fish. Bull. 105:348–355 (2007).

Harbor seals (*Phoca vitulina*) in Alaska occupy a geographically extensive range and topographically diverse haul-out habitats. They are present in U.S. waters from approximately 172°E to 130°W (over 3500 km east to west) and from 51°N to 61°N (over 1000 km north to south), hauling out on a variety of substrates including sand, rock, and, in Alaska, glacial ice. Alaska harbor seal populations have declined at several locations since the late 1970s. For example, counts of harbor seals at Tugidak Island (southwest of Kodiak Island, Alaska) declined 85% between 1976 and 1988 (Pitcher, 1990), and counts in Prince William Sound indicate population declines of approximately 63% between 1984 and 1997 (Frost et al., 1999). Additional evidence indicates that harbor seal numbers near Kodiak Island, including those at Tugidak Island, increased 6.6%/yr during 1993–2001 (Small et al., 2003), but that seals in Prince William Sound have continued to decline 3.3%/yr during 1988–99 (Ver Hoef and Frost, 2003). In Glacier Bay, Alaska, harbor seal numbers declined by 75% (−14.5%/yr) during 1992–2002 at terrestrial resting sites and by 64% (−9.6%/yr) from 1992 to 2001 in Johns Hopkins Inlet, the primary breeding site, which is a glacial fjord where seals haul out on floating ice (Mathews and Pendleton, 2006). Because it is estimated that 10% or more of harbor seals in Alaska use glacial ice habitats during the molting season (August–September) (J. L. Bengtson, unpubl. data), there is a pressing need to develop reliable survey methods to assess harbor seal abundance in such areas. Here we evaluate two such survey methods: counts from shore-based observations and counts from large-format aerial photography.

Shore-based surveys of harbor seals in two glacial fjords in Glacier Bay National Park, Alaska, have been made from elevated shore sites over the past three decades (Calambokidis et al., 1987; Mathews, 1995; Mathews and Pendleton, 2006) and in Aialik Bay, a glacial fjord in the Gulf of Alaska (Hoover, 1983). In 1997, Mathews et al.[1] conducted a pilot study in Johns Hopkins Inlet, Glacier Bay, and determined that it was feasible to count harbor seals on glacial ice from medium-format aerial photographs, and comparisons of these counts were made to simultaneous shore counts. In our study, we employed higher resolution (large-format) film, conducted three simultaneous aerial and shore surveys (vs. one in the pilot study), and used data from different altitudes to assess sources of counting error within aerial photographs.

---

[1] Mathews, E. A., W. L. Perryman, and L. B. Dzinich. 1997. Use of high-resolution, medium-format aerial photography for monitoring harbor seal abundance at glacial ice haulouts, 15 p. Unpubl. report to Glacier Bay National Park and Preserve, P. O. Box 140, Gustavus, AK 99826. Website: http://www.uas.alaska.edu/biology/faculty/mathews/publications.html (accessed 1 December 2006).

Aerial surveys of harbor seals are most often conducted when peak numbers are hauled out, which usually occurs during the annual molt in late summer. During such surveys, low altitude (100–300 m) photographs of harbor seal groups are obtained, from which seal counts are made (Olesiuk et al., 1990; Boveng et al., 2003). Surveying seals in glacial fjords is more difficult than on terrestrial sites because the moving, large expanses of scattered ice on which seals haul out offer little spatial reference to aid in counting seals. Furthermore, there is often insufficient maneuvering room for low-altitude aerial surveys in the fjords. The main objective of our study was to compare the relative effectiveness of shore-based and aerial survey methods to estimate harbor seal abundance.

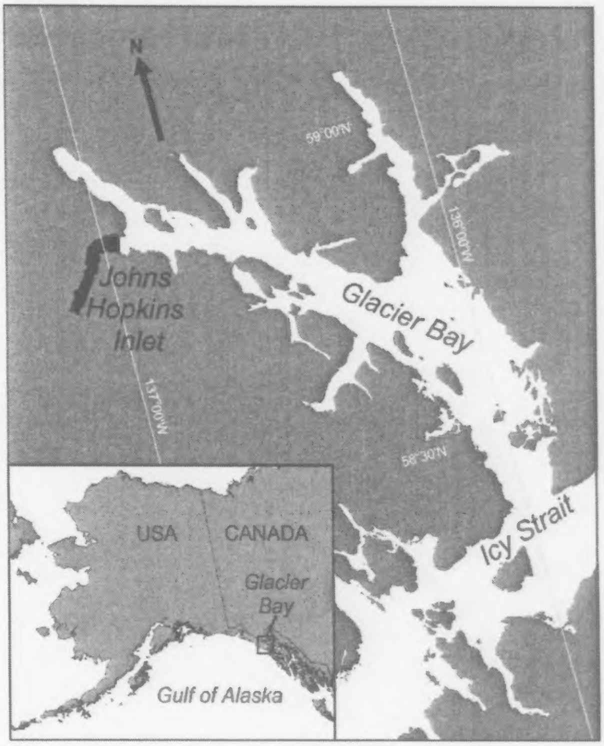

Figure 1

Map of Glacier Bay, Alaska, showing Johns Hopkins Inlet (shaded).

Materials and methods

Study area

Johns Hopkins Inlet is located in the northwest arm of Glacier Bay (58°N, 138°30′W) in southeastern Alaska (Fig. 1). At the head of the inlet is an active tidewater glacier that is currently advancing. The fjord walls are steep, rising to 640 m and 884 m within one km of the western and eastern shores, respectively. Harbor seals rest, nurse, and molt on ice calved from the glacier. Pieces of ice occupied by seals are typically around 8–24 m^2, although they vary widely in size and can be much larger (up to ~890 m^2, n=105) (E. A. Mathews, unpubl. data). Ice that has above-water features taller than about 2 m is rarely occupied. The percent of ice cover in the inlet was estimated by shore observers before seal counts during August for the years 1995–2001; for most surveys, 6–25% or 26–50% of the inlet was covered by ice (n=83 shore surveys). Approximately 60–70% of harbor seals in Glacier Bay use glacial ice in Johns Hopkins Inlet during the pupping, breeding, and molting periods from spring to early fall (Mathews, 1995).

Shore-based surveys

Observers counted seals from an elevated (~35 m) site located along the western shore of the inlet about 2.5 km from the terminus of Johns Hopkins Glacier (Fig. 2A). From this site, the observers' field of view comprised approximately 9 km (from the glacier to Jaw Point). The northwestern edge of the inlet and a small area near the northwest edge of the glacier face were not visible to the shore observers because of obstruction by headlands and other geographic features (i.e., "blind spots," Fig. 2A). Ice in the inlet more commonly drifted closer to the east than the west shore because of current and wind patterns; therefore, the location of the observation site along the western shore was selected as the observation site. Two of the four observers involved in this study simultaneously counted seals 2 or 3 times each day between 12 and 23 August 2001 and 9 and 26 August 2002. Seals on ice and in the water were tallied, but only seals on ice were included in this analysis. Observers conducted shore-based counts of harbor seals in Johns Hopkins Inlet during, or within an hour of, the aerial surveys conducted on 15 and 16 August 2001, and 15 August 2002. Surveys targeted the period around solar noon when the largest number of seals hauls out on glacial ice (Hoover, 1983; Calambokidis et al., 1987).

Observers counted seals using 20×60 binoculars mounted on tripods. After each tripod was leveled, observers locked the vertical orientation of the tripod head and counted all seals in the field of view as the binoculars were pivoted horizontally in one direction. To facilitate systematic counting in the study area, observers visually divided the field of view into three or four subareas using markers such as landmarks or natural breaks in the ice as viewed from the observation site. When a marker came into the field of view, the binoculars were lowered exactly one field of view, locked again, and a pass in the opposite direction was made (Mathews, 1995). Each of the subareas typically required only two nonoverlapping, parallel passes across ice habitat to completely cover the width of a subarea. Counts from all subareas were summed for each observer to estimate total counts, and the two observers' total counts were then averaged to estimate the total count for each survey. The variance for each survey's total count was estimated as the variance among the two observers' total counts.

Aerial surveys

Aerial surveys were conducted from a twin engine aircraft on 15 and 16 August 2001 and 15 August 2002 by a commercial photographic surveying company (Aeromap U.S., Anchorage, AK). In 2001, each aerial survey over Johns Hopkins Inlet was completed in three transects: two transects at 1465 m altitude covering the entire inlet, and an additional transect at 915 m covering the central portion of the inlet a second time from Johns Hopkins Glacier to the point north of Jaw Point (Fig. 2B). In 2002, the survey aircraft flew two transects at 1465 m covering Johns Hopkins Inlet from the glacier to Jaw Point; a lower-altitude, central transect was not flown (Fig. 2C). Shore observers observed no reaction by the seals (e.g., entering the water) to the aerial surveys.

During each survey, large-format (23 × 23 cm) photographic images were taken automatically at a predetermined rate on Agfa Aviphot Color X100 PE1 negative film (Agfa Corp., Ridgefield Park, NJ), with a belly-mounted Zeiss RMK TOP 15 camera (Carl Zeiss, Inc., Thornwood, NY) with forward-motion compensation (15 August 2001) or with a Zeiss RMK A 15/23 camera (Carl Zeiss, Inc., Thornwood, NY) (16 August 2001 and 15 August 2002). We did not notice any substantial improvement with the use of forward-motion compensation. The resulting photographic frame widths (i.e., the on-the-ground width of the area photographed in each photo frame) were 2200 m for high-altitude (1465 m) images and 1400 m for low-altitude (915 m) images. The images had approximately 10% endlap (i.e., overlapping duplication of the same area in separate, successive images) within transects, 20% sidelap between high-altitude transects, and 75% sidelap between the central transect and the neighboring high-altitude transects in 2001. Large-format negatives were scanned at 1600 dpi (the maximum resolution available to us) with a digital scanner and converted to positive-color digital images. The pixel resolutions of the resulting digital images were 0.10 m and 0.15 m for low- and high-altitude transects, respectively. At that resolution, we found that seals could be identified from the scanned imagery, and we were satisfied with this resolution for the purposes of counting seals.

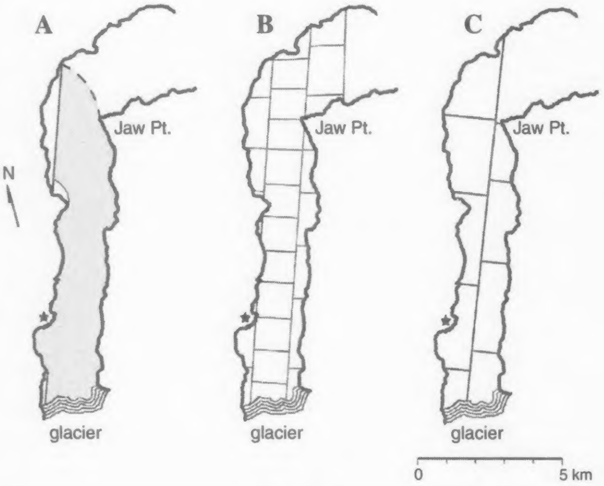

Figure 2

Survey coverage of Johns Hopkins Inlet, Glacier Bay, achieved by each survey type in this study. (**A**) Field of view (shaded area) observed from shore-based observation site (indicated with a star). Note that the northwestern edge of the inlet and a small area near the glacier are obscured from view ("blind spots") by geographical features. The outer range of visibility varied with conditions and is denoted by a dashed, curved line. (**B**) Photographic coverage of aerial transects flown on 15 and 16 August 2001. The straight lines in the inlet reflect the approximate boundaries between photographs. For simplicity, only the nonoverlapping areas (i.e., no endlap or sidelap) of each image are shown. The central transect was flown at a lower altitude (915 m) than the two adjacent transects (1465 m). (**C**) Photographic coverage of aerial transects (1465 m altitude) flown on 15 August 2002; the overlap between neighboring photographs was ignored.

Seals were counted from the digital images by using the "geospatial light table" feature of ERDAS Imagine 8.6 software (Leica GeoSystems Inc., Atlanta, GA). No distinction was made between adults, pups, or juvenile seals. A virtual mosaic was created by delineating overlapping zones on adjacent images based on the relative positions of identifiable pieces of ice. This mosaic allowed the analyst to account for ice movement when counting seals. In some cases, delineation of overlapping zones was difficult, particularly

Table 1

Shore-based and aerial photographic counts of harbor seals (*Phoca vitulina*) at Johns Hopkins Inlet, Glacier Bay, Alaska, in 2001 and 2002. Means, standard errors (SE), and coefficients of variation (CV) are derived from two simultaneous counts during each shore-based census and from three independent counts of aerial survey imagery (times are given in local solar time).

Date	Survey type	Survey time (h)	Mean count	SE	CV
15 Aug 2001	Shore-based	1406–1449	1970	57.0	0.029
	Aerial	1457–1512	1581	20.0	0.013
16 Aug 2001	Shore-based	1401–1439	1906	192.5	0.101
	Aerial	1421–1442	1294	25.6	0.020
15 Aug 2002	Shore-based	1249–1349	1562	4.0	0.003
	Aerial	1231–1245	1511	46.6	0.031

when ice moved substantially during the time that elapsed between neighboring photographs. Seals in overlapping zones were counted only once (i.e., only counted in one of the overlapping images). In 2001, the resolution in the low-altitude transects was superior to that in the high-altitude transects; therefore we counted all seals within the low-altitude imagery first and then added counts of seals in the nonoverlapping portions of the high-altitude imagery. Three replicate total counts were calculated for each survey by counting the seals in each image three separate times and tallying the resulting counts for each replicate. All replicates were counted by a primary analyst, and at least one week elapsed between each replicate count to minimize bias caused by the analyst remembering the location of seals from previous replicate counts. The number of images analyzed varied between surveys, depending on the survey tracks flown and the distribution of ice. Sixty-two total images were analyzed: 15 August 2001=21 images, 16 August 2001=30 images, and 15 August 2002=11 images. A subsample of five images from Johns Hopkins Inlet was also counted by a secondary analyst to provide independent verification of counts. The mean count (of the three counts by the primary analyst) for each image was calculated, and the mean counts for all images from each survey were summed to estimate the total survey count. The variance of the total count estimate was estimated as the sum of the variances for each mean count included in the total estimate.

Comparison of detection rates at different altitudes

To compare the detection rates in low- and high-altitude imagery from 2001, we counted all seals in the overlapping zones of low- and high-altitude images. Next, we visually compared the location of each seal in the overlapping portions of low- and high-altitude images and classified seals as either 1) counted in both images or 2) counted in only one of the images. Seals counted in only one of the images were further categorized as follows: 1) light-colored seal not detected in the other image, 2) seal in a group not resolved as an individual in the other image, 3) seal definitely not present in the other image (e.g., seal went into the water or hauled out between transects), or 4) shadow or dirty ice classified as a seal in other image. These comparisons were conducted to help us understand the relative accuracy of counting seals from images taken at different altitudes. The less accurate high-altitude counts were not used when estimating mean counts for each survey; mean counts were estimated by triplicate counts with priority given to low-altitude counts as described above.

Results

Comparison of total counts

In 2001, counts made from shore were consistently higher than counts made with the use of aerial photography (Table 1). In contrast, both counting methods produced similar results in 2002. The standard errors and coefficients of variation (CV) presented in Table 1 reflect variance between counts by shore-based observers or between independent counts of aerial photographs. Although the CVs for counts of individual images were generally larger than the CVs for total estimates, 91% of the CVs for individual images were less than 0.1. Of the five images counted by a secondary analyst, all counts were within 8% of the mean of the three replicate counts conducted by the primary analyst. Imprecision or inaccuracies in counts caused by the distance of seals from the observation site or the altitude of the aerial survey were not easily quantified, although altitude-related errors were evaluated separately by comparing counts of seals in overlapping low- and high-altitude images.

Spatial distribution of seals in Johns Hopkins Inlet

The distribution of seals in Johns Hopkins Inlet was different during each of the surveys and appeared to be associated with the pattern of ice in the inlet. Generally, seals were found in aggregations, although solitary seals were frequently observed outside of the main seal concentrations (Fig. 3). On 15 August 2001, seals were distributed in groups of 200–500 animals, ranging from 1 to 6 km from the glacier terminus (Fig. 3A). On 16 August 2001, a large group of 800–900 seals was aggregated in a band stretching from 0.5 km from the glacier terminus to the shore-based observation site, and another group of 300–400 seals was found 3–5 km from the glacier (Fig. 3B). On 15 August 2002, all of the seals were within 3 km of the glacier face between the glacier and the shore-based observation site (Fig. 3C). Of these, a group of 350–450 seals was observed on the southwest side of the inlet, and the remaining 1100–1200 seals formed a dense concentration on the east side of the inlet. No seals were located in the blind areas (from the view point of the shore-based observers) on any of the three survey days (Figs. 2A and 3).

Comparison of detection rates at different altitudes

An examination of seals in overlapping zones of low- and high-altitude images revealed a difference in the rates of seal detection between the two altitudes. Seals were more easily detected and confirmed to be seals in the low-altitude imagery; therefore, seals identified in low-altitude imagery were considered to be "true" observations for comparison to seals counted in high-altitude imagery. For the 15 August 2001 survey, 32.7% of the seals counted in the low-altitude images (i.e., "true" seals) were misclassified in high-altitude images: 8.6% were counted as seals when no seals were present (i.e., shadows or dirty ice misidentified as seals) and 24.1% were not counted as seals when seals were present (i.e., 23.3% were dark seals dismissed as shadows or dirty ice, 0.5% were light-colored seals that were not detected, and 0.3% were so close to other seals that they could not be identified from their neighbors). In the 16 August 2001 survey, 34.3% of the seals counted in the low-altitude images were misclassified in the high-altitude images, including 12.5% that were shadows or dirty ice misidentified as seals and 21.8% that were not detected in the high-altitude imagery (21.5% dark seals and 0.3% light-colored seals). The net effect of the misclassifications was that counts from higher-altitude images were underestimates of the number of seals compared to counts from lower altitudes (i.e., the proportion of seals missed exceeded the proportion of false identifications).

Discussion

Comparison of total counts

Both shore-based and aerial counts indicated that more than 1500 seals haul out on glacial ice in Johns Hopkins Inlet in mid-August, making the inlet one of the most important haul-out sites in Glacier Bay (as suggested by Mathews [1995]). The total number of seals that use the inlet might be substantially larger because some unknown proportion of seals was in the water (i.e., not hauled out on ice) during the surveys. In 2001, counts made from shore were consistently higher than counts made with aerial photography (Table 1). In contrast, both counting methods produced similar results in 2002. Several sources of error for each method likely contributed to these inconsistencies in results between the two methods.

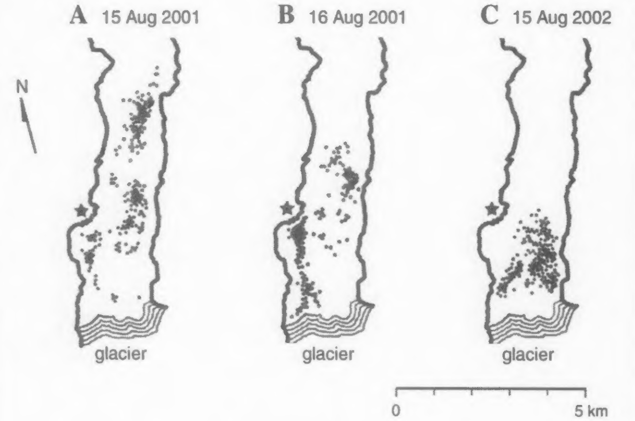

Figure 3

Relative distribution of patches of harbor seals (*Phoca vitulina*) in Johns Hopkins Inlet, Glacier Bay, determined by aerial photography, on (**A**) 15 August 2001, (**B**) 16 August 2001, and (**C**) 15 August 2002. Dots indicate groups of seals and are meant to illustrate generalized locations of seals, rather than a precise indication of seal abundance. The shore-based observation site is indicated with a star.

Sources of error for each survey method

Both counting methods were susceptible to common errors of either double-counting or missing seals. These errors were most likely to occur within overlapping zones between neighboring photographic images, between parallel passes with binoculars, or between shore-based counts of subareas. If overlapping zones were not accurately delineated, individual seals within the overlapping zone could be counted twice, or missed entirely. The permanent record provided by photography provided the best opportunity to minimize such errors by allowing for careful delineation of overlapping zones based on the relative positions of identifiable pieces of ice on adjacent images. The shore-based method did not allow re-identification of individual pieces of ice; therefore shore-based observers attempted to eliminate overlapping by adjusting binoculars carefully. Seals could be missed, however, if the binoculars were

Table 2

Comparison of the percent difference ([shore-based count - aerial photography count]/shore-based count) in the number of harbor seals (*Phoca vitulina*) counted by two survey methods. Potential sources of error for harbor seal counts in Johns Hopkins Inlet included maximum distance between harbor seals and shore observers, degree of clumping of harbor seals on ice, and the degree of movement of ice.

Date	Percent difference in counting method	Maximum distance between seals and shore site (km)	Degree of seal clumping	Degree of ice movement
15 Aug 2001	25%	4.25	moderate	high
16 Aug 2001	47%	2.40	high	high
15 Aug 2002	3%	2.75	low	high

lowered more than one field of view. Similarly, seals could be counted twice, if the binoculars were lowered less than one field of view before the second survey pass.

Counting errors could be caused by movement of ice on which seals were hauled out. Shore-based observers could not track the movement of ice between parallel passes; therefore some counting errors caused by ice movements were unavoidable. Depending on ice drift patterns, seals that were already counted could drift into an uncounted zone and be double counted, or uncounted seals could drift into a counted zone and be missed. On both days surveyed in 2001, we observed considerable movement of ice between aerial transects, particularly along the eastern side of the inlet, farthest away from the shore-based observation site. Thus, it is likely that seals would have drifted between the shore-based observers' counting areas, resulting in either missed or double counts. In contrast, the ice was less mobile during the 2002 survey day. Ice did not drift much between adjacent photographic images along a transect because only 5–10 seconds elapsed between each image. However, ice sometimes drifted substantially between images along neighboring transects, which were typically separated by 10–15 minutes. Although such ice movements sometimes made identification of individual seals between neighboring images more difficult, spatial clues from recognizable pieces of ice aided identification and made us confident that seals on moving ice were properly counted.

The distribution of seals could also influence counting errors for both survey methods. In 2001, ice was distributed up to 4.5–6 km from the glacier terminus and seal distribution was clumped (Fig. 3, A and B). In contrast, during the 2002 survey day the ice was more densely packed near the glacier terminus and seals were more evenly distributed (Fig. 3C). The distance between the shore observers and seals was also expected to affect shore counts, and to produce greater error as distance increased. Our results, however, did not exhibit a clear pattern in the percent difference between counting methods and distance between shore observers and seals. In 2001, seals were within 4.25 km of observers on 15 August and within 2.4 km on 16 August; during the 2002 survey seals were located within 2.75 km (Table 2). Overall, the counts recorded by both methods were most similar when ice movement and seal clumping were minimal (Table 2).

Counting errors could also be caused by misidentifying seals as shadows or dirty ice. Occasionally, ice ridges cast shadows that looked remarkably like seals. Some glacial ice contained veins of dirt that also had the similar shape and color of seals. When comparing seals identified in overlapping imagery from the two aerial survey altitudes, we found that 22–24% of seals counted in the low-altitude (high-resolution) imagery either were not detected or were dismissed as shadows or dirty ice in counts of the high-altitude imagery. However, 9–13% of seals counted in the high-altitude imagery were actually shadows or dirty ice, according to the low-altitude imagery. These two types of errors tended to offset each other, although high-altitude counts still exhibited a general bias toward 10–15% lower seal counts. As a result, the aerial counts (especially from high-altitude imagery) likely produce underestimates of the actual number of seals hauled out on ice. The aerial counts from 2001 were based primarily on low-altitude counts, and, thus probably represent less biased estimates than the counts for the 2002 survey, which was based solely on high-altitude imagery. No correction was applied to the high-altitude counts because the likelihood of misidentifying or missing seals varied according to conditions specific to each image (e.g., dirty ice and shadows); therefore applying a correction based on images from one part of the fjord probably was not applicable to images from other parts of the fjord, let alone images from an entirely different day. Further, no correction was available for the proportion of seals misidentified or missed in the low-altitude imagery and for an unknown number of seals that were in the water during the surveys.

Shore-based observers had the advantage of a three-dimensional "live" view of seals and were able to distinguish between actively moving seals and shadows or dirty ice, although this advantage probably diminished with distance. Stationary seals could still be difficult to distinguish at any distance, although their characteristic profiles and the reflectivity of their fur helped to distinguish seals from rocks or dirt of similar size. As was the case for the aerial estimates, no correction was available for seals missed or misidentified by shore-based observers, and some unknown number of seals were in the water during the observation periods.

Advantages of each method

Shore-based counts The main benefit associated with counting harbor seals from land is the ability to obtain multiple counts throughout the day, and on successive days, relatively inexpensively.[1] Counts can also be made from land under suboptimal weather conditions, when aerial surveys are impossible or when the resulting photographs would be of poor quality. Repeated surveys allow an assessment of changes in seal counts related to covariates such as time of day, ice conditions, and weather (Mathews and Pendleton, 2006). The number of harbor seals counted on ice in Johns Hopkins Inlet varies from day to day and thus increases the probability that a small number of aerial surveys could yield misleading results. For example, on 10 consecutive days in August 1999 the number of seals counted from shore near midday ranged from 1465 to 2534. If surveys are conducted when pups are nursing (generally during June in Alaskan waters), shore observers can identify seal pups based on size, shape, and relative position of seals within a group hauled out on ice. By August, however, almost all pups are weaned and the number of seals in groups on ice is much larger than in June, making it much more difficult to distinguish weaned pups or juveniles from adults except at very close range. With the aerial surveys there were also difficulties in distinguishing pups and juveniles (i.e., the resolution of the aerial photographs in the August study was not high enough to distinguish weaned pups, and no large-format aerial surveys were conducted during June when dependent pups are more likely to be distinguishable from adults).

Aerial photography Large-format aerial photography allows investigators to count seals from a set of images taken at a consistent distance (altitude) from the seals without potential "blind spots" caused by land or ice features. Photographs can be taken with overlapping images so that a mosaic of the complete study area can be obtained for each sampling event, and so that ice movement can be taken into account. The ability to view seals from a vertical perspective, rather than obliquely from a shore-based observation site, removes many of the potential biases associated with sighting seals at variable distances from the shoreline. The photographs also represent a permanent record of the distribution of the seals within a fjord—a record that allows recounts or re-analyses of images. For example, the primary analyst was able to count seals in each image independently three times to estimate variance in the number of seals recorded; a secondary analyst was also able to count seals in a subsample of the same images to provide an independent verification of the final estimates. Aerial photography also offers one the ability to evaluate the spatial distribution of seals within a study area in relation to other seals (e.g., social interactions) and to environmental features (e.g., ice types or shifting ice patterns). A final advantage of using aerial photography is that researchers are not required to establish and maintain a remote field camp throughout the study period.

Future surveys of harbor seals in glacial fjords

The development of reliable methods for surveying harbor seal abundance in glacial ice habitats is a fundamental requirement for estimating the population size of these seals in Alaska. Conventional aerial surveys of harbor seals at terrestrial haul-out sites indicate that approximately 180,000 seals may be found at terrestrial sites. Preliminary counts of harbor seals from large-format photographs taken in glacial ice habitats throughout Alaska indicate that as many as 20,000 to 25,000 additional harbor seals may be using glacial ice habitats (J. L. Bengtson, unpubl. data). If 10% or more of Alaska's harbor seal population are using glacial ice habitats at various times of the year, monitoring trends in seal abundance in these areas will be very important to resource managers and to subsistence hunters in the Alaska Native community. In some regions, a much larger proportion of harbor seals may use glacial ice habitats. Within Glacier Bay, an average of 72% of harbor seals surveyed between 1992 and 2001 (2400–4700 seals per year) were found within glacial fjords during the breeding season (Mathews and Pendleton, 2006). At present, there are about 20 sites in Alaska where harbor seals are known to haul out in glacial ice habitats. Several of these fjords are of special interest to resource managers because 1) some local seal populations may be declining, 2) the fjords are important hunting areas to Alaska Natives, and 3) logistical difficulties have hampered past efforts to monitor changes in seal abundance with standard survey methods.

In the future, which survey methods seem most appropriate for monitoring the abundance of harbor seals in glacial ice habitats? Both shore-based counts and aerial photography are valuable methods for monitoring seals in glacial fjords, and each method has different limitations and potential applications. Unlike Johns Hopkins Inlet, many glacial fjords in Alaska do not have an overlook with such a full view of seal habitat, and thus large-format aerial photography may be the only option for surveying seals in these important breeding areas. The present study demonstrates that large-format aerial photography is a promising method for surveying the abundance of harbor seals using glacial ice habitats in Alaska.

Acknowledgments

L. Dzinich, O. Harding, K. Blejwas, and N. Tex provided field assistance with shore-based counts at Johns Hopkins Inlet. Funding for this project was provided by the National Park Service to E. A. Mathews and J. L. Bengtson and by the National Oceanic and Atmospheric Administration and the National Park Service to J. L. Bengtson. We thank M. Kralovec and M. B. Moss at the Glacier Bay National Park for their support in helping to secure funding. S. Slade at Leica GeoSystems provided technical assistance for Erdas Imagine for the aerial photography counts. S. Tackley produced Figures 2 and 3. This manuscript was improved by comments from J. K. Jansen, J. M. Waite, and three anonymous reviewers. This research was conducted under Marine Mammal Protection Act permits 527-1461, 782-1355, and 782-1676.

Literature cited

Boveng, P. L., J. L. Bengtson, D. E. Withrow, J. C. Cesarone, M. A. Simpkins, K. J. Frost, and J. J. Burns.
2003. The abundance of harbor seals in the Gulf of Alaska. Mar. Mamm. Sci. 19(1):111–127.

Calambokidis, J., B. L. Taylor, S. D. Carter, G. H. Steiger, P. K. Dawson, and L. D. Antrim.
1987. Distribution and haul-out behavior of harbor seals in Glacier Bay, Alaska. Can. J. Zool. 65:1391–1396.

Frost, K. J., L. F. Lowry, and J. M. Ver Hoef.
1999. Monitoring the trend of harbor seals in Prince William Sound, Alaska, after the *Exxon Valdez* oil spill. Mar. Mamm. Sci. 15(2):494–506.

Hoover, A. A.
1983. Behavior and ecology of harbor seals *(Phoca vitulina richardsi)* inhabiting glacial ice in Aialik Bay, Alaska. M.S. thesis, 132 p. Univ. Alaska, Fairbanks, AK.

Mathews, E. A.
1995. Longterm trends in abundance of harbor seals (*Phoca vitulina richardsi*) and development of monitoring methods in Glacier Bay National Park, Southeast Alaska. *In* Proceedings of the third Glacier Bay science symposium, Glacier Bay National Park & Preserve, P.O. Box 140, Gustavus, Alaska, U.S.A., Sept. 15–18, 1993 (D. R. Engstrom, ed.) p. 254–263. U.S. National Park Service, Anchorage, AK.

Mathews, E. A., and G. W. Pendleton.
2006. Declining trends in harbor seal *(Phoca vitulina)* numbers at glacial ice and terrestrial haulouts in Glacier Bay National Park, 1992–2002. Mar. Mamm. Sci. 22(1):167–189.

Olesiuk, P. F., M. A. Bigg, and G. M. Ellis.
1990. Recent trends in the abundance of harbor seals, *Phoca vitulina*, in British Columbia. Can. J. Fish. Aquat. Sci. 47:992–1003.

Pitcher, K. W.
1990. Major decline in the number of harbor seals *(Phoca vitulina)* on Tugidak Island, Gulf of Alaska. Mar. Mamm. Sci. 6(2):121–134.

Small, R. J., G. W. Pendleton, and K. W. Pitcher.
2003. Trends in abundance of Alaska harbor seals, 1983–2002. Mar. Mamm. Sci. 19(2):344–362.

Ver Hoef, J., and K. J. Frost.
2003. A Bayesian hierarchical model for monitoring harbor seal changes in Prince William Sound, Alaska. Environ. Ecol. Sta. 10:210–219.

Age and growth of swordfish (*Xiphias gladius*) caught by the Hawaii-based pelagic longline fishery

Edward E. DeMartini (contact author)
James H. Uchiyama
Robert L. Humphreys Jr.
Jeffrey D. Sampaga
Happy A. Williams
Email address for E. E. DeMartini: Edward.Demartini@noaa.gov
Pacific Islands Fisheries Science Center
National Marine Fisheries Service, NOAA
2570 Dole Street
Honolulu, Hawaii 96822-2396

Abstract—We verified the age and growth of swordfish (*Xiphias gladius*) by comparing ages determined from annuli in fin ray sections with daily growth increments in otoliths. Growth of swordfish of exploitable sizes is described on the basis of annuli present in cross sections of the second ray of the first anal fins of 1292 specimens (60–260 cm eye-to-fork length, EFL) caught in the region of the Hawaii-based pelagic longline fishery. The position of the initial fin ray annulus of swordfish was verified for the first time with the use of scanning electron micrographs of presumed daily growth increments present in the otoliths of juveniles. Fish growth through age 7 was validated by marginal increment analysis. Faster growth of females was confirmed, and the standard von Bertalanffy growth model was identified as the most parsimonious for describing growth in length for fish greater than 60 cm EFL. The observed growth of three fish, a year-old in size when first caught and then recaptured from 364 to1490 days later, is consistent with modeled growth for fish of this size range. Our novel approach to verifying age and growth should increase confidence in conducting an age-structured stock assessment for swordfish in the North Pacific Ocean.

Manuscript submitted 21 September 2006 to the Scientific Editor's Office.

Manuscript approved for publication 20 December 2006 by the Scientific Editor.

Fish. Bull. 105:356–367 (2007).

Swordfish (*Xiphias gladius*) constitute an economically important fishery resource and have historically supported many large-scale commercial fisheries throughout the world's oceans. During the 1990s, however, declining catches and average sizes of swordfish in Atlantic and Mediterranean fisheries indicated possible or likely overexploitation of these populations, and the status and management of these stocks became a highly publicized issue.

Swordfish began to be a major species targeted by the Hawaii-based pelagic longline fishery in 1990 and continued as such through the late 1990s, with landings peaking at 4000–6000 t in 1991–93 (Ito et al., 1998). This longline fishery targeted swordfish within, and adjacent to, fronts of the Subtropical Convergence Zone north of Hawaii during winter and late spring (Bigelow et al., 1999). Beginning in 1999, gear restrictions were imposed and in mid-2001 a moratorium on shallow-set (swordfish style) longlining within the swordfish fishery grounds north of the equator was instated to reduce interactions of fishing gear with, and incidental take of, protected species—primarily loggerhead turtles (*Caretta caretta*). The moratorium was lifted in March 2004 and a regulated (by annual effort cap, gear restrictions, take limit) longline fishery was reinstated.

A preliminary stock assessment for swordfish caught in the North Pacific Ocean, based on surplus production models, was conducted in early 1999 and was updated in early 2002 to include body length composition. No age-structured assessment as yet exists for swordfish in the central North Pacific. With the subsequent re-opening of the Hawaii-based fishery, there has been renewed interest in swordfish management in the North Pacific and a recognized need for a more robust, age-structured basis for stock assessment and documentation of age distributions and growth rates. For example, Sun et al. (2005) recently assessed the population status of swordfish taken by the tuna longline fishery in the waters around Taiwan in the western North Pacific.

Our objectives in this study were the following: 1) to evaluate the accuracy and precision of our age estimates; 2) to provide several complementary data supporting a predictable periodicity (on a yearly basis) of annulus formation in cross sections of anal-fin rays of swordfish caught in the region of the Hawaii-based longline fishery and examine evidence verifying our age estimates for these specimens; and 3) to estimate sex-specific patterns of size-at-age and growth to provide input for pending age-structured assessments of swordfish stock(s) in the central North Pacific.

Materials and methods

Collections and measurements of fish

All swordfish used for age determination in this study were collected from within the general region of the Hawaii-based pelagic longline fishery (Ito et al., 1998; DeMartini et al., 2000, Fig. 2 therein). About 95% of the specimens used were caught by commercial longlines during March 1994–June 1997; specimen collections were conducted and fish measurements were recorded by National Oceanic and Atmospheric Administration (NOAA) Fisheries, Southwest Region observers. The remaining 5% of the fish were caught on research cruises conducted during April–May 1992 and 1993, September 1996, and March–April 1997. Fish were measured (eye-to-fork length, EFL, in cm) before dressing (removal of head, entrails, tail, and fins) at sea. As they were dressed, sex was scored according to macroscopic criteria and later validated by microscopic evaluation of histological preparations of gonads for subsamples of the fish (DeMartini et al., 2000). When the fins of swordfish were removed at sea, either a portion or the entire first anal fin was collected and frozen. The braincase section, including the region of the semicircular canals was collected from juvenile and young adult swordfish, either when fish were beheaded at sea or when whole frozen bycatch specimens were thawed and dissected ashore. Additional larval and early young-of-year specimens (4 mm to 20 cm EFL) were collected by a neuston trawl (5-mm and 0.505-mm mesh in wings and codend, respectively) leeward of Hawaii Island during 1995–97; intact specimens were stored frozen before otolith extraction.

Laboratory processing and specimen examination

Frozen first anal fins were thawed, and the second spiny ray was selected (Berkeley and Houde, 1983), removed, and cleaned of all tissue. It was then dried in a dehydrator for 24–48 h at about 60°C, and three adjacent, transverse sections were cut with a low-speed saw. The first cut was made according to standard protocol (Ehrhardt et al., 1996) but at a newly defined position (distal end of the medial suture, hereafter "suture terminus") located about 15% of the distance beyond the basal condyle. Subsequent cuts were made distal to the first, spaced to provide wafers ~1 mm thick (Uchiyama et al., 1998). The location chosen for the cuts was different from the conventional standard (i.e., at a distance above the basal condyle equal to one-half the condyle width=$d/2$) currently used in swordfish aging studies (Sun et al., 2002). The unconventional cut was necessary because the condyle of the second ray is often severed or lost during the removal of fins by fishermen at sea. A small series of matched (same fish) fin ray samples were cut at the suture terminus and at the $d/2$ positions; some of these were also cut immediately distal to the condyle (basal cut) and the numbers of annuli were counted and compared. Cross sections of rays were preserved in mounting media on glass microscope slides and stored (without cover slips) in sealed boxes. Otoliths (sagittae) were dissected from frozen larvae and young adults at the NOAA Fisheries, Pacific Islands Fisheries Science Center (Honolulu Laboratory), and stored dry after having been cleaned, rinsed with water, and dried with 95% ethanol (EtOH).

Fin ray annuli, each defined as a single pair of opaque and translucent bands completely encircling the cross-section hemisphere without partial and split checks (Ehrhardt et al., 1996; Sun et al., 2002), were enumerated. At first examination, about 1% of all cross sections were deemed unreadable and discarded. The distances separating the distal edges of the translucent band of each annulus were measured, the opaque versus translucent nature of cross-section edges was noted, and marginal increment ratios (MIRs) were measured in marginal increment analysis (Campana, 2001). A series of MIRs was calculated for each specimen of age 1 or older by using the formula (Prince et al., 1988; Sun et al., 2002):

$$MIR = (R_{\mathrm{tot}} - R_n) / (R_n - R_{n-1}),$$

where R_{tot} = total radius of fin ray specimen; and
R_n and R_{n-1} = the distance from ray focus to the nth and $(n-1)$th annuli, respectively.

The focus was identified at the proximal confluence of growth striations (Ehrhardt et al., 1996). Because only one image analyzer was available and multiple readers had to work concurrently, several methods were used to examine specimens: 1) slide-mounted ray cross sections were viewed with a dissecting microscope (10–60×) by reflected light against a black background; 2) grey-scale TIFF file images of slide-mounted cross sections were prepared by using a digital camera system (Sony DKC-5000 and VCL-713BXS macro-zoom lens; Sony USA, New York, NY), processed to enhance contrast and sharpness using Adobe PhotoShop vers. 3, and viewed by means of two shareware available in the public domain (NIH Image vers. 1.58; National Institutes of Health, Bethesda, MD; and Scion Image vers. Beta 4.0.2; Scion Corporation, Frederick, MD), for MAC and PC, respectively. Annuli were counted independently by two primary readers (1 and 2) without reference to length, sex, or month of capture. Each reader made two or more readings, spaced by at least several months to cloak the identity of individual specimens. Presumed daily growth increments (DGIs) were enumerated by using digitized composite images (scanning electron micrographs of sagittae) (Humphreys, 2000).

If known-age specimens are unavailable for use in calibrating age assignments, a reference collection should be evaluated and a consensus or majority agreement used to provide a reference standard (Campana, 2001). We therefore enlisted the services of four other North and South Pacific laboratories that either recently had or were presently conducting aging studies of swordfish (Institute of Oceanography, National Taiwan University [NTU]; the National Research Institute of Far Seas

Fisheries [NRIFSF], Japan; the Centro de Investigacion Cientifica y de Educacion Superior de Ensenada [CICESE], Mexico; and the Instituto de Fomento Pesquero [IFOP], Chile). They provided 20 representative and usable fin ray specimens for swordfish caught by their respective regional fisheries. Specimens spanned all available months of capture and body sizes of both sexes.

Specimens were processed in identical fashion within each laboratory (e.g., the $d/2$ cut was used by the Honolulu Laboratory for select Hawaii-based fishery specimens). Digitized images of all 100 specimens were prepared at the Honolulu Laboratory and file images were distributed among laboratories. Most laboratories conducted multiple readings by two or more readers, thus enabling evaluation of precision and bias within and among laboratories.

Statistical analyses

Conventional descriptive statistics (Zar, 1984) were used to evaluate several interrelated data necessary for verification or corroboration of annular periodicity and size-at-age. We evaluated interrelations among fin ray radius (in mm) and estimated age (in days) based on enumeration of DGIs and EFL (in cm). Regression models were fitted by using nonlinear least squares (Marquardt algorithm) and the best model was chosen on the basis of relative r^2 values (proc nlin, SAS, vers. 8, SAS Inst., Inc., Cary, NC). Likely sexual dimorphisms in relationships (Sun et al., 2002) were evaluated with ANCOVA (proc glm; SAS, vers. 8, SAS Inst., Inc., Cary, NC).

Standard graphical methods and statistics (Campana, 2001) were used to evaluate between- and within-reader bias (age-bias plots) and precision gauged by the coefficient of variation (CV: deviation [=SD] (100/mean) (Campana et al., 1995; Campana, 2001). Observer bias (accuracy) also was evaluated partly in terms of the majority agreement standard generated by the aforementioned inter-laboratory calibration exercise. Precision was evaluated by comparing the repeatability of estimates made by readers 1 and 2 for both the specimen series provided by the inter-laboratory exercise and the much larger group of specimens that were used for the main study described in this article. CVs were compared both within- and between-readers.

Growth was described by fitting fin ray-based age estimates to back-calculated body length-at-age by using von Bertalanffy growth formulas (VBGFs). Both standard and generalized VBGFs (Richards, 1959) were evaluated:

Standard VBGF: $L_t = L_\infty (1 - \mathrm{e}^{-k\,(t - t_0)});$
Generalized VBGF: $L_t = L_\infty (1 - e^{-K\,(1-m)(t - t_0)})^{(1/(1-m))};$

where L_t = mean eye-to-fork length (EFL, in cm) at age t;
L_∞ = asymptotic length;
t = a specific age;
t_0 = hypothetical age at length zero;
k and K = growth coefficients; and
m = fitted fourth parameter.

Individual length-at-age was back-calculated by using method II of Sun et al. (2002) which is based on the formula of Ehrhardt et al. (1996):

$$EFL_t = (R_n/R_{\mathrm{tot}})^b\ \mathrm{EFL},$$

where EFL_t = back-calculated eye-to-fork length at age t;
R_n and R_{tot} are as previously defined; and
b = parameter derived from the relation of EFL to R_{tot}.

EFL was related to R_{tot} using the power equation,

$$EFL = a\,R_{\mathrm{tot}}{}^b,$$

where a, b = fitted parameters.

This model was chosen because of the obvious curvilinearity of the relationship. Sex effects were evaluated by using ANCOVA.

Likelihood ratio (LR) tests (Cerrato, 1990; Quinn and Deriso, 1999) were used to evaluate the effects of sex and type of VBGF model for describing the length-at-age relationship. For LR test statistics, the additivity of untransformed data was assumed and the statistics were calculated as two times the log-likelihood:

$$LR = [-n/2]\left[\ln(2\pi[SSE/n]) + 1\right],$$

where SSE = error sum of squares; and
n = number of age classes.

In both cases, LR test statistics were compared against χ^2 with df = 1 by using the Akaike information criterion.

Results

Accuracy and precision

A pilot evaluation of the two methods used for viewing fin ray preparations (microscope, digital image analyzer) indicated nearly congruent results (mean difference only 0.12 ±0.087 yr or 3% of a mean age of 3.8 years; matched-pairs t-test; t=1.38; P=0.17). Directly viewed and image analyzed preparations were therefore considered equivalent (no bias from methods) and were pooled in all subsequent analyses.

Age-bias plots for readers 1 and 2 indicated variable deviations, small in relation to the age estimates, which lacked major pattern over the range of all putative ages. Reader 1's mean age estimates regressed on reader 2's age estimates deviated insignificantly from a slope of 1 and an intercept of 0, even if additional positive deviations for ages > 8 were included (Table 1A). Readers

Table 1

Summary statistics from a comparison of the (**A**) bias (accuracy), and (**B**) precision (repeatability) of swordfish (*Xiphias gladius*) ages estimated by readers 1 and 2; precision was evaluated both between- and within-readers. Bias and precision were evaluated by age-bias plots and coefficient of variation (CV), respectively (Campana et al., 1995; Campana, 2001). Sexes were pooled in (A) because the effect of sex insignificantly influenced aging differences between readers, both for ages <8 and for all ages (ANCOVA: P=0.21 and 0.06, respectively). H_0 = null hypothesis. SE = standard error.

A Hypothesis	Main study data subset	Parameter estimate ±SE (test statistic)	df	Prob > F
Bias				
H_0: slope = 1	ages < 8	0.985 ± 0.034	1,6	0.67
H_0: intercept = 0		(F=0.20)	1,6	0.85
		0.015 ±0.078		
		(F=0.04)		
H_0: slope = 1	all ages	1.010 ± 0.019	1,10	0.93
H_0: intercept = 0		(F=0.01)	1,10	0.62
		−0.006 ±0.070		
		(F=0.27)		

B Type	Specimen series	Median CV[1]	Number of fish
Precision			
Within-reader, reader 2	inter-laboratory[2]	9.7	100
Within-reader, reader 1	main study	13.3	377
Within-reader, reader 2	main study	12.9	790
Between-reader	inter-laboratory	15.7	100
Between-reader	main study	10.8	1055

[1] Weighted equally over all age groups.

[2] Unavailable for reader 1, who made only one set of readings.

1 and 2 aged specimens used in the inter-laboratory calibration exercise with negligible (<2%) deviation from the majority agreement standard. The age assignments of both readers 1 and 2 were henceforth used for growth analyses. If the readers did not agree, reader 2 re-examined the specimen to resolve the discrepancy. Specimens with unresolvable ages were omitted from subsequent analysis.

Age estimates were adequately precise, as well as accurate. CVs of within- and between-reader age estimates were generally 10–15 % (Table 1B). CVs of the inter-laboratory and main study readings were similar, as were the within- and between-reader CVs within each series (Kruskal-Wallis 1-way ANOVAs; all P>0.3).

Verification and validation of annuli

The results of marginal increment analysis (Fig. 1) provided consistent quantitative support for the contention that fin rays form a single pair of opaque and translucent bands per year (Campana, 2001). Formation of the annulus is complete by September in central North Pacific swordfish; MIRs were wider in June and narrower in September (for fish of both sexes) than during the rest of the year (2-way ANOVA on sex and month; interaction effect: F=0.80, df=11,732, P=0.64; month effect: F=2.05, df=11,743, P=0.02). The pattern generally applied to fish of all ages through at least age-group 7 of adequate sample sizes (Fig. 1), although considerable variability existed throughout the year.

Verification and corroboration of annuli (Kalish et al., 1995; Campana, 2001) were further explored using several complementary methods. These consisted of comparisons of ages that were based on otolith sagittae and fin rays from matched (same) fish and on quantitative relations among fin ray cross-section dimensions, fish body length, and ages based on sagittal DGIs and fin ray annuli. Measurements of total and incremental radii in fin ray cross-sections were obtained for a total 1336 swordfish (733 females, range 46–260 cm EFL; 603 males, range 36–229 cm EFL). Numbers of DGIs on sagittae were enumerated for a total 63 larval, older juvenile, and small adult swordfish of the two sexes (range 4–135 cm EFL). The EFL-at-age relation was described for 49 fish (range 4–133 cm EFL) for which there were adequately precise DGI counts. Fin ray preparations were available for 50 specimens with matched DGI counts.

Total cross-section radius of the second ray of the first anal fin was significantly related to fish age in days for older juveniles and small adults (Fig. 2). The best fitted power equation relationship:

$$R_{tot} = 0.0197 \text{ DGI}^{0.7877}, r^2 = 0.877,$$

predicted an R_{tot} of 2.055 ±0.069 (mean ±SE) mm at an age of 365 days. For a larger sample of fish aged to be 1 yr old by using fin rays, the radius R_1 (the just-completed first annulus) was 2.23 ±0.091 mm from the focus on cross sections cut as described and was unrelated to sex of fish (Student's t=0.88; n=71 fish; P=0.38).

Cross sections taken at the suture terminus were located about 14% of the conforming total length (distal surface) of the ray above the condyle. In a comparison between cross sections from matched (same) fish, where the cross sections were taken at our suture terminus and the $d/2$ position for 115 specimens (sexes pooled) ranging from 82–241 cm EFL, the conventional cross-section radius was located at a shorter average distance (about 10%) above the condyle. Total radii of cross sections produced by the two different types of cuts necessarily differed slightly (by 3%; ANCOVA; P<0.001) but were independent of fish size and sex (ANCOVA; P=0.6 and 0.3, respectively). Despite these numeric differences, there was no discernible average difference in annuli counts with sections cut at the suture terminus and $d/2$ positions. Core regions of basal cut sections were obscure in 77% of the specimens whose ages ranged from 1 to 11 years (ages estimated by using suture terminus sections). Either the first annulus was missing or the section could not be aged for 21% of the basal cut specimens. Ages averaged 0.8 yr younger with basal sections (matched-pairs signed-ranks test; P<0.01) for 25 of the specimens whose age estimates differed between basal and distal sections, and averaged 0.2 yr younger overall. For basal cuts only, mean back-calculated body lengths at age 1 yr, based on the presumed "first annulus," differed in predicted fashion among age groups (i.e., they were greater for older fish in which the real first annulus was more apt to be missing with age (2-way ANOVA on age-group and type of section; age-group effect: P<0.0001; Penha et al., 2004).

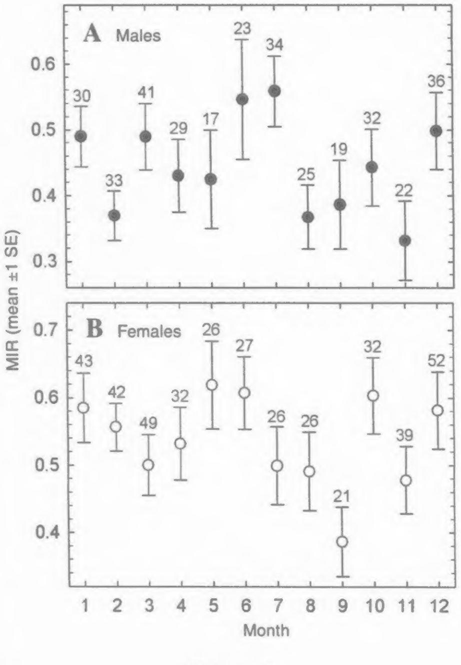

Figure 1

Monthly means of the marginal increment ratio (MIR) for (**A**) male and (**B**) female swordfish (*Xiphias gladius*) caught in the region of the Hawaii-based pelagic longline fishery during 1993–97. Vertical lines indicate ±1 standard error (SE). Number of fish specimens is noted above each monthly estimate. Code to months: 1 = January, 2 = February, ... 12 = December.

Daily growth of young swordfish based on counts of DGIs on otoliths strongly corroborated our estimates of size-at-age for age-group 0 (age 0+) and yearling fish based on fin ray cross sections (Fig. 3). Body length was nonlinearly related to presumed age in days and the most parsimonious, best fit was the hyperbolic, two-parameter relation:

$$EFL = (136.6 \text{ DGI}) / (140.8 + \text{DGI}), r^2=0.937, n=49.$$

This best fit relation indicated a body length of 98.6 ±3.0 (95 % CI) cm EFL at an age of 365 days (Fig. 3).

Development of growth model

The relations between EFL and cross-section fin ray radius were strongly curvilinear, and doubly log-transformed data differed in elevation for females and males (ANCOVA; $F_{1,1333}$=6.41; P=0.01) but shared a common slope (ANCOVA; $F_{1,1332}$=0.84; P=0.36). For R_{tot} measured in mm and EFL (in cm), the best fit relations were

$$\text{Females} \quad EFL = 64.3725 R_{tot}^{0.5539}, r^2=0.939;$$
$$\text{Males} \quad EFL = 66.3090 R_{tot}^{0.5175}, r^2=0.936.$$

R_{tot} regressed on EFL indicated that R_1 should be about 2.16 mm, using the independent length-at-age 1-yr estimate of 98.6 cm EFL. An R_1 of 2.055 mm would be equivalent to a length of about 96 cm EFL (Figs. 2 and 3).

Table 2 lists our sex-specific, back-calculated EFL-at-age estimates. Summary statistics for the corresponding estimates of ray radii are provided in Table 3 for males and females, respectively, by age group and averaged over all age groups. We estimated an age of 0.58 yr (213 days) at an observed mean EFL of 82.2 cm from the otolith-based length-at-age relation (Fig. 3) and used this estimate to represent the mean length of age-group-0 fish ≥60 cm EFL in the aged population.

Table 2

Summary of eye-to-fork length (EFL, cm) statistics and estimated mean back-calculated lengths-at-age for swordfish (*Xiphias gladius*) of each sex and age-group, caught in the region of the Hawaii-based pelagic longline fishery during 1993–97. SD=standard deviation.

	Males			Females		
Age group	Sample size	Back-calculated EFL	Mean ±SD EFL	Sample size	Back-calculated EFL	Mean ±SD EFL
0	136		82.1 ±18.4	137		82.3 ±18.8
1	145	102.0	114.3 ±13.2	114	100.5	115.1 ±14.2
2	97	127.4	137.0 ±13.5	109	126.3	138.3 ±15.1
3	69	147.9	155.3 ±16.0	64	147.7	155.4 ±15.5
4	41	159.9	164.1 ±14.2	58	167.1	171.4 ±18.2
5	29	166.3	172.8 ±18.0	59	179.6	185.3 ±18.0
6	34	174.7	181.0 ±17.6	63	189.7	195.0 ±17.8
7	15	188.4	189.7 ±17.2	36	204.7	209.9 ±12.4
8	10	196.7	197.3 ±19.7	29	208.5	212.3 ±15.4
9	4	202.2	212.5 ±12.9	20	208.0	210.3 ±16.6
10				12	223.4	228.0 ±15.6
11	2	197.5	198.5 ±6.4	9	219.6	222.8 ±17.6
12				5	216.0	218.2 ±14.5

Back-calculated lengths-at-age were used to evaluate length versus age by using several versions of the von Bertalanffy growth model, for a total 1292 fish (712 females, 580 males) ≥60 cm EFL. Less than 4% of all fin ray preparations were deemed unreadable and not used. Age-group-0 fish (0.58 yr; 82.3 cm [females], 82.1 cm [males]) were included in the model fits. Male and female swordfish clearly grow in length at different rates after age 1 (Table 4; likelihood-ratio test; $P<0.001$; Table 5A). Furthermore, for central North Pacific swordfish spanning the length range of most fish in the commercial catch (60-cm EFL as an average minimum), the standard three-parameter VBGF fit the length-at-age data more efficiently than Richards' generalized VBGF (likelihood-ratio test; males: $P>0.2$, females: $P=0.5$; Table 5B). Hence, the standard VBGF is the more parsimonious growth model and should be applied to the sexes separately for central North Pacific swordfish of exploitable sizes (Table 4; Fig 4).

Three fish, whose ship-side, visually estimated weights were equivalent to lengths of 88, 98, and 93 cm EFL when initially tagged and released, were recaptured after 364, 610, and 1490 days at liberty and had grown 38, 58, and 90 cm, respectively, based on round weights at market (Uchiyama et al., 1998). The sex of none of these fish was determined when they were tagged

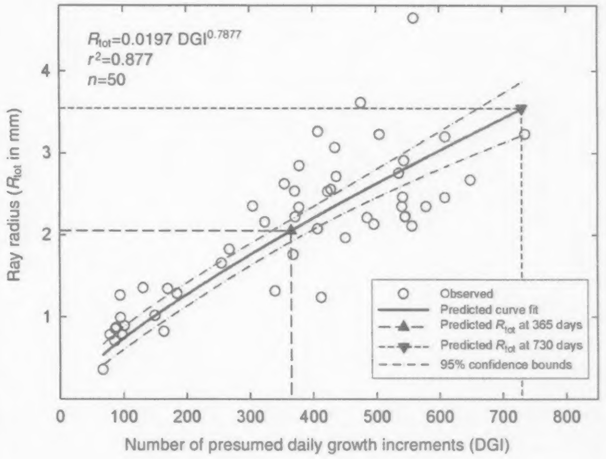

Scatterplot and fitted relationship between the total cross-section radius (R_{tot}, in mm) of the second ray of the first anal fin and the number of daily growth increments (DGI; estimated age in presumed days based on microincrement counts) on sagittae for the same young-of-year and yearling swordfish (*Xiphias gladius*) (sexes pooled) caught in the region of the Hawaii-based pelagic longline fishery during 1993–97. The power equation, $R_{tot} = a \text{ DGI}^{b}$, was used to model the fitted relationship. The extended lines intercepting the x and y axes represent the estimated radii at ages 365 and 730 days. Confidence in the R_{tot} at age 730 days (3.5–3.6 mm) is low because of the poor readability of DGIs at and beyond this age, for fish of either or both sexes.

or recaptured. If estimated length increments are related to a fit of the standard VBGF (sexes pooled) for central North Pacific swordfish, the growth trajectories of these fish agreed reasonably well with those expected for fish of their sizes at liberty for the observed durations (Fig. 5).

Discussion

Verification and validation of age

Our comparisons of ages based on annuli in fin ray sections and DGIs in otoliths, coupled with those of ray radii and otolith ages, represent a novel approach to verifying the age and growth of swordfish and other species for which validation is difficult. The good agreement we observed between our estimates of size at age 365 days based on otoliths and of size at age 1 yr based on fin rays provides a strong partial verification of our aging protocols for young swordfish. Our detailed cross-validation of fin ray annuli against otolith DGIs has conclusively identified the location of the first annulus on swordfish fin rays for the first time. Marginal increment analysis further corroborates that a single annulus forms once each year in anal-fin rays and is complete for swordfish through age 7 caught in the central North Pacific by the end of the spawning period in late summer (DeMartini et al., 2000), when somatic condition is lowest (Uchiyama et al., 1999). Others have similarly observed that the time of annulus formation occurs at the end of the growing season for swordfish in the western North Pacific (Sun et al., 2002) and eastern South Pacific (Cerna[1]), although other drains on physiological condition, such as migration, may be involved (Sun et al., 2002). We also present final proof that basal cross sections of fin rays underestimate ages as a result of partial or complete resorption of the first annulus, as first proposed by Berkeley and Houde (1983) and subsequently observed by Tserpes and Tsimenides (1995) and others. Our comparison of age readings derived from basal, $d/2$, and suture terminus cuts of anal-fin rays demonstrates the equivalence of the latter two types of ray cross sections.

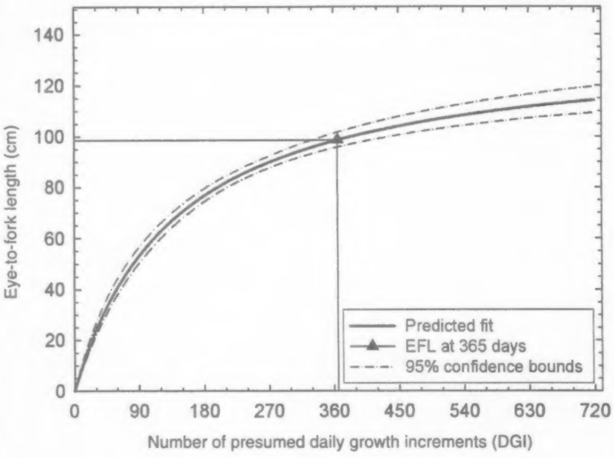

Fitted relationship between eye-to-fork length (EFL, in cm) and number of daily growth increments (DGIs) on sagittae for young-of-year (age 0+) and yearling swordfish (*Xiphias gladius*) (sexes pooled) caught in the region of the Hawaii-based pelagic longline fishery during 1993–97. A hyperbolic equation, $EFL = (a\ DGI)/(b+DGI)$, provided the best two-parameter relationship. The extended lines intercepting the x and y axes represent the estimated EFL at age 365 days.

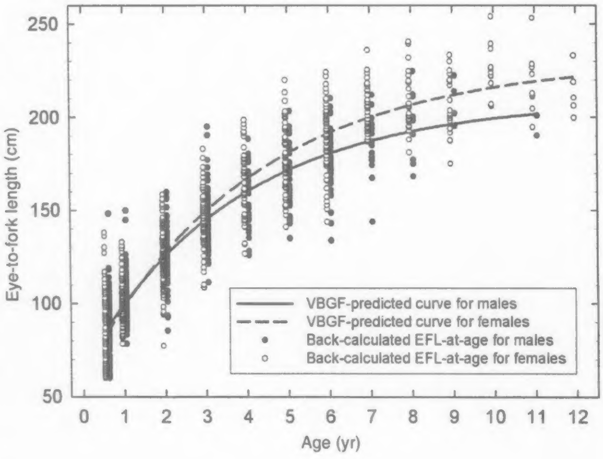

scatterplots of means of back-calculated EFL-at-age describing mean length (cm)-at-age (yr) separately for male and female swordfish (*Xiphias gladius*), caught in the region of the Hawaii-based pelagic longline fishery during 1993–97. Scatterplots for the two sexes were offset slightly for readability. EFL = eye-to-fork length..

---

[1] Cerna, F. J. 2006. Unpubl. data. Sección Edad y Crecimiento, División de Investigación Pesquera, Instituto de Fomento Pesquero, Blanco 839, Valparaiso 5a Region, Chile.

Table 3

Mean R_n (radius from focus to distal edge of each annulus) for each age-group of male and female swordfish (*Xiphias gladius*) caught in the region of the Hawaii-based pelagic longline fishery during 1993–97. Roman numerals indicate the number of presumed annuli. SD = standard deviation. "Increment" refers to the increase in mean R_n from the preceding annulus.

		Mean R_n (mm) from focus to distal edge of each annulus										
Males Age-group (yr)	Sample size	I	II	III	IV	V	VI	VII	VIII	IX	X	XI
0	136											
1	145	2.22										
2	97	2.23	3.34									
3	68	2.20	3.38	4.30								
4	41	2.17	3.36	4.32	5.04							
5	29	2.19	3.33	4.35	5.11	5.76						
6	33	2.09	3.27	4.25	5.09	5.87	6.43					
7	15	2.39	3.41	4.27	4.98	5.62	6.15	6.61				
8	10	2.08	3.23	4.19	4.87	5.53	6.09	6.57	6.96			
9	4	2.28	3.24	4.23	5.24	5.85	6.50	7.15	7.76	8.22		
10	—										—	
11	2	2.02	3.15	3.86	4.96	5.54	6.17	6.59	6.91	7.28		8.03
Mean		2.19	3.30	4.22	5.04	5.69	6.26	6.73	7.21	7.75		8.03
SD		0.11	0.09	0.15	0.12	0.15	0.18	0.28	0.48	0.66		—
Increment			1.11	0.92	0.82	0.65	0.57	0.47	0.48	0.54		0.28

		Mean R_n (mm) from focus to distal edge of each annulus											
Females Age-group (yr)	Sample size	I	II	III	IV	V	VI	VII	VIII	IX	X	XI	XII
0	137												
1	114	2.22											
2	108	2.26	3.37										
3	63	2.15	3.36	4.28									
4	58	2.15	3.25	4.22	4.99								
5	58	2.27	3.42	4.40	5.28	5.95							
6	63	2.17	3.28	4.29	5.25	6.04	6.65						
7	36	2.24	3.42	4.47	5.42	6.16	6.79	7.25					
8	29	2.23	3.31	4.24	5.14	5.88	6.56	7.19	7.62				
9	20	2.15	3.27	4.20	5.06	5.75	6.39	6.98	7.48	7.89			
10	12	2.13	3.23	4.19	5.08	5.94	6.60	7.21	7.75	8.24	8.67		
11	9	2.18	3.11	4.02	4.99	5.77	6.52	7.19	7.71	8.14	8.56	8.90	
12	5	2.28	3.31	4.33	5.14	5.71	6.40	6.97	7.45	7.90	8.34	8.70	9.08
Mean		2.20	3.30	4.27	5.15	5.90	6.56	7.13	7.60	8.04	8.52	8.80	9.08
SD		0.05	0.09	0.12	0.14	0.16	0.14	0.12	0.13	0.17	0.17	0.14	
Increment			1.10	0.97	0.88	0.75	0.66	0.57	0.47	0.44	0.48	0.28	0.28

Selection of growth model

Unlike swordfish caught in waters near Taiwan (Sun et al., 2002), swordfish of exploitable size in the central North Pacific near Hawaii grow in length at rates best described by the standard, rather than generalized, VBGF. We suggest that this model primarily reflects the different size structure of catches from the two regions. By truncating the application of our growth model at the approximate minimum size of fish caught by the Hawaii-based longline fishery (60-cm EFL), we eliminate the markedly allometric growth effects that half-year-old and younger fish have on the ascending limb of the VBGF curve. The disproportionately low body mass of young juveniles reflects the fact that swordfish, perhaps like most pelagic fishes that are reliant on swimming speed as their primary antipredator adaptation (and unlike typical nonpelagic fish with less pronounced allometric growth), must experience intense selection for growth in length (swimming speed) at the expense of growth in mass during the juvenile stage. A related issue is the fact that swordfish >180–200 cm EFL are more abundant in the Hawaiian than in Taiwanese fisheries, and these larger fish provide an extended scope for resolving the asymptote of VBGF models, especially the standard VBGF which lacks a fourth parameter (shape function) to help resolve curvature of the ascending limb. Not surprisingly, growth of swordfish caught

Table 4

Parameter estimates (±standard error, SE) for the standard von Bertalanffy and the generalized von Bertalanffy growth formulas (VBGFs) fitting mean back-calculated eye-to-fork length (EFL)-at-age against age for male and female swordfish (*Xiphias gladius*) ≥60 cm EFL caught in the region of the Hawaii-based longline fishery during 1993–97. L_∞= asymptotic length; k and K = growth coefficients; t_0 = hypothetical age at length zero; m = fitted fourth parameter; n = number of age-classes. r^2=coefficient of determination; n = sample size.

	Standard VBGF		Generalized VBGF	
Parameter	Male	Female	Male	Female
L_∞	208.9 ±5.60	230.5 ±3.94	221.0 ±20.1	227.2 ±6.18
k	0.271 ±0.034	0.246 ±0.019		
K			0.070 ±0.080	0.524 ±0.871
t_0	−1.37 ±0.259	−1.24 ±0.167	−0.15 ±0.576	−2.41 ±2.968
m			−1.27 ±1.122	0.448 ±0.771
r^2	0.989	0.995	0.991	0.995
n	11	12	11	12
P	<0.001	<0.001	<0.001	<0.001

Table 5

Summary statistics for likelihood ratio (LR) tests evaluating (**A**) potential differences between the estimated von Bertalanffy growth (VBGF) parameters for male and female swordfish (*Xiphias gladius*), and (**B**) the standard versus generalized VBGF models of length-on-age for males and females caught in the region of the Hawaii-based pelagic longline fishery during 1993–97. H_0=null hypothesis.

	Sexes pooled	By sex (male+female)
A Male versus female		
Log-likelihood	−64.7	−79.1
X^2 (prob $>\chi^2$)	28.8 (<0.001)	
Conclusion	Reject H_0 : male = female	

	Male		Female	
	Standard	Generalized	Standard	Generalized
B Standard versus generalized VBGF				
Log-likelihood	−30.7	−29.9	−34.0	−33.8
X^2 (prob $>\chi^2$)	1.62 (P>0.2)0.46 (P=0.5)			
Conclusion	Accept H_o: standard = generalized		Accept H_o: standard = generalized	

by the Chilean longline fishery (Cerna[1]), like those caught near Hawaii, is better described by the standard VBGF, and large swordfish are also abundant in the relatively undeveloped Chilean fishery. Chapman's five-parameter version of the generalized VBGF would be the most appropriate for describing size-at-age of swordfish only if there was a compelling reason to fit the growth curve through zero length at zero age (see Arocha et al., 2003).

Our growth-at-liberty data for tagged-recaptured swordfish in the central North Pacific, albeit limited to only three fish, are consistent with modeled growth of small- to medium-size adult fish. Restrepo (1990) and Brown (1995) provide the only other data of this type for swordfish, limited to fish caught in the Atlantic Ocean and Gulf of Mexico. The usefulness of such data is limited because of inaccuracies in estimates of body size at time of first capture (Restrepo, 1990)—as it was for our tagged swordfish—and uncertain units of size measurement (Brown, 1995), but some general growth patterns are nonetheless evident. For nearly 100 swordfish with a median length of about 100 cm at initial capture and of 135 cm when recaptured after a median period at liberty of 1.5 years, the growth rate was about 24 cm per yr (Brown, 1995). Given that body size when a fish is tagged is usually overestimated (Restrepo, 1990), and this body size yields an underestimate of incremental growth at liberty and given also the likely faster growth of swordfish in the Pacific—especially the central North Pacific—see below, the average growth increment (35 cm per yr) that we observed for the three tagged-recaptured fish, yearlings in size when first caught and at liberty for 1, 2, and 4 years, is reasonable, as well as consistent, with our modeled growth trajectories for fish of this size range. We nonetheless caution, however, that these few consistencies by themselves do not verify our growth curves.

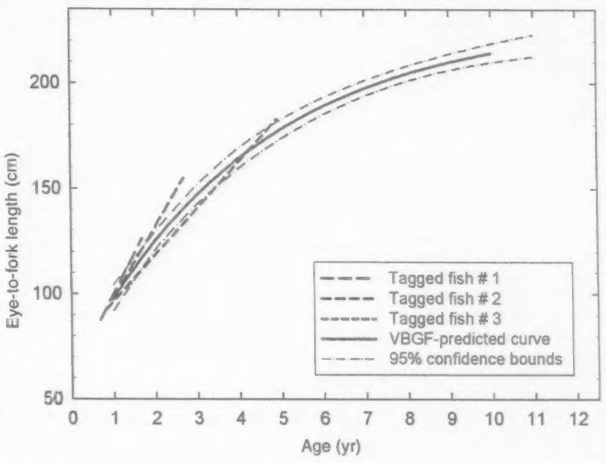

VBGF) describing eye-to-fork length (in cm)-at-age (in yr) for swordfish (*Xiphias gladius*) (both sexes pooled); calculated growth trajectories for each of three tagged-recaptured swordfish (sexes unknown) are indicated.

Sexually dimorphic growth

By now there can be no doubt that female swordfish grow faster and attain larger maximum body sizes than do males in the Pacific (Castro-Longoria, 1995; Sun et al., 2002; Cerna[1]; this study), as many others (e.g., Berkeley and Houde, 1983) have observed for swordfish in the Atlantic. That females on average live longer than males is less certain, and this uncertainty will likely persist because of the rarity of the largest, oldest fish captured by fisheries —especially in developed fisheries—and associated difficulties in validating estimates of their ages. Even though sexually dimorphic growth does not become prominent in either body length or fin rays until after age 1, it is obvious that the sexes should be evaluated separately in stock assessments (Wang et al., 2005) for retained swordfish (generally greater than 1 yr old in most fisheries) whenever landings data allow. The sexual differences in body size and growth that we observed reinforce the argument that sex-specific, age-based stock assessments are needed for swordfish.

The greater probability of error in estimating the ages of larger swordfish affects females disproportionately as the larger-bodied fish. Sex-specific stock assessments need to explicitly evaluate the greater uncertainty of age estimates for the largest, mostly female, fish as well as the more generally recognized influences of gear bias on the capture efficiency (hence sex ratio) for male and female swordfish of different sizes.

Unresolved issues and future research needs

In prior studies of swordfish age and growth there has been the conspicuous need to validate the periodicity of annulus formation for all age groups present in a fishery, including the oldest age groups, which are typically relegated to a catch-all plus group that complicates stock assessment computations (Restrepo and Powers, 1991). Validation of the age and growth of these largest, oldest fish likewise has been a problem in our study, and our estimates of growth-at-liberty for tag-recaptured fish only provide insights into growth (not absolute age) of juveniles and young adults. There is still great need to verify the accuracy of age estimates for swordfish in older age-groups. Radiometric aging (Watters et al., 2006), one alternative method for aging the hard parts of large, old fish, is inappropriate for swordfish because the oldest living tissue is reabsorbed within fin rays and because their tiny otoliths provide insufficient material for analysis of individual fish. Resolution of the problem would almost certainly require a dedicated, large-scale, and expensive conventional tagging effort targeting large and old fish, preferably one in which a rigorous protocol is implemented for accurately estimating size at initial capture and labeling body size at time of release with a fluorescent biomarker. Such a study is unlikely to be implemented unless greater reductions in stock sizes, increases in value, or (more likely) both in concert, justify the great cost of such an enterprise. Of course, such a study could provide data on fish movements whose importance might dwarf that of age and growth validation.

Geographic variation in growth rates is evident for swordfish in regional Pacific fisheries. Size-at-age is appreciably greater for swordfish caught in the region of the Hawaii-based fishery (versus the Taiwanese fishery) and the regional difference includes juvenile and small adult, as well as larger adult fish. For example, the mean length at age 1 of swordfish in the Taiwanese fishery is about 96 cm lower-jaw-to-fork length, which is equivalent to only 83 cm EFL (Sun et al., 2002), whereas the mean length at age 1 in the Hawaii-based fishery is 99 cm EFL. The results of our study indicate that swordfish caught in the central North Pacific grow in length at a rate faster than swordfish caught by several other Pacific regional fisheries (Fig. 6), and this finding was confirmed by readers from other laboratories during the inter-laboratory exercise. Faster growth in the central North Pacific (versus the western North Pacific) may reflect the high planktonic productivity of swordfish feeding grounds in the Subtropical Convergence Zone (Seki et al., 2002), perhaps similar to that in the productive upwelling region off Chile in the eastern South Pacific. Consistent with this observation, data on body condition (weight-at-length) indicate that central North Pacific swordfish are heavier at a given length than swordfish from the western North Pacific (Uchiyama et al., 1999; Sun et al., 2002). Regional differences in growth rates are also apparent for swordfish throughout the Atlantic and Mediterranean (Tserpes and Tsimenides, 1995; Ehrhardt et al., 1996; Alicli and Oray, 2001).

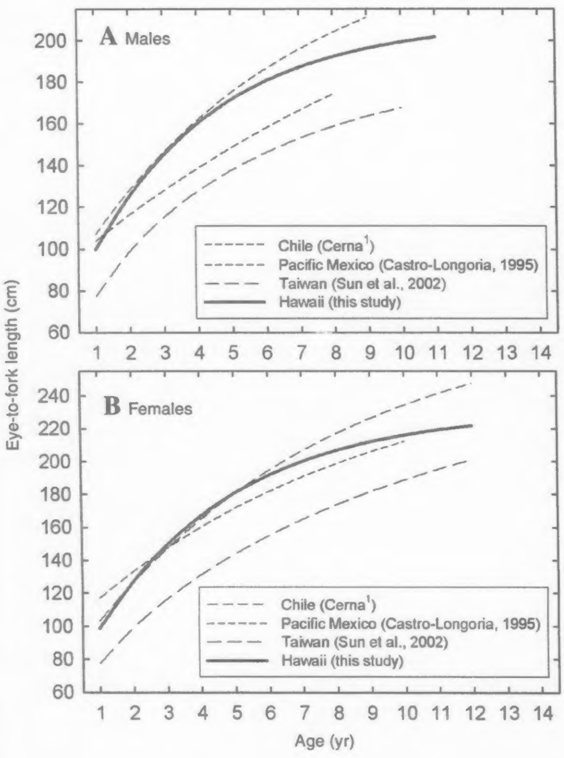

9

Fitted curves describing body length-at-age relationships for (**A**) male and (**B**) female swordfish (*Xiphias gladius*) captured by three other regional Pacific fisheries; length-at-age curves for swordfish caught in the region of the Hawaii-based fishery are provided for comparison. To facilitate the comparison, lower jaw-to-fork lengths were converted to eye-to-fork lengths (EFL). EFL-at-age relationships were fitted by using parameters of the standard von Bertalanffy growth formula (VBGF) in all cases except that of Taiwan, for which the generalized VBGF was used, as recommended by Sun et al. (2002).

Stock structure is still incompletely understood for Pacific swordfish and regional variations in growth rates complicate rather than resolve the issue. Present understanding of the population genetics of swordfish indicates that separate stocks exist in the North and South Pacific and that there likely is some stock structuring between east and west in the North Pacific (Reeb et al., 2000). Detailed comparisons among the nuclear (microsatellite) DNAs and mtDNAs of planktonic spawning products (eggs and larvae) and fish of exploitable sizes, coupled with analyses of phenotypic traits like growth and environmental markers, such as trace element signatures in otoliths (Humphreys et al., 2005), are needed for swordfish collected from all regional fisheries in order to fully resolve the stock issue for swordfish in the Pacific.

Acknowledgments

We gratefully acknowledge C.-L. Sun (National Taiwan University), K. Yokawa (National Research Institute of Far Seas Fisheries), O. Sosa-Nishizaki (Centro de Investigacion Cientifica y de Educacion Superior de Ensenada), and F. Cerna (Instituto de Fomento Pesquero) for their cooperation in implementing the inter-laboratory calibration exercise mandated at the Second Meeting of the Interim Scientific Committee for Tuna and Tuna-like Fishes in the North Pacific (ISC2) held January 15–23, 1999, in Honolulu, Hawaii. We also thank M. McCracken for statistical advice, D. Yamaguchi for assistance with preparing all of the final figures, and P. Kleiber, D. Kobayashi, R. Nishimoto, C. Boggs, and three anonymous reviewers for constructive criticisms of a draft of the manuscript.

Literature cited

Alicli, T. Z., and I. K. Oray.
2001. Age and growth of swordfish (*Xiphias gladius* L., 1758) in the eastern Mediterranean Sea. Int. Comm. Conserv. Atl. Tunas, Coll. Vol. Sci. Pap. 52:698–707.

Arocha, F., C. Moreno, L. Beerkircher, D. W. Lee, and L. Marcano.
2003. Update on growth estimates for swordfish, *Xiphias gladius*, in the northwestern Atlantic. Int. Comm. Conserv. Atl. Tunas, Coll. Vol. Sci. Pap. 55(4):1416–1429.

Berkeley, S. A., and E. D. Houde.
1983. Age determination of broadbill swordfish, *Xiphias gladius*, from the Straits of Florida, using anal fin spine sections. NOAA Tech. Rep. NMFS 8:137–143, 211 p.

Bigelow, K. A., C. H. Boggs, and X. He.
1999. Environmental effects on swordfish and blue shark catch rates in the US North Pacific longline fishery. Fish. Oceanogr. 8:178–198.

Brown, C. A.
1995. Preliminary examination of size and location data for U.S. tagged and recaptured swordfish. Int. Comm. Conserv. Atl. Tunas, Coll. Vol. Sci. Pap. 44(3): 217–224.

Campana, S. E.
2001. Accuracy, precision and quality control in age determination, including a review of the use and abuse of age validation methods. J. Fish Biol. 59:197–242.

Campana, S. E., M. C. Annand, and J. I. McMillan.
1995. Graphical and statistical methods for determining the consistency of age determinations. Trans. Am. Fish. Soc. 124:131–138.

Castro-Longoria, R.
1995. Analysis of age, growth, and gonadal maturity of swordfish, *Xiphias gladius*, in the Mexican Pacific longline fishery. Ph. D. diss., 114 p. Departmento de Ecologia, Division de Oceanologia, Centro de Investigacion Cientifica y de Educacion Superior de Ensenada, Ensenada, Mexico [In Spanish].

Cerrato, R. M.
1990. Interpretable statistical tests for growth comparisons using parameters in the von Bertalanffy equation. Can. J. Fish. Aquat. Sci. 47:1416–1426.

DeMartini, E. E., J. H. Uchiyama, and H. A.Williams.
2000. Sexual maturity, sex ratio, and size composition of swordfish, *Xiphias gladius*, caught by the Hawaii-based pelagic longline fishery. Fish. Bull. 98:489–506.

Ehrhardt, N. M., R. J. Robbins, and F. Arocha.
1996. Age validation and growth of swordfish, *Xiphias gladius*, in the northwest Atlantic. Int. Comm. Conserv. Atl. Tunas, Coll. Vol. Sci. Pap. 45(2):358–367.

Humphreys, R. L., Jr.
2000. Otolith-based assessment of recruitment variation in a North Pacific seamount population of armorhead *Pseudopentoceros wheeleri*. Mar. Ecol. Prog. Ser. 204:213–223.

Humphreys, R. L., Jr., S. E. Campana, and E. E. DeMartini.
2005. Otolith elemental fingerprints of juvenile Pacific swordfish (*Xiphias gladius* L.). J. Fish Biol. 66:1660–1670.

Ito, R., R. A. Dollar, and K. E. Kawamoto.
1998. The Hawaii-based longline fishery for swordfish, *Xiphias gladius*. *In* Biology and fisheries of swordfish, *Xiphias gladius* (I. Barrett, O. Sosa-Nishizaki, and N. Bartoo, eds.), p. 77–88. NOAA Tech. Rep. NMFS 142, 276 p.

Kalish, J. M., R. J. Beamish, E. B. Brothers, J. M. Casselman, R. I. C. C. Francis, H. Modegaard, J. Panfili, E. D. Prince, R. E. Thresher, C. A. Wilson, and P. J. Wright.
1995. Glossary for otolith studies. *In* Recent developments in fish otolith research. (D. H. Secor, J. M. Dean, and S. E. Campana, eds.), p. 723–729. Belle W. Baruch Library in Marine Science Number 19. Univ. So. Carolina Press, Columbia, SC.

Penha, J. M. F., L. A. F. Mateus, and M. P. Petrere, Jr.
2004. A procedure to improve confidence in identification of the first annulus in fin-spines of fishes. Fish. Manage. Ecol. 11:135–137.

Prince, E. D., D. W. Lee, and S. A. Berkeley.
1988. Use of marginal increment analysis to validate the anal spine method for ageing Atlantic swordfish and other alternatives for age determination. Int. Comm. Conserv. Atl. Tunas, Coll. Vol. Sci. Pap. 27:194–201.

Quinn, T. J., II, and R. B. Deriso.
1999. Quantitative fish dynamics, 542 p. Oxford Univ. Press, New York, NY.

Reeb, C. A., L. Arcangeli, and B. A. Block.
2000. Structure and migration corridors in Pacific populations of the swordfish *Xiphias gladius*, as inferred through analyses of mitochondrial DNA. Mar. Biol. 136:1123–1131.

Restrepo, V.
1990. An update of swordfish tagging data for use in growth analyses. Int. Comm. Conserv. Atl. Tunas, Coll. Vol. Sci. Pap. 32:360–370.

Restrepo, V. R., and J. E. Powers.
1991. A comparison of three methods for handling the "plus" group in Virtual Population Analysis in the presence of ageing errors. Int. Comm. Conserv. Atl. Tunas, Coll. Vol. Sci. Pap. 35(2):346–354.

Richards, F. J.
1959. A flexible growth function for empirical use. J. Exp. Bot. 10:290–300.

Seki, M. P., J. J. Polovina, D. R. Kobayashi, R. R. Bidigare, and G. T. Mitchum.
2002. An oceanographic characterization of swordfish (*Xiphias gladius*) longline fishing grounds in the springtime subtropical North Pacific. Fish. Oceanogr. 11:251–266.

Sun, C.-L., S.-P. Wang, C. E. Porch, and S.-Z. Yeh.
2005. Sex-specific yield per recruit and spawning stock biomass per recruit for the swordfish, *Xiphias gladius*, in the waters around Taiwan. Fish. Res. 71:61–69.

Sun, C.-L., S.-P. Wang, and S.-Z. Yeh.
2002. Age and growth of the swordfish (*Xiphias gladius* L.), in the waters around Taiwan determined from anal-fin rays. Fish. Bull. 100:822–835.

Tserpes, G., and N. Tsimenides.
1995. Determination of age and growth of swordfish, *Xiphias gladius* L., 1758, in the eastern Mediterranean using anal-fin spines. Fish. Bull. 93:594–602.

Uchiyama, J. H., E. E. DeMartini, and H. A. Williams.
1999. Length-weight interrelationships for swordfish *Xiphias gladius* L. caught in the central North Pacific. NOAA Tech. Memo. NMFS-SWFSC-284, 82 p.

Uchiyama, J. H., R. A. Skillman, J. D. Sampaga, and E. E. DeMartini.
1998. A preliminary assessment of the use of hard parts to age central Pacific swordfish, *Xiphias gladius*. *In* Biology and fisheries of swordfish, *Xiphias gladius* (I. Barrett, O. Sosa-Nishizaki, and N. Bartoo, eds.), p 261–273. NOAA Tech. Rep. NMFS 142, 276 p.

Wang, S.-P., C.-L. Sun, A. E. Punt, and S.-Z. Yeh.
2005. Evaluation of a sex-specific age-structured assessment method for the swordfish, *Xiphias gladius*, in the North Pacific Ocean. Fish. Res. 73:79–97.

Watters, D. L., D. E. Kline, K. H. Coale, and G. M. Cailliet.
2006. Radiometric age confirmation and growth of a deepwater marine fish species: the bank rockfish, *Sebastes rufus*. Fish. Res. 81:251–257.

Zar, J. H.
1984. Biostatistical analysis, 2nd ed., 718 p. Prentice-Hall, Englewood Cliffs, NJ.

Systematics of the North American menhadens: molecular evolutionary reconstructions in the genus *Brevoortia* (Clupeiformes: Clupeidae)

Joel D. Anderson

Email address: Joel.Anderson@tpwd.state.tx.us

Perry R. Bass Marine Fisheries Research Station
Texas Parks and Wildlife Department
HC02 Box 385
Palacios, Texas 77465.

Abstract—Evolutionary associations among the four North American species of menhadens (*Brevoortia* spp.) have not been thoroughly investigated. In the present study, classifications separating the four species into small-scaled and large-scaled groups were evaluated by using DNA data, and genetic associations within these groups were explored. Specifically, data from the nuclear genome (microsatellites) and the mitochondrial genome (mtDNA sequences) were used to elicit patterns of recent and historical evolutionary associations. Nuclear DNA data indicated limited contemporary gene flow among the species, and also indicated higher relatedness within the small-scaled and large-scaled menhadens than between these groups. Mitochondrial DNA sequences of the large-scaled menhadens indicated the presence of two ancestral lineages, one of which contained members of both species. This result may indicate genetic divergence (reproductive isolation) followed by secondary contact (hybridization) between these species. In contrast, a single ancestral lineage indicated incomplete genetic divergence between the small-scaled menhaden. These results are discussed in the context of the biology and demographics of each species.

Manuscript submitted 28 July 2006 to the Scientific Editor's Office.

Manuscript approved for publication 12 January 2007 by the Scientific Editor.

Fish. Bull. 205:368–378 (2007).

The North American species of menhaden (*Brevoortia* spp. Gill, 1861) support large commercial fisheries on the eastern Atlantic and Gulf of Mexico (hereafter, Gulf) coasts. Historically, this industry represented as much as 40% of all commercial landings in the United States (Vaughan and Merriner, 1991), and the Gulf menhaden (*B. patronus* Goode, 1878) supported, by weight, one of the largest single fisheries in the United States. In addition, menhaden are one of the most important participants in estuarine and nearshore food webs along the Atlantic coast (Gottlieb, 1998) and support various recreational fisheries in the Gulf and Atlantic (Kroger and Guthrie, 1972; Scharf and Schlicht, 2000; Bethea et al., 2004).

There are four species of menhaden present in North American waters, three of which are found in the Gulf of Mexico (Fig. 1). These species are further classified into two general groups, the small-scaled and large-scaled menhadens. These groups are named according to the relative size of scales adjacent to the lateral line but also reflect contrasts in other morphological characteristics (Dahlberg, 1970), population demographics (Christmas and Gunter, 1960), and migratory behavior (Gunter, 1945; Simmons, 1957; Tolan and Newstead, 2004). The Gulf menhaden (*B. patronus*) and Atlantic menhaden (*B. tyrannus* Latrobe, 1802) are members of the large-scaled group. *Brevoortia patronus* occurs wholly in the Gulf of Mexico, and dominates the menhaden fishery in the Gulf, with other menhaden species representing less than 1% of the annual catch (Ahrenholz, 1981). *Brevoortia tyrannus* is a semimigratory species found in large schooling populations and is targeted by a second reduction fishery. This species is found only on the Atlantic coast, and does not inhabit the Gulf (Ahrenholz, 1991). The small-scaled menhadens, yellowfin menhaden (*B. smithi* Hildebrand, 1941) and finescale menhaden, (*B. gunteri* Hildebrand, 1948), are present in smaller population sizes and have slightly overlapping distributions in the Gulf. *Brevoortia gunteri* has a distribution range restricted entirely to the northern and western Gulf coastal region. In contrast, *B. smithi* exists mainly in the eastern Gulf, although it ranges north on the Atlantic coast to Cape Lookout, North Carolina (Reintjes, 1959; Ahrenholz, 1991). *Brevoortia smithi* overlaps the eastern range of *B. patronus*, and also overlaps the southern range *B. tyrannus*. Considerable hybridization is thought to occur between *B. patronus* and *B. smithi* along the west coast of Florida, and between *B. tyrannus* and *B. smithi* along the east coast of Florida (Turner, 1969; Hettler, 1984).

Although the evolutionary relationships among the four North American menhaden species have not been explicitly examined, early investigations in species morphology indicated that *B. tyrannus* and *B. patronus* were Atlantic and Gulf complements of one another, and that *B. gunteri* and *B.*

smithi were western and eastern Gulf cognates (Christmas and Gunter, 1960). Dahlberg (1970) conducted an extensive morphological investigation of the Atlantic and Gulf menhadens, including compilation of older data as well as 14 novel physical character assessments that provided morphological support for the notion of small-scaled and large-scaled groups. Subsequent morphological assessments of menhaden at various life stages support this generally accepted taxonomic arrangement (Hettler, 1984; Ahrenholz, 1991; Tolan and Newstead, 2004). Avise et al. (1989) and Bowen and Avise (1990) examined mitochondrial DNA (mtDNA) fingerprints of the large-scaled menhaden complex (*B. patronus+tyrannus*), and two divergent lineages of large-scaled menhadens were identified, one of which was shared between the two species, and the other occurring only in *B. tyrannus*. Avise (1992) suggested that this type of pattern is what would be expected from historical divergence, followed by secondary contact between the species. Anderson and McDonald (2007) used microsatellites to characterize populations of western Gulf menhadens (*B. patronus* and *B. gunteri*) and found significant genetic differences between these species. However, the latter work was limited in its phylogenetic scope because 1) it included only two of the four species of *Brevoortia* found in North America, and 2) it did not include genomic or mtDNA sequence data, which are typically more reliable than microsatellites in discerning relationships among species.

In the present study, the taxonomic relationships among the four North American menhaden species are examined by using both nuclear satellite DNA (microsatellites) and mitochondrial DNA sequences (mtDNA). Microsatellites are short runs of repetitive sequence (usually a two to four base motif repeated multiple times) that tend to be highly variable in vertebrates, are codominant (both parental copies of the marker can be scored for progeny), and are selectively neutral. Because of these properties, they are used extensively for examinations of population structure, paternity, and kinship in vertebrates (Wright and Bentzen, 1994; Jarne and Lagoda, 1996). Five DNA microsatellites were scored in populations of menhaden comprising the range of the four North American species. In addition, mtDNA sequencing was conducted on a short segment of the mtDNA control region for a subset of menhaden representing the four species. Mitochondrial DNA assays are beneficial because the mitochondrial genome of fishes is presumably not affected by recombination, and direct maternal lineages can be examined in contrast to the potentially admixed genotypes of nuclear DNA. In addition, genome-wide genetic studies (i.e., those that include both nuclear and mitochondrial data) are favored over single-locus or single-genome treatments because different genetic loci may yield conflicting results (Hare and Avise, 1998). These data revealed distinctive patterns which, when examined in the context of the biogeographic setting of each species, broaden the existing information with which the evolutionary history of North American menhadens may be elucidated.

Materials and methods

Sample collection and DNA isolation

Fin clips from individual menhaden were collected from bay systems covering the extent of the North American range of *Brevoortia* (Fig. 1) from 2002 through 2004 (see Brown et al., 1996 for a discussion of the implications and assumptions of pooling multiple year genetic data in clupeids). Adult fish samples from Texas were collected with a 184 m gill net partitioned into four sections ranging in mesh sizes from 76 mm to 152 mm, and all juveniles and young adult menhaden were collected in bag-seine hauls. Menhaden from locations outside of Texas were obtained through appropriate state and federal agencies (see "Acknowledgments" section). Fin tissue was excised from larger fish and placed in 70% ethanol; for smaller fish, whole individuals were preserved in ethanol. DNA was extracted from 200 mg of each fin clip or whole fish by using a Puregene® miniprep kit (Gentra Systems, Minneapolis, MN) and following the manufacturer's instructions.

Microsatellite data set

Genomic DNA from 20 sampling locales (Fig. 1) was used as a template to amplify microsatellite loci by touchdown polymerase chain reaction (PCR) with fluorescent end-labeled forward primers. Primer pairs were designed around microsatellite regions initially isolated from another clupeid, American shad (*Alosa sapidissima* Wilson, 1811); these primers have subsequently been evaluated for examinations of the genus *Brevoortia* (Anderson and McDonald, 2007). PCR products were electrophoresed with a Beckman-Coulter CEQ™ 8000 automated capillary system, with a 400 base pair (bp) standard (Beckman Coulter, Inc., Fullerton, CA), according to the manufacturer's suggested protocol. Microsatellite allele sizes were estimated with Beckman-Coulter fragment analysis software (Beckman Coulter, Inc., Fullerton, CA), by using allelic bins that were based on the analysis of 1276 DNA samples from the four North American menhaden species collected over four years (data not shown).

The freeware program FSTAT vers. 2.9.3.2 (Goudet, 1995) was used to calculate observed (H_o) and expected (H_e) heterozygosity and allelic diversity (k_a), and to identify microsatellite loci which deviated significantly from Hardy-Weinberg equilibrium expectations (HWE). Deviation from HWE was tested by calculating the inbreeding coefficient (F_{is}) in the overall data set, and within each individual sampling locale. Statistical significance was assessed in a randomization procedure with 100 iterations. For this analysis, 13 populations of *B. patronus* (n=20) ranging from southern Texas to southern Florida were used. Individuals were then pooled into species and sampling locales (n=20 in each sampling locale, in locales where two species were captured, 20 of each species were used). The genetic divergence (F_{st}, Weir and Cockerham, 1984) among the four

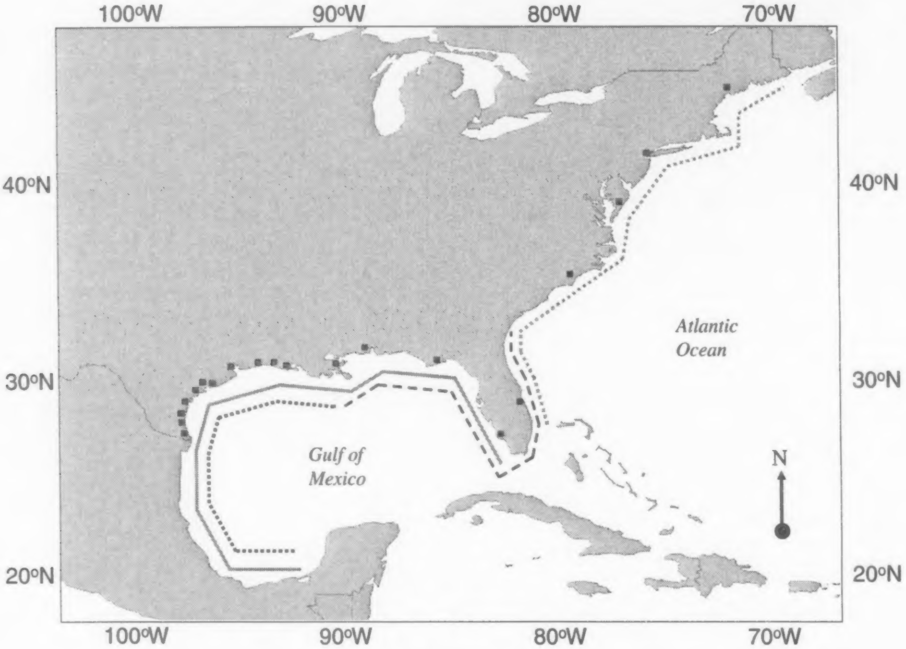

Figure 1

Geographic range of the four menhaden species: Gulf menhaden (*Brevoortia patronus*)—smooth gray line, Gulf; Atlantic menhaden (*B. tyrannus*)—dotted gray line, Atlantic; finescale menhaden (*B. gunteri*)—dotted black line, western Gulf; and yellowfin menhaden (*B. smithi*)—dashed black line, eastern Gulf). Sample sites are indicated by black boxes.

species, and among all populations, was determined by using FSTAT software. A neighbor-joining (N-J) dendrogram was constructed with genetic divergence as a distance metric, and populations were revealed as terminal nodes by using the freeware program MEGA, vers. 2.1 (Kumar et al., 2001).

With a small subset of the data (to accommodate differences in sample size among species), we used a Bayesian procedure, as implemented in the freeware program Structure 2.1 (Pritchard et al., 2000), to examine historical admixture among species. Admixture may be defined as any measure of combination and introgression of genotypes (through hybridization) between two distinctive genetic sources, such as definitive populations, subspecies, or species. Structure 2.1 uses a Markovian chain Monte Carlo method (MCMC) to assign individuals to population clusters such that satisfaction of Hardy-Weinberg and linkage equilibrium expectations are maximized within populations. Because of the mechanics of the MCMC method, each iteration in a simulation is necessarily connected to the previous iteration, and therefore initial iterations are subject to the stochastic nature of random sampling. In order to account for this, data from simulations should not be collected until summary statistics begin to converge (to "burn-in"). A burn-in length of 10,000 repetitions was chosen by examination of summary statistics for convergence in preliminary runs. A run length of 100,000 repetitions was chosen after several preliminary trials, after which parameter values were evaluated for consistency. For all analyses, the admixture model was used, and allele frequencies were assumed to be independent among species. Although this procedure allows estimation of the number of populations present (K), while simultaneously assigning individuals, we constrained the population number to $K = 4$, to reflect the prior assumption that only four species were present. Individuals were then assigned profiles that included the proportion of their genotype contributed by each species cluster. These profiles were then aligned by species in order to visually examine the influence of genetic admixture upon species groups.

Multilocus expected heterozygosity, estimated from microsatellite allele frequencies, was used to generate relative estimates of the value $N_e\mu$ for each of the four species, where N_e is the effective population size and μ represents the overall mutation rate, assuming a stepwise mutation model (Valdes et al., 1993). The estimator θ_F (Xu and Fu, 2004) was used to approximate $N_e\mu$ and was calculated as follows:

$$\theta_F = 0.5\ (F^{-2} - 1),$$

where F = multilocus mean homozygosity ($1 - H_e$).

Although estimates of N_e from small genetic samples are notoriously inaccurate and may do a poor job of reflecting overall census size, relative estimates of N_e have been used to test evolutionary hypotheses (Nielsen, 1997), and theoretically may be used to examine relative differences in multiple populations at the same loci. The assumptions of the present study are that the mutation rate (μ) is not significantly different among the four examined species, and that genetic variability is related to population size. For this analysis, four loci were used because of the highly significant deviation from equilibrium frequencies that was observed at locus AF39660 (see "Results" section).

Sequencing data set

Sequencing templates were generated with PCR by using primers specific to an 840-bp fragment of the mtDNA control region. The heavy strand primer (HN20) was a previously described universal primer (Bernatchez and Danzmann, 1993) (5′-CGGGGTTTGACATGAATAT), whereas the light strand primer (940r) was a novel sequence primer designed specifically for menhaden (3′-TGTAATACTAGTGCGCAGATGGTAC). Each sample was amplified twice, and the amplicons were combined before purification to assure a high quality, concentrated product. PCR products were purified by using QIAquick® PCR purification kits (Qiagen Inc., Valencia, CA). The resulting purified fragments were used in two sequencing reactions in a nested design. The novel heavy strand primer (520f) was internal (5′-GGAACCAAATGCCAGGAATAGT), whereas the light strand primer was the same used in PCR. This nested design resulted in fragments which overlapped one another for 360 bp and which resided within the original 840-bp PCR fragment. Sequences were electrophoresed and analyzed on a Beckman-Coulter CEQ™ 8000 capillary sequencer by using default module (LFR-1) parameters (Beckman Coulter, Inc., Fullerton, CA). Raw sequences were trimmed and edited, and forward and reverse sequences were conjoined by using the software package Sequencher™ vers. 4.2 (Gene Codes Corp., Ann Arbor, MI). Whole sequences were then aligned by using Clustal X freeware (Jeanmougin et al., 1998). Sequences were submitted to GenBank by means of Sequin freeware (National Center for Biotechnology Information, Bethesda, MD) as batch submissions (accession numbers EF119342-EF119454).

Sequence data were obtained from 113 individuals from the four species (*B. tyrannus*, n=37; *B. smithi*, n=32; *B. patronus*, n=30; *B. gunteri*, n=14), and samples were selected to represent the full geographic range of each species (sampling locations in Maine, New Jersey, Virginia, North Carolina, Atlantic and Gulf Florida, and Texas). Sequence statistics, including nucleotide diversity (π) and haplotype diversity (h), were estimated for each species, and the genetic similarity among populations (measured using D_a, Nei, 1987) was calculated by using the freeware program DnaSP 4.0 (Rozas et al., 2003). The variances of sequence diversity estimates were used to construct 95% confidence intervals around each mean. The averaged frequency of each base and the estimated ratio of transitions to transversions (ts/tv) were calculated with the freeware program DAMBE (Data Analysis in Molecular Biology and Evolution, Xia and Xie, 2001). Because of the extreme level of variation found in menhaden mtDNA, both in this study and in a previous study (Bowen and Avise, 1990), we employed a mutation saturation test as instituted in DAMBE. With this analysis, we compared the genetic distance between sequences to the number of transitions and transversions occurring between them. When all pairwise comparisons of sequences were plotted in this manner, mutation saturation was indicated by a plateau at which transversions approach or outnumber transitions at higher genetic distances. The genetic distance employed for this analysis (*K2P*) is described in Kimura (1980).

Both transitions and transversions were included in phylogenetic analyses. Before evolutionary reconstruction of haplotypes, the freeware program Modeltest 3.7 (Posada and Crandall, 1998) was used to determine the model of sequence evolution which had the highest likelihood. Briefly, 56 nested models of evolution were tested against raw sequence data with the program PAUP 4.0b1 (Phylogenetic Analysis Using Parsimony, available from Sinauer Associates, Inc., Sunderland, MA). Modeltest was then used to perform hierarchical likelihood ratio testing (hLRT) in order to identify the model with the highest likelihood. Concurrently, the Akaike information criterion (AIC) weights of the four most likely models were also examined during model selection. The appropriate model was subsequently used in a maximum-likelihood (ML) procedure in PAUP 4.0b1, with 10 replicates, to reconstruct an unrooted haplotype phylogeny. Because of the enormous computational load associated with maximum likelihood of highly variable loci, a concurrent N-J tree was constructed by using the 2-parameter distance of Kimura (1980); this tree was bootstrapped (1000 replicates over nucleotides, Felsenstein, 1985) to evaluate the significance of major interior nodes that correlated with nodes on the maximum-likelihood tree.

Results

Microsatellite data set

Microsatellite samples were distributed from southern Texas to the Gulf of Maine, the northern extent of *B. tyrannus*. *Brevoortia tyrannus* was sampled in three locations (all Atlantic coast), *B. smithi* in two locations (one Atlantic, one eastern Gulf), *B. patronus* in 14 locations (all Gulf coast), and *B. gunteri* in three locations (all western Gulf coast). Of the five microsatellite markers used in this study, all had observed levels of heterozygosity that were lower than anticipated under Hardy-Weinberg expectations when tested by using samples

Table 1

Short tandem repeat locus statistics (listed by National Center for Biotechnology Information accession number) averaged over 13 populations of Gulf menhaden (*Brevoortia patronus*, n=260). Statistics include the DNA base motif (each allele is distinguished by "x" number of repetitions of the motif), observed (H_o) and expected (H_e) heterozygosity, number of alleles (k_a), and deviation from Hardy-Weinberg expected genotype frequencies (measured by deviation of F_{is} from 0).

Locus	Primer sequence	Motif	H_o	H_e	k_a (overall)	F_{is} (overall)
AF049462	*F: GGAGGCACAGGTGTGGTATT* *R: TTTGGAGGGAGAGAAACGTC*	$[GTT]_x$	0.84	0.93	31	0.09
AF039658	*F: TAATAAACCCCGTTGGGACA* *R: GCTGATGTTCCTCCATCTCC*	$[CAA]_x$	0.78	0.87	23	0.10
AF039657	*F: GCCATTACTCCAAGTTGCTTTT* *R: CGTGGCACAACATAGTCATCA*	$[CTT]_x$	0.70	0.73	20	0.05
AF039661	*F: TGCTTTAATCCGGAATGGAC* *R: GGGGAGTGAGAGAACGAGTG*	$[CTTT]_x$	0.15	0.20	10	0.24
AF039660	*F: GGAGCTCAGCACATCTCTCC* *R: CTGACATGGCCCAGTAGGTT*	$[GTTT]_x$	0.26	0.58	13	0.55*

* indicates that F_{is} is significantly different from zero in a majority of *B. patronus* populations sampled after correction for multiple tests, determined by a randomization procedure with 1000 iterations.

of *B. patronus* individuals from the Gulf of Mexico (n=260, Table 1). One locus (AF39661) had a high overall value of F_{is}, but was not significantly different than zero based on randomization tests. However, a second locus (AF39660) had lower than expected heterozygosity at a significant level in a majority of the populations assayed. Whether the explanation for decreased levels of heterozygosity is biological or simply sampling error is unclear; however analyses excluding this marker had little effect on tree topology or other results. Multilocus estimates of genetic divergence (F_{st}) were lowest within the predefined menhaden groups; that is, the level of divergence seen in the comparisons between *B. patronus+tyrannus* and *B. smithi+gunteri* was lower than any other pairwise comparisons among species (Table 2). Similarly, the N-J tree constructed from microsatellite data was deeply bifurcated (Fig. 2) and the two major groupings on this tree corresponded to populations of small-scaled and large-scaled menhaden, exclusively. Four major clusters on this tree corresponded to the populations of each of the four assayed species. The greatest level of within-species divergence was observed between the Atlantic and Gulf populations of *B. smithi*. The divergence among these populations was an order of magnitude higher than the mean divergence from comparisons among populations of the same species, and was 5.5 standard deviations removed from the mean of all F_{st} comparisons combined (F_{st}^{smithi}=0.0523, $F_{st}^{overall}$=0.0054, σ^2=0.0094).

Table 2

Genetic divergence among Atlantic menhaden (*Brevoortia tyrannus*), Gulf menhaden (*B. patronus*), yellowfin menhaden (*B. smithi*), and finescale menhaden (*B. gunteri*), as measured by using multilocus microsatellite data (F_{st}, above the diagonal) and mtDNA sequence similarity among populations (D_a, below the diagonal).

	B. tyrannus	*B. patronus*	*B. smithi*	*B. gunteri*
B. tyrannus	0	0.110	0.448	0.412
B. patronus	0.005	0	0.411	0.378
B. smithi	0.077	0.093	0	0.355
B. gunteri	0.071	0.088	0.004	0

Bayesian analysis of population structure resulted in four well-defined clusters corresponding to the four assayed species (Fig. 3). However, no single species contained exclusively one cluster; each species had individuals with composite genotypes including influence from other clusters. In particular, admixture among the two large-scaled species was indicated by individuals of each species in which a majority of the genotype was contributed by the complimentary species. A smaller level of admixture was indicated in the small-scaled species. However, one interesting result was a single individual *B. gunteri* which had 0.723 of its genotype contributed by the *B. patronus* cluster. This is significant in that, although the possibility of hybridization in the western Gulf has not been ruled out (Anderson and McDonald, 2007), a verified F1 *B. patronus+gunteri* hybrid has not been documented in the Gulf.

Estimates of genetic variability including H_e, k_a, and θ_F were higher in large-scaled species of menhaden than in small-scaled species (Table 3). Multilocus expected heterozygosity ranged from 0.672 in *B. patronus* and

Table 3

Genetic diversity estimates over four nuclear loci (AF49462, AF39658, AF39657, and AF39661) and the mtDNA control region locus, for Atlantic menhaden (*Brevoortia tyrannus*), Gulf menhaden (*B. patronus*), finescale menhaden (*B. gunteri*), and yellowfin menhaden (*B. smithi*). The diversity estimates include allelic diversity (k, alleles/locus) at each microsatellite locus and overall (k_a), multilocus expected heterozygosity (H_e), relative effective population size estimated from multi-locus heterozygosity (θ_F), the 95% confidence range of mtDNA nucleotide diversity (π), and the 95% confidence range of mtDNA haplotype diversity (h). Sample sizes were equal (n=39) in all comparisons unless otherwise noted.

Species	*AF49462* (k)	*AF39658* (k)	*AF39657* (k)	*AF39661* (k)	k_a	H_e	θ_F	π	h
Brevoortia tyrannus	20	14	15	3	13.0	0.67	4.15	0.064–0.086 (n=37)	0.99–1.00 (n=37)
Brevoortia patronus	19**	16**	9**	4**	12.0	0.67	4.15	0.046–0.054 (n=30)	0.99–1.00 (n=30)
Brevoortia gunteri	11	11	3	1	6.5	0.41	0.90	0.038–0.055 (n=14)	0.95–1.00 (n=14)
Brevoortia smithi	8	4	2	2	4.0	0.37	0.76	0.030–0.037 (n=32)	0.92–1.00 (n=32)

** Allelic counts for *B. patronus* are different from those presented in Table 1 because fewer individuals were used to account for smaller sample sizes in the three remaining species.

B. tyrannus, to 0.413 in *B. gunteri* and 0.370 in *B. smithi*. This disparity is due to near fixation of alleles in both small-scaled species at a single locus which is highly polymorphic in both large-scaled species (AF39657), but also reflects decreased variability at all marker loci. As a result, the estimates of θ_F in large-scaled species were four to five times larger than those for small-scaled species.

Sequencing data set

The mtDNA sequencing data set indicates an enormous amount of genetic variation in the control region of menhaden (Table 3), although this variation was not evenly distributed across the entire alignment. In particular, regions of sequence conservation in the data set were directly adjacent to highly degenerate regions more typical of the mitochondrial control region of clupeids (Grant et al., 1998). Over a total dataset of 360 bp, 149 sites were polymorphic, and pairwise sequence comparisons resulted in an average of 28.7 nucleotide differences among haplotypes. Of 113 individuals assayed, 106 haplotypes were identified in the four species. Despite this high level of sequence divergence, only three single-base deletions were detected in the multiple alignment of 113 individuals (deletions were treated as missing data). The control region of menhaden is A-T rich (contains greater than 50% adenine and thymine bases), with averaged base frequencies of A = 0.269, T = 0.487, C (cytosine) = 0.156, and G (guanine) = 0.167, and with no evidence for heterogeneity of base frequencies among taxa (χ^2=59.40, P~1.00).

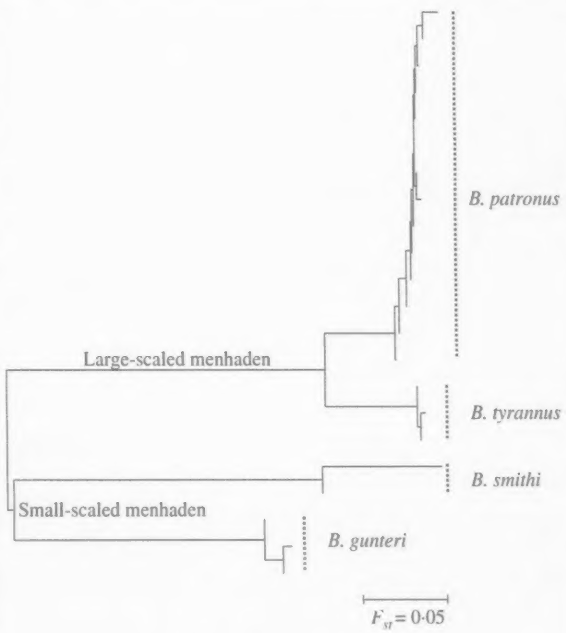

Figure 2

Neighbor-joining dendrogram of populations (n=20, in each population) of Gulf menhaden (*Brevoortia patronus*), Atlantic menhaden (*B. tyrannus*), finescale menhaden (*B. gunteri*), and yellowfin menhaden (*B. smithi*). The distance metric used for neighbor-joining was F_{st} (Weir and Cockerham, 1984), which is the estimated proportion of genetic variance that is due to between-population effects.

The estimated ts/tv ratio was 2.1:1. As was the case in comparisons using microsatellites, the mtDNA distance among species (D_a) was lowest in comparisons between species within small-scaled and large-scaled groups (Table 2).

Hierarchical likelihood ratio tests indicated that the K81uf+I+Γ model (Kimura, 1981) was the most appropriate model of sequence evolution at the control region locus. This model also had the second highest AIC weight, at 0.23. The K81uf+I+Γ model approximates the rate of heterogeneity across sites (a property which can simply be described as unequal probabilities of mutations among sites) by using a gamma distribution, after variant sites have been removed. Haplotype phylogenies generated with both the M-L method and the N-J cluster method indicated three divergent lineages of menhadens (Fig. 4), and these lineages were identical in haplotype membership between the two tree-building methods. The first lineage had 99% bootstrap support and included haplotypes contributed from both *B. patronus* and *B. tyrannus*. This main group of large-scaled haplotypes ($n=59$) was characterized primarily by transitions and had minimal (<7) transversions among haplotypes. A second, small group of divergent Atlantic menhaden occurred in the haplotype phylogeny, with 100% bootstrap support. This second group comprised the remaining eight large-scaled haplotypes and differed from the first group by 14+ transversions per haplotype, likely the result of mutation saturation. Plots of transitions and transversions indicated that this data set was saturated; the rate of transversions begins to rival that of transitions at approximately a Kimura distance of 0.10 (Fig. 5A). Although saturation is indicated in cases where divergent haplotype clades are compared, saturation is not indicated in comparisons involving within-clade comparisons (Fig. 5, B–D). Thus, the main effect of saturation on this data set was on longer (more divergent) branches. A third lineage on the maximum likelihood tree had 100% bootstrap support and consisted of haplotypes contributed by *B. gunteri* and *B. smithi* in paraphyly. Haplotypes in this clade indicated incomplete sorting of mtDNA haplotypes within the small-scaled menhadens. However, there was clear evidence for genetic divergence between this group and both large-scaled clades, and 100% bootstrap support for monophyly of the small-scaled haplotypes.

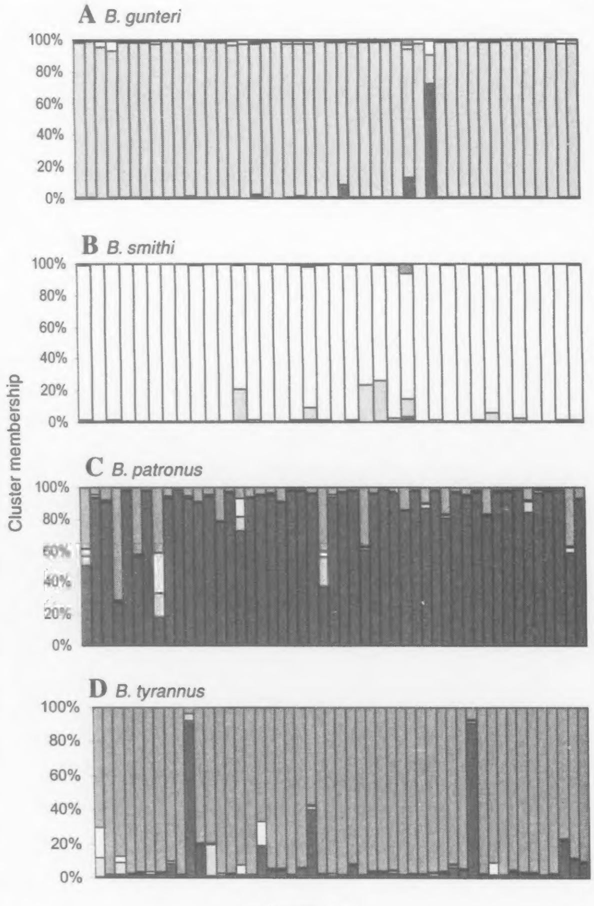

Figure 3

Bayesian assignment tests resulted in recovery of four putative source populations of genotypic data. Individuals were separated into their respective species groups (**A–D**), and genetic identity was assigned based upon the percentage of an individual's genotype contributed by each of the four source populations, as indicated on the *y*-axis. Genetic source populations are represented by light grey (finescale menhaden [*Brevoortia gunteri*], white (yellowfin menhaden, [*B. smithi*]), black (Gulf menhaden [*B. patronus*]), and dark grey (Atlantic menhaden [*B. tyrannus*]).

Discussion

The morphological differences among the four North American menhaden species have been examined previously at egg, larval, juvenile, and adult stages (Dahlberg, 1970 [and references therein]; Hettler, 1984; Ahrenholz, 1991; Tolan and Newstead, 2004), and previous classifications have the species divided between small-scaled and large-scaled groups (Dahlberg, 1970). The results presented here reinforce the conventional hypothesis that *B. smithi* and *B. gunteri* share recent common ancestry as do *B. patronus* and *B. tyrannus*. Both classes of genetic markers showed significant genetic divergence between the two menhaden types, and this distinction is reinforced by demographic characteristics shared within these groups. Specifically, overall census sizes (Christmas and Gunter, 1960), species ranges (Christmas and Gunter, 1960), and migratory behavior (Gunter, 1945; Simmons, 1957; Tolan and Newstead, 2004) are markedly different between the small-scaled and large-scaled species pairs, yet similar between species within these pairs. The differences in the demographics of small-scaled and large-scaled menhaden are reflected in nuclear-based estimates of $N_e\mu$, which are four to five times larger in large-scaled species. Smaller population sizes, and relatively shorter overall coastal ranges, are reflected in the lower genetic variability of small-scaled menhaden compared to large-scaled menhaden. In addition, nutritional and trophic differences among these species in the western Gulf have previously been documented (Castillo-Rivera et al., 1996; Castillo-Rivera and Kobelkowsky, 2000) and may represent mechanisms for the divergence of population demographic parameters among these groups.

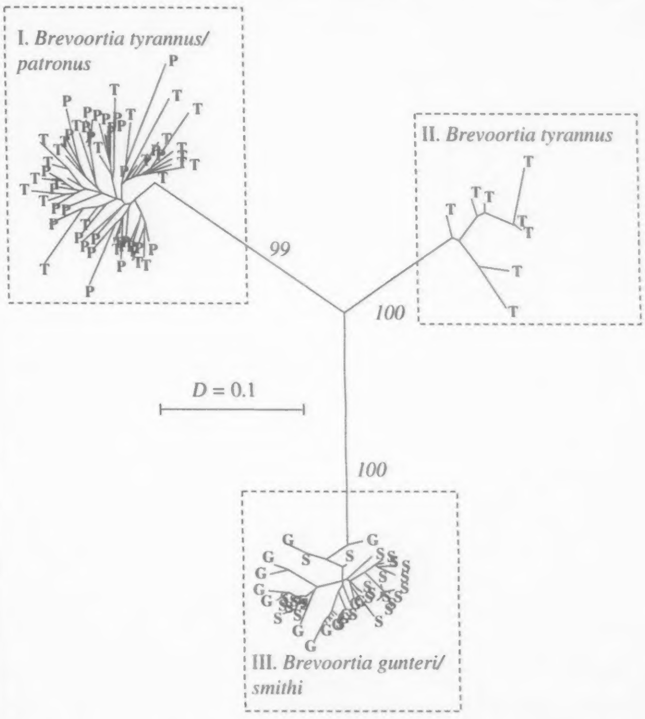
I. *Brevoortia tyrannus/ patronus*
II. *Brevoortia tyrannus*
99
100
D = 0.1
100
III. *Brevoortia gunteri/ smithi*

Figure 4

Maximum likelihood plot of unrooted menhaden mtDNA samples. The numbers at the base of each of three divergent clades (99, 100, and 100) are the bootstrap support values from a neighbor joining analysis. The genetic distance (*D*) between links in the phylogeny is a modified version of Kimura's distance (1981), which includes gamma-distributed rate variation after invariant sites are removed, as outlined in Modeltest software (Posada, 1998). The roman numerals correspond to clade numbers as discussed in the text, including clade I (mixture of haplotypes from Gulf menhaden [*Brevoortia patronus*] and Atlantic menhaden [*B. tyrannus*]), clade II (haplotypes from *B. tyrannus* only), and clade III (mixture of haplotypes from yellowfin menhaden, *B. smithi* and finescale menhaden, *B. gunteri*).

In both the present study and the study of Bowen and Avise (1990), high levels of genetic variation were detected in the mtDNA genome of menhaden. Indeed, because of the high mutation rate of the mtDNA region surveyed in this study, saturation was a likely source of bias in comparisons among divergent lineages. A second similarity between this study and that of Bowen and Avise (1990) is the presence of two divergent large-scaled haplotype groups, one that is confined to *B. tyrannus*, and a second which includes haplotypes from both species. Avise (1992) suggested that a likely explanation for this pattern is recent gene flow between these species, rather than incomplete lineage sorting. A Bayesian population assignment of nuclear genotypes seems to support the possibility of admixture between these species, with individuals from both species containing genetic signatures of the complementary group. Epperly (1989, [and references therein]), suggested the existence of two subpopulations of *B. tyrannus* in the Atlantic: one on the southern Atlantic coast (below 40°N) and a subpopulation north of Long Island, New York. Juveniles from these subpopulations differed in meristic and morphological characteristics, and also had different biochemical profiles (Epperly, 1989). Epperly (1989) suggested that the spawning times for these two subpopulations may be different, allowing for recruitment to occur in these areas at different times of the year. Variance in spawning times may be a mechanism for maintenance of divergence between haplotype clades for large-scale menhaden recovered in this study. However, it is likely that the variation in morphology and biochemistry seen in northern and southern forms of Atlantic menhaden is affected by the influence of recurrent gene flow between this species and its Gulf cognate. Avise (1992) demonstrated a broad-scale demographic break between Atlantic and Gulf forms of both terrestrial and marine vertebrates (including menhaden); however, in many species, haplotypes representative of Gulf forms were present in individuals collected in the southern Atlantic. Locales farther north in the Atlantic lack the Gulf haplotypes; in this scenario it would be expected that Atlantic menhaden collected farther north would lack the Gulf menhaden influence. Indeed, in the divergent group of Atlantic menhaden examined in the present study, four of the eight haplotypes came from juveniles collected from the northernmost sampling locale (Maine). The remaining haplotypes came from a single adult from a northern locale (New Jersey), two adults from southern locales (North Carolina), and a southern locale juvenile (North Carolina).

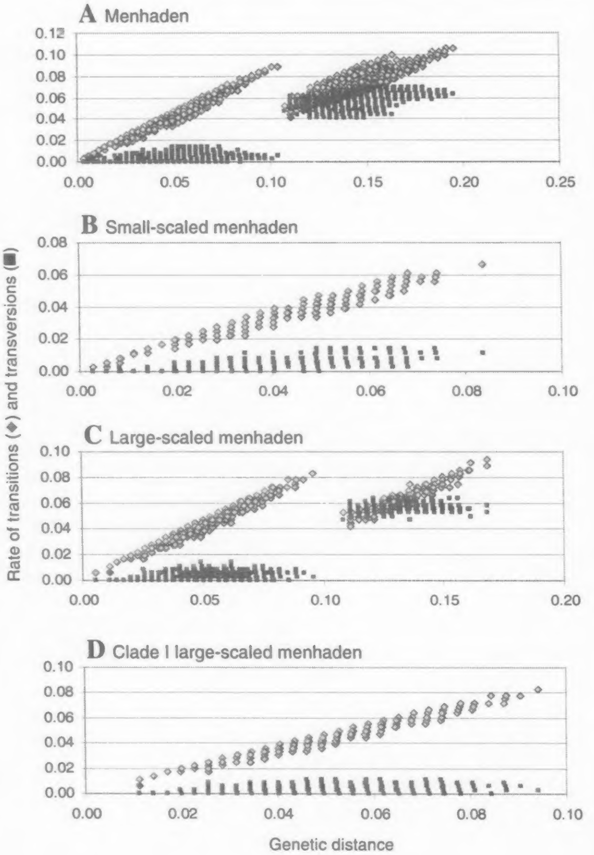

Figure 5

Saturation plots of menhaden mtDNA data. The x-axis represents Kimura (1980) distances between sequences, whereas the y-axis represents the rate of transitions (♦) and transversions (■). A saturation plot was constructed for (**A**) mtDNA samples from all four species, (**B**) samples from small-scaled menhaden only (yellowfin menhaden [*Brevoortia smithi*] and finescale menhaden [*B. gunteri*]), (**C**) samples from large-scaled menhaden only (Gulf menhaden [*B. patronus*] and Atlantic menhaden [*B. tyrannus*]), and (**D**) large-scaled menhaden from mtDNA clade I only.

Previous treatments have recognized two subpopulations of *B. smithi* in the Gulf and Atlantic, and Hildebrand (1963) characterized the eastern Gulf *B. smithi* as intermediate in form between *B. gunteri* and the Atlantic form of *B. smithi*. An interesting note in our data set is the large divergence estimate between two sampled populations of *B. smithi* obtained in the microsatellite analysis. This estimate of divergence between these populations ($F_{st}^{smithi}=0.0523$) is the largest of any comparison and is an order of magnitude greater than the mean comparison among populations of the same species ($F_{st}^{mean}=0.0054$). *Brevoortia smithi* is the only species of menhaden that has significantly large populations in both the Gulf and Atlantic, and populations of this species are rare towards the southern tip of Florida (Reintjes, 1959; Dahlberg, 1970). Thus, vicariance may play a role in divergence between these populations. It is clear that biological differences between Atlantic and Gulf forms of *B. smithi* extend into the genetic data presented here, resulting in long branches in the microsatellite-based topology. In addition, the smaller relative census sizes of small-scaled menhaden species has likely resulted in a faster and more distinctive pattern of divergence among populations of these species than what has occurred in large-scaled species. Further investigation is needed in order to determine if the genetic divergence between Gulf and Atlantic forms of *B. smithi* is genome-wide.

A final peculiarity of the data was a single individual *B. gunteri* which had a genotype that indicated influence from *B. patronus* (Fig. 3). Specifically, this individual had an estimated 72.3% of its genotype contributed by a cluster roughly representative of *B. patronus*, whereas all other individuals of this species had less than a 10% contribution from this cluster (averaged around 2.7%). Although high rates of hybridization between *B. smithi* and both large-scaled menhaden species have been documented in peninsular Florida (Turner, 1969; Hettler, 1984), hybrids between *B. gunteri* and *B. patronus* have not been documented (Anderson and McDonald, 2007). Visual inspection of the individual in question yielded no morphological evidence of hybridization. In addition, Bayesian assignment can be expected to perform better if more loci are sampled. Although five microsatellite loci were adequate to recover evidence for population structure in the present data set, individual assignments based on limited genetic loci will comprise a high level of uncertainty

(Corander et al., 2006). However, given the result here and a similar individual possible occurrence documented in Anderson and McDonald (2007), rare hybridization events between *B. gunteri* and *B. patronus* cannot be ruled out.

Acknowledgments

The following are to be acknowledged for their assistance in completing this work. B. Mobley, K. Anderson, and H. Hendrickson provided technical laboratory assistance. B. Bumguardner, B. Karel, M. Fisher, J. Mambretti, T. Stelly, D. McDonald, S. Grant, and four anonymous reviewers provided thoughtful comments on the manuscript. Texas samples were collected by numerous individuals during routine monitoring of Texas estuarine ecosystems by staff of Texas Parks and Wildlife Department, Coastal Fisheries Division. The following provided samples from outside of Texas: R. McMichael and the staff of the fisheries-independent monitoring program at the Florida Fish and Wildlife Conservation Commission, especially T. Tuckey, D. Adams, and C. Idelberger; J. W. Smith at the National Marine Fisheries Service, National Oceanic and Atmospheric Administration, Beaufort Laboratory in Beaufort, NC; and B. Tarbox at the Southern Maine Community College. This research was funded in part by a Federal Aid in Sport Fish Restoration Grant (F-144-R).

Literature cited

Ahrenholz, D. W.
1981. Recruitment and exploitation of Gulf menhaden, *Brevoortia patronus*. Fish. Bull. 79:325–335.
1991. Population biology and life history of the North American menhadens, *Brevoortia* spp. Mar. Fish. Rev. 53:3–19.

Anderson, J. A., and D. L. McDonald.
2007. Morphological and genetic investigations of two western Gulf of Mexico menhadens (*Brevoortia* spp.). J. Fish Biol. 70(S):139–147.

Avise, J. C.
1992. Molecular population structure and the biogeographic history of a regional fauna: a case history with lessons for conservation biology. Oikos 63:62–76.

Avise, J. C., B. W. Bowen, and T. Lamb.
1989. DNA fingerprints from hypervariable mitochondrial genotypes. Mol. Biol. Evol. 6:258–269.

Bernatchez, L., and R. G. Danzmann.
1993. Congruence in control-region sequence and restriction-site variation in mitochondrial DNA of brook charr (*Salvelinus fontinalis* Mitchill). Mol. Biol. Evol. 10:1002–1014.

Bethea, D. M., J. A. Buckel, and J. K. Carlson.
2004. Foraging ecology of the early life stages of four sympatric shark species. Mar. Ecol. Prog. Ser. 268:245–264.

Bowen, B. W., and J. C. Avise.
1990. Genetic structure of Atlantic and Gulf of Mexico populations of sea bass, menhaden and sturgeon: influence of zoogeographic factors and life-history patterns. Mar. Biol. 107:371–381.

Brown, B. L., J. M. Epifanio, P. E. Smouse, and C. J. Kubiak.
1996. Temporal stability of mtDNA haplotypes frequencies in American shad stocks: to pool or not to pool across years? Can. J. Fish. Aquat. Sci. 53:2274–2283.

Castillo-Revera, M., and A. Kobelkowsky.
2000. Distribution and segregation of two sympatric *Brevoortia* species (Teleostei:Clupeidae). Estuar. Coast. Shelf Sci. 50:593–598.

Castillo-Revera, M., A. Kobelkowsky, and V. Zamayoa.
1996. Food resource partitioning and trophic morphology of *Brevoortia gunteri* and *B. patronus*. J. Fish Biol. 49:1102–1111.

Christmas, J. Y., and G. Gunter.
1960. Distribution of menhaden, genus *Brevoortia*, in the Gulf of Mexico. Trans. Am. Fish. Soc. 89:338–343.

Corander, J., P. Marttinen, and S. Mäntyniemi.
2006. A Bayesian method for identification of stock mixtures from molecular marker data. Fish. Bull. 104:550–558.

Dahlberg, D. W.
1970. Atlantic and Gulf of Mexico menhadens, genus *Brevoortia* (Pisces: Clupeidae). Bull. Fla. Mus. Nat. Hist. Biol. Sci. 15:91–162.

Epperly, S. P.
1989. A meristic, morphometric and biochemical investigation of Atlantic menhaden, *Brevoortia tyrannus* (Latrobe). J. Fish Biol. 35:139–152.

Felsenstein, J.
1985. Confidence limits on phylogenies: An approach using the bootstrap. Evolution 39:783–791.

Gottlieb, S. J.
1998. Ecological role of Atlantic menhaden (*Brevoortia tyrannus*) in Chesapeake Bay and implications for management of the fishery. M.S. thesis, 126 p. Univ. of Maryland, College Park, MD.

Goudet, J.
1995. FSTAT (vers. 1.2): a computer program to calculate F-statistics. J. Hered. 86:485–486.

Grant, W. S., A. M. Clark, and B. W. Bowen.
1998. Why restriction fragment length polymorphism analysis of mitochondrial DNA failed to resolve sardine (*Sardinops*) biogeography: insights from mitochondrial DNA cytochrome *b* sequences. Can. J. Fish. Aquat. Sci. 55:2539–2547.

Gunter, G.
1945. Studies on marine fishes of Texas. Publ. Inst. Mar. Sci. 1:1–190.

Hare, M. P., and J. C. Avise.
1998. Population structure in the American oyster as inferred by nuclear gene genealogies. Mol. Biol. Evol. 15:119–128.

Hettler, W. F.
1984. Description of eggs, larvae, and early juveniles of gulf menhaden, *Brevoortia patronus*, and comparisons with Atlantic menhaden, *B. tyrannus*, and yellowfin menhaden, *B. smithi*. Fish. Bull. 82:85–95.

Hildebrand, S. F.
1963. Family Clupeidae. *In* Fishes of the western North Atlantic Memoir 1, Part 3 (Y. H. Olsen, ed.), p.257–454. Sears Foundation Mar. Res., Yale Univ., New Haven, CT.

Jarne, P., and J. L. Lagoda.
1996. Microsatellites, from molecules to populations and back. Trends Ecol. Evol. 11:424–429.

Jeanmougin, F., J. D. Thompson, M. Gouy, D. G. Higgins, and T. J. Gibson.
1998. Multiple sequence alignment with Clustal X. Trends Biochem. Sci. 23:403–405.

Kimura, M. A.
1980. Simple method for estimating evolutionary rates of base substitutions through comparative studies of nucleotide sequences. J. Mol. Evol. 16:111–120.
1981. Estimation of evolutionary distances between homologous nucleotide sequences. Proc. Nat. Acad. Sci. 78:454–458.

Kroger, R. L, and J. F. Guthrie.
1972. Effect of predators on juvenile menhaden in clear and turbid estuaries. Mar. Fish Rev. 34:78–80.

Kumar, S., K. Tamura, I. B. Jakobsen, and M. Nei.
2001. Mega2: Molecular Evolutionary Genetics Analysis Software. Bioinformatics 12:1244–1245.

Nei, M.
1987. Molecular evolutionary genetics, 1st ed., 512 p. Columbia Univ. Press, New York, NY.

Nielsen, R.
1997. A likelihood approach to populations samples of microsatellite alleles. Genetics 146:711–716.

Posada, D., and K. A. Crandall.
1998. Modeltest: testing the model of DNA substitution. Bioinformatics 14:817–818.

Pritchard, J. K, M. Stephens, and P. Donnelly.
2000. Inference of population structure using multilocus genotype data. Genetics 155:945–959.

Reintjes, J. W.
1959. Continuous distribution of menhaden along the south Atlantic and Gulf coasts of the United States. Proc. Gulf Carib. Fish. Inst. 12:31–35.

Rozas, J., J. C. Sanchez-DelBarrio, X. Messeguer, and R. Rozas.
2003. DnaSP, DNA polymorphism analyses by the coalescent and other methods. Bioinformatics 19:2496–2497.

Scharf, F. S., and K. K. Schlicht.
2000. Feeding habits of red drum (*Sciaenops ocellatus*) in Galveston Bay, Texas: Seasonal diet variation and predator-prey size relationships. *Estuaries* 23:128–139.

Simmons, E. G.
1957. An ecological survey of the upper Laguna Madre of Texas. Publ. Inst. Mar. Sci. Univ. Tex. 4:156–200.

Tolan, J. M., and D. A. Newstead.
2004. Descriptions of larval, prejuvenile, and juvenile finescale menhaden (*Brevoortia gunteri*) (family Clupeidae), and comparisons to Gulf menhaden (*B. patronus*). Fish. Bull. 102:723–732.

Turner, W. R.
1969. Life history of menhadens in the eastern Gulf of Mexico. Trans. Am. Fish Soc. 98:216–224.

Valdes, A. M., M. Slatkin, and N. B. Freimer.
1993. Allele frequencies at microsatellite loci: the stepwise mutation model revisited. Genetics 133:737–749.

Vaughan, D. S., and J. V. Merriner.
1991. Assessment and management of Atlantic and Gulf menhaden stocks. Mar. Fish Rev. 53:47–55.

Weir, B. S., and C. C. Cockerham
1984. Estimating F-statistics for the analysis of population structure. Evolution 38:1358–1370.

Wright, J. M., and P. Bentzen.
1994. Microsatellites: genetic markers for the future. Rev. Fish Biol. 4:384–388.

Xia, X., and Z. Xie.
2001. DAMBE: Data analysis in molecular biology and evolution. J. Heredity 92:371–373.

Xu, H., and Y. X. Fu.
2004. Estimating effective population size or mutation rate with microsatellites. Genetics 166:555–563.

Vertical movement patterns of skipjack tuna (*Katsuwonus pelamis*) in the eastern equatorial Pacific Ocean, as revealed with archival tags

Kurt M. Schaefer (contact author)
Daniel W. Fuller
Email address for K. M. Schaefer: kschaefer@iattc.org
Inter-American Tropical Tuna Commission
8604 La Jolla Shores Drive
La Jolla, California 92037-1508

Abstract—Thirty-three skipjack tuna (*Katsuwonus pelamis*) (53–73 cm fork length) were caught and released with implanted archival tags in the eastern equatorial Pacific Ocean during April 2004. Six skipjack tuna were recaptured, and 9.3 to 10.1 days of depth and temperature data were downloaded from five recovered tags. The vertical habitat-use distributions indicated that skipjack tuna not associated with floating objects spent 98.6% of their time above the thermocline (depth=44 m) during the night, but spent 37.7% of their time below the thermocline during the day. When not associated with floating objects, skipjack tuna displayed repetitive bounce-diving behavior to depths between 50 and 300 m during the day. The deepest dive recorded was 596 m, where the ambient temperature was 7.7°C. One dive was particularly remarkable because the fish continuously swam for 2 hours below the thermocline to a maximum depth of 330 m. During that dive, the ambient temperature reached a low of 10.5°C, and the peritoneal cavity temperature reached a low of 15.9°C. The vertical movements and habitat use of skipjack tuna, revealed in this study, provide a much greater understanding of their ecological niche and catchability by purse-seine fisheries.

Manuscript submitted 10 October 2006 to the Scientific Editor's Office.

Manuscript approved for publication 12 January 2007 by the Scientific Editor.

Fish. Bull. 105:379–389 (2007)

Limited information on the vertical movements of skipjack tuna (*Katsuwonus pelamis*) is available from analyses of catch data for tuna longline gear (Yabe et al., 1963), ultrasonic telemetry (Dizon et al., 1978; Schaefer and Fuller, 2005; Matsumoto et al.[1]), and archival tags (Ogura[2]). These studies have indicated that skipjack tuna inhabit predominantly the mixed layer but make occasional brief dives below the thermocline.

Skipjack tuna are distributed throughout the world's tropical and subtropical oceans (Collette and Nauen, 1983; Matsumoto et al., 1984). In the eastern Pacific Ocean (EPO), catches of this species have occurred from about 34°N off southern California to about 27°S off northern Chile. The species is limited to surface temperatures of about 17° to 30°C (Wild and Hampton, 1994). Skipjack tuna are one of three principal targets of a large-scale purse-seine fishery in the EPO and are caught mostly in association with floating objects between about 10°N and 15°S. The purse-seine catch of skipjack tuna in the EPO during 1995–2004 averaged 197 thousand metric tons (t) (range: 129 to 295 thousand t), which is 160% greater than the average of 76 thousand t (range: 51 to 95 thousand t) during the previous 10-year period (Anonymous, 2005).

The anatomical and physiological adaptations of skipjack tuna characterize them as highly efficient opportunists for exploiting their oceanic vertical habitat. Their body shape, fin configurations, and musculature are close to optimum for relatively fast, sustained, and burst swimming (Magnuson, 1978; Altringham and Shadwick, 2001). They lack a swim bladder (Godsil and Byers, 1944), are capable of physiological thermoregulation (Dizon and Brill, 1979), and have relatively rapid gastric evacuation rates (Magnuson, 1969).

Skipjack tuna possess a well-developed large central rete, in addition to epaxial and hypaxial vessels and retia (Stevens et al., 1974; Graham and Dickson, 2001). The counter-current retia provide a thermoconserving mechanism enabling metabolic heat to be retained within the muscles and thus elevate body temperatures above that of ambient water temperatures (Graham, 1975; Stevens and Neill, 1978). The anatomical specializations enhance the thermal inertia of this species and enable this species to slow the cooling rate of the body. Thermal inertia allows skipjack tuna to undertake brief dives into cooler waters below the thermocline to exploit deep prey resources or to escape predators (Neill et al., 1976; Stevens and Neill, 1978).

---

[1] Matsumoto, T., H. Okamoto, and M. Toyonaga. 2006. Behavioral study of small bigeye, yellowfin and skipjack tunas associated with drifting FADs using ultrasonic coded transmitter in the central Pacific Ocean. Information Paper 7, 25 p. Second regular session of the scientific committee. Western and Central Pacific Fisheries Commission, P.O. Box 2356, Kolonia, Pohnpei FM 96941.

[2] Ogura, M. 2003. Swimming behavior of skipjack, *Katsuwonus pelamis*, observed by the data storage tag at the northwestern Pacific, off northern Japan, in summer of 2001 and 2002. Working Paper SKJ-7, 10 p. Sixteenth meeting of the standing committee on tuna and billfish, Sec. Pac. Comm., Noumea, New Caledonia, B.P. D5 Noumea Cedex, New Caledonia.

The objectives of this investigation were to elucidate vertical movement patterns of and habitat use by skipjack tuna in the equatorial EPO. By examining the behavioral and physiological constraints and environmental variables that define skipjack tuna vertical habitat, we can improve our ecological understanding and provide useful data for inclusion in stock assessments.

Materials and methods

Tag releases

Thirty-three skipjack tuna were captured, tagged, and released during 9–10 April 2004 in close proximity to a Tropical Atmosphere-Ocean (TAO) mooring at 1°59′N 95°19′W in the equatorial EPO. The estimated depth of the seafloor at the TAO mooring was 3091 m. Tagging was conducted on the chartered FV *Her Grace*, a 17.7-m pole-and-line fishing vessel. The tagged fish (tagged from an aggregation estimated at 10 t of skipjack tuna), remained associated with the tagging vessel as it drifted away from the TAO mooring at 0520 h on 11 April 2004 until 0940 h and about 15 km west of the mooring, when the aggregation dispersed as the vessel departed at about at a cruising speed of 8 kt.

The archival tags (ATs) used in this study were model LTD_1100 (Lotek Wireless Inc., St. John's, Newfoundland, Canada). The tag is a rectangular solid, measuring 8 mm × 16 mm × 27 mm, and weighing 5 g in air. Information on how to report the recovery of the tag and how to claim the associated reward (US$50) was printed in Spanish on a label encased in the epoxy of the tag.

Depth and temperature data were stored in the memory of the ATs at 28-s intervals. At this sampling rate, the memory of each AT (64 KB) was capable of storing 10.7 days of data. The maximum depth sensing was 1000 m (with a resolution of 0.4%, and an accuracy of ±1%). The temperature sensing range was from −5° to 35°C, with a resolution of 0.2°C and an accuracy of better than 0.3°C.

Skipjack tuna were captured with fishing rods and reels (n=18) and handline gear (n=9) equipped with chrome jigs and barbless hooks during the night, and with pole-and-line gear (n=6) and by chumming live bait during the day. Each fish was lifted directly into a padded aluminum cradle that was covered with wet smooth vinyl. The fish were placed ventral side up, their eyes were immediately covered with a wet synthetic chamois, the hook was removed, and the condition of the fish was determined. If the fish was in excellent condition (i.e., no damage to the eyes or gills and no significant bleeding), the surgery required for implanting an AT was initiated. An incision about 2 cm long was made with a sterile surgical scalpel blade in the abdominal wall about 1/3 of the distance between the anus and the base of the pelvic fins and about 2 cm to the left of the centerline of the fish. Special care was taken to cut through the dermis and only partially through the muscle, but not into the peritoneal cavity. A gloved finger was inserted into the incision and forced through the muscle into the peritoneal cavity. The tag, sterilized in Betadine solution, was inserted through the incision into the peritoneal cavity, and a 13-cm length of 64-kg spectra line was tied to the tag that protruded outside. The incision was closed with three staples, by using a surgical staple gun.

After implantation of the AT, each fish was also tagged with one numbered 12.5-cm green plastic dart tag (Hallprint, Victor Harbor, Australia), by using tubular stainless steel applicators. Tags were inserted into the dorsal musculature with the barbed heads passing between the pterygiophores below the base of the second dorsal fin, from either side of the fish.

The 33 skipjack tuna released with ATs were measured to the nearest centimeter (mean=66.9 cm fork length (FL), range: 53–73 cm). The fish were then picked up by hand from the cradle and released back into the ocean. The total time that fish were out of the water was less than 1 min. All fish released with ATs were observed to swim away from the vessel after release, and all appeared to be in good condition.

Tag recoveries

Six of 33 skipjack tuna released in 2004 were recaptured (18.2%), but just five of the archival tags were recovered. Data on the fish lengths, release and recapture dates and locations, numbers of days at liberty, and linear displacements of the six fish are given in Table 1. Recapture locations ranged from 341 km to 2548 km and 123° (southeast) to 260° (west) of the release location. Of the six fish recaptured, four were initially caught by using fishing rods and reels, one by using handline gear, and one by using pole-and-line gear.

Data processing

Data were downloaded from the tags, and initial exploratory data analyses were conducted with software provided by the tag manufacturer. For the five skipjack tuna, the behavior for each day at liberty was classified as associated or unassociated with floating objects, on the basis of behavioral characteristics from ultrasonic telemetry observations of skipjack tuna associated with floating objects (reported by Schaefer and Fuller [2005]). For each day at liberty, surface-oriented and deep diving behavior were also classified. Behavior associated with floating objects was characterized by tunas remaining primarily at depths of less than 50 m during the day. Behavior unassociated with floating objects was defined as the behavior of fish that made 10 or more dives to depths greater than 150 m during the daytime within

Table 1

Release and recapture information for six skipjack tuna (*Katsuwonus pelamis*) from which five archival tags were recovered. Archival tag 6553 was not recovered. The lengths given for each skipjack tuna were those recorded at the time of tagging. The release and recapture locations are given in decimal degrees. The linear displacements, in kilometers and directions (degrees), from the release to the recapture locations are given.

		Release		Recapture			Linear displacement	
Tag no.	Length (cm)	Date	Location	Date	Location	Days at liberty	Kilometers	Direction
4881	67	10 Apr 2004	1.98°N 95.32°W	18 Oct 2004	0.17°S 103.18°W	190	906	255°
4885	68	9 Apr 2004	1.98°N 95.32°W	30 Aug 2004	3.33°S 106.07°W	142	1332	244°
4908	67	9 Apr 2004	1.98°N 95.32°W	14 Nov 2004	2.42°S 117.82°W	218	2548	260°
4930	66	10 Apr 2004	1.98°N 95.32°W	6 May 2004	1.25°S 92.35°W	25	487	137°
6553	68	9 Apr 2004	1.98°N 95.32°W	25 May 2004	4.25°S 92.25°W	45	772	153°
6740	69	9 Apr 2004	1.98°N 95.32°W	21 June 2004	0.33°N 92.73°W	72	341	123°

a 24-h period. Surface-oriented behavior was defined as the behavior of fish that remained less than 10 m below the surface for periods greater than 10 minutes. Deep-diving behavior was defined as the behavior of fish that whose dives exceeded 500 m in depth. The quantitative characteristics describing the different types of behavioral events were derived from the AT records for the five fish.

The AT data sets were separated into periods of nighttime and daytime by the times of nautical twilight. Nighttime was classified as the period between the time of the first evening record after nautical twilight until the time of the last morning record before nautical twilight. The individual data sets for night and day were used in evaluations of diel differences in behavior and in habitat use.

The depth data obtained from the archival tags were analyzed in conjunction with ambient ocean temperatures, as measured by a calibrated Sea-Bird SBE 39 time-temperature-depth probe (Sea-Bird Electronics, Seattle, WA) deployed on 9 April 2004 to about 500 m depth near the TAO mooring at which the fish were tagged and released. For ambient temperatures at depths greater than 500 m we utilized the temperatures measured by a CTD (conductivity-depth-temperature) probe deployed off the National Oceanic and Atmospheric Association (NOAA) ship *Ka'imimoana* by the TAO Project Office (NOAA/Pacific Marine Environmental Laboratory) on 15 April 2004 to 1000 m depth near the same TAO mooring. These two temperature-depth profiles to depths of about 500 m, obtained from hydrocasts conducted six days apart, were virtually identical.

Results

Behavior patterns

Evaluations of the complete AT depth records, which ranged from 9.3 to 10.1 days, for the five skipjack tuna (Table 1; tag numbers: 4881, 4885, 4908, 4930, 6740) indicated that all five fish remained associated with the drifting vessel, following separation from the TAO mooring, until the vessel departed the area at 0940 h on 11 April 2004. Within 48 h of the time of separation, all five fish demonstrated distinct behavior unassociated with a floating object, including repetitive bounce diving during the day, and for each of the six subsequent days of the AT depth records. The variability in the daytime unassociated behavior patterns for each of the five fish during the approximate 8 days of AT depth records, following separation from the vessel, indicated that all five fish did not remain together.

The depth records for two representative fish (Fig. 1) showed similarities for both day and night for the first 48-h period, including a change in behavior when the vessel departed. The following day, both fish showed deeper average swimming depths, and the day after that both fish began to show repetitive bounce-diving behavior which continued for the remaining 7 days. The first day in which bounce diving occurred for a skipjack tuna (tag no. 4930), included the deepest dive, to a depth of 596 m, recorded for any of the five fish. During the last 3 days of depth records, in addition to the distinct diel differences seen for both fish, the average depth after a dive for the fish with tag 4930 (mean=47.1 m, 95% confidence interval (CI)=1.1) was significantly deeper (ANOVA: $F=3.9$, $P<0.05$) than for the fish with tag 4885 (mean=20.3 m, 95% CI=3.7). These depth differences and behavior patterns indicate that these two similar-size skipjack tuna did not remain together for long after their separation from the vessel.

Evaluations of the depth records for the five skipjack tuna carrying ATs in the equatorial EPO resulted in the discrimination of four distinct behaviors: 1) behavior associated with floating objects (abbreviated to "associated behavior" in this article; 2) behavior unassociated with floating objects (abbreviated to "unassociated behavior", 3) deep diving behavior, and 4) surface-oriented behavior. For the five archival tag data

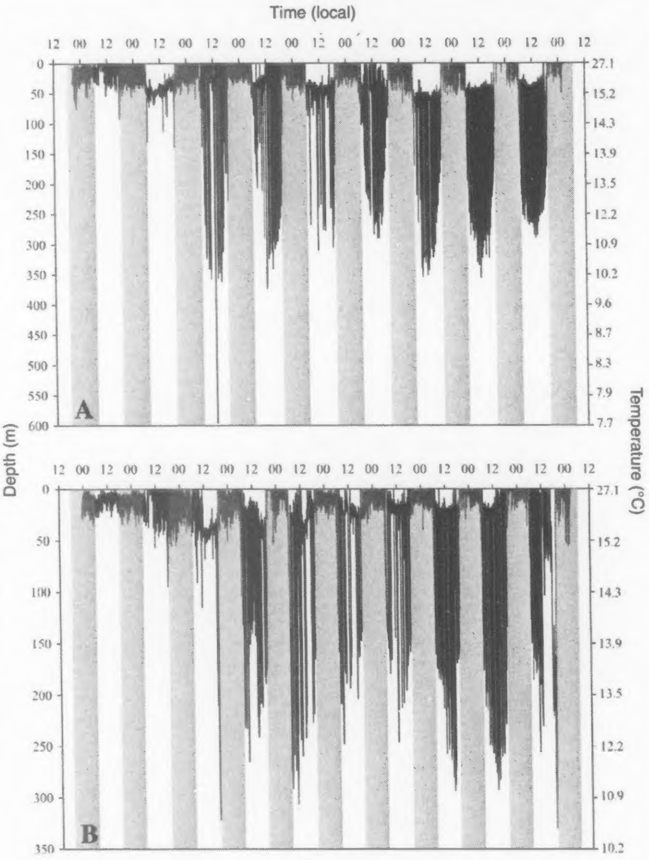

Figure 1

Depth and temperature records for skipjack tuna (*Katsuwonus pelamis*) with implanted archival tags after release. (**A**) Skipjack tuna (tag no. 4930) during April 10–20, 2004. (**B**) Skipjack tuna (tag no. 4885) during April 9–20, 2004. Time periods shaded gray indicate nighttime.

sets, behavior types 1, 2, 3, and 4 were evaluated for each day at liberty, and the descriptive characteristics presented.

Behavior associated with floating objects

The behaviors of the skipjack tuna released at the TAO mooring were distinct and discernible from the behaviors 48 h after the tuna separated from the mooring and the vessel. When the fish were associated with the mooring and the vessel, they remained primarily between the surface and 50 m during the night and day (Fig. 2A). The mean swimming depths were 13.6 m (range: 1–57.4 m) at night and 10.8 m (range: 1–92.3 m) during the day. Shortly before dusk, several dives to about 90 m were recorded, which were followed by an apparent change in the vertical movements during the night. The greater frequency of vertical movements observed during the night (1900 h to 0700 h) within the mixed layer probably represented foraging activity on prey organisms of the deep-scattering layer (DSL).

The delta T values, differences between the peritoneal cavity temperatures and the ambient temperatures (Fig. 2B), corresponding to the simultaneous depth records (Fig. 2A), showed an average of 2.2°C (95% CI=0.1°C, range:–0.4 to 14.1°C) during the day, and an average of 1.8°C (95% CI=0.1°C, range: –0.9 to 12.9°C) during the night. The depths of the mixed layer and the thermocline (depth of the 20°C isotherm) (Fiedler, 1992) were approximately 15 and 44 m, respectively. Whenever skipjack tunas made dives in excess of the thermocline depth, the delta T values were observed

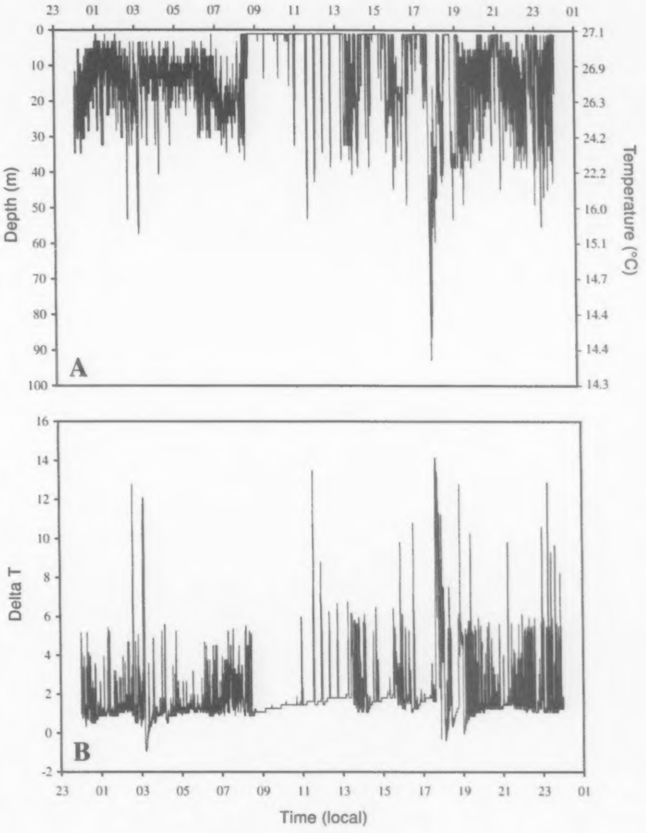

Figure 2

Depth and temperature records for a skipjack tuna (*Katsuwonus pelamis*) with an implanted archival tag (no. 4930) on 11 April 2004. (**A**) Skipjack tuna exhibiting behavior associated with floating objects. (**B**) Delta T's (differences between peritoneal cavity and ambient temperature) for the same time period as in (A).

to spike upward, indicative of the thermal excess of the peritoneal cavity in relation to the ambient temperature.

Behavior unassociated with floating objects

Within 48 hours after the skipjack tuna were unassociated with the vessel, they showed a distinct change in their vertical movements and behavior, exhibiting repetitive bounce diving between about 50 and 300 m during the day (Figs. 1 and 3A). They remained close to the surface at night, primarily within 50 m, showing distinct diel differences in behavior. Figure 3A shows 50 dives in excess of 150 m, and an average duration of 6.8 min (range: 3 to 17 min). The mean depth of these dives was 257 m (range: 153–355 m). During ascents following dives the fish returned to an average depth of 44 m, the approximate depth of the thermocline, before undertaking another dive. The delta T values (Fig. 3B), corresponding to the simultaneous depth records (Fig. 3A), showed an average of 1.9°C (95% CI=0.09°C, range: 0.8–13.5°C) during the night when the fish were primarily in the mixed layer. The delta T values during the day corresponding to the maximum depths of bounce dives were an average of 12.2°C (95% CI=0.3°C, range: 10.2–13.9°C). At the maximum depths of these bounce dives, the mode of the minimum ambient temperature experienced was 11.7°C and the peritoneal cavity temperature was 25.1°C.

For the five skipjack tuna, during days of unassociated repetitive bounce diving behavior, the mode for the time the first dive of the day occurred was 07:10 h (95%

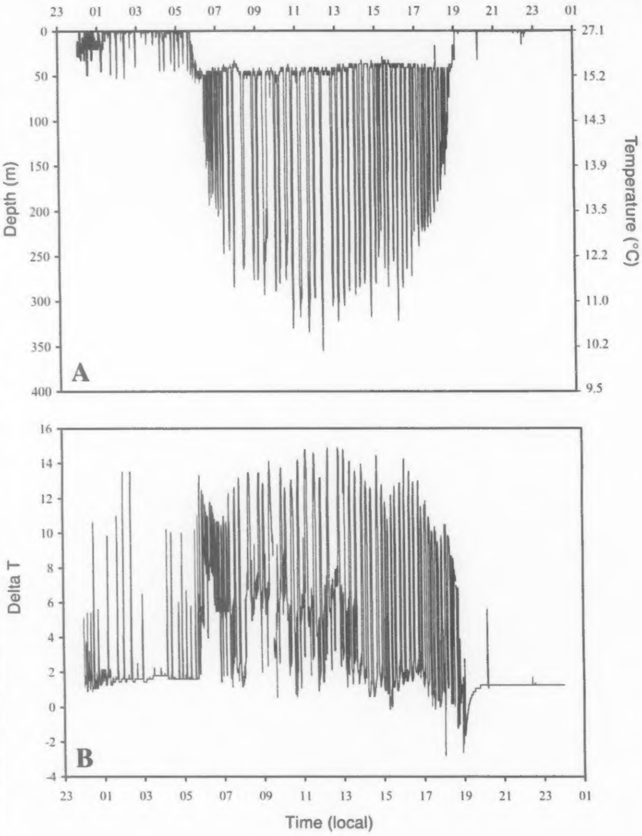

Figure 3

Depth and temperature records for a skipjack tuna (*Katsuwonus pelamis*) with an implanted archival tag (no. 4930) on 18 April 2004. (**A**) Skipjack tuna exhibiting unassociated repetitive bounce diving behavior. (**B**) Delta T's (differences between peritoneal cavity and ambient temperature) for the same time period as in (A).

CI=00:25 h) (Fig. 4A), the mean number of dives made per day was 21.2 (95% CI=4.9) (Fig. 4B), the mean duration of dives was 10.0 min (95% CI=0.9 min), and the mean depth of all dives was 230 m (95% CI=5.7) (Fig. 4C).

One skipjack tuna (tag no. 4885) made an extraordinary dive below the thermocline that lasted 119 min at 1700 h on 19 April 2004. From a depth of 36 m (22.3°C) with a peritoneal cavity temperature of 24.1°C, the fish dived to about 180 m (13.7°C) where it presumably foraged for 1 h 12 min. The fish then dived fairly rapidly to a maximum depth of 330 m (10.5°C) from which it gradually ascended toward the surface, remaining below the thermocline for another 47 min. From echosounder data collected aboard the vessel, it appeared that this fish was tracking the slowly ascending DSL and foraging on prey during this period. The minimum peritoneal cavity temperature observed in this study of 15.9°C was recorded continuously over a period of 7 mintes as this skipjack tuna ascended from 197 to 105 m depth.

Deep diving behavior

Only one of the five skipjack tuna (tag no. 4930) dived in excess of 500 m on 13 April 2004, beginning at 12:16 (Fig. 5). The maximum depth was 596 m, with a duration of 14 min in excess of 300 m (11.0°C), and 1 min 52 seconds in excess of 500 m (8.3°C). The dive profile shows that the fish dived initially to about 300 m where it remained for 4 minutes before continuing to 596 m and returning after about 2 minutes to between

300 m and 250 m, where it remained for about 12 minutes before returning to depths within the mixed layer. The peritoneal cavity temperature and delta T were 28.7°C and 3.8°C, respectively, at the beginning of the dive, 26.1°C and 18.4°C at the bottom of the dive, and 21.8°C and 9.8°C before the quick ascent at 12:38 h from 271 m to above the thermocline.

Surface-oriented behavior

For unassociated behavior, the mean number of surface-oriented events per day ranged from 5 to 23 (grand mean=9.4, 95% CI=2.4). The greatest number and longest duration of surface-oriented events occurred between 01:00 and 12:00 h (Fig. 6, A and B). The duration of events ranged from 10 to 214 min (mean=48.8 min, 95% CI=6.2 min) (Fig. 6 C).

Vertical habitat use

The vertical habitat use by the five skipjack tuna, for unassociated behavior, is presented as composite distributions by night and day along with the thermal profile in Figure 7. The vertical habitat-use distributions indicated that the fish remained above the depth of the thermocline (44 m) during the night 98.6% of the time but spent 37.7% of their time below the thermocline during the day.

Discussion

The results obtained in our study are useful for evaluating vertical movement patterns and habitat use for skipjack tuna on temporal scales previously undocumented. Knowledge about skipjack tuna movements, behavior, and habitat use, when tuna are associated and unassociated with floating objects, specifically in oceanic regions where large-scale industrial purse-seine fisheries operate, are important for understanding the ecology of this species, assessing catchability of the species for inclusion in stock assessments, and for evaluating potential modifications in fishing techniques for reduction of the bycatches of nontarget species.

In the present study, the vertical movement patterns of skipjack tuna when associated with floating objects were similar to those reported by Schaefer and Fuller (2005) for both skipjack and bigeye (*Thunnus obesus*) tunas associated with floating objects in the equatorial EPO. In both studies, the behavior of skipjack tuna was characterized by swimming depths predominantly shallower than the depth of the thermocline, throughout the day and night, and average nighttime depths were slightly deeper than those during the day. A plausible explanation for the greater average depths at night than during the day in these studies is the observed nighttime vertical distribution of the DSL and the foraging behavior of these tunas while associated with the moored buoys and the drifting vessel in this study area (Schaefer and Fuller, 2005). Ultrasonic telemetry

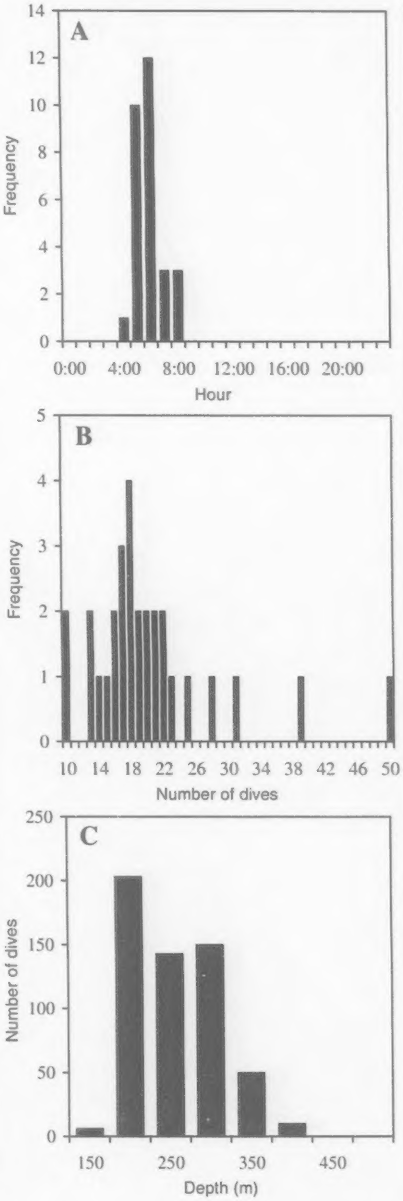

Figure 4

Summary of frequency data for repetitive bounce diving behavior not associated with floating objects for five skipjack tuna (*Katsuwonus pelamis*) over all dives. (**A**) Time the first dive of the day occurred. (**B**) Total number of dives for each day. (**C**) Depth of all dives.

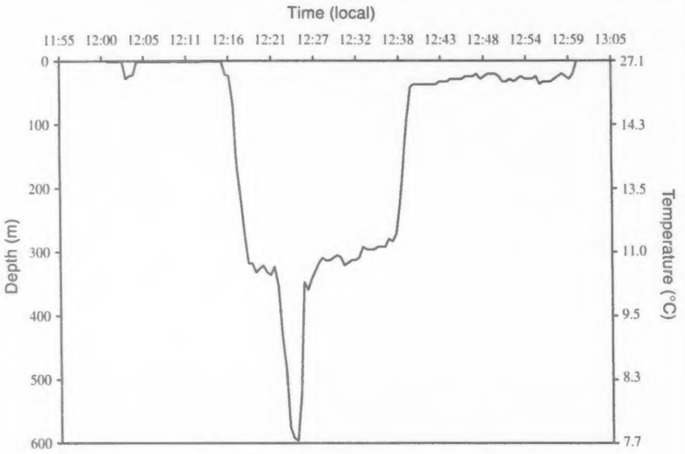

Figure 5

Depth and temperature data for a skipjack tuna (*Katsuwonus pelamis*) (tag no. 4930) exhibiting deep-diving behavior.

studies on the simultaneous behavior of skipjack, bigeye, and yellowfin (*Thunnus albacares*) tunas associated with drifting fish aggregation devices in the central Pacific Ocean also revealed that skipjack tuna swimming depths are predominantly shallower than the thermocline depth, about 115 m, throughout the day and night, but average nighttime depths are shallower than those during the daytime (Matsumoto et al.[1]).

The vertical movement patterns observed in this study for unassociated behavior of skipjack tuna, seen mostly as relatively high frequency repetitive bounce diving between dawn and dusk, was unexpected on account of the data from previously published studies (Matsumoto et al., 1984). There are, however, most likely other vertical movement patterns for skipjack tuna when unassociated with floating objects, from that observed in the present study. This pattern is probably dependent on the spatial and temporal habitat as well as forage availability. In the first published paper on acoustic tracking of tunas (Yuen, 1970), ultrasonic transmitters were used to study the behavior and movements of skipjack tuna off Hawaii. One individual, tracked for 8 days, undertook daily cyclical movements away from and back to a bank at consistent times, and from these movements Yuen (1970) first suggested that skipjack tuna can navigate and have a sense of time. The method Yuen (1970) used was suitable only to conclude that the fish remained close to the surface at night but could be found at various depths during the day. In a subsequent tracking study in Hawaiian waters, three skipjack tuna tagged with ultrasonic transmitters spent time between the surface (23.5°C) and 263 m (13.5°C) during the day, but remained above 75 m (22°C) depth at night (Dizon et al., 1978). Vertical positions of the skipjack tuna were determined only every 3 minutes, but indicated many rapid vertical movements, including some to depths below the thermocline. Although the three tracked skipjack tuna spent 85% of the time in water above 20°C (about 160 m), there were brief dives to temperatures between 12° and 14°C. The data retrieved from seven archival tags recovered from skipjack tuna released off northern Japan indicated that their nighttime movements were normally between the surface and depths of about 30 m, but during the daytime they exhibited frequent dives to depths below the thermocline and below ambient temperatures of 12°C; the greatest depth was reported to be 267 m (Ogura[2]). The lowest peritoneal cavity temperatures recorded in that study were around 17°C, whereas in the present study it was about 16°C. Skipjack tuna held in land-based tanks in Hawaii subjected to gradually lowered temperatures resulted in one mortality at 17°C, and none survived at 15°C for more than a few hours (Dizon et al., 1977).

A relatively dense DSL was observed at night on the echosounder during the time the skipjack tuna were associated with the vessel in this study. Skipjack tuna associated with a TAO mooring in this study area have been documented to be feeding at night near the surface on prey organisms of the DSL (Schaefer and Fuller, 2005). The repetitive bounce diving observed in the present study for unassociated skipjack tuna during the day apparently reflects foraging activity on prey organisms of the diurnally migrating DSL (Kuznetsov et al., 1982). The profile in Figure 3A of repetitive bounce diving shows a higher frequency of dives during the first hour at around dawn when the DSL is descending and during the 1.5 h period preceding dusk during the ascent of the DSL. Sonic tracking studies have also shown that the diel vertical migrations of bigeye tuna are closely associated with vertical movements of organisms of the DSL (Josse et al., 1998; Dagorn et al., 2000). When in areas with a high density DSL it appeared that skipjack tuna were also commonly foraging on DSL prey organisms near the surface at night and at depths well below the thermocline during the day. Depths of the DSL in the eastern tropical Pacific have been reported to be 300–400 m during the day and 0–100 m at night (Fiedler et al., 1998). Variation in daytime DSL depths is probably a function of light penetration (which is regulated by biological production) and absorption of light by chlorophyll and phaeopigments (Tont, 1976).

The depths and temperatures to which skipjack tuna were repetitively bounce diving during the day in this study were mostly between 200 to 300 m and 10.9° to 13.5°C, respectively. In the same general area of the equatorial EPO, bigeye tuna unassociated with floating objects have been reported to undertake prolonged dives to similar depths and temperatures during the day to forage on DSL prey organisms (Schaefer and Fuller, 2002). A recent study of yellowfin tuna behavior off northern Mexico in the EPO, based on archival tag data, has revealed that yellowfin tuna are also capable of exploiting the vertical habitat below the thermocline by repetitively bounce diving during the day between about 150 and 250 m and between 11°C and 13.5°C, respectively (Schaefer et al., in press).

An ecological benefit of endothermy in tunas is an expanded thermal niche, including exploitation of vertical habitat by skipjack tuna (Block, 1991; Graham and Dickson, 2001). There are several anatomical and physiological differences between skipjack and bigeye tunas (Brill and Bushnell, 2001; Graham and Dickson, 2001) that would explain why skipjack, unlike large bigeye (Holland and Sibert, 1994), are unable to remain for extensive periods at optimal foraging depths below the thermocline. Instead they exhibit repetitive bounce diving behavior to employ both behaviorally and physiologically induced thermoregulation for partial independence from cold water effects on temperature-dependent functions (Graham and Dickson, 2004). Thermal inertia also helps stabilize body temperatures during dives, and larger bigeye tuna have been shown to have slower cooling rates than smaller individuals (Schaefer and Fuller, 2002). The heart rates of tunas are reduced by lower temperatures and hypoxia; therefore excursions below the thermocline may be limited by the diminished capacity of the heart to supply the oxygen requirements of the endothermic tissues (Brill and Bushnell, 2001; Blank et al., 2004).

Skipjack tuna surface-oriented behavior was observed in this study to occur primarily between 0100 h and 1200 h. Skipjack tuna within large multispecies aggregations associated with floating objects have previously been reported to show monospecific horizontal separation and "breezing" (rippling of the water surface) behavior near dawn (Schaefer and Fuller, 2005). Informa-

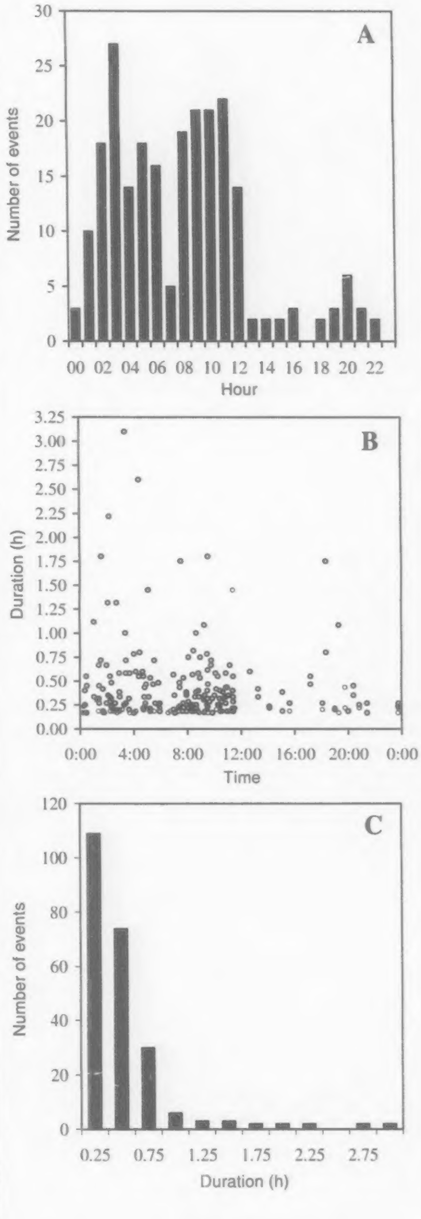

Figure 6

Summary of surface-oriented events for skipjack tuna (*Katsuwonus pelamis*). (**A**) Hour of the day at which the events occurred. (**B**) Beginning time and duration of each event. (**C**) Duration of events.

tion on surface-oriented behavior of skipjack is relevant to understanding catchability (vertical vulnerability plus spatial vulnerability) by purse-seine vessels and may be useful to incorporate into the standardization of catch and effort data. In addition, this information on occurrence and duration of surface-oriented behavior is useful for evaluating optimal detection periods for the use of remote-sensing techniques for conducting fisheries-independent abundance estimation of this species with the use of airborne optical equipment, including LIDAR (light detection and ranging) (Gauldie et al., 1997).

Large-scale studies with archival tags are needed to improve our understanding of skipjack tuna movements, behavior, and habitat use, all of which, in turn, will provide useful information for stock assessments of this valuable resource. Elucidating skipjack tuna behavior may also permit the design of optimal fishing strategies for this species, including the reduction of current bycatch levels associated with purse-seine fishing around floating objects. Archival tags are now capable of storing data for multiple years; this capacity provides a remarkable opportunity to evaluate ontogenetic changes and the influence of seasonal and annual environmental variability on the behavioral characteristics of tuna.

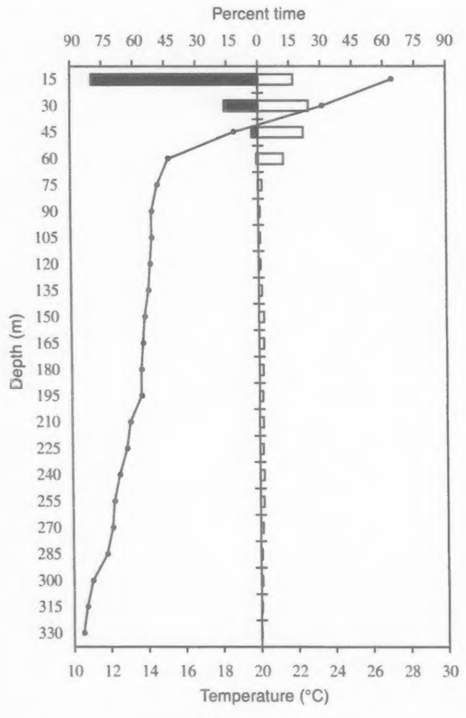

Figure 7

Composite vertical habitat-use distribution for five skipjack tuna (*Katsuwonus pelamis*) for all days of behavior unassociated with floating objects. Depth frequencies during the night are represented by the black bars and depth frequencies during the day are represented by open bars; the average ambient temperatures (line of connected dots) are shown within depth intervals.

Acknowledgments

This research was made possible through financial contributions by the Japan Fisheries Agency, Taiwan Fisheries Agency, and the United States Tuna Foundation. We are grateful to vessel owners, captains, fishermen, unloaders, industry representatives, and Inter-American Tropical Tuna Commission field office staff in Ecuador for assistance in recovering the archival tags. We appreciate the constructive comments on drafts of the manuscript provided by W. Bayliff, E. Calvert, A. Moles, M. Scott, and three anonymous reviewers.

Literature cited

Altringham, J. D., and R. E. Shadwick.
2001. Swimming and muscle function. *In* Tuna physiology, ecology, and evolution. Fish physiology series, vol. 19 (B. A. Block, and E. D. Stevens, eds.), p. 313–344. Academic Press, San Diego, CA.

Anonymous.
2005. Tunas and billfishes in the eastern Pacific Ocean in 2004. Fishery Status Report No. 3. Inter-Am. Trop. Tuna Comm., 119 p.

Blank, J. M., J. M. Morrissette, A. M. Landeira-Fernandez, S. B. Blackwell, T. D. Williams, and B. A. Block.
2004. In situ cardiac performance of Pacific bluefin tuna hearts in response to acute temperature change. J. Exp. Biol. 207:881–890.

Block, B. A.
1991. Endothermy in fish: thermogenesis, ecology, and evolution. *In* Biochemistry and molecular biology of fishes, vol. 1 (P. W. Hochachka, and T. P. Mommsen, eds.), p. 269–311. Elsevier Publishing, New York, NY.

Brill, R. W., and P. G. Bushnell.
2001. The cardiovascular system of tunas. *In* Tuna physiology, ecology and evolution, Fish physiology series, vol. 19 (B. A. Block, and E. D. Stevens, eds.), p. 79–120. Academic Press, San Diego, CA.

Collette, B. B., and C. E. Nauen.
1983. FAO species catalogue. Vol. 2: Scombrids of the world: an annotated and illustrated catalogue of tunas, mackerels, bonitos, and related species known to date. FAO Fish. Synop. 125, 137 p. FAO, Rome.

Dagorn, L., P. Bach, and E. Josse.
2000. Movement patterns of large bigeye tuna (*Thunnus obesus*) in the open ocean, determined using ultrasonic telemetry. Mar. Biol. 136:361–371.

Dizon, A. E., and R. W. Brill.
1979. Thermoregulation in tunas. Am. Zool. 19:249–265.

Dizon, A. E., R. W. Brill, and H. S. H. Yuen.
1978. Correlations between environment, physiology, and activity and the effects on thermoregulation in

skipjack tuna. *In* The physiological ecology of tunas (G. D. Sharp, and A. E. Dizon, eds.), p. 233–259. Academic Press, New York, NY.

Dizon, A. E., W. H. Neill, and J. J. Magnuson.
1977. Rapid temperature compensation of volitional swimming speeds and lethal temperatures in tropical tunas (Scombridae). Environ. Biol. Fish. 2:83–92.

Fiedler, P. C.
1992. Seasonal climatologies and variability of eastern tropical Pacific surface waters. NOAA Tech. Rep. NMFS 109, 65 p.

Fiedler, P. C., J. Barlow, and J. Gerrodette.
1998. Dolphin prey abundance determined from acoustic backscatter data in eastern Pacific surveys. Fish. Bull. 96:237–247.

Gauldie, R. W., S. K. Sharma, and C. E. Helsey.
1997. LIDAR applications to fisheries monitoring problems. Can. J. Fish. Aquat. Sci. 53:1459–1468.

Godsil, H. C., and R. D. Byers.
1944. A systematic study of the Pacific tunas. Calif. Div. Fish Game, Fish Bull. 60, 131 p.

Graham, J. G.
1975. Heat exchange in the yellowfin tuna, *Thunnus albacares*, and skipjack tuna, *Katsuwonus pelamis*, and the adaptive significance of elevated body temperatures. Fish. Bull. 72:219–229.

Graham, J. B., and K. A. Dickson.
2001. Anatomical and physiological specializations for endothermy. *In* Tuna physiology, ecology, and evolution, Fish physiology series, vol. 19 (B. A. Block, and E. D. Stevens, eds.), p. 121–165. Academic Press, San Diego, CA.
2004. Tuna comparative physiology. J. Exp. Biol. 207:4015–4024.

Holland, K. N., and J. R. Sibert.
1994. Physiological thermoregulation in bigeye tuna, *Thunnus obesus*. Environ. Biol. Fish. 40:319–327.

Josse, E., P. Bach, and L. Dagorn.
1998. Simultaneous observations of tuna movements and their prey by sonic tracking and acoustic surveys. Hydrobiologia 371/372:61–69.

Kuznetsov, I. L., S. R. Stefanov, and V. I. Savagov.
1982. A migrating sound scattering layer in the equatorial Pacific Ocean. Oceanology 22:702–703.

Magnuson, J. J.
1969. Digestion and food consumption by skipjack tuna (*Katsuwonus pelamis*). Trans. Am. Fish. Soc. 98:379–392.
1978. Locomotion by scombrid fishes: hydromechanics, morphology, and behavior. *In* Fish physiology series, vol. 7 (W. S. Hoar, and D. J. Randall, eds.), p. 239–313. Academic Press, New York, NY.

Matsumoto, W. M., R. A. Skillman, and A. E. Dizon.
1984. Synopsis of biological data on skipjack tuna, *Katsuwonus pelamis*. NOAA Tech. Rep. NMFS Circ. (451), 92 p.

Neill, W. H., R. K. C. Chang, and A. E. Dizon.
1976. Magnitude and ecological implications of thermal inertia in skipjack tuna, *Katsuwonus pelamis* (Linnaeus). Environ. Biol. Fish. 1:61–80.

Schaefer, K. M., and D. W. Fuller.
2002. Movements, behavior, and habitat selection of bigeye tuna (*Thunnus obesus*) in the eastern equatorial Pacific, ascertained through archival tags. Fish. Bull. 100:765–788.
2005. Behavior of bigeye (*Thunnus obesus*) and skipjack (*Katsuwonus pelamis*) tunas within aggregations associated with floating objects in the equatorial eastern Pacific. Mar. Biol. 146:781–792.

Schaefer, K. M., D. W. Fuller, and B. A. Block.
In press. Movements, behavior, and habitat utilization of yellowfin tuna (*Thunnus albacares*) in the northeastern Pacific Ocean, ascertained through archival tag data. Mar. Biol.

Stevens, E. D., H. M. Lam, and J. Kendall.
1974. Vascular anatomy of the counter-current heat exchanger of skipjack tuna. J. Exp. Biol. 61:145–153.

Stevens, E. D., and W. H. Neill.
1978. Body temperature relations of tunas, especially skipjack. *In* Fish physiology series, vol. 7 (W. H. Hoar, and D. J. Randall, eds.), p. 316–359. Academic Press, New York, NY.

Tont, S. A.
1976. Deep scattering layers: patterns in the Pacific. Calif. Coop. Ocean Fish. Investig. Rep. 18:112–117.

Wild, A., and J. Hampton.
1994. A review of the biology and fisheries for skipjack tuna, *Katsuwonus pelamis*, in the Pacific Ocean. FAO Fish. Tech. Pap. 336(2):1–51.

Yabe, H., Y. Yabuta, and S. Ueyanagi.
1963. Comparative distribution of eggs, larvae and adults in relation to biotic and abiotic environmental factors. FAO Fish. Rep. 6(3):979–1009.

Yuen, H. S. H.
1970. Behavior of skipjack tuna, *Katsuwonus pelamis*, as determined by tracking with ultrasonic devices. J. Fish. Res. Board Can. 27:2071–2079.

Abstract—The northern bluefin tuna (*Thunnus thynnus*) is a highly mobile apex predator in the Gulf of Maine. Despite current stock assessments that indicate historically high abundance of its main prey, Atlantic herring (*Clupea harengus*), commercial fishermen have observed declines in the somatic condition of northern bluefin tuna during the last decade. We examined this claim by reviewing detailed logbooks of northern bluefin tuna condition from a local fishermen's co-operative and applying multinomial regression, a robust tool for exploring how a categorical variable may be related to other variables of interest. The data set contained >3082 observations of condition (fat and oil content and fish shape) from fish landed between 1991 and 2004. Energy from stored lipids is used for migration and reproduction; therefore a reduction in energy acquisition on bluefin tuna feeding grounds could diminish allocations to growth and gamete production and have detrimental consequences for rebuilding the western Atlantic population. A decline in northern bluefin tuna somatic condition could indicate substantial changes in the bottom-up transfer of energy in the Gulf of Maine, shifts in their reproductive or migratory patterns, impacts of fishing pressure, or synergistic effects from multiple causes.

Manuscript submitted 23 June 2006 to the Scientific Editor's Office.

Manuscript approved for publication 16 January 2007 by the Scientific Editor.

Fish. Bull. 105:390–395 (207)

Decline in condition of northern bluefin tuna (*Thunnus thynnus*) in the Gulf of Maine

Walter J. Golet (contact author)[1]

Andrew B. Cooper[1]

Robert Campbell[2]

Molly Lutcavage[1]

Email address for W. J. Golet: wgolet@cisunix.unh.edu

[1] Large Pelagics Research Center, Room 177
Spaulding Hall, College Rd.
University of New Hampshire
Durham, New Hampshire 03824

[2] Yankee Fisherman's Co-op
Seabrook, New Hampshire 03874

The Gulf of Maine is a highly productive region of the northwest Atlantic where substantial aggregations of forage fish attract northern bluefin tuna (*Thunnus thynnus*) and other top predators, including sharks, marine mammals, and seabirds. Atlantic herring (*Clupea harengus*), Atlantic mackerel (*Scomber scomber*), and sand lance (*Ammodytes dubius*) form a major part of this prey base (Bigelow and Schroeder, 1953). As seasonal migrants, northern bluefin tuna arrive in the Gulf of Maine in limited numbers in late May and early June (Bigelow and Schroeder, 1953; Mather et al., 1995). Fish landed in the Gulf of Maine during June and early July are typically lean and have little to no perigonadal or body fat reserves (Estrada et al., 2005; Goldstein et al., in press). Presumably, energy stores of mature northern bluefin tuna entering the Gulf of Maine have been exhausted after spawning, a time when shifts in fat and energy stores are pronounced (Mourente et al., 2001) and mesenteric lipid stores are used for gametogenesis and for subsequent migration to feeding grounds.

Given its size, speed, and wide thermal tolerance, the northern bluefin tuna is a formidable predator, capable of exploiting diverse prey species. Having visceral retes that warm the stomach (Carey et al., 1971) and digestive enzymes with fast turnover rates, northern bluefin tuna can rapidly process prey (Stevens and McLeese, 1984). During the 1950s and 1970s, individual northern bluefin tuna gained 7% (Rivas, 1955) and 10% (Butler[1]), respectively, of their body mass per month on the northwest Atlantic feeding grounds. The majority of this mass gain was reflected in the accumulation of intramusculature and perigonadal fat stores, which presumably provide the necessary reserves for migration to the spawning grounds and subsequent gamete production following their departure from the Gulf of Maine in late September to mid November (Lutcavage and Kraus, 1995; Wilson et al., 2005).

Recent observations by fishermen, brokers, and co-operative managers have identified two declining trends in the Gulf of Maine commercial northern bluefin tuna fishery. First, there appears to be fewer mature fish now than in the last decade. Hundreds of surface schools were detected annually between 1994 and 1996 in aerial surveys (Lutcavage and Kraus, 1995), but catches in 2004 and 2005 decreased dramatically, and only 30% of the commercial quota was landed in the New England region. Second, coincident with the reduction in catch, over the past decade fishermen and dealers have reported a decline in fish quality irrespective of season. Fish landed in September and October had the same somatic condition as those landed in June, indicating that northern bluefin tuna are not establishing the fat reserves they once did. Given that energy allocation is a key factor in growth, maturation, reproduction, and migration in long-lived fishes (Marshall et al., 1999; Rideout et al., 2005; Jørgenson et al., 2006), a decline in the somatic condition of northern bluefin tuna would be expected to affect the population.

---

[1] Butler, M. J. A. 1974. Prince Edward Island bluefin tuna research program 1974. Prince Edward Island marine fisheries and training center and department of tourism, parks, and conservation, Prince Edward Island, 65 p. Agriculture, Fisheries and Aquaculture P. O. Box 2000, Charlottetown, Prince Edward Island, Canada C1A7N8.

Catch rates of highly migratory species, especially northern bluefin tuna, have fluctuated over the years in many different regions of the world (Anderson and Piatt, 1999; Ravier and Fromentin, 2001). These top pelagic predators may have altered their distribution because of environmental shifts (Anderson and Piatt, 1999), or may have suffered localized depletion because of fishing pressures (Tiews, 1978; Fromentin and Powers, 2005). Although these causes may explain why northern bluefin tuna distribution or abundance in the Gulf of Maine has changed, they do not account for the apparent decline in quality of those fish remaining in the area. In this study, we examined records of the fat and oil content and shape of northern bluefin tuna captured in the Gulf of Maine from 1991 to 2004 in order to investigate whether the observations of a decline in quality (as advanced by commercial fishermen and dealers) represents a significant change in somatic condition of these fish.

Materials and methods

Fish condition is most often assessed through the use of Fulton's K or linear regression, both of which give a quantitative value to the physical condition of fish. Such analyses were not possible in this study because individual lengths and weights were not recorded for many of the fish. As a substitute, we used grade data from brokers in the commercial northern bluefin tuna fishery who grade every fish before purchase. This procedure is quite involved and often requires schooling or an apprenticeship to learn the trade. Grading involves a qualitative assessment of the condition of fish, defined by the characteristics of freshness, color, fat and oil content, and fish shape (Bestor, 2004). Fat grade is assessed by evaluating the amount of marbling in a tail cut sectioned between the third and fourth finlet, the thickness of the midsection, and the amount of fat present in a small core of muscle (near the mid-line) extracted for biopsy. Shape grade is determined by the overall appearance of the fish, the more rotund the better. A good quality fish will receive high marks in all categories. Even though different graders may use different terms, ranking of fish quality is consistent between experienced graders (Foote[2]).

We used two of these characteristics, fat and oil content and fish shape, as proxies for fish condition. Fish with large fat reserves and rotund appearance are presumably feeding in excess of their daily metabolic requirements and hence, are in good condition. Fat and oil content and fish shape are reasonable proxies to assess condition because, unlike freshness and color, they cannot be altered by either the time fishermen are at sea or type of gear used.

Detailed logbooks were obtained from a local fishermen's co-operative that consisted of 3834 observations of fat and oil content and 3082 observations of shape from fish landed between 1991 and 2004. Fish ranged in size from the commercial minimum of 185 cm curved fork length (CFL) to 300 cm CFL and weighed from 54 kg to 351 kg dressed (i.e., after head, gill plate, and internal organs were removed). All of the grading was carried out by the same individual using the same grade scale for the entire 14-year period.

To examine temporal trends in fish quality, as defined separately by fat and oil content and fish shape, we used multinomial logit regression with fat and oil grade or shape grade as the dependent variable, and month and year as independent variables. The multinomial logit model estimates the probability of a fish being in grade j in month m and year y as

$$\pi_j(m,y) = \frac{\exp\left(\eta_j(m,y)\right)}{\sum_{\forall i} \exp\left(\eta_i(m,y)\right)} .$$

where $\eta_j(m,y)$ is a linear equation consisting of the variables for month (m) and year (y) and any month-year interactions.

The coefficients for these variables can take on different values for each grade (McCullagh and Nelder, 1989). For example, if we treat month as a categorical variable, $n_j(m,y)$ can be written as

$$\eta_j(m,y) = \beta_{0,j} + (\beta_{1,k,j} \times m_k) + (\beta_{2,j} \times y) + (\beta_{3,k,j} \times m_k \times y)$$

where $B_{0,j}$ = the intercept for grade j;
$B_{1,k,j}$ = the coefficient for the effect of month k on grade j;
m_k = an indicator variable denoting the month as a categorical variable;
$B_{2,j}$ = the effect of year on grade j; and
$B_{3,k,j}$ = the interaction between month k and year y.

The model was fitted by using the multinomial command in the NNET library of S-PLUS vers. 6.2 (Insightful Corporation, Seattle, WA). The significance of each variable was tested by using likelihood ratios for nested

---

[2] Foote, J. 2005. Personal commun. Jensen Tuna Inc., 8 Seafood Way, Boston, MA 02210.

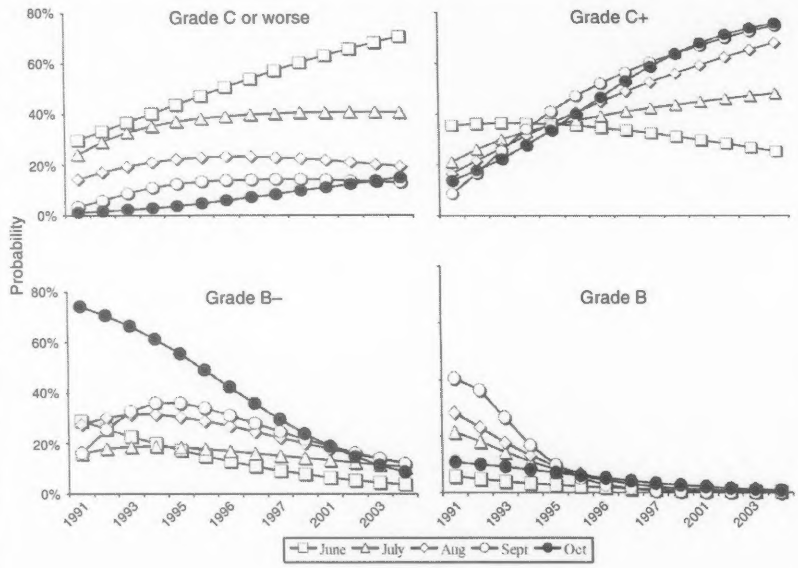

Figure 1

The predicted probabilities of a northern bluefin tuna (*Thunnus thynnus*) being in grade j in month m and year y, $\hat{\pi}_j(m,y)$ for fat and oil grades of C or worse, and for grades C+, B–, and B. The most dramatic shifts occurred in the C+ fish which made up between 68% and 75% of the catch in 2004 as opposed to 10–20 % in the early 1990s. Good quality (grade B) fish comprised <1% of the total commercial catch in 2004.

models, and Akaike's information criterion (AIC) for non-nested models.

Results

Our analysis identified significant declines in the somatic condition (fat and oil content and fish shape) of northern bluefin tuna in the Gulf of Maine. For fat and oil content, the effect of month, year, and the month-year interaction were each significant (all $P<0.0001$; $\chi_4^2=429$, $\chi_4^2=1088$, and $\chi_4^2=29.95$, respectively). Fish landed in the month of June arrived in poorer condition than they did in the early 1990s (Fig. 1). For example, the probability of landing a poor quality fish (grade C or worse) in June 1991 was 30% compared with 70% in 2004. Similar, but more striking results were observed in the C+ category during August and September (Fig. 1). In 1991, the probability of landing a fish in the C+ category was 16% and 9% for August and September, respectively. In 2004, the probability increased to 68% and 76% in the C+ category for August and September, respectively. Good quality fish, such as B or better now comprise <1% of the commercial catch at this particular co-operative (Fig. 1).

For fish shape, the effect of month, year, and the month-year interaction were each significant (all $P<0.0001$; $\chi_3^2=207$, $\chi_3^2=388$, and $\chi_3^2=47.18$, respectively). Results for shape were similar to fat and oil content, likely because shape and fat and oil content are closely related (fat fish should have a more rotund shape). The probability of landing a fish that received a B– (lesser quality) grade for shape increased by 30%, 32%, 43%, and 28% from 1991 to 2004 for the months of July, August, September, and October, respectively (Fig. 2). For the same time period, fish with a good shape (B or better) decreased by 18%, 22%, 47%, and 25% for the months of July, August, September, and October, respectively (Fig. 2).

Discussion

Our multinomial regression analysis demonstrated highly significant declines in the fat and oil content and shape of northern bluefin tuna landed in the Gulf of Maine over the last 14 years, corroborating the observations of fishermen. Northern bluefin tuna arrive in leaner condition and are not increasing their fat stores on the feeding grounds as they did in the early 1990s. This was particularly true in late summer and early fall, when fish usually fatten and become more rotund (Butler[1]).

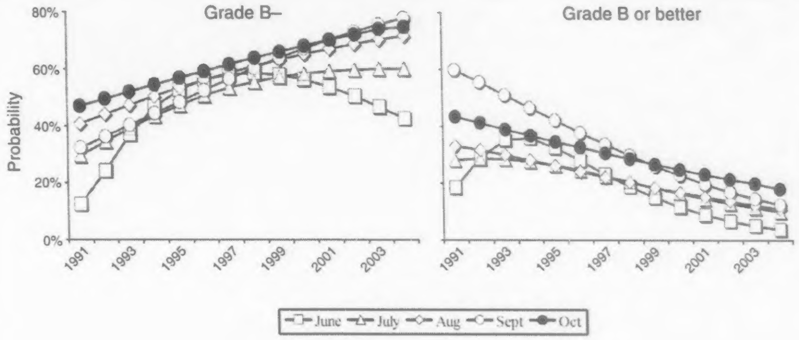

The predicted probabilities of a northern bluefin tuna (*Thunnus thynnus*) being in grade j in month m and year y, $\hat{\pi}_j(m,y)$ for shape grade B– and grade B or better. Similar to fat and oil content, there is a consistent increase in poor fish shape and a decline in the good shape grades for all months, except June, throughout the 14-year period.

Seasonal migrations of adult northern bluefin tuna are believed to be bound by reproduction and feeding constraints: spawning in warm (>24°C) regions in spring and early summer followed by dispersal to continental shelves at higher latitudes for intensive foraging through late fall (Rivas, 1955; Clay, 1991). Their body condition also varies through this cycle: feeding periods presumably put individuals into positive lipid balance, creating energy stores for gonadal development and metabolism (Medina et al., 2002; Carruthers et al., 2005). Since the mid 1990s, mixed size classes of northern bluefin tuna appeared in North Carolina coastal waters from December to February (Block et al., 2001), extending the range of their inshore foraging on Atlantic menhaden (*Brevoortia tyrannus*) and possibly other species. If the temporal or spatial aspects of migration, reproduction, and feeding patterns have changed over the past decade, alterations in the somatic and bioenergetic condition of fish feeding in the Gulf of Maine could be expected. Other possible explanations for changes in somatic and bioenergetic condition of fish include increased growth rates due to selective fishing pressure (Polacheck et al., 2004), or skipped spawning to increase growth (Jørgensen et al., 2006), but the general declines in condition in fish of such large body size are difficult to explain based on intrinsic changes in growth. This is particularly true in this study where every fish was larger than 110 cm, the size at which the seasonal length-weight relationship begins to decrease (Mather et al., 1995) and northern bluefin tuna gain more in mass than length.

In pelagic fishes, migrations require a substantial energetic cost (Harden Jones, 1984), and migration distance has been linked to body size and available fat stores (Nøttestad et al., 1999). The longstanding migration paradigm is that western Atlantic northern bluefin tuna spawn in the Gulf of Mexico and Straits of Florida from April to June and then migrate northward along the continental shelf to New England and Canadian waters (Rivas, 1955; Mather et al., 1995; Block et al,. 2005). A substantial increase in migrants from the Eastern Atlantic may explain why the condition of fish in this region has declined. Northern bluefin tuna migrating to the Gulf of Maine from the eastern Atlantic would have to swim a greater distance, travel against major currents and through unproductive waters using more stored energy than individuals coming from western Atlantic spawning grounds. To date, there is insufficient data to confirm that such a shift has occurred (Fromentin and Powers, 2005). Another possibility is that the timing and location of spawning has shifted. The long held assumption that the New England assemblage spawns exclusively in the Gulf of Mexico and adjacent regions (Rivas, 1955; Block et al., 2005) may be incorrect (Lutcavage et al., 1999; Fromentin and Powers, 2005; Goldstein et al., in press). If fish are spawning outside of these traditional spawning grounds during May and June (Mather et al., 1995; Lutcavage et al., 1999; Wilson et al., 2005), or at different times, their somatic condition and lipid allocations would be expected to shift from historical patterns (Rajasilta, 1992).

Given that northern bluefin tuna spend up to five months on the feeding grounds, a decline in somatic condition intuitively points to changes in the forage base and energy transfer within the Gulf of Maine. Northern bluefin tuna exploit several trophic levels, including krill, before arrival in the Gulf of Maine (Estrada et al., 2005), but while there, they forage extensively on herring (Chase, 2002), which has the highest energy density of prey in the region (Lawson et al., 1998). The observed decline in condition could result from a decrease in the amount, quality, or availability of herring (Marshall et al., 1999; Diamond and Devlin, 2003), or an increase in the energy required for northern bluefin tuna to acquire and process sufficient amounts of prey (Marshall et al., 1999; Nøttestad et al., 1999; Carruthers et al., 2005).

Atlantic herring spawning stocks in the Gulf of Maine and Georges Bank-Nantucket Shoals are at historically high levels (Overholtz et al.[3]); this fact argues against a reduction in herring abundance as a causal factor for the declining condition in northern bluefin tuna. A reduction in the energy density of herring itself, as seen in seabird-herring-copepod ecosystem studies (Diamond and Devlin, 2003; Durant et al., 2003) are other possible reasons for the decline. A coincident decline in northern bluefin tuna and Atlantic herring condition in the Gulf of St. Lawrence indicate that similar changes are occurring in other Northwest Atlantic shelf systems. In view of changes also detected in other predators, such as seabirds, and in the distribution and abundance of baleen whales, there appears to be a major shift in energy transfer and dynamics across the Gulf of Maine ecosystem over a period when oceanographic changes linked to the North Atlantic Oscillation were also evident (Greene and Pershing, 2003).

If the abundance of forage fish has been reduced, dispersed into smaller schools, or shifted, northern bluefin tuna would have to expend more energy in search of prey, shift their diet to less energetic prey (i.e., the junk food hypothesis [Piatt and Anderson, 1996; Golet et al., 2002]), or move to regions with a greater biomass of forage fish (Anderson and Piatt, 1999). Northern bluefin tuna are arriving in poorer condition than they were 10–14 years ago, and despite long residency in the area they are no longer attaining the good condition of previous decades. Of additional concern is that after disappearances in the North Sea and in some historic locations on the Canadian Atlantic shelf, northern bluefin tuna have not returned to these areas (Tiews, 1978; Clay and Hurlbut, 1989).

Condition data alone do not allow us to identify the cause of observed declines in this top predator, but decreased energy stores on feeding grounds could reduce energetic allocations to growth and reproduction, as observed in gadids in the northwest Atlantic and elsewhere (Marshall et al., 1999; Lambert and Dutil, 2000), and may have unexpected and detrimental consequences for rebuilding the northern bluefin tuna population. Given that northern bluefin tuna are currently overexploited throughout most of their range, it is essential to identify root causes for these declines on one of their most important foraging grounds in the western Atlantic.

Acknowledgments

This work was supported by a National Oceanic and Atmospheric Administration Grant NA04NMF4550391 to M. Lutcavage. We thank M. Perkins for all his work processing the bluefin tuna, and several anonymous reviewers for their constructive comments that improved our manuscript.

Literature cited

Anderson, P. J., and J. F. Piatt.
1999. Trophic reorganization in the Gulf of Alaska following ocean climate regime shift. Mar. Ecol. Prog. Ser. 189:117–123.

Bestor, T. C.
2004. Tsukiji. The fish market at the center of the world, p. 257–258. Univ. California Press, Berkeley and Los Angeles, CA.

Bigelow, H. B., and W. C. Schroeder.
1953. Fishes of the Gulf of Maine. Fish. Bull. Wild. Ser. 53:1–577.

Block, B. A., H. Dewar, S. B. Blackwell, T. D. Williams, E. D. Prince, C. J. Farwell, A. Boustany, S. L. H. Teo, A. Seitz, A. Walli, and D. Fudge.
2001. Migratory movements, depth preferences, and thermal biology of Atlantic bluefin tuna. Science 293:1310–1314.

Block, B. A., S. L. H. Teo, A. Walli, A. Boustany, M. J. W. Stokesbury, C. Farwell, K. Weng, H. Dewar, and T. D. Williams.
2005. Electronic tagging and population structure of Atlantic bluefin tuna. Nature 434:1121–1126.

Carey, F. G., J. M. Teal, J. W. Kanwisher, K. D. Lawson, and J. S. Beckett.
1971. Warm-bodied fish. Am. Zool. 11:137–145.

Carruthers, E. H., J. D. Neilson, C. Waters, and P. Perley.
2005. Long-term changes in the feeding of *Pollachius virens* on the Scotian Shelf: responses to a dynamic ecosystem. J. Fish Biol. 66:327–347.

Chase, B. C.
2002. Differences in the diet of Atlantic bluefin tuna (*Thunnus thynnus*) at five seasonal feeding grounds on the New England continental shelf. Fish. Bull. 100:168–180.

Clay, D.
1991. Atlantic bluefin tuna (*Thunnus thynnus thynnus* (L.)): a review. *In* World meeting on stock assessment of bluefin tunas: strengths and weaknesses (R. B. Deriso, and W. H. Bayliff, eds), p. 89–180 p. Inter-Am. Trop. Tuna Comm., La Jolla, CA.

Clay, D., and T. Hurlbut.
1989. Catch and effort for Canadian Atlantic bluefin tuna (*Thunnus thynnus* L.). ICCAT Coll. Vol. Sci. Pap. 30:335–342.

Diamond, A. W., and C. M. Devlin.
2003. Seabirds as indicators of changes in marine ecosystems: Ecological monitoring on Machias Seal Island. Environ. Monit. Assess. 88:153–175.

Durant, J. M., T. Anker-Nilssen, and N. C. Stenseth.
2003. Trophic interactions under climate fluctuations: the Atlantic puffin as an example. Proc. R. Soc. Lond., Ser. B: Biol. Sci. 270:1461–1466.

Estrada, J. A., M. Lutcavage, and S. R. Thorrold.
2005. Diet and trophic position of Atlantic bluefin tuna

---

[3] Overholtz, W. J., L. D. Jacobson, G. D. Melvin, M. Cieri, M. Power, D. Libby, and K. Clark. 2004. Stock assessment of the Gulf of Maine-Georges Bank Atlantic herring complex, 2003. Northeast Fish. Sci. Cent. Ref. Doc. 04-06, 300 p.

(*Thunnus thynnus*) inferred from stable carbon and nitrogen isotope analysis. Mar. Biol. 147:37–45.

Fromentin, J. M., and J. E. Powers.
2005. Atlantic bluefin tuna: population dynamics, ecology, fisheries and management. Fish Fish. Ser. 6:281–306.

Goldstein, J., S. Heppell, A. Cooper, S. Brault, and M. Lutcavage.
In press. Variability in the reproductive status and body condition of Atlantic bluefin tuna in the Gulf of Maine, 2000–2002. Mar. Biol.

Golet, G. H., P. E. Seiser, A. D. McGuire, D. D. Roby, J. B. Fischer, K. J. Kuletz, D. B. Irons, T. A. Dean, S. C. Jewett, and S. H. Newman.
2002. Long-term direct and indirect effects of the Exxon Valdez oil spill on pigeon guillemots in Prince William Sound, Alaska. Mar. Ecol. Prog. Ser. 241:287–304.

Greene, C. H., and A. J. Pershing.
2003. The flip-side of the North Atlantic Oscillation and modal shifts in slope-water circulation patterns. Limnol. Oceanogr. 48:319–322.

Harden Jones, F. R.
1984. A view from the ocean. *In* Mechanisms of migration in fishes (J. D. McCleave, G. P. Arnold, J. J. Dodson, and W. H. Neill, eds.), 26 p. Plenum Press, New York, NY.

Jørgensen, C., B. Ernande, Ø. Fiksen, and U. Dieckmann.
2006. The logic of skipped spawning in fish. Can. J. Fish. Aquat. Sci. 63:200–211.

Lambert, Y., and J. Dutil.
2000. Energetic consequences of reproduction in Atlantic cod (*Gadus morhua*) in relation to spawning level of somatic energy reserves. Can. J. Fish. Aquat. Sci. 57:815–825.

Lawson, J. W., A. M. Magalhães, and E. H. Miller.
1998. Important prey species of marine vertebrate predators in the northwest Atlantic: proximate composition and energy density. Mar. Ecol. Prog. Ser. 164:13–20.

Lutcavage, M., R. W. Brill, G. B. Skomal, B. C. Chase, and P. W. Howey.
1999. Results of pop-up satellite tagging of spawning size class fish in the Gulf of Maine: Do North Atlantic bluefin tuna spawn in the mid-Atlantic? Can. J. Fish. Aquat. Sci. 56:173–177.

Lutcavage, M., and S. Kraus.
1995. The feasibility of direct photographic assessment of giant bluefin tuna, *Thunnus thynnus*, in New England waters. Fish. Bull. 93:495–503.

Marshall, C. T., N. A. Yaragina, Y. Lambert, and O. S. Kjesbu.
1999. Total lipid energy as a proxy for total egg production by fish stocks. Nature 402:288–290.

Mather, F. J., J. M. Mason Jr., and A. Jones.
1995. Historical document: life history and fisheries of Atlantic bluefin tuna. NOAA Tech. Memo. NMFS-SEFSC-370, 412 p.

McCullagh, P., and J. A. Nelder.
1989. Generalized linear models, 511 p. Chapman and Hall, London.

Medina, A., F. J. Abascal, C. Megina, and A. Garcia.
2002. Stereological assessment of reproductive status of female Atlantic northern bluefin tuna during migration to the Mediterranean spawning grounds through the Strait of Gibraltar. J. Fish Biol. 60:203–217.

Mourente, G., C. Megina, and E. Díaz-Salvago.
2001. Lipids in female northern bluefin tuna (*Thunnus thynnus thynnus* L.) during sexual maturation. Fish. Pysiol. Biochem. 24:351–363.

Nøttestad, L., J. Giske, J. C. Holst, and G. Huse.
1999. A length-based hypothesis for feeding migration in pelagic fish. Can. J. Fish. Aquat. Sci. 56:26–34.

Piatt, J. F., and P. Anderson.
1996. Response of common murres to the Exxon Valdez oil spill and long-term changes in the Gulf of Alaska marine ecosystem. Am. Fish. Soc. Symp. 18:720–737.

Polacheck, T., J. P. Eveson, and G. M. Laslett.
2004. Increase in growth rates of southern bluefin tuna (*Thunnus maccoyii*) over four decades:1960–2000. Can. J. Fish. Aqaut. Sci. 61:307–322.

Rajastilta, M.
1992. Relationship between food, fat, sexual maturation, and spawning time of Baltic herring (*Clupea harengus*) in the Archipelago Sea. Can. J. Fish. Aquat. Sci. 49:644–654.

Ravier, C., and J-M. Fromentin.
2001. Long-term fluctuations in the Eastern Atlantic and Mediterranean bluefin tuna population. ICES J. Mar. Sci. 58:1299–1317.

Rideout, R. M., G. A. Rose, and M. P. M. Burton.
2005. Skipped spawning in iteroparous fishes. Fish Fish. Ser. 6:50–72.

Rivas, L. R.
1955. A comparison between giant bluefin tuna (*Thunnus thynnus*) from the straits of Florida and the Gulf of Maine with reference to migration and population identity. Proc. Gulf and Caribbean Fish. Inst. Seventh Ann. Sess. 133–149.

Stevens, E. D., and J. M. McLeese.
1984. Why bluefin tuna have warm tummies: temperature effect on trypsin and chymotrypsin. Am. J. Physiol-Reg I. 246:R487-R494.

Tiews, K.
1978. On the disappearance of bluefin tuna in the North Sea and its ecological implications for herring and mackerel. Rapp. P-V. Réun. Cons. Int. Explor. Mer172:301–309.

Wilson, S. G., M. E. Lutcavage, R. W. Brill, M. P. Genovese, A. B. Cooper, and A. W. Everly.
2005. Movements of bluefin tuna (*Thunnus thynnus*) in the northwestern Atlantic recorded by pop-up satellite archival tags. Mar. Biol. 146:409–423.

Abstract—This study investigates the temporal stability of length- and age-at-maturity estimates for female Pacific cod (*Gadus macrocephalus*) in the Gulf of Alaska and eastern Bering Sea. Females reached 50% maturity (A_{50}) at 4.4 years in the Gulf of Alaska and at 4.9 years in the eastern Bering Sea. Total body length at 50% maturity (LT_{50}) was significantly smaller (503 mm) in the Gulf of Alaska than in the eastern Bering Sea (580 mm). The estimated length- and age-at-maturity did not differ significantly between winter and spring in either the Gulf of Alaska (1999) or Bering Sea (2003) areas. The results of this study raised the spawning biomass estimate of female Alaskan Pacific cod from 298×10^3 t for 2005 to 499×10^3 t for 2006. The increased spawning biomass estimate resulted in an increased over-fishing limit for Pacific cod.

Geographic and seasonal variations in maturation and growth of female Pacific cod (*Gadus macrocephalus*) in the Gulf of Alaska and Bering Sea

James W. Stark

Email address: jim.stark@noaa.gov

Resource Assessment and Conservation Engineering Division
Alaska Fisheries Science Center
NOAA/National Marine Fisheries Service
7600 Sand Point Way NE
Seattle, Washington 98115

Pacific cod (*Gadus macrocephalus*) was the fourth most important commercial species landed in the United States during 2003 by volume, and catches totaled 27×10^4 metric tons (t) and had a value of $160 million. The Pacific cod stocks in Alaska were not considered to be overfished in 2005 (Thompson and Dorn, 2005; Thompson et al., 2005). Pacific cod range from California, around the North Pacific Rim, to the Sea of Japan (Hart, 1973). In Alaska, this species is found along the continental shelf and upper slope, primarily at depths <300 m (Matarese et al., 2003). The objectives of this study were to determine the length- and age-at-maturity, as well as growth of female Pacific cod, in order to provide for significantly improved stock management in the Gulf of Alaska, eastern Bering Sea, and Aleutian Islands. Previous estimates of Pacific cod length-at-maturity were based on visual (macroscopic) observations of ovaries taken during the spawning season (Welch and Foucher, 1988; Thompson et al., 2005), or on a gonadosomatic index (*IG*) (Teshima, 1985; Hattori et al., 1992).

The macroscopic observation and *IG* methods can introduce sampling bias through misclassifications of the stage of oocyte maturity (Hunter et al., 1992). The macroscopic method of maturity classification is contingent upon differentiating between ova that contain yolk (mature ova) which can appear transparent to the naked eye, and opaque ova that do not contain yolk. The change in opacity is the result of yolk sequestering within the ova, resulting in distension and transparency of the chorion (external covering of the ova). Opacity is more difficult to discern in the small ova that are produced by smaller fish. Therefore, the macroscopic method of classification can result in a bias against smaller fish.

With macroscopic classification, there is also a bias against specimens in early vitellogenesis, because during this period only a small quantity of yolk has been sequestered within the ova, resulting in an opaque chorion that is not distended. With macroscopic observation methods, an ovary containing only postovulatory follicles and opaque ova would be classified as immature; postovulatory follicles can be detected only through the use of histological methods.

Macroscopic observations also have the disadvantage of generally being conducted under less than ideal lighting and weather conditions. Maturity classifications based on histological examination are not subject to these biases because the maturity classifications are based on a comprehensive microscopic assessment of ova and associated structures, such as postovulatory follicles, under controlled laboratory conditions. Histological methods provide a high probability that yolk sequestered within ova will be detected because ova are sectioned and stained with eosin that renders yolk pink.

Manuscript submitted 20 September 2006 to the Scientific Editor's Office.

Manuscript approved for publication 23 March 2007 by the Scientific Editor.

Fish. Bull. 105:396–407 (2007).

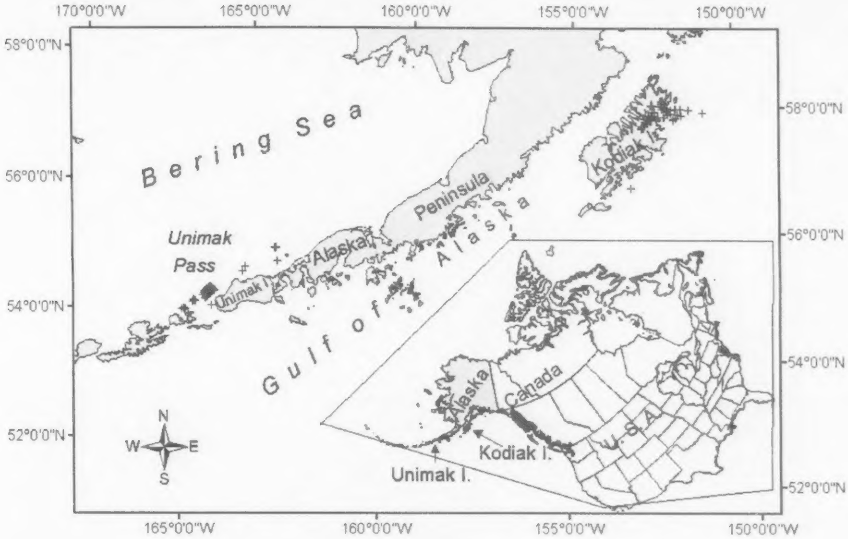

Figure 1

Locations (+) sampled during Alaska Fisheries Science Center survey cruises from October 1988 through January 2004 for assessment of the maturity stages of Pacific cod (*Gadus macrocephalus*).

Materials and methods

Ovaries and otoliths were collected from Pacific cod in two geographic areas, the Gulf of Alaska and eastern Bering Sea (Fig. 1). Seasonal sampling was used to estimate the time of spawning, rate of ovary development, and length- and age-at-maturity for female Pacific cod. The first area, located in the central Gulf of Alaska, was sampled during October 1998, January 1999, and April 1999 (Table 1) during a cooperative seasonal maturity study conducted by the Alaska Department of Fish and Game (ADFG) and the National Oceanic and Atmospheric Administration Alaska Fisheries Science Center (NOAA/AFSC). The area was sampled with bottom trawl gear again in June 1999 during the annual ADFG crab survey and during the commercial fishery in January 2004. Seawater temperature, and depth data were collected with a calibrated trawl-mounted microbathythermograph. The second area, within Unimak Pass and the adjacent southeastern Bering Sea, was sampled during the January, February, and March 2003 AFSC Pacific cod pot study. Growth was determined by using the cod length- and geographic area-stratified otolith collections from the 2003 AFSC area wide surveys in the Gulf of Alaska and eastern Bering Sea (Table 1). Otoliths were aged by using the methods developed during 2002 for Pacific cod (Roberson et al., 2005; Thompson and Dorn, 2005) by personnel of the AFSC Age and Growth Program.

In both the Gulf of Alaska and Bering Sea collections, ovaries were removed and placed in individually labeled cloth bags and stored in a solution of 4% buffered formaldehyde. The ovary samples for the Gulf of Alaska consisted of whole ovaries and samples from the Bering Sea area were excised ovarian cross-sections (minimum of two 16.4-mm-diameter samples per individual). For each whole ovary sample, a section was taken from the posterior region of the ovary. From 50 of these specimens, two additional sections were taken from the anterior and median regions.

Oocytes within each ovary were classified into five histological stages based on criteria used by Hunter et al. (1992) and Stark and Somerton (2002). The five stages were perinucleus, cortical alveoli, vitellogenesis, hydrated oocytes, and postovulatory follicles. Individual ovaries were classified according to the most advanced stage of oocytes present in the histological sections. Individuals classified as spawners were those with ovaries containing either hydrated oocytes or post-ovulatory follicles. Mature individuals were defined by using two different classification criteria in order to compare results from each method. One method classified mature specimens as those with ovary stages ranging from vitellogenesis through postovulatory follicles. The other method included the additional stage of cortical alveoli ovaries in the mature category.

Ovarian development was compared across months, by tabulating the proportion of fish classified within each of the five histological stages only for females that had reached the minimum total body length (*LT*) at maturity, as determined by a length-at-maturity analysis. A selection of samples from the entire length range of

Table 1

Summary of data on samples collected by the National Oceanic and Atmospheric Administration Alaska Fisheries Science Center used to estimate maturity and growth of Pacific cod (*Gadus macrocephalus*). Categories include date of sample collections, location of sample collections, sources of sample collections, types and numbers (n) of specimen samples. The ovaries and otoliths used to estimate length- and age-at-maturity and timing of the reproductive cycle were taken from specimens collected in the Gulf of Alaska (GOA) and Bering Sea (BS). The GOA sampling was conducted during surveys extending from October 1998 to June 1999, and additional specimens were collected from a seafood processing plant (referred to as "Plant" in table) during 2004. The BS ovary and otolith specimens were collected during the 2003 Pacific cod surveys. The length data and the otoliths (of both sexes) used to estimate growth were collected during the 2003 bottom trawl surveys conducted in the GOA and BS.

Period of sample collections	Location of sample collections	Source of sample collections	No. of specimens sampled for histological examination of ovaries	No. of specimens aged
For maturity estimates				
October 1998	GOA	Survey	59	58
January 1999	GOA	Survey	107	104
April 1999	GOA	Survey	60	57
June 1999	GOA	Survey	66	48
January 2004	GOA	Plant	50	50
	GOA	Total	342	317
January 2003	BS	Survey	30	29
February 2003	BS	Survey	133	129
March 2003	BS	Survey	96	92
	BS	Total	259	250
	GOA and BS	Total	601	567
For growth estimates				
May–July 2003	GOA	Survey females		375
May–July 2003	GOA	Survey males		336
June–July 2003	BS	Survey females		676
June–July 2003	BS	Survey males		684
	GOA and BS	Total		2071

mature females allowed the investigation of the full seasonal progression of ovary development. The proportion of females in spawning condition was estimated for each month by dividing the sum of the fish classified as spawning by the sum of the fish classified as mature. The length- and age-at-maturity estimates that were chosen as representing the standard for each area were based on specimens collected during the prespawning or initial yearly spawning period, January 1999 and 2004 and February 2003. By January and February, all specimens that would mature that year had matured according to the results of seasonal sampling from this study. The data from January of 1999 and 2004 were combined to obtain length- and age-at-maturity estimates with the lowest variance. The monthly length and age composition of females in mature condition were estimated by using standard length- and age-at-maturity analysis.

Maturity as a function of length was estimated by fitting a logistic function to the maturity data with generalized linear modeling (Venables, 1997); for this procedure, S-Plus software (vers. 2000 Professional release 3, MathSoft Inc., Cambridge, MA) was used. The significance of between-area, between-month, and between-classification methods differences were tested by fitting the model of maturity as a function of L_T with a term distinguishing area, month, and method and by recalculating without each term. Significance of the area, month, and method terms were determined by using analysis of deviance (Venables, 1997). Length at 50% maturity was also estimated by evaluating the fitted model at 50% maturity and algebraically solving for length. The variance of $L_{T_{50}}$ was estimated for each area, month, and method by using bootstrapping (Efron and Tibshirani, 1993) based on 200 resamplings, with replacement, of the maturity and length data. Between-area, between-month, and between-method differences in $L_{T_{50}}$ were then tested with a z-test (Sokal, 1969). With these same procedures, maturity was described as a function of age, and spawning was estimated as a function of L_T, age, month, and ambient water temperature.

With the use of S-Plus software, length-at-age was described by the von Bertalanffy growth function, which incorporated nonlinear least-squares fitted to

L_T and age data (Venables, 1997). Between-sex and between-area differences in growth were tested by first fitting the von Bertalanffy model with a term distinguishing sex and area and again tested for the combined sexes and areas. The likelihood ratio of the two models was then determined for each category (Kimura, 1980). Significance of the likelihood ratio was tested to determine if growth differed by sex or area.

The gonadosomatic index (I_G) was calculated from the specimens sampled for maturity as the ratio of gonad weight (W_G) to body weight (W) with the gonads removed ($IG=100\ W_G/W$). The body weight portion of the data included food contents for the Gulf of Alaska specimens, whereas stomachs were emptied for all 250 Bering Sea specimens that were weighed. However, weight of the stomach contents represented less than 1% of the total body weight for the Bering Sea specimens. A z-test (Sokal, 1969) was performed with S-Plus software to determine if there were between-area and between-month differences in I_G.

Table 2

Length-at-maturity results based on samples of ovaries (n) collected between the late prespawning and initial spawning period for female Pacific cod (*Gadus macrocephalus*) in the Gulf of Alaska (GOA) and Bering Sea (BS) areas, by date of collection. The parameters of the logistic equation that were used to fit the data are given: B (slope of the line) and A (Y intercept), variance (the square of the standard deviation of B and A), covariance (the product of the standard deviations of B and A and the coefficient of correlation between them), length (mm) at which 50% of females were expected to reach sexual maturity (L_{T50}), and variance of L_{T50}.

	Gulf of Alaska	Bering Sea
Sampling statistics	January 1999 and 2004	February 2003
n	157	133
B	0.0222	0.0132
A	−11.1425	−7.6248
Variance (B)	2.0649	1.3807
Variance (A)	6.5528	3.2433
Covariance (B,A)	−0.0002	0.0001
$LT_{50\,(\mathrm{mm})}$	502.5543	579.9599
Variance (LT_{50})	212.5733	309.3380

Results

The results provided information on the relationship between ovary growth and maturation for Pacific cod in the Gulf of Alaska and Bering Sea. The I_G data were available for 95% of the Gulf of Alaska specimens and 99% of the Bering Sea specimens sampled for maturity. For both areas, the I_G cycled according to the season (Fig. 2). The observed I_G was highest during the winter months (Jan=4.24 I_G and February=8.48 I_G), declined through the spring (March=6.37 I_G and April=3.50 IG), and reached the lowest levels in early summer (June=1.02 I_G). Maturation of the population of oocytes to be spawned the following year occurred at a slow rate through October (1.74 I_G).

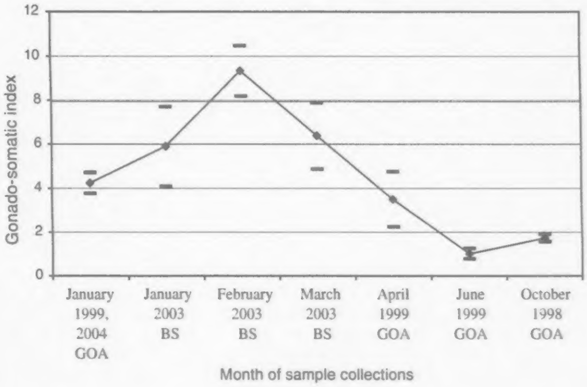

Figure 2

Mean gonadosomatic index of female Pacific cod (*Gadus macrocephalus*). Sample sites were located in the Gulf of Alaska (GOA) during January 1999 and 2004, April and June 1999, and October 1998 (total n=327), and the Bering Sea (BS) during January, February, and March 2003 (total n=261). The 95% confidence intervals are represented by bars located adjacent to each data point.

Similarly linked to the Pacific cod spawning cycle, was the development of oocytes within the ovaries (Fig. 3), which was consistent in all quadrants of each ovary. By January, over 70% of the sampled ovaries were in the vitellogenesis stage of development in preparation for spawning, in both the Gulf of Alaska and Bering Sea Pacific cod. Females that had vitellogenesis-stage oocytes during the spring were expected to develop and spawn those oocytes that year. By June, all stocks of vitellogenesis-stage oocytes had been exhausted. In the Gulf of Alaska, over half of the female Pacific cod spawned during April and June. Pacific cod spawning began during February in the Bering Sea area, and approximately 10% of the fish population participated. During October, 5% of female Pacific cod had vitellogenesis-stage ovaries, whereas 95% of Gulf of Alaska cod were in earlier stages of maturation. The likelihood of female Pacific cod spawning was significantly

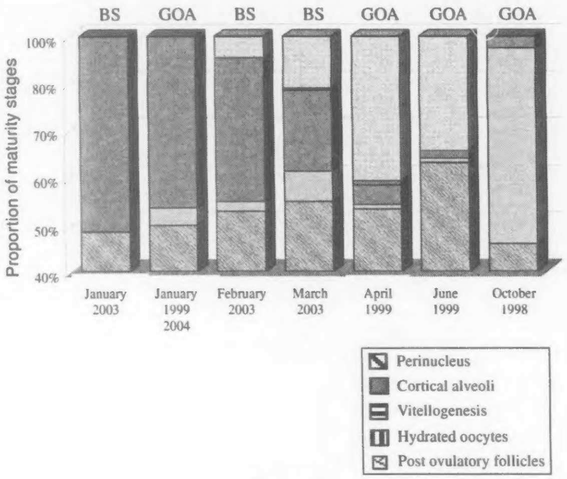

Figure 3

Ovary development of Pacific cod (*Gadus macrocephalus*), based on maturity-stage classification results from specimens that had reached the minimum length at maturity and that had been collected from 1998 through 2004 in the Gulf of Alaska (GOA) and 2003 Bering Sea (BS). Selecting samples from the entire length range of mature females provided for the investigation of the full seasonal progression of ovary development.

($P<0.001$) associated with the time of month and not significantly associated with L_T ($P=0.06$), age ($P=0.06$), or ambient water temperature ($P=0.21$). However, by April and June in the Gulf of Alaska, L_T was slightly ($P=0.01$) associated with the likelihood of spawning. Spawners ranged in L_T from 420 mm to 1060 mm. The age-at-spawning ranged from 4 year olds up to the oldest females taken, at 10 years of age. Spawning female Pacific cod were found in all areas, including bays and offshore gullies, sampled during April and June 1999 in the Gulf of Alaska. Ambient seawater temperatures were similar in 1999 during January and April (2.21°C to 6.10°C), and increased only slightly in June (3.7°C to 7.01°C).

The estimates of L_{T50} did not differ significantly between the two histology-based methods used to define mature females, except for a slight difference ($P=0.02$) with January Gulf of Alaska estimates, which used the combined data from 1999 and 2004. The January L_{T50} estimates were 503 mm based on a mature classification that did not include cortical alveoli (CA) stage ovaries, and 437 mm when CA-stage ovaries were included as part of the mature category.

However, there was a significant area difference ($P<0.001$, Fig. 4, Table 2) between the January 1999, 2004 Gulf of Alaska LT_{50} (503 mm) and the February 2003 Bering Sea LT_{50} (580 mm). In both areas, the estimates of length-at-maturity did not differ significantly between months, with the exception of a slight difference ($P=0.03$) between January (496 mm) and June (601 mm) 1999. In the present study the expected L_T range of mature female P. cod was adequately assessed from a sample L_T distribution that extended to 130 mm L_T in the Gulf of Alaska and 350 mm L_T in the Bering Sea (Table 3) and on the documentation of only a single specimen smaller than 420 mm L_T.

The estimated age at which 50% of the females reached maturity (A_{50}) did not differ significantly between the two histological methods for assigning maturity. With either method, the A_{50} differed slightly ($P=0.02$) between the Gulf of Alaska (4.4 years) and Bering Sea (4.9 years, Table 4, Fig. 5). However, within each area, the estimated ages at maturity did not differ significantly between months ($P>0.16$). Similarly, the January 1999 and 2004 Gulf of Alaska female cod ages at maturity did not differ significantly ($P=0.19$).

The otoliths taken during the 2003 AFSC bottom trawl surveys of the Gulf of Alaska ($n=711$) and eastern Bering Sea ($n=1360$) provide the largest and most comprehensive collection of age data available for female and male Pacific cod. The otolith specimens were selected by region, sex, and L_T. Pacific cod had wide variations in age at length (Fig. 6, Table 5). Based on these collections, the von Bertalanffy growth function differed significantly ($P<0.001$) between the Gulf of Alaska and Bering Sea for both males and females (Table 5). Female Pacific cod length at age was smaller in the Gulf of Alaska than in the Bering Sea. The Gulf

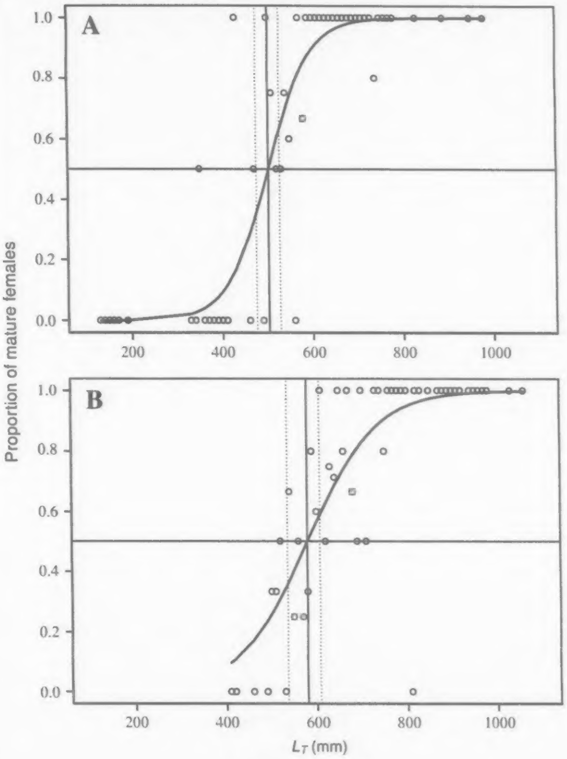

Figure 4

The proportion of mature female Pacific cod (*Gadus macrocephalus*) by total length (L_T, mm) in (**A**) the Gulf of Alaska January 1999 and 2004 collection (n=157) and in (**B**) the Bering Sea February 2003 collection (n=133). The mean length at 50% maturity=502.56 (A) and 579.96 mm (B), and the 95% confidence intervals are represented by parallel dotted lines.

of Alaska female Pacific cod growth differed significantly (P<0.001) from the growth of males. The rate of growth declined more with age for males than for females in the Gulf of Alaska (Fig. 6). However, in the Bering Sea, male growth was nearly as rapid (P=0.015) as that of females. Males were estimated to reach a slightly smaller maximum theoretical L_∞ of 1044 mm in the Gulf of Alaska than in the Bering Sea (1101 mm).

Discussion

This study provides the most extensive and representative estimates of female Pacific cod length- and age-at-maturity and growth available. This is the first Pacific cod study to rely on histological methods to assess ovary maturity, and the first to make temporal comparisons of maturity. It is the first northeast Pacific Ocean study to assess Pacific cod age-at-maturity. Before this study, managers of the Alaska Pacific cod fishery (Thompson and Dorn, 2005; Thompson et al., 2005) used a female L_{T50} estimate of 670 mm from macroscopic maturity classifications made by commercial fishery observers on specimens collected after March in 1993 and 1994. However, the macroscopic maturity classification method can introduce sampling bias and misclassifications. In contrast, in this study, it was determined that the most representative method for estimating L_{T50} relied on making histological maturity assessments of large numbers of ovary samples from a wide L_T range of specimens collected before the late spawning period.

The results from this study are similar to the results from studies conducted in other areas. The estimated female Pacific cod A_{50} differed only slightly between the Gulf of Alaska and Bering Sea study areas and were similar to the ages estimated for Sea

Table 3

Total length (mm) and age (years) composition of female Pacific cod (*Gadus macrocephalus*) specimens collected in the Gulf of Alaska (GOA) during January 1999 and 2004 and in the Bering Sea (BS) during February 2003 to estimate the length and age at which 50% reached sexual maturity. The objective was to collect a minimum of five specimens per length class, subject to availability. *n* = number of fish in the sample.

Length (mm)	GOA *n*	BS *n*	Length (mm)	GOA *n*	BS *n*	Age (years)	GOA *n*	BS *n*
130	1		660	4	5	1	6	
140	1		670	4	2	2	3	
150	1		680	8	6	3	20	3
160	1		690	5	2	4	16	16
170	1		700	4	2	5	32	32
190	1		710	6	6	6	42	22
330	1		720	8		7	26	30
340	1		730	8	1	8	6	18
350	2		740	5	5	9	2	6
360	3		750	2	5	10	1	2
370	5		760	5	3			
380	7		770	2	1			
390	3		780	1	2			
400	3		790		3			
410	4	1	800		4			
420		2	810		1			
430	1		820		3			
460	1	3	830	1	2			
470	2		850		1			
490	1	1	870		1			
500	1	3	880		3			
510	4	3	890	1	2			
520	4	2	900		1			
530	4	1	910		1			
540	4	3	920		1			
550	5	4	940		1			
560	1	2	950	1	1			
570	2	4	960		1			
580	3	3	970		1			
590	3	5	980	1	1			
600	4	5	1030		1			
610	4	2	1060		1			
620	2	4						
630	5	2						
640	4	3						
650	1	4						

of Okhotsk (5 years of age, Rovnina et al., 1997) and Sea of Japan (4 years of age, Hattori et al., 1992) female Pacific cod. Results from previous studies support the between-area differences in female Pacific cod length-at-maturity found during the present study. Like Gulf of Alaska Pacific cod, female Pacific cod from Canadian waters were estimated to mature at a smaller L_{T50} (median 450 mm during the 1970s and 550 mm during the 1960s; Welch and Foucher, 1988) than Bering Sea Pacific cod. The Bering Sea estimate of L_{T50} was within the range estimated for the Sea of Okhotsk female Pacific cod (550 mm L_T to 600 mm L_T; Rovnina et al., 1997). In the present study, no significant differences were found in female Pacific cod L_{T50} or A_{50} for any of the months sampled, within either the Gulf of Alaska or Bering Sea areas. The temporal agreement for female Pacific cod A_{50} and L_{T50} estimates indicates they are reliable. Results were also similar between the two histology-based methods of classifying mature female Pacific cod, indicating that either method could be used to define A_{50} or L_{T50}.

Table 4

Age-at-maturity results based on ovary samples (n) collected between the late prespawning and initial spawning periods for female Pacific cod (*Gadus macrocephalus*) in the Gulf of Alaska (GOA) and Bering Sea (BS) areas, by date of collection. The parameters of the logistic equation that were used to fit the data are given: B (slope of the line) and A (Y intercept), variance (the square of the standard deviation of B and A), covariance (the product of the standard deviations of B and A and the coefficient of correlation between them), age (years) at which 50% of females were expected to reach sexual maturity (A_{50}), and variance of A_{50}.

	Gulf of Alaska	Bering Sea
Sampling statistics	January 2003 and 2004	February 2003
n	154	129
B	1.9632	0.9654
A	−8.5395	−4.7143
Variance (B)	0.0145	0.0065
Variance (A)	2.1246	1.3680
Covariance (B,A)	0.0059	0.0013
A_{50}	4.3499	4.8832
Variance (A_{50})	0.0224	0.0663

Spawning participants sampled during this study, included female Pacific cod as small as 420 mm L_T in the Gulf of Alaska and 460 mm in the Bering Sea area. In comparison, cod (*Gadus morhua*) from the northwest Atlantic Ocean initiated spawning in 1995 at 400 mm—a decline from 500 mm in 1992 (Saborido-Rey and Junquera, 1998).

Spawning is an annual occurrence for female Pacific cod according to the results of seasonal ovary development, the I_G cycle, and the wide range in age and body length composition of the spawning population each month. This conclusion was consistent with that from Teshima's (1985) study, which found that the Bering Sea Pacific cod gonadosomatic index increased in November and December because of maturation and that spawning was not expected to occur until the following year. Similarly, Atlantic cod individuals have an annual reproductive cycle (Norberg et al., 2004) and spawn despite being raised in captivity under conditions of starvation (Kjesbu et al., 1991).

Based on results from this study, the spawning activity for female Pacific cod is believed to begin during late winter and peak during the spring. This estimated period of peak spawning, based on results summarizing ovarian maturities by month of collection, is validated by larval abundance estimates from the Gulf of Alaska and Bering Sea ichthyoplankton surveys conducted since 1980 by the AFSC (Matarese et al., 2003). Similarly, the Sea of Okhotsk population is estimated to have a peak spawning period that includes the months of March and May, based on a 1995 study (Rovnina et al., 1997). Spawning probably ends in early summer in the Gulf of Alaska, as indicated by the lack of any specimens in June with vitellogenesis-stage ovaries.

The likelihood of female Pacific cod spawning was strongly associated ($P<0.001$) with the time of month, and later in the spawning season, spawning was associated ($P=0.01$) with LT. There were no associations with spawning and age, or ambient water temperature; consequently these factors probably do not regulate the timing of spawning for Pacific cod. Similarly, seawater temperature was not the most important environmental cue regulating the maturation and spawning of Atlantic cod and other commercially cultured Atlantic Ocean fish species, including rainbow trout (*Oncorhynchus mykiss*), Atlantic halibut (*Hippoglossus hippoglossus*) and sole (*Solea solea*) (Norberg et al., 2004). For these cultured Atlantic species, photoperiod is the most important regulator of the reproductive cycle. Pacific cod maturation and spawning was significantly associated with time of month, as determined by this study, which would indicate that photoperiod may regulate the reproductive cycle in this species. Photoperiod should be similar for both the Gulf of Alaska and Bering Sea study areas sampled by this survey, given their similar latitudes (Fig. 1), and could account for the similarity in the timing of spawning within the Gulf of Alaska and Bering Sea waters found during this study and during the ichthyoplankton surveys.

Regardless of where spawning occurs, the reproductive effort by the fish represents a substantial investment, based on ovary weight that represents up to 30% of the total female Pacific cod body weight and Atlantic cod body weight (Lambert and Dutil, 2000). Pacific cod have among the highest fecundities of any tele-

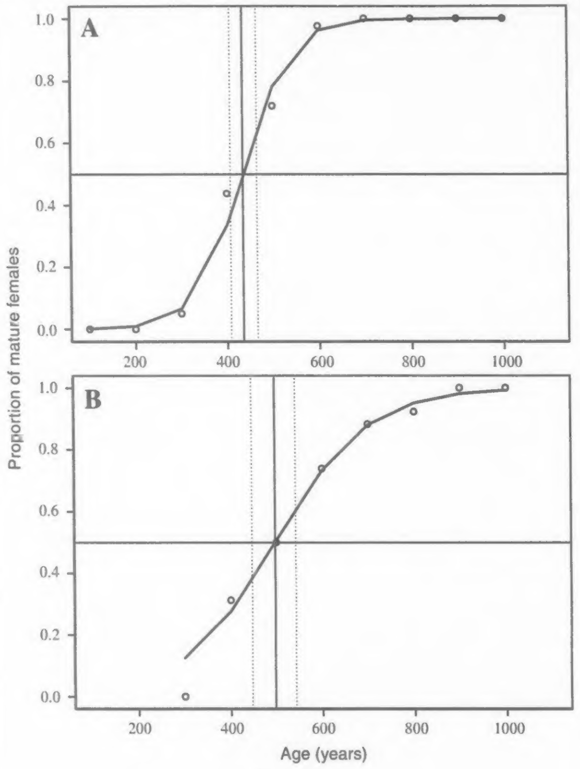

Figure 5

The proportion of mature female Pacific cod (*Gadus macrocephalus*) by age in (**A**) the Gulf of Alaska, based on the January 1999 and 2004 (n=154) collection and in (**B**) the Bering Sea, based on the February 2003 (n=129) collection. The mean age at 50% maturity=4.4 (A) and 4.9 years (B), and the 95% confidence intervals are represented by the parallel dotted lines.

ost (Waiwood, 1982; Foucher and Tyler, 1990) and can produce up to 5.7 million ova each year. However, it appears that the metabolic costs of spawning do not diminish female Pacific cod growth.

Female Pacific cod growth does not significantly decline upon reaching A_{50} in either the Gulf of Alaska or Bering Sea. Males in the Gulf of Alaska area reach a smaller maximum length than females. Similarly, in the eastern Sea of Okhotsk, male Pacific cod reach a smaller total length than females (Rovnina et al., 1997). In contrast male Pacific cod in the Bering Sea area reach a maximum length similar to that of females, and female Pacific cod grow significantly faster in the Bering Sea than in the Gulf of Alaska. The growth results support the maturity-at-length results in the present study that indicate a much larger L_{T50} for the Bering Sea females. Longevity, however, is similar for Gulf of Alaska and Bering Sea Pacific cod and does not differ between sexes. Pacific cod growth probably occurs primarily during the summer and fall, as does growth in Atlantic cod (Norberg et al., 2004), and not during the winter through early summer months, the period used by the present study to assess length- and age-at-maturity.

With the estimates of A_{50} and L_{T50} from this study, the spawning stock biomass of female Pacific cod for the Gulf of Alaska and eastern Bering Sea increased from the 2005 estimate of 300×10^3 t that was based on a previous study, to an 2006 estimate of 500×10^3 t (Thompson and Dorn, 2005; Thompson et al., 2005). The spawning biomass estimates are of critical importance for stock management models from which are determined the allowable commercial catch quotas of Pacific cod in the northeast Pacific Ocean and Bering Sea (Thompson and Dorn, 2005; Thompson et al., 2005). The increased spawning stock biomass estimates of female Pacific cod resulting from this study support the establishment of higher over-fishing limits for Pacific

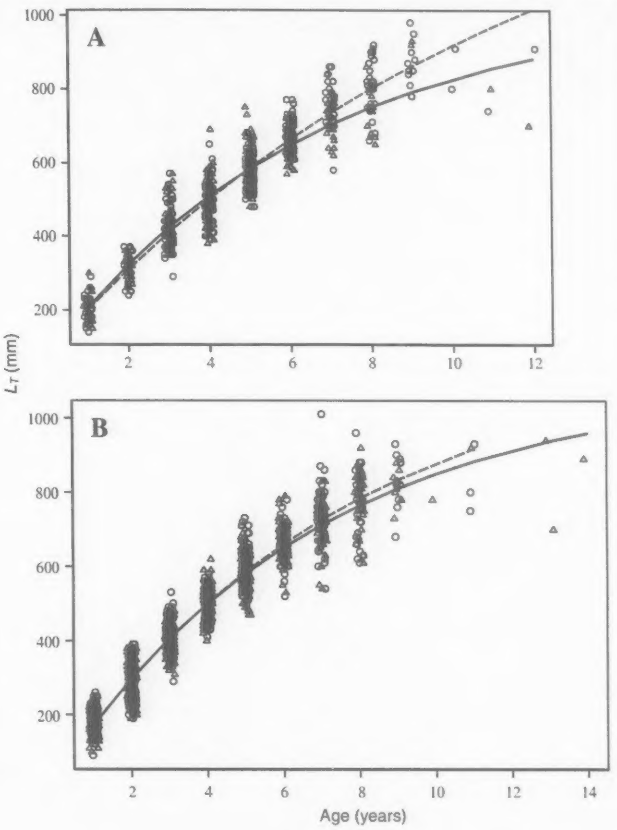

Figure 6

Total length (L_T, mm) at age of Pacific cod (*Gadus macrocephalus*) females (○, ---) and males (△, ——) in (**A**) the Gulf of Alaska (♀ n=375, ♂ n=336) and (**B**) the Bering Sea (♀ n=676, ♂ n=684), based on area-wide groundfish assessment surveys conducted by the National Oceanic and Atmospheric Administration Alaska Fisheries Science Center during 2003.

cod than would have otherwise occurred. As a result, the revised 2006 management plan increased the estimated spawning stock biomass by 80% in the Gulf of Alaska and by 10% in the eastern Bering Sea and Aleutian Islands, over the 2005 plan estimates. These increases offset declines in the estimated biomass of Pacific cod over 2 years of age for the Gulf of Alaska (4%) and for the eastern Bering Sea and Aleutian Islands (19%) during the same period. Consequently, the recommended over-fishing limit increased 51% in the Gulf of Alaska and declined only 18% in the Bering Sea and Aleutian Islands.

Although temporal stability was found for Pacific cod A_{50} and L_{T50} estimates in the present study, maturity assessments should be conducted on a periodic basis in the future to ensure that managers continue to receive representative estimates of Pacific cod A_{50} and L_{50} and timing of spawning, which are essential for rational stock management. Maturity assessments would be particularly important during periods of significant change in climate or habitat.

Acknowledgments

Thanks to the following Alaska Fisheries Science Center personnel for their contributions: D. Somerton, G. Stauffer, R. Nelson, A. Hollowed, D. Nichol,

Table 5

Length-at-age described by the von Bertalanffy growth equation for male and female Pacific cod (*Gadus macrocephalus*) in the Gulf of Alaska (GOA) and Bering Sea (BS). Also provided are sample size (n) and parameters L_∞ (length at maximum age in mm), k (estimated growth increment), t_0 (theoretical age when fish length is 0). Numbers in parentheses represent the number of fish in the sample.

	Gulf of Alaska		Bering Sea	
	Males	Females	Males	Females
n	347	389	684	676
L_∞ (mm)	1043.7900	1567.2000	1100.630	1203.9400
var (L_∞)	3564.9736	24716.8707	1281.3393	2641.7441
k	0.1498	0.0825	0.1449	0.1277
var (k)	0.0003	0.0002	0.0001	0.0001
t_0	−0.4670	−0.6712	−0.1814	−0.2233
var (t_0)	0.0182	0.0246	0.0032	0.0042
cov (L_∞,k)	−0.9892	−2.0091	−0.3052	−0.4808
cov (L_∞,t_0)	−6.1381	−20.3573	−1.4960	−2.5903
cov (k,t_0)	0.0020	0.0018	0.0004	0.0005

E. Acuna, R. MacIntosh, C. Armistead, J. Haaga, M. Wilkins, S. Neidetcher, L. Logerwell, P. Munro, C. Johnston, M. Nelson, G. Duker, and J. Lee. Thanks to the following Alaska Department of Fish and Game staff for sample collections: J. Blackburn, D. Urban, D. Pengilly, K. Phillips, T. Dinnocenzo, I. MacIntosh, M. Ruccio, D. Jackson, the Captain R. Kutchick, and crew of the RV *Resolution*. K. MacIntosh from the Alaska Groundfish Databank collected the plant samples.

Literature cited

Efron, B., and R. J. Tibshirani.
1993. An introduction to the bootstrap, 436 p. Chapman and Hall, New York, NY.

Foucher, R. P., and A. V. Tyler
1990. Estimation of the fecundity of Pacific cod *Gadus macrocephalus*. Can. Man. Rep. Fish. Aquat. Sci. 2088, 49 p.

Hart, L.
1973. Pacific fishes of Canada. Fish. Res. Board Can. Bull. 180,740 p.

Hattori, T., Y. Kasurai, and K. Shimazaki.
1992. Maturation and reproductive-cycle of female Pacific cod in waters adjacent to the southern coast of Hokkaido, Japan. Nihon. Suisan. Gakkai-Shi 58:2245–2252.

Hunter, J. R., B. J. Macewicz, N. C. H. Lo, and C. A. Kimbrell.
1992. Fecundity, spawning, and maturity of female Dover sole, *Microstomus pacificus*, with an evaluation of assumptions and precision. Fish. Bull. 90:101–128.

Kimura, D. K.
1980. Likelihood methods for the von Bertalanffy growth curve. Fish. Bull. 77:765–776.

Kjesbu, O. S., J. Klungsoyr, H. Kryvi, P. R. Witthames, and M. Greer-Walker.
1991. Fecundity, atresia, and egg size of captive Atlantic cod (*Gadus morhua*) in relation to proximate body composition. Can. J. Fish. Aquat. Sci. 48:2333–2343.

Lambert, Y., and J. D. Dutil.
2000. Energetic consequences of reproduction in Atlantic cod *Gadus morhua* in relation to spawning level of somatic energy reserves. Can. J. Fish. Aquat. Sci. 57:815–825.

Matarese, A. C., D. M. Blood, S. J. Picquelle, and J. L. Benson.
2003. Atlas of abundance and distribution patterns of ichthyoplankton from the Northeast Pacific Ocean and Bering Sea ecosystems based on research conducted by the Alaska Fisheries Science Center 1972–1996. U.S. Dep. Commer. NOAA Prof. Pap. NMFS 1, 281 p.

Norberg, B., C. L. Brown, O. Halldorsson, K. Stensland, and B. T. Bjornsson.
2004. Photoperiod regulates the timing of sexual maturation, spawning, sex steroid and thyroid hormone profiles in the Atlantic cod *Gadus morhua*. Aquaculture 229:451–467.

Roberson, N. E., D. K. Kimura, D. R. Gunderson, and A. M. Shimada.
2005. Indirect validation of the age-reading method for Pacific cod (*Gadus macrocephalus*) using otoliths from marked and recaptured fish. Fish. Bull. 103:153–160.

Rovnina, O. A., N. V. Klovach, A. I. Glubokov, and A. P. Selyutin.
1997. On the biology of Pacific cod *Gadus macrocephalus* in the eastern part of the Sea of Okhotsk. J. Ichthyol. 37:21–26. Translated from Russian [1997 Voprosy Ikhtiologii 37:27–32] by Interperiodica Publishing, Russia.

Saborido-Rey, F., and S. Junquera.
1998. Histological assessment of variations in sexual maturity of cod (*Gadus morhua* L.) at the Flemish Cap (north-west Atlantic). ICES J. Mar. Sci. 55:515–521.

Sokal, R. R.
1969. Biometry, 776 p. W.H. Freeman and Company, San Francisco, CA.

Stark, J. W., and D. A. Somerton.
2002. Maturation, spawning and growth of rock soles off Kodiak Island in the Gulf of Alaska. J. Fish Biol. 61:417–431.

Teshima, K.
1985. Maturation of Pacific cod in the eastern Bering Sea. Bull. Jap. Soc. Sci. Fish. 51:21–31.

Thompson, G. G., and M. W. Dorn.
2005. Stock assessment and fishery evaluation: Bering Sea and Aleutian Island cod, 90 p. North Pacific Fishery Management Council. Anchorage, AK.

Thompson, G. G., H. H. Zenger, and M. W. Dorn.
2005. Stock assessment and fishery evaluation: Gulf of Alaska Cod, 112 p. North Pacific Fishery Management Council. Anchorage, AK.

Venables, W. N.
1997. Modern applied statistics with S-Plus, 548 p. Springer-Verlag, New York, NY.

Waiwood, K. G.
1982. Growth history and reproduction in Atlantic cod (*Gadus morhua*). *In* Proceedings of the international symposium on reproductive physiology of fish (C. J. J. Richter, and H. J. Th. Goos, eds.), 256 p. Pudoc Press, Wageningen, The Netherlands.

Welch, D. W., and R. P. Foucher.
1988. A maximum-likelihood methodology for estimating length-at-maturity with application to Pacific cod (*Gadus macrocephalus*) population dynamics. Can. J. Fish. Aquat. Sci. 45(2):333–343.

Interactions between marine mammals and pelagic longline fishing gear in the U.S. Atlantic Ocean between 1992 and 2004

Lance P. Garrison

Email address: Lance.Garrison@noaa.gov

National Marine Fisheries Service
Southeast Fisheries Science Center
75 Virginia Beach Dr.
Miami, Florida 33149

Abstract—The U.S. East Coast pelagic longline fishery has a history of interactions with marine mammals, where animals are hooked and entangled in longline gear. Pilot whales (*Globicephala* spp.) and Risso's dolphin (*Grampus griseus*) are the primary species that interact with longline gear. Logistic regression was used to assess the environmental and gear characteristics that influence interaction rates. Pilot whale interactions were correlated with warm water temperatures, proximity to the shelf break, mainline lengths greater than 20 nautical miles, and damage to swordfish catch. Similarly, Risso's dolphin interactions were correlated with geographic location, proximity the shelf break, the length of the mainline, and bait type. The incidental bycatch of marine mammals is likely associated with depredation of the commercial catch and is increased by the overlap between marine mammal and target species habitats. Altering gear characteristics and fishery practices may mitigate incidental bycatch and reduce economic losses due to depredation.

Manuscript submitted 11 December 2006 to the Scientific Editor's Office.

Manuscript approved for publication 27 March 2007 by the Scientific Editor.

Fish. Bull. 105:408–417 (2007).

Marine mammal mortalities and injuries occur in gillnet fisheries (Perrin et al., 1994), trawl fisheries (Fertl and Leatherwood, 1997), and longline fisheries (e.g., Garrison, 2005; Kock et al., 2006). The U.S. East Coast pelagic longline fishery targeting swordfish, tunas, and sharks has long been the focus of bycatch reduction efforts for nontarget fish species (e.g., billfish; Goodyear, 1999) and for marine turtles (Watson et al., 2005). In addition, marine mammal bycatch in the pelagic longline fishery is common, particularly of pilot whales (*Globicephala* spp.) and Risso's dolphins (*Grampus griseus*). An estimated average of 132 (CV [coefficient of variation]=0.49) pilot whales and 45 (CV=0.38) Risso's dolphins either died or were seriously injured because of interactions with pelagic longline gear each year between 1999 and 2003 (Waring et al., 2006). These numbers account for 63% of the total commercial fishery-related mortality for pilot whales and 88% for Risso's dolphins along the U.S. East Coast. The total fishery mortality for pilot whales approaches the potential biological removal (PBR) benchmark (PBR=249 for pilot whales and 129 for Risso's dolphins), and it exceeds the requirement that mortality caused by commercial fishing approach insignificant levels as mandated by the U.S. Marine Mammal Protection Act (MMPA) (Waring et al., 2006).

In addition to marine mammal conservation concerns, the occurrence of depredation, or marine mammals feeding on the catch or bait from commercial fishing gear, is an emerging global issue. Depredation has been observed on both bottom and pelagic longlines by killer whales (*Orcinus orca*; Secchi and Vaske, 1998; Kock et al., 2006), false killer whales (*Pseudorca crassidens*), pilot whales, and sperm whales (*Physeter macrocephalus*; Kock et al., 2006). Fishermen in the Atlantic longline fleet indicate that damage to commercial catch by pilot whales is common (Angliss and DeMaster, 1998). Depredation has a direct economic impact on commercial fishermen by removing commercially valuable catch.

Identification of the fishing practices and environmental processes that drive interactions between marine mammals and longline fishing gear is important to understanding and reducing both incidental mortality and depredation. In this study, pelagic longline fishery observer data collected between 1992 and 2004 were analyzed to describe the number of interactions, seasonal and spatial patterns, and the types of interactions associated with serious injuries and mortalities of marine mammals. Logistic regression was used to examine factors affecting the probability of interactions with pilot whales and Risso's dolphins. The results of these analyses will help managers make informed decisions to reduce both marine mammal bycatch and economic losses due to depredation.

Materials and methods

Pelagic observer program

The U.S. East Coast pelagic longline fishery has been observed since 1992.

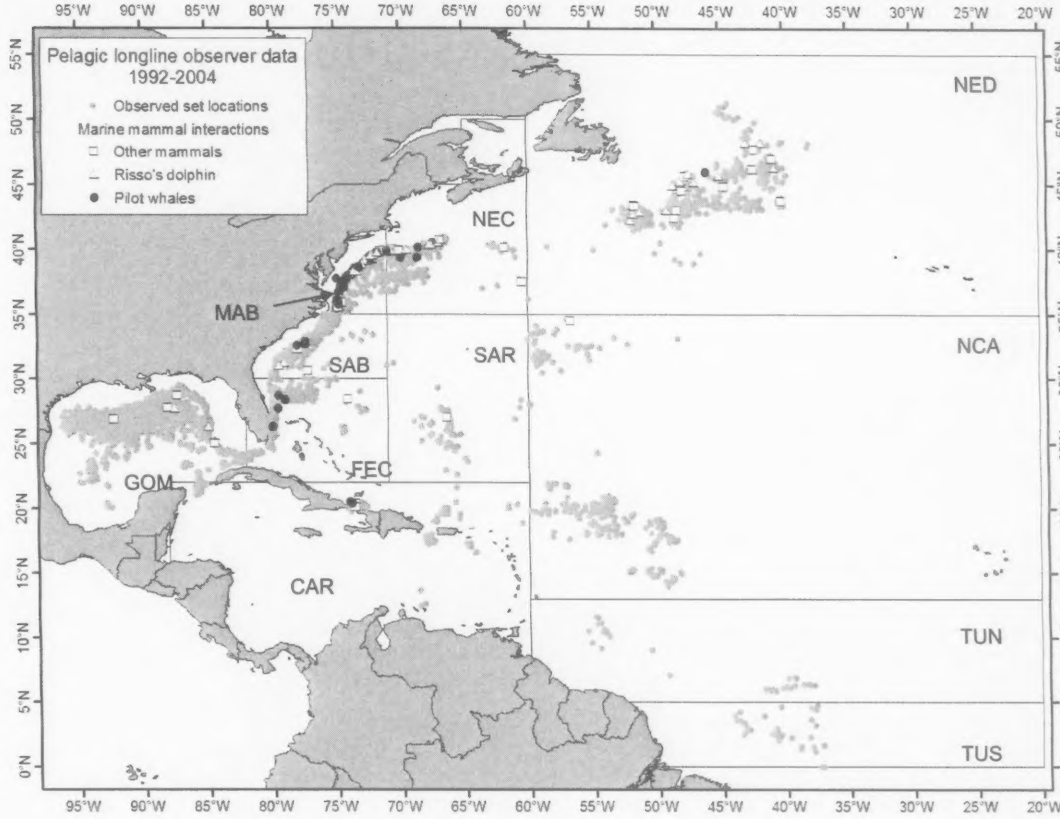
Pelagic longline observer data
1992-2004
Observed set locations
Marine mammal interactions
Other mammals
Risso's dolphin
Pilot whales
NED
NEC
NCA
MAB
SAB
SAR
GOM
FEC
CAR
TUN
TUS
95°W
90°W
85°W
80°W
75°W
70°W
65°W
60°W
55°W
50°W
45°W
40°W
35°W
30°W
25°W
20°W
55°N
50°N
45°N
40°N
35°N
30°N
25°N
20°N
15°N
10°N
5°N
0°N

Mexico, NEC=Northeast Coastal, NED=Northeast Distant, NCA=North Central Atlantic, MAB=Mid-Atlantic Bight, SAB=South Atlantic Bight, SAR=Sargasso Sea, TUN=Tuna North, and TUS=Tuna South.

Observer coverage was allocated randomly among fishing vessels by calendar quarter and fishing area. Achieved annual observer coverage typically ranged between 3–4% of longline sets between 1992–2001 and was near 7% during 2002–04. The observers collected detailed information on gear characteristics, set and haul locations, environmental data, and composition of the fish catch. Observers also documented incidental takes of marine mammals including estimated lengths and written descriptions of each animal and its interaction with the fishing gear (Beerkircher et al., 2004).

During 2001–04, the Northeast Distant (NED) fishing area (Fig. 1) was closed to the longline fishery because of concerns over marine turtle bycatch. An experimental program was initiated, in cooperation with the fishing industry, to explore potential gear and bait combinations to reduce interactions with marine turtles. During the study, fishermen used larger circle hooks rather than traditional, smaller, straight-shanked "J" hooks (Watson et al., 2005). There was 100% observer coverage of this experimental fishing. Because the fishing operations were prescribed by experimental design, and differed from standard commercial fishing operations, data from these experimental sets, including data on marine mammal interactions, were excluded from the current analysis.

Observed marine mammal interactions

When a marine mammal interacted with the longline gear (i.e., was hooked or entangled), the observers noted the condition of the captured animal and the type of fishing gear, documented efforts to remove the animal from the gear, and recorded the behavior of the animal after release. Observer comments were summarized to assess the most frequent types of interactions with longline gear. Two species of pilot whales inhabit the waters along the U.S. East Coast: the short-finned pilot whale (*G. macrorhynchus*) and long-finned pilot whale (*G. melas*). However, the two could not be reliably distinguished at sea by the observers and therefore were combined in this analysis.

Determination of serious injury to marine mammals

The MMPA requires that incidental mortality of and serious injury to marine mammals during commercial fishing operations be reduced below the PBR benchmark. Serious injury has been defined as an injury likely to result in mortality (Angliss and DeMaster, 1998). A workshop of National Marine Fisheries Service (NMFS) and nongovernmental experts was convened in 1997 to evaluate the types of injuries occurring in commercial fisheries and to develop guidelines to determine if a given marine mammal observed interacting with commercial fishing gear was seriously injured. For small cetaceans, including pilot whales and other delphinids, it was concluded that animals that ingested hooks, that were released with significant amounts of trailing fishing gear, that were swimming abnormally, or that suffered severe external trauma would be considered seriously injured (Angliss and Demaster, 1998). Serious injury determinations were made by NMFS staff on a case-by-case basis after reviewing the observations and comments of fishery observers.

Logistic regression analysis

Logistic regression was used to evaluate the effects of environmental conditions and fishing practices on the probability of interactions with pilot whales and Risso's dolphins. The vast majority (>85%) of interactions with marine mammals involved only one individual with a set. Therefore, the data were transformed to a binary response variable indicating whether or not a marine mammal interaction was observed.

Only longline sets made along the U.S. Atlantic and Caribbean coasts, including the Florida East Coast (FEC), South Atlantic Bight (SAB), Mid-Atlantic Bight (MAB), Northeast Coastal (NEC), and Caribbean (CAR) fishing areas (Fig. 1), were included in this analysis because interaction rates in most other areas were extremely low or zero. Although Risso's dolphin interactions were observed during experimental fishing in the NED, the fishing characteristics of these sets were different from those of the normal commercial fishing operations. Therefore, sets observed in the NED (experimental and nonexperimental) were excluded from the analysis. This included two observed interactions with Risso's dolphins and none with pilot whales in nonexperimental fishing. The analysis focused on the Atlantic fishing areas with the highest overall interaction rates with pilot whales and Risso's dolphin and comprised 3187 observed longline sets.

Explanatory variables were drawn from a broad suite of data collected during each set by the fishery observer (Table 1), or they were derived from the date and location of the set (Table 1). Variables were categorized broadly as environmental conditions, space or time variables, gear characteristics, fishing effort level, and catch characteristics. However, each was considered independently in developing the best fitting, most parsimonious logistic regression model following strategies for model selection outlined in Hosmer and Lemeshow (1989). Briefly, each variable was examined individually to assess its explanatory power, and the subset of significant single terms was included in the initial model. Following this initial exploratory step, the single terms and all two-way interactions were examined by using stepwise selection. The explanatory power and significance of each potential model term was examined through chi-square tests and Akakie's information criterion (AIC; Hosmer and Lemeshow, 1989; McCullagh and Nelder, 1989). Terms were retained in the model if they were significant (at a *P*-value <0.10) based upon chi-square tests and if their addition resulted in a reduction in AIC. The resulting models were examined for overdispersion by using the ratio between the residual model chi-square and degrees of freedom (Burnham et al., 1987; McCullagh and Nelder, 1989). For both the pilot whale model and the Risso's dolphin model, this ratio was approximately equal to one, which indicated no significant problems with overdispersion and hence accurate estimates of variance for model parameters.

Results

Observed marine mammal interactions

Between 1992 and 2004, a total of 200 interactions between marine mammals and pelagic longline gear were observed. Of these, there were 10 observed mortalities and 94 observed serious injuries (Table 2). One hundred of the observed interactions were with pilot whales, 64 were with Risso's dolphin, and all other species had six or fewer observed interactions. Other marine mammal interactions of note occurred with a killer whale, unidentified beaked whales (family Ziphiidae), a pygmy or dwarf sperm whale (*Kogia* spp.), a northern bottlenose whale (*Hyperoodon ampullatus*), and two baleen whales (Table 2).

The majority of marine mammal interactions were observed near the shelf break along the U.S. Atlantic coast between North Carolina and Georges Bank (Fig. 1). Pilot whale interactions were concentrated in the MAB fishing area between North Carolina and New Jersey, whereas Risso's dolphin interactions primarily occurred in the NEC region (Fig. 1). Thirteen Risso's dolphins, one pilot whale, and eight additional animals of various species interacted with fishing gear during experimental fishing operations in the NED during 2001–03 (Fig. 1).

The observed interaction rates (number of sets with a marine mammal interaction/number of observed sets) fluctuated across the time series. The highest rates were observed during 1992–95 and in the most recent years from 2000 through 2004 (Fig. 2A). There were generally low interaction rates and very few pilot whale

Table 1

Environment, space or time, gear type, fishing effort, and catch variables examined in logistic regression analyses of the probability of marine mammal interactions in the U.S. pelagic longline fishery. The fishing areas included in the study were the following: Florida East Coast (FEC), Mid-Atlantic Bight (MAB), South Atlantic Bight (SAB), Northeast Coastal (NEC), and Carribbean (CAR) (see Fig. 1).

Type of variable	Variable name	Description
Environment	Average temperature	Average of sea surface temperature reported by observer at beginning and end of haul and set
Environment	Water depth	Water depth based on average location of set determined from a global bathymetry grid
Environment	Wave height	Recorded by observers at time of set
Environment	Wind speed	Recorded by observers at time of set
Environment	Weather conditions	Calm, cloudy, mild storm, stormy—recorded by observers at time of set
Space or time	Distance from 200-m isobath	Distance of the set (km) from the 200-m isobath
Space or time	Average location	Average of latitude and longitude for beginning set, end set, beginning haul, end haul
Space or time	Month	Calendar month of beginning set
Space or time	Quarter	Calendar quarter of beginning set
Space or time	Year	Calendar year of beginning set
Space or time	Fishing area	Fishing area of set: includes FEC, MAB, SAB, NEC, CAR
Space or time	Geographic area	Combined area categories MAB versus other areas
Space or time	Lunar phase	Lunar age since full moon
Gear type	Hook shape	Type(s) of hooks reported on the set. Categories include J-hook only, C-hook only, or both types
Gear type	Hook size	Size categories of hooks on the set were 7/0, 8/0, 9/0, 10/0, 12/0, 16/0, and 18/0
Gear type	Light sticks	Binary variable, whether or not light sticks were used on the set
Gear type	Bait type	Type(s) of bait recorded. Includes fish only, squid only, or both
Gear type	Live bait	Binary variable, whether or not live bait was used on the set
Gear type	Hook depth	Average of reported minimum and maximum hook depths (fathoms)
Gear type	Day set	Binary variable, whether or not set occurred during daylight
Gear type	Day soak	Binary variable, whether or not gear soaked during daylight
Gear type	Day haul	Binary variable, whether or not haulback occurred during daylight
Effort	Mainline length	Mainline length reported in miles
Effort	Number of hooks	Number of hooks set
Effort	Set duration	Number of hours to set the gear
Effort	Soak duration	Number of hours the gear soaked between the end of the set and the beginning of the haul
Effort	Haul duration	Number of hours spent hauling the gear
Effort	Total duration	Estimated number of hours the average hook was in the water (1/2 set duration + soak duration + 1/2 haul duration)
Effort	Hook density	Number of hooks/mainline length
Effort	Hook hours	Number of hooks×total duration
Catch	Bigeye tuna(*Thunnus obesus*)	Bigeye tuna catch (numbers)
Catch	Sharks	Shark catch (numbers)
Catch	Swordfish (*Xiphias gladius*)	Swordfish catch (numbers)
Catch	Other tunas	Other tuna catch (numbers)
Catch	Yellowfin tuna (*Thunnus albacares*)	Yellowfin tuna catch (numbers)
Catch	All tunas	Sum of yellowfin tuna, bigeye tuna, and other tunas
Catch	Damage	Binary variable, whether or not damage to the catch was observed
Catch	Swordfish damage	Binary variable, whether or not damage to swordfish catch was observed
Catch	Tuna damage	Binary variable, whether or not damage to tuna catch was observed

Table 2

Marine mammal interactions with pelagic longline fishing gear between 1992 and 2004. The totals include interactions observed during experimental fishing in the Northeast Distant Water (NED) fishing area. Determination of serious injury was based on observer descriptions and National Marine Fisheries Service criteria (Angliss and Demaster, 1998).

Species	Total captured	Total observed dead	Total seriously injured
Pilot whale (*Globicephala* spp.)	100	4	52
Risso's dolphin (*Grampus griseus*)	64	6	30
Common dolphin (*Delphinus delphi*)	6	0	0
Bottlenose dolphin (*Tursiops truncatus*)	6	0	2
Unidentified dolphin	4	0	2
Unidentified marine mammal	4	0	2
Unidentified beaked whales (*Mesoplodon* spp.)	3	0	1
Pantropical spotted dolphin (*Stenella attenuata*)	3	0	0
Atlantic spotted dolphin (*Stenella frontalis*)	2	0	2
Striped dolphin (*Stenella coeruleoalba*)	2	0	0
Unidentified whale	1	0	1
Northern bottlenose whale (*Hyperoodon ampullatus*)	1	0	1
Unidentified baleen whale	1	0	0
Killer whale (*Orcinus orca*)	1	0	0
Minke whale (*Balaenoptera acutorostratus*)	1	0	0
Pygmy or dwarf sperm whale (*Kogia* spp.)	1	0	1

Table 3

Types of serious injuries observed in marine mammals interacting with pelagic longline fishing gear between 1992 and 2004.

Species	Mouth hooked	Animal released with entangling gear	Mouth hooked and animal released with entangling gear	Total
Pilot whales (*Globicephala* spp.)	3	19	30	52
Risso's dolphin (*Grampus griseus*)	7	12	11	30
Other species	1	3	8	12
Totals	11	34	49	94

interactions were observed during 1996–98. Interaction rates for both pilot whales and Risso's dolphins peaked during the late summer and fall (Fig. 2B).

Types of serious injury

Of the 94 observed serious injuries, there were 60 cases where marine mammals were released with hooks remaining in the mouth. In 49 of these cases, monofilament line (typically 15–60 feet in length) remained with the animal (Table 3). In the remaining 11 cases, the animal was released with less than five feet of monofilament line and with the hook remaining in the mouth. In four of the 11 documented mortalities, the animal was hooked in the mouth.

There were 34 serious injuries in which the animal was released entangled with fishing gear that did not involve ingestion of a hook (Table 3). The majority of these cases were injuries to animals that became entangled in the mainline which typically consists of 700-lb test monofilament. In most of these cases, the animal was released with multiple wraps of mainline around its tail or body, and the gear remained with the animal after the line was cut. In five of the 10 documented mortalities, the animal was entangled in the mainline. Fishermen were typically able to cut the mainline away from entangled animals. Thus, the majority of animals entangled in the mainline were released without entangling gear, and these animals were not considered to be seriously injured.

Logistic regression results: Pilot whales

Geographic area (MAB vs. other areas; chi-square=31.24, df=1, $P<0.0001$), distance from the 200-m isobath (chi-square=11.31, df=1, $P=0.0008$), and observed damage to the swordfish catch (chi-square=7.26, df=1, $P=0.0071$) were significant factors correlated with the occurrence of pilot whale interactions with longline gear. A linear term for water temperature was also highly significant and, on inspection of initial regression results, there was a unimodal relationship between water temperature and interaction rate. Water temperature (chi-square=8.53, df=1, P=0.0035) and its second-order term (chi-square=7.87, df=1, P=0.0050) were included in the model and were statistically significant. There was also an apparent nonlinear relationship with mainline length, with a step increase in interaction rate for mainlines greater than 20 nautical miles in length. The continuous mainline length variable was replaced with a binary response (mainline ≥20 miles). This variable was highly significant (chi-square=13.24, df=1, P=0.0003) and provided greater explanatory power and a better model fit than the continuous variable. The final model was highly significant (total chi-square=146.67, df=6, P<0.0001), and both examination of residuals and goodness-of-fit tests indicated strong model fit.

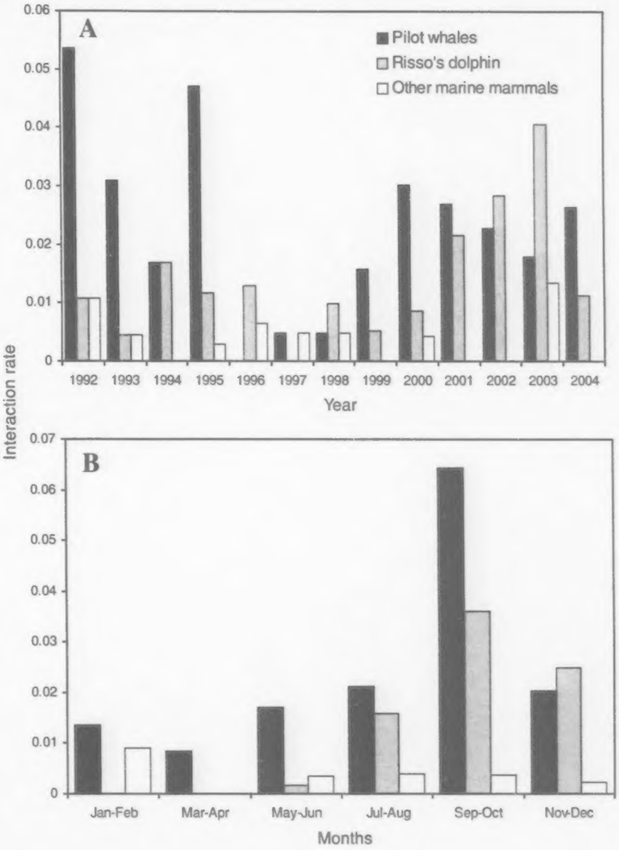

Figure 2

Annual (**A**) and seasonal (**B**) patterns in observed marine mammal interaction rates (number of positive sets/total number of observed sets) for pilot whales (*Globicephala* spp.), Risso's dolphins (*Grampus griseus*), and other marine mammal species.

Interactions with pilot whales were much more likely to occur in the MAB fishing area than in other regions. Both mainline length and damage to swordfish catch on the set also significantly increased the probability of observing a pilot whale interaction (Fig. 3). There was a strong decrease in the probability of a pilot whale interaction with increasing distance from the 200-m isobath (Fig. 4), and this trend was apparent in the MAB and other regions. No pilot whale interactions were observed in sets greater than 30 km away from the 200-m isobath. The correlation with water temperature was generally weaker than that for other factors; however, there was a peak in interaction rates in warm waters between 70 and 80°F in the MAB and between 75 and 85°F in the other geographic areas. This warm water peak was associated with late summer and fall in these regions.

Logistic regression results: Risso's dolphins

Risso's dolphin interaction rates were significantly higher in the MAB (chi-square=4.56, df=1, P=0.0328) and the NEC fishing areas (chi-square=13.03, df=1, P=0.0003) than in areas farther south. The highest interaction rates overall were observed in the NEC. As with pilot whales, distance from the 200-m isobath (chi-square=4.58, df=1, P=0.0306) and damage to swordfish catch (chi-square=4.68, df=1, P=0.0297) were important explanatory factors. However, overall, the strength of these effects was weaker than that for pilot whales. The mainline length effect, although improving the explanatory power of the model, was not a statistically significant factor (chi-square=3.284, df=1, P=0.07). The use of fish bait, either alone or in addition to squid bait, significantly decreased the probability of observing a Risso's dolphin interaction (chi-square=4.33, df=1, P=0.0375). The overall model was highly significant (chi-square=71.68, df=6, P<0.0001) and provided a good fit to the data.

The bait effect was apparent only in the observed data from the MAB region and the southern Atlantic areas and was not observed in the NEC region, but the positive correlation with damage to swordfish catch was observed across all regions (Fig. 5). The negative correlation with distance from the 200-m isobath for Risso's dolphins was somewhat weaker than that for pilot whales; however, no interactions were observed in waters greater than 30 km from the 200-m isobath, with the exception of one interaction observed in the south Atlantic areas (Fig. 6).

Discussion

Interactions of marine mammals with pelagic longlines are concentrated primarily in the MAB and NEC fishing areas along the shelf break. Interaction rates were consistent across the time series, with the exception of the period between 1996–99. There was relatively low observer coverage in the MAB fishing area during these years, and the low observed interaction rates may be a sampling artifact. Pilot whales and Risso's dolphins are the primary species interacting with the longline fishery, and mortality and serious injury of these species are a significant conservation concern. Assessing the impact of fishery-induced mortality on the two pilot whale species (longfin and shortfin pilot whales) is difficult because the species cannot be distinguished in either assessment surveys or when caught on fishing gear. Thus, although the total fishery mortality is below the PBR limit for the combined species, it is possible that the longline fishery disproportionately impacts one species. The shortfin pilot whale (*G. macrorhyncus*) generally has a more southern distribution than the longfin pilot whale (*G. melas*), and therefore the impact of the longline fishery may be more severe than current stock assessments indicate. Research is currently underway to determine the spatial distributions of the two species in order to assess their status more accurately.

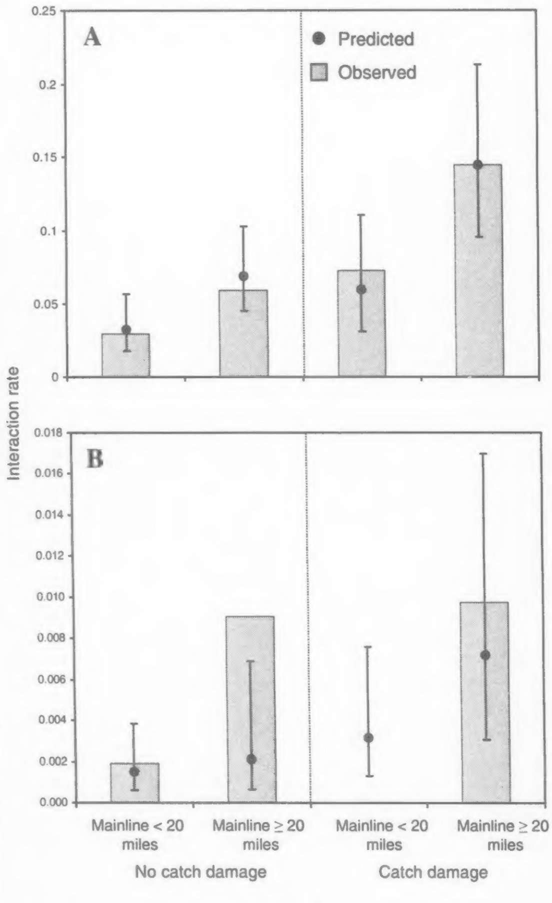

Figure 3

Predicted (black dots) and observed (bars) interaction rates with pilot whales (*Globicephala* spp.) by mainline-length category and observed catch damage for the Mid-Atlantic Bight fishing area (A) and other fishing areas (B). Error bars indicate 95% confidence intervals of predicted values. Note the difference in *y*-axis scale.

Approximately equal proportions of interactions involve hookings versus entanglement in the mainline for both species. Hooking almost exclusively involves the animal being hooked in the mouth. In most cases, the animal is released after the gangion line is either cut or broken; however the animal either trails or is entangled in a significant amount of monofilament line upon release. These animals are considered seriously injured and likely to die, and hence they are of greatest concern for conservation and management agencies. Marine turtle interactions with longlines also generally involve the animal swallowing the hook or being hooked externally. Therefore, developing and implementing guidelines for the removal of hooks and careful release of turtles is a major focus of management efforts (Watson et al., 2005). The challenges for release of marine mammals are more severe because larger animals can break gangion lines before these animals can be brought close to the boat, and there can be considerable risk of injury to the vessel crew. However, the development of equipment and protocols to more effectively remove ingested hooks from marine mammals would be an important step to reduce the severity of injuries.

The shape of the hook had no effect on marine mammal interaction rates in these analyses. This factor was examined closely because of recent changes in longline fishery gear—changes mandated to reduce the catch and mortality of endangered sea turtles. As of August 2004, all U.S. East Coast pelagic longline fishermen were required to use larger circle hooks rather than "J" hooks. In the data examined in the present study, there were relatively few circle hooks observed in the fishery and thus there was limited power to test this potential gear effect. Marine mammal interactions with the fishery will continue to be closely monitored to verify that actions to reduce turtle interactions do not inadvertently increase marine mammal interactions.

The logistic regression results demonstrate that longline fishery interactions with both pilot whales and Risso's dolphins are largely driven by environmental factors and spatial overlap of marine mammals and fishery operations. Pilot whales are concentrated along the shelf break between the 200- and 1000-m isobaths, and the highest densities are found between Cape Hatteras, NC, and New Jersey and along the southern flank of Georges Bank (Payne and Heinemann, 1993; Mullin and Fulling, 2003; Waring et al., 2006). Risso's dolphins are similarly concentrated along the shelf break, but they have a more northern distribution from New Jersey to southern New England (Waring et al., 2006). Both species are found along the southeast Atlantic U.S. coast from North Carolina to Florida; however, they have much lower densities and are not as strongly associated with the shelf break (Mullin and Fulling, 2003; Waring et al., 2006) as in the former region. The fishery effort is similarly concentrated along the shelf break in both the MAB and NEC (Fig. 1; Abercrombie et al., 2005). Fishery effort is generally concentrated just north of Cape Hatteras, NC, during the winter months from January through April. The fishery then expands northward and overall effort increases through the MAB and NEC fishing areas, reaching peak effort levels during September and October and remaining high through December.

The strong overlap between fishery effort and high marine mammal presence is related to prey distribution. The pelagic longline fishery targets tunas and swordfishes that feed on small fish and squids. Both pilot whales and Risso's dolphins are also pelagic predators, and squids are a major component of their diets (Overholtz and Waring, 1991; Gannon et al., 1997; Kruse et al., 1999). Both longfin (*Loligo pealei*) and shortfin (*Illex illecebrosus*) squids are primary prey items, and both concentrate near the convergence zone of shelf-slope waters during summer and autumn (Brodziak and Hendrickson, 1999). The high interaction rate in the MAB area during summer and fall, and in warmer water temperatures, is therefore likely a function of environmental features driving availability of squid and small pelagic fishes that are prey for both the target fish species and marine mammals.

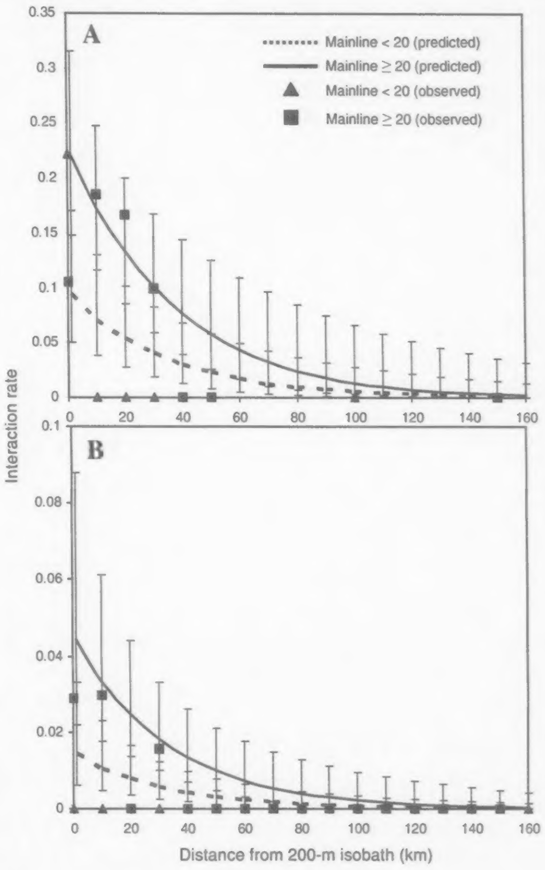

Figure 4

Predicted (lines) and observed (symbols) interaction rates (number of positive sets/total number of observed sets) for pilot whale (*Globicephala* spp.) in the Mid-Atlantic Bight fishing area (A) and other areas (B), with increasing distance from the 200-m isobath and by mainline-length category. Error bars indicate 95% confidence intervals of predicted values. Note the difference in the *y*-axis scale.

For both pilot whales and Risso's dolphins, there was a correlation between observed damage to swordfish catch and the likelihood of an interaction with a marine mammal. It should be noted that damage to catch may also be related to feeding by sharks, as well as by marine mammals. The strong correlation with damage to catch indicates that marine mammals are likely feeding upon the catch or bait. Similarly, the negative correlation between fish bait and Risso's dolphin interactions indicates that the animals were attracted to gear with squid bait as a ready food source.

The consistent effect of mainline length may also be related to depredation of catch on the longline gear. Longer mainlines represent a larger, more attractive food source or may be more easily detectable. Marine mammals therefore likely spend a longer time around the gear, creating greater opportunities for hooking

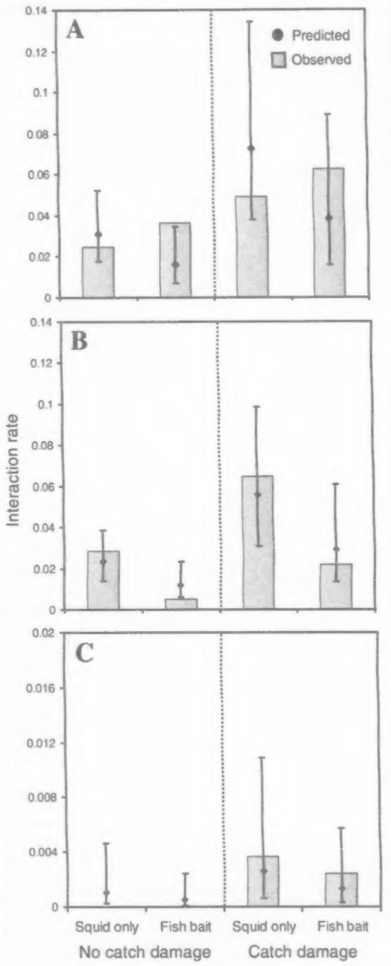

Figure 5

Predicted (symbols) and observed (bars) interaction rates (number of positive sets/total number of observed sets) for Risso's dolphins (*Grampus griseus*) in the Northeast Coastal fishing area (**A**), the Mid-Atlantic Bight fishing area (**B**), and other areas (**C**) as a function of bait type and observed catch damage. Error bars indicate 95% confidence intervals of predicted values. Note the difference in the *y*-axis scales.

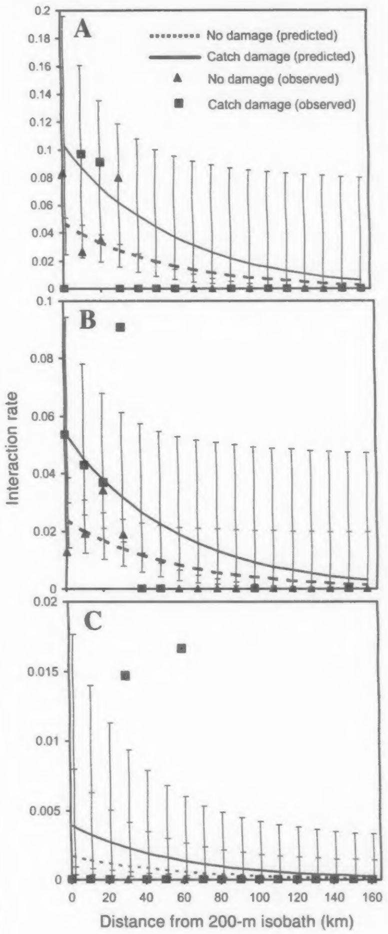

Figure 6

Predicted (lines) and observed (symbols) interaction rates of gear (number of positive sets/total number of observed sets) with Risso's dolphins (*Grampus griseus*) in the Northeast Coastal fishing area (**A**), the Mid-Atlantic Bight fishing area (**B**), and other areas (**C**) with increasing distance from the 200-m isobath and observed catch damage. Error bars indicate 95% confidence intervals of predicted values. Note the difference in the *y*-axis scales.

or entanglement. In other regions, sperm whales and killer whales are thought to respond to the sound of the vessel engines and winches when bottom longlines are hauled back on board (Kock et al., 2006). Longer haulback times associated with longer mainlines may thus further increase the opportunity for marine mammals to detect fishing gear. Improving the understanding of how and why marine mammals are attracted to longline gear will help both to reduce the economic losses due to depredation of catches and the impacts of commercial fishing activities on marine mammal populations.

Marine mammal bycatch in longline gear is driven to a large extent by the overlap of marine mammal and pelagic fish habitat with the area of longline fishery operations. In addition, this analysis demonstrates that longer mainlines had a significantly higher bycatch rate than shorter mainlines. Reducing mainline lengths below 20 nautical miles, particularly within the seasons and areas where interactions occur, has the potential to reduce the rate of interactions and the impact of the longline fishery on pilot whale and Risso's dolphin populations. This management option, along with a suite of other measures, is currently being considered by NMFS within the framework of the Pelagic Longline Take Reduction plan.

Acknowledgments

I am indebted to the diligent efforts of the observers who have participated in the Pelagic Longline Observer Program throughout its history. C. Brown, D. Abercrombie, L. Beerkircher, and D. Lee of the National Marine Fisheries Service, Southeast Fisheries Science Center provided invaluable assistance. The analytical approach was developed in cooperation with members of the Pelagic Longline Take Reduction Team who made many useful suggestions and provided insights into the operation of the fishery. I would like to recognize the late N. Beideman, commercial fisherman and head of the Blue Water Fisherman's Association, for his contributions to the conservation of protected species during pelagic longline fishing operations. This work is a contribution of the Protected Species and Biodiversity Division, Southeast Fisheries Science Center, National Marine Fisheries Service.

Literature cited

Abercrombie, D. L., H. A. Balchowsky, and A. L. Paine.
2005. 2002 and 2003 annual summary: large pelagic species. NOAA Tech. Memo. NMFS-SEFSC-529, 33 p.

Angliss, R. P., and D. P. DeMaster.
1998. Differentiating serious and non-serious injury of marine mammals taken incidental to commercial fishing operations: Report of the serious injury workshop 1–2 April, 1997, Silver Spring, Maryland. NOAA Tech. Memo. NMFS-OPR-13, 48 p.

Beerkircher, L. R., C. J. Brown, D. L. Abercrombie, and D. W. Lee.
2004. SEFSC Pelagic Observer Program Data Summary for 1992–2002. NOAA Tech. Memo. NMFS-SEFSC-522, 25 p.

Burnham, K. P., D. R. Anderson, G. C. White, C. Brownia, and K. Pollack.
1987. Design and analysis methods for fish survival experiments based on release-recapture. American Fisheries Society, Monograph 5, 433 p. Am. Fish. Soc., Bethesda, MD.

Brodziak, J., and L. Hendrickson.
1999. An analysis of environmental effects on survey catches of squids *Loligo pealei* and *Illex illecebrosus* in the northwest Atlantic. Fish. Bull. 97:9–24.

Fertl, D., and S. Leatherwood.
1997. A review of cetacean interactions with trawls. J. NW Atl. Fish. Sci. 22:209–218.

Gannon, D. P., A. J. Read, J. E. Craddock, K. M. Fristrup, and J. R. Nicolas.
1997. Feeding ecology of long-finned pilot whales *Globicephala melas* in the western North Atlantic. Mar. Ecol. Prog. Ser. 148:1–10.

Garrison, L. P.
2005. Estimated bycatch of marine mammals and turtles in the U.S. Atlantic pelagic longline fleet during 2004. NOAA Tech. Memo. NMFS-SEFSC-531, 57 p.

Goodyear, C. P.
1999. An analysis of the possible utility of time-area closures to minimize billfish bycatch by U.S. pelagic longlines. Fish. Bull.97:243–255.

Hosmer, D. W., and S. Lemeshow.
1989. Applied logistic regression, 307 p. John Wiley and Sons, Inc., New York, NY.

Kock, K.-H., M. G. Purves, and G. Duhamel.
2006. Interactions between cetaceans and fisheries in the Southern Ocean. Polar Biol. 29:379–388.

Kruse, S., D. K. Caldwell, and M. C. Caldwell.
1999. Risso's dolphin—*Grampus griseus* (G. Cuvier 1812). *In* Handbook of marine mammals (S. H. Ridgeway, and R. Harrison, eds.), p. 183–212. Academic Press, San Diego, CA.

McCullagh, P., and J. A. Nelder.
1989. Generalized linear models, 511 p. Chapman and Hall, London.

Mullin, K. D., and G. L. Fulling.
2003. Abundance of cetaceans in the southern U.S. north Atlantic ocean during summer 1998. Fish. Bull. 101:603–613.

Overholtz, W. M., and G. T. Waring.
1991. Diet composition of pilot whales *Globicephala* sp. and common dolphins *Delphinus delphis* in the mid-Atlantic bight during spring 1989. Fish. Bull. 89:723–728.

Payne, P. M., and D. W. Heinemann.
1993. The distribution of pilot whales (*Globicephala* sp.) in the shelf/shelf edge and slope waters of the northeastern United States, 1978–1998. Reports of the International Whaling Commission (special issue 14):51–68.

Perrin, W. F., G. P. Donovon, and J. Barlow.
1994. Gillnets and cetaceans. International Whaling Commission. Special issue 15, p. 1–53.

Secchi, E. R., and T. Vaske.
1998. Killer whale (*Orcinus orca*) sightings and depredation on tuna and swordfish longline catches. Aquat. Mamm. 24:117–122.

Waring, G. T., E. Josephson, C. P. Fairfield, and K. M. Foley.
2006. U.S. Atlantic and Gulf of Mexico marine mammal stock assessments—2005. NOAA Tech. Memo. NMFS-NE-194, 352 p.

Watson, J. W., S. P. Epperly, A. K. Shah, and D. G. Foster.
2005. Fishing methods to reduce sea turtle mortality associated with pelagic longlines. Can. J. Fish. Aquat. Sci. 62:965–981.

Changes in egg production of the western rock lobster (*Panulirus cygnus*) associated with appendage damage

Roy Melville-Smith (contact author)
Simon de Lestang
Email address for R. Melville-Smith: rmsmith@fish.wa.gov.au

Department of Fisheries (Western Australia)
Western Australian Marine Research Laboratories
39 Northside Drive
Hillarys, Western Australia 6025, Australia

Abstract—Data collected during fishery-independent sampling programs were used to examine the impact of appendage damage (indicated by lost or regenerated legs and antennae) on the reproductive output of female western rock lobster (*Panulirus cygnus*). Most of the damaged females sampled had one (53%), two (27%), or three (13%) appendages that had been lost or that were regenerating. Appendage damage was associated with the reduced probability of a female developing ovigerous setae; and if setae were produced, with the reduced probability that females would produce more than one batch of eggs within a season. These effects were more pronounced as the number of damaged appendages increased. From data collected in 2002, it was estimated that the total number of eggs produced by mature females caught in the fishery was significantly reduced ($P<0.001$) by 3–9% when the impact of appendage damage was included.

Manuscript submitted 8 September to the Scientific Editor's Office.

Manuscript approved for publication March 28 2007 by the Scientific Editor.

Fish. Bull. 105:418–425 (2007).

Western rock lobster (*Panulirus cygnus*) are found only off Western Australia, where they form the basis of an intensive commercial fishery (Phillips and Melville-Smith, 2005). One result of the high exploitation rates experienced by western rock lobster (Brown and Caputi, 1985, 1986), and other decapod species (Krouse, 1976; Smith and Howell, 1987), is the damage sustained by the catch that is returned to the water. Damage, whether caused by aggression between conspecifics trapped in pots, desiccation on board boats before processing, or rough handling during sorting, is generally a combination of dehydration, broken body parts, and the loss of entire appendages. Apart from the mortality of animals due to processing, both the growth rate and fecundity of the surviving animals can be significantly reduced (Davis, 1981; Brouwer et al., 2006). Damaged animals appear to reallocate energy stores towards regenerating damaged appendages and away from growth and reproduction (Norman and Jones, 1992; Juanes and Smith, 1995; Mariappan and Balasundaram, 2001).

In the western rock lobster fishery, sustainability of the resource has been achieved by management regulations that include limited entry to the commercial fishery, a closed fishing season from July to mid-November, and return to the water of all lobsters that are outside the maximum and minimum legal size limits or that are in a breeding condition (i.e., bearing ovigerous setae) (Caputi et al., 2000; de Lestang and Melville-Smith, 2006). Anecdotally, these regulations are believed to result in 55% of the *P. cygnus* catch being returned to the sea. This species is especially susceptible to autotomizing (dropping) limbs (Brown and Caputi, 1983, 1985): 40–80 tonnes of legs are estimated to be lost from the landed catch of *P. cygnus* each year (Davidson and Hosking, 2002).

We used data from a variety of existing and new sources to examine the effect of appendage loss and regeneration (both antennae and legs) on the reproductive biology of female *P. cygnus*. We believe this study to be the first comprehensive assessment of the impact that appendage damage has on the reproductive output of a decapod species. This study assesses the impact of appendage damage on the proportion of females developing ovigerous setae, the proportion of females that will produce one or more batches of eggs within a breeding season, and the number of eggs in a batch.

Materials and methods

Sampling regime

Data were collected during a fishery-independent breeding stock survey (hereafter referred to as "the survey"), which has been conducted annually at three localities (Lancelin, Dongara, and Abrolhos Islands) and intermittently at three others (Fremantle, Jurien, and Kalbarri) since 1992. The commercial fishery in Western Australia is divided into three management zones: the Abrolhos Islands (zone A), north coastal (zone B), and south coastal (zone C) (Fig. 1). In some cases data were pooled into these zones for analysis.

The surveys were undertaken over the course of ten days before the start of the commercial lobster fishing season on 15 November. This period is very close to the annual peak of the egg-bearing season, which is considered to occur in November of each year (Chubb, 1991). Because this survey was designed to be repeatable, the same fishing gear (batten pots with closed escape gaps), bait (a combination of north sea herring [*Clupea harengus*] and Australian salmon [*Arripis truttaceus*]), and locations (same GPS coordinates) were used. The results are therefore directly comparable between years. For more details on the survey sampling regime see Chubb (2000).

Measurements and records

During the surveys, the carapace length (CL) of each lobster was measured to the nearest 1 mm from midpoint between the preorbital spines down the mid-dorsal line to the posterior edge of its carapace. The presence of gonopores on the base of the fifth pair of pereiopods was used to identify males. For females, the presence of ovigerous setae attached to the endopodites, the visual appearance of the ovaries through the dorsothoracic musculature, the presence and developmental stage of external ova attached to the setae, and the presence of a spermatophoric mass attached to the fifth abdominal segment were recorded. These data have been used to predict whether a female would produce one or two batches of eggs in a spawning season (such females are known as "single breeders" and "double breeders, respectively)"—see Melville-Smith and de Lestang (2005) for a full description of this method).

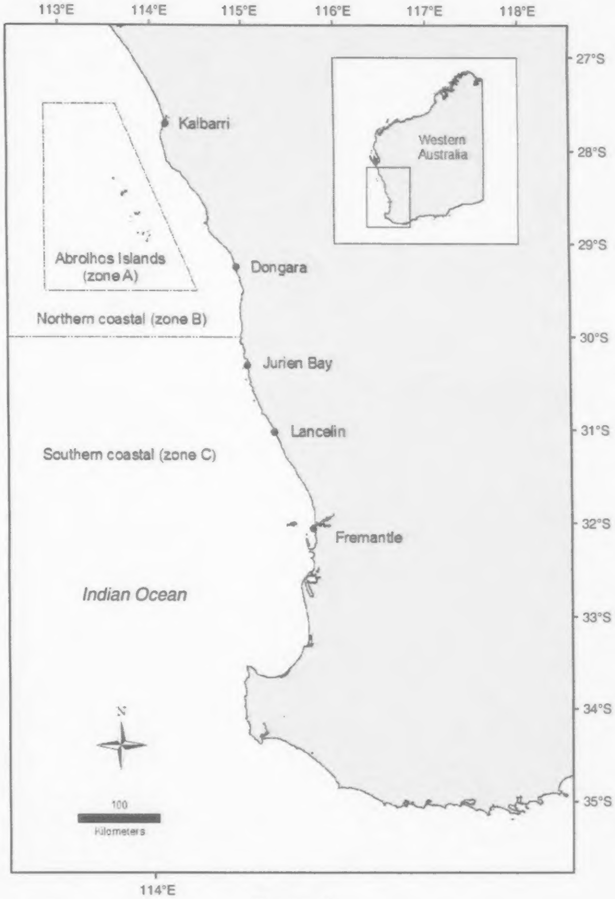

Figure 1

Management zones (zone A, Abrolhos Islands; zone B, northern coastal; zone C, southern coastal) in the western rock lobster (*Panulirus cygnus*) fishery, and six sites (five on the coast of Western Australia and one comprising the Abrolhos Islands) used for fishery-independent breeding stock surveys and commercial monitoring of the catch.

Loss and regeneration of antennae and limbs were also recorded during the survey as either an old loss, new loss, or as a regenerated appendage and all three categories were grouped collectively and referred to as "appendage damage." Old loss was identified by dark melanization at the site of the lost appendage and new loss by exposed flesh without melanization. Although new leg losses were recorded, nearly all were considered to have resulted from capture and handling during the survey and therefore were excluded from our analysis of the impact of appendage damage on reproductive output. Regenerated limbs of *P. cygnus* were only easily identifiable in the first intermoult period after the limb was lost and were distinguished by being greenish in color and noticeably smaller or thinner than existing limbs. Because old and new losses have been recorded since 1992 and regenerated limbs have been recorded since 2001, we used only the data collected since the 2001 survey. The incidence of old losses, new losses, and regenerated appendages between zones, sex, and carapace size was compared by using ANOVA.

Effect of appendage damage on fecundity estimates

Because most of the lobsters sampled in zone A (the Abrolhos Islands) during the 2001–03 surveys were larger than the size at maturity (Melville-Smith and de Lestang, 2006), data derived from sampling in this location were used to examine whether the incidence of old appendage-losses and regenerated appendages affects the reproductive state of female *P. cygnus*.

The batch fecundity (number of eggs in one batch) of 50 female *P. cygnus* with early-stage eggs that ranged in carapace length (CL) from 67.1 to 96.2 mm was determined. Twenty-three females had either one or two damaged appendages and 27 had no damaged appendages; females with early-stage eggs and more than two damaged appendages were seldom caught and therefore were not assessed. The endopodites with eggs were removed from the lobsters and dried in an oven for 24 hours. The eggs were then separated from the setae and weighed to the nearest 0.0001 g. Three subsamples of each brood (each of ~0.05 g) were taken and weighed. The number of eggs in each subsample was counted to determine the mean number of eggs per gram of dry egg weight, and the mean of these values was used to estimate the total number of eggs in the brood. The mean fecundity per spawning season was compared for females with and without appendage damage after standardizing for carapace length with ANCOVA.

The total number of eggs produced by all mature female *P. cygnus* caught during the 2002 survey in each of the three commercial fishing zones was estimated by using an equation that incorporates the number of broods of eggs produced each spawning season and the effects of appendage damage on the likelihood of spawning once or twice.

$$(TF = NB \times F \times PO_{DA}),$$

where TF = the total fecundity (number of eggs produced) by mature females;

NB = the probability of a female producing one or two broods each spawning season, on the basis of their CL;

F = s the relationship of fecundity to carapace length; and

PO = the probability that females with damaged appendages DA will produce eggs.

$$P_1 = \left(1/1+\exp\left(-\ln(19)\times(CL-SB_{50})/(SB_{95}-SB_{50})\right)\right),$$

$$P_2 = \left(1/1+\exp\left(-\ln(19)\times(CL-DB_{50})/(DB_{95}-DB_{50})\right)\right),$$

where SB_{50} and SB_{95} = the CLs at which 50 and 95%, respectively, of the population at each location produced one brood of eggs (P_1); and

DB_{50} and DB_{95} = the CLs at which 50 and 95%, respectively, of the population at each location produced two broods of eggs (P_2) per spawning season (de Lestang and Melville-Smith, 2006).

Results

Frequency of appendage damage in 2001–05 surveys

The percentage of western rock lobster with damaged appendages in the 2001–05 survey catches decreased as the number of damaged appendages increased (Fig. 2, A–C). For example, in zone A, about 82% of all female and male *P. cygnus* in the catches had no appendage damage, whereas about 9%, 4%, and 2% of both sexes had one, two, and three damaged appendages, respectively. Only 1% of the catch of each sex had four damaged appendages and less than 0.5% of all lobsters had more than five damaged appendages.

Table 1

Percentage of all female and male western rock lobster (*Panulirus cygnus*) with old damage, or regenerated appendages, in the three management zones of the fishery. Data are from the 2001–05 fishery-independent breeding stock survey.

	Fishing zone		
Sex	Zone A	Zone B	Zone C
Female	17.8%	12.4%	20.9%
Male	18.9%	8.7%	17.2%

The incidence of appendage damage was significantly different between zones ($P<0.001$) and both zones A and C had higher incidences than zone B (Table 1) . In addition, within zones B and C, significantly ($P<0.001$) more females than males were caught with appendage damage. There was no significant difference ($P=0.14$) in the incidence of appendage damage for females and males caught at the Abrolhos Islands.

Relationship between appendage damage and carapace length

The incidence of new appendage loss differed significantly ($P<0.001$) between the two sexes in the various size classes (Fig. 3A). New appendage loss in females remained at about 17% in all the size classes, whereas in males this loss decreased from 15% to 8% in the first four size classes, then increased substantially to 28% and 20% in the larger size classes (110–119 and 120–129 mm CL, respectively).

The incidence of old appendage loss also differed significantly ($P<0.001$) between sexes in different size classes (Fig. 3B). Old appendage damage was slightly more common as females increased in size, i.e., from 7% to 11% between the 60–69 and 100–109 mm CL size classes. This increase also occurred for males but to a much greater extent, i.e., from 4% to 23% between the 60–69 and 100–109 mm CL size classes. The incidence of old appendage damage in males then declined slightly over the two largest size classes (110–119 and 120–129 mm CL) 22 and 16%, respectively (Fig. 3B).

Regenerated appendages in the catches of lobster differed significantly ($P<0.001$) between sex and size classes (Fig. 3C). Regenerated appendages were more commonly recorded for females than for males, but regenerated appendages for each sex remained relatively

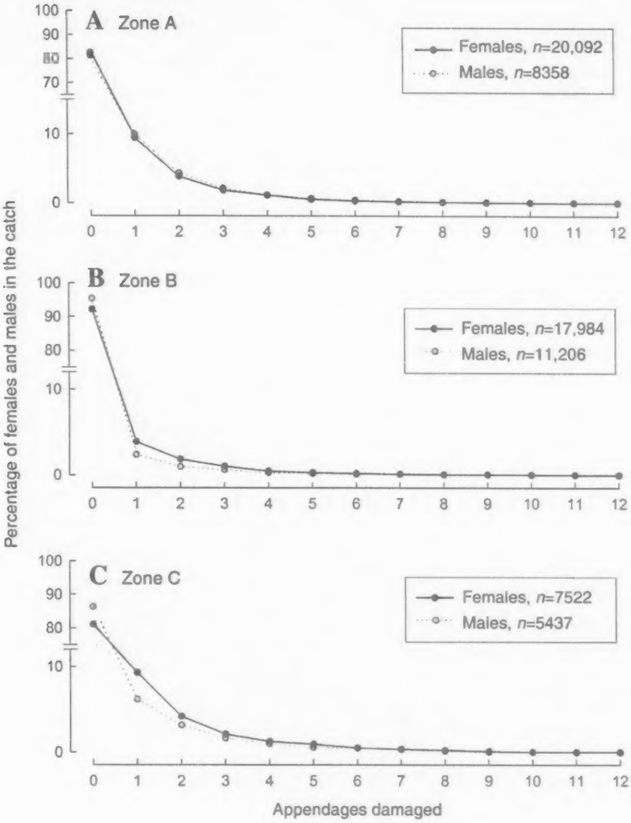

constant at about 4% and 3%, respectively, in all size classes below 120 mm CL. Above this size class, the incidence of regenerated appendages increased markedly in females (10%) and declined to zero for males (Fig. 3C).

The influence of appendage damage on egg production

The proportions of female *P. cygnus* (CL>65 mm) from the Abrolhos Islands that were classified as having ovigerous setae, as being single breeders, and as being double breeders, all declined with increasing appendage damage (Fig. 4, A–C). A consistent trend existed between the various reproductive states and the magnitude of their appendage damage. For females at the Abrolhos Islands above the size at maturity, the likelihood of developing ovigerous setae declined with the number of appendages damaged: 98% likelihood (one appendage damaged), 95% (two), 80% (five), and 58% (six). This likelihood continued to decline until it reached zero for all females with either 11 or 12 damaged appendages (Fig. 4A).

For ovigerous females with damaged appendages, the likelihood of producing either one or two batches of eggs each spawning season declined more rapidly than the likelihood of developing ovigerous setae. Females with one damaged appendage were 20% and 19% less likely to produce one or two batches of eggs, respectively, whereas those with five damaged appendages were around 85% and 65% less likely to produce one or two batches of eggs, respectively. Females with more than seven damaged appendages did not produce eggs (Fig. 4, B and C). Equations describing the relationships between appendage damage and the likelihood of spawning once for single breeders and twice for double breeders were not significantly ($P=0.42$) different from each other and were thus combined to produce a single equation to describe the likelihood of producing one or two broods of eggs:

$$PO_{DA} = \exp[-0.31 \times \ln(DA+1) + 0.742] - 1.$$

The above relationship between appendage damage and the likelihood of lobsters developing ovigerous setae, or the likelihood of lobsters producing one or two broods of eggs at the Abrolhos Islands, was very similar in the other two coastal management zones.

The influence of appendage damage on fecundity

The mean fecundity per spawning season of female *P. cygnus* with a standardized CL of 77.0 mm did not differ significantly ($P>0.05$) between females with and without damaged appendages (i.e., 249,885 ±7873 eggs and 234,164 ±7094 eggs, respectively). Furthermore, regressions between fecundity (F) and carapace length (CL) of female *P. cygnus* with and without damaged appendages (Fig. 5) did not differ from each other ($P>0.05$) and were both very similar to the relation of carapace length to fecundity recorded for this species by Chubb (1991).

The effect of damaged appendages on the number of eggs produced per spawning season by female *P. cygnus* at the Abrolhos Islands was greater for large than for small females (Fig. 6). For example, two damaged appendages reduced the fecundity of a 70-mm-CL lobster by about 114,000 eggs, whereas the fecundity of a 120-mm-CL lobster was reduced by about 1,000,000 eggs (Fig. 6).

The total number of eggs produced in the 2002 survey was estimated for each of the three management zones separately for females with and without appendage damage. The inclusion of appendage damage significantly (all $P<0.001$, paired t-test) reduced egg production estimates by 8.5%, 3%, and 9% in zones A, B, and C, respectively.

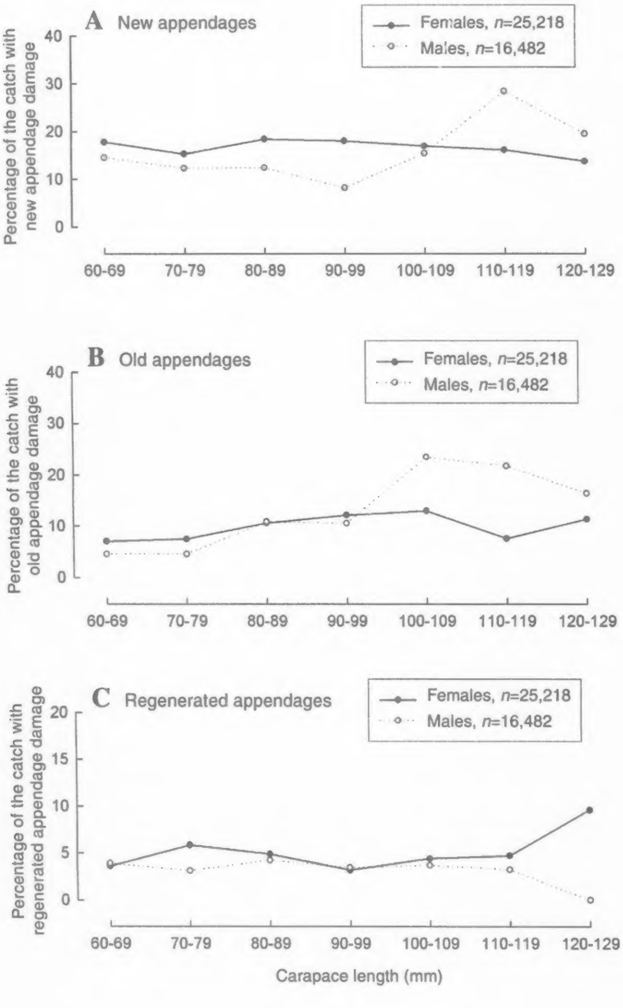

Discussion

The incidence of appendage damage

The proportions of lobsters with damaged appendages varied markedly between sexes, sizes, and locations sampled. However, the timing and frequency within a year that molting takes place for the sexes, and for different-size animals, plays only a relatively minor role in influencing these differences. Female western rock lobsters generally molt twice a year: February–March and again in May. A significant proportion of large breeding females occasionally skip the February–March molt, but all take part in the May molt (de Lestang and Melville-Smith, 2006).

New appendage damage occurred around the time of capture and could mostly be attributed to the survey sam-

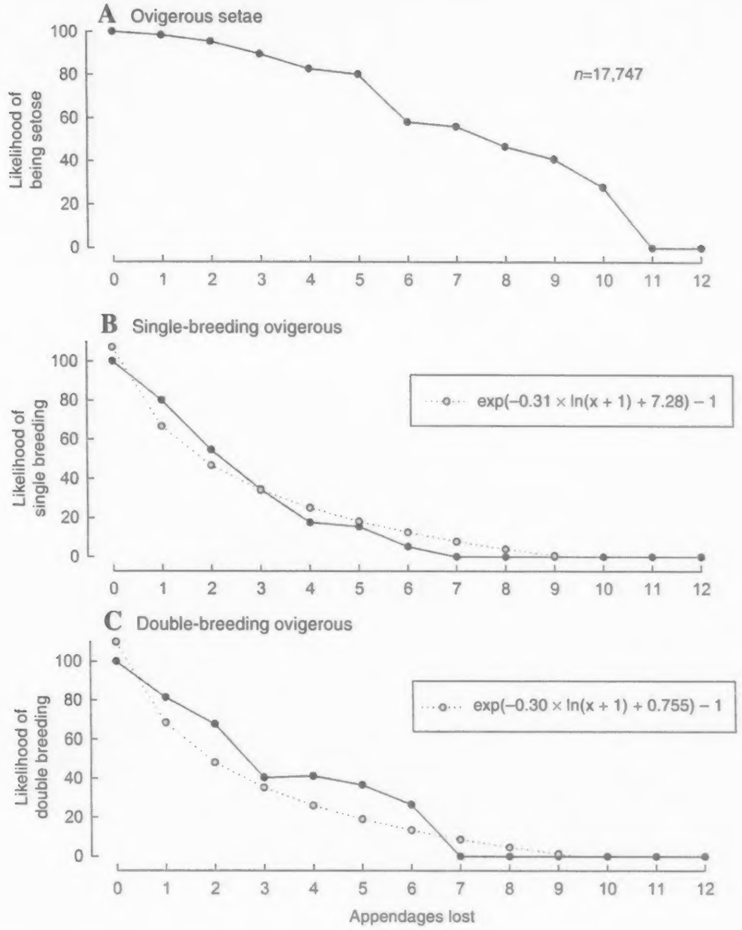

pling methods, either to capture in the pots or handling on deck. The slightly higher proportions of females than males recorded with new damage are possibly the result of the longer handling time needed to make additional observations, such as recording the presence or absence of eggs and spermatophores and visually assessing the condition of the ovary. In contrast to new appendage damage, the events that resulted in old damage and regenerated appendages occurred before the survey and, in the latter case (regenerated appendages), before the lobster's last molt, i.e., about May (de Lestang and Melville-Smith, 2006). It is therefore likely that much of this damage is inflicted during the commercial fishing season, possibly as a result of capture and handling. It is thus not surprising that the lobsters showing the greatest incidence of regenerated appendages are females above the maximum legal size (115 mm CL in zone C and 105 mm CL in zones A and B); many of these animals were likely handled and returned to the water many times during a season. Predators may be an additional cause of appendage damage. The fact that the incidence of old appendage damage increased in

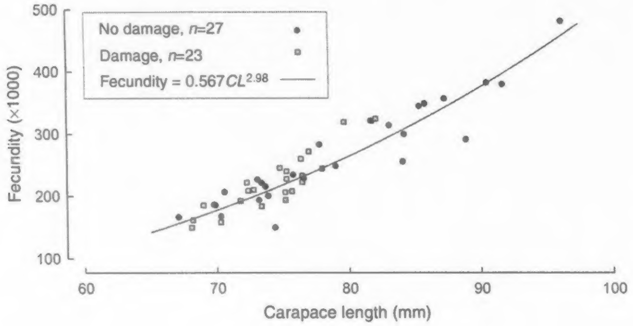

both sexes with size may indicate that larger individuals are more likely to survive the attack of a predator, although perhaps with the loss of appendages.

The effect of appendage damage on reproductive output

Appendage damage can lead to an associated reduction in the reproductive output of female *P. cygnus* directly, namely as reduced proportions of females that develop ovigerous setae, and as a reduction in the proportions of ovigerous females that will produce one or two batches of eggs within a season. Reproductive output is also affected indirectly when females with appendage damage do not molt into breeding condition (with ovigerous setae); a female above the legal minimum size without ovigerous setae can be legally retained by commercial and recreational fishermen and thus her contribution to the broodstock is removed.

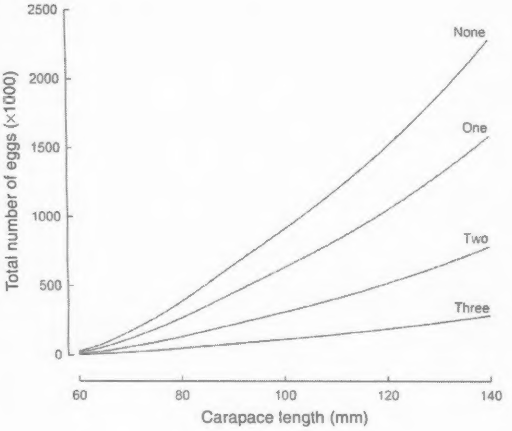

The significant reduction in reproductive output of female *P. cygnus* with appendage damage is not surprising, because regeneration places large demands on energy reserves, often in the form of a reallocation of resources that were originally destined for reproduction and growth (Démeusy, 1965; Norman and Jones, 1992; Juanes and Smith, 1995). Moreover, if appendage damage is extensive, the process of regenerating multiple appendages may result in a long-term reallocation and an overall increase in energy demand (McVean, 1982).

Most *P. cygnus* caught during the survey were intact when examined; less than 15% of the entire catch had damaged appendages. This 15% was probably due, in part, to management measures based on previous work on the effects of appendage damage (Brown and Caputi, 1985, 1986) to initiate changes aimed at reducing limb loss. Methods for limiting appendage damage even further are being developed, i.e., cold stunning (Davidson and Hoskin, 2002). However, even with the best intentions, some appendage damage through handling is unavoidable.

This study has highlighted that management measures aimed at protecting the western rock lobster broodstock inevitably result in the animals being handled more than once (or multiple times) in the course of the fishing season, and the damage to appendages caused by handling produces a significant, and previously unrecognized, effect on the overall egg production of this resource. These effects need to be taken into account when considering the benefits of these management measures in this and other crustacean fisheries.

Acknowledgments

Thanks are expressed to research staff and crew of the RV *Naturaliste* for assistance with sampling. R. Campbell, N. Caputi, C. Lawrence, V. Mawson, and J. Penn provided constructive criticisms to earlier drafts of the paper. This work was undertaken as part of Fisheries Research and Development Corporation Project 2003/005. All experiments were conducted in compliance with the current laws of Australia.

Literature cited

Brouwer, S. L., J. C. Groeneveld, and B. Blows.
2006. The effects of appendage loss on growth of South African west coast rock lobster *Jasus lalandii*. Fish. Res. 78:236–242.
Brown, R. S., and N. Caputi.
1983. Factors affecting the recapture of undersize western rock lobster *Panulirus cygnus* George returned by fishermen to the sea. Fish. Res. 2:103–128.
Brown, R. S., and N. Caputi.
1985. Factors affecting the growth of undersize western rock lobster *Panulirus cygnus* George returned by fishermen to the sea. Fish. Bull. 83:67–574.
Brown, R. S., and N. Caputi.
1986. Conservation and recruitment of the western rock lobster (*Panulirus cygnus*) by improving survival and growth of undersize rock lobsters captured and returned by fishermen to the sea. Can. J. Fish. Aquat. Sci. 43:2236–2242.
Caputi, N., C. F. Chubb, N. G. Hall, and R. S. Brown.
2000. Measurement of catch and fishing effort in the western rock lobster fishery. *In* Spiny lobsters fisheries and culture (B. F. Phillips, and J. Kittaka, eds.), p. 334–356. Fishing News Books, Oxford.
Chubb, C. F.
1991. Measurement of spawning stock levels for the western rock lobster, *Panulirus cygnus*. Rev. Invest. Mar. 12:223–233.
2000. Reproductive biology: issues for management. *In* Spiny lobsters fisheries and culture (B. F. Phillips and J. Kittaka, eds.), p. 245–275. Fishing News Books, Oxford.
Davidson, G., and W. Hosking.
2002. Development of a method for alleviating leg loss during post-harvest handling of rock lobsters. *In* Proceedings of the fourth annual rock lobster enhancement and aquaculture subprogram/rock lobster post-harvest subprogram (R. van Barneveld, and B. Phillips, eds.), p. 85–89. Rock Lobster Enhancement and Aquaculture Subprogram Publication No. 7. Barneveld Nutrition Pty Ltd. Springwood, Queensland, Australia.
Davis, G. E.
1981. Effects of injuries on spiny lobsters, *Panulirus argus*, and implications for fishery management. Fish. Bull. 78:979–984.
de Lestang, S., and R. Melville-Smith.
2006. Interannual variation in the moult cycle and size at double breeding of mature female western rock lobster *Panulirus cygnus*. ICES J. Mar. Sci. 63:1631–1639.
Démeusy, N.
1965. Somatic growth and reproductive function in the female brachyuran decapod *Carcinus maenas* Linn. [In French.] Arch. Zool. Exp. Gen. 106:625–663.
Juanes, F., and L. D. Smith.
1995. The ecological consequences of limb damage and loss in decapod crustaceans: a review and prospectus. J. Exp. Mar. Biol. Ecol. 193:197–223.
Krouse, J. S.
1976. Incidence of cull lobsters, *Homarus americanus*, in commercial and research catches off the Maine coast. Fish. Bull. 74:717–724.
Mariappan, P., and C. Balasundaram.
2001. Limb autotomy along with exuvium in freshwater prawn, *Macrobrachium malcolmsonii*. Indian J. Animal Sci. 71:1001–1002.
McVean, A.
1982. Autotomy. *In* The biology of crustaceans, neural integration and behaviour (D. C. Sandeman, and H. L. Atwood, eds.), p. 107–246. Academic Press Inc., New York, NY.
Melville-Smith, R., and S. de Lestang.
2005. Visual assessment of the reproductive condition of female western rock lobsters (*Panulirus cygnus*). N. Z. J. Mar. Freshw. Res. 39:557–567.
2006. Spatial and temporal variation in the size at maturity of the western rock lobster *Panulirus cygnus*. Mar. Biol. 150:183–195.
Norman, C. P., and M. B. Jones.
1992. Reproductive ecology of the velvet swimming crab, *Necora puber* (Brachyura: Portunidae), at Plymouth. J. Mar. Biol. Assoc. U.K. 73:379–389.
Phillips, B. F., and R. Melville-Smith.
2005. Sustainability of the western rock lobster fishery: a review of past progress and future challenges. Bull. Mar. Sci. 76:485–500.
Smith, E. M., and P. T. Howell.
1987. The effects of bottom trawling on American lobsters *Homarus americanus* in Long Island Sound. Fish. Bull. 85:737–744.

Diversity of estuarine movements of striped bass (*Morone saxatilis*): a synoptic examination of an estuarine system in southern New Jersey

Kenneth W. Able (contact author)

Thomas M. Grothues

Email address for K. W. Able: able@marine.rutgers.edu

Marine Field Station, Institute of Marine and Coastal Sciences
Rutgers University
800 c/o 132 Great Bay Boulevard
Tuckerton, New Jersey 08087-2004

Abstract—We determined the distribution of multiple ($n=68$; 508–978 mm total length [TL]) striped bass (*Morone saxatilis*) along the estuarine salinity gradient in the Mullica River–Great Bay in southern New Jersey over two years to determine the diversity of habitat use and the movements of striped bass. Ultrasonically tagged fish were detected in this estuarine area by means of wireless hydrophones deployed at four gates inside the entrance of the study area and farther up to tidal freshwater (38 km). Numerous individuals frequently departed and returned to the estuary, primarily in the spring and late fall over periods of 15–731 days at liberty. The period of residency and degree of movement of individuals to and from the estuary varied extensively among seasons and years. The diversity of movements in and out of, as well as within, the estuary differed from the less-complex patterns reported in earlier studies, perhaps because of the comprehensive and synoptic nature of this study.

Manuscript submitted 10 April 2006 to the Scientific Editor's Office.

Manuscript approved for publication 30 March 2007 by the Scientific Editor.

Fish. Bull. 105:426–435 (2007).

Striped bass (*Morone saxatilis*) are an economically and ecologically important species along most coasts of the United States, and especially along the east coast and into Canada (Klein-MacPhee, 2002). The degree to which this species uses estuaries along the east coast appears to vary among and within estuaries. From North Carolina southward most striped bass remain in rivers and estuaries (Haeseker et al., 1996; Bjorgo et al., 2000), as does the northernmost population in the Gulf of St. Lawrence (Coutant, 1985). North of North Carolina to the Bay of Fundy, striped bass can be highly migratory (Waldman et al., 1990; Rulifson and Dadswell, 1995). Much of the research effort in this region has focused on the coastal migrations and there has been less effort on within-estuary movements. Both coastal and within-estuary movements have become more important to understand because 1) the recovery of the species (Wooley et al., 1990; Richards and Rago, 1999), especially at the current higher densities, may influence its movement patterns, and 2) there is the possibility that there are distinct contingents, including estuarine residents, that are critical to understanding stock structure for fishes in general (Begg and Waldman, 1999), but especially for striped bass (Secor et al., 2001).

In the past, most attempts to examine estuarine movements have been based on fish caught in local fisheries (Rulifson and Dadswell, 1995) and tagged-recaptured fish (Boreman and Lewis, 1987; Waldman et al., 1990). However, in recent years the development of otolith microchemistry has helped scientists to recognize the importance of distinct substocks or contingents and their migrations (Secor, 1999) that have the potential to be indicative of homing (Thorrold et al., 2001; Gillanders, 2005). These concepts have been applied to striped bass as well, and resident, mesohaline, and coastal migratory contingents have been recognized within the same estuarine and river system (Secor, 1999; Zlokovitz et al., 2003), as well as the annual variation in the migratory patterns of these contingents (Morris et al., 2003). Additionally, the development of biotelemetry in general (Cooke et al., 2004; Heupel et al., 2006) and smaller ultrasonic tags and passive receivers has increased the possibility for more accurate and frequent detection of fish and has enhanced our ability to study fish movements (Arnold and Dewar, 2001; Sibert and Nielsen, 2001). These efforts conducted on striped bass previously focused on introduced populations in freshwater reservoirs (e.g., Jackson and Hightower, 2001; Young and Isley, 2002), with exceptions in North Carolina (Haeseker et al., 1996; Carmichael et al 1998), Maryland (Hocutt et al., 1990), and New Jersey (Tupper and Able, 2000). More detailed studies are necessary to determine how estuarine and ocean use varies among individuals over seasons and years. This is especially necessary because much of the past focus has been on large estuarine and river systems such as the

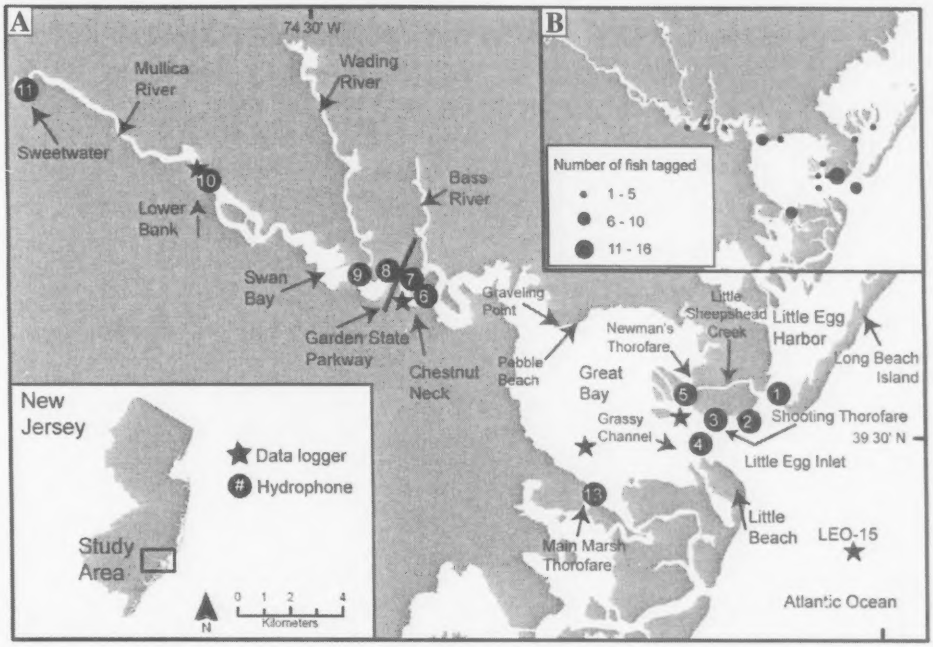
A
74 30' W
Mullica River
Wading River
Sweetwater
Bass River
Lower Bank
Swan Bay
Garden State Parkway
Chestnut Neck
Graveling Point
Pebble Beach
New Jersey
Study Area
Data logger
Hydrophone
0 1 2 4
Kilometers
N
B
Number of fish tagged
1 - 5
6 - 10
11 - 16
Little Sheepshead Creek
Little Egg Harbor
Long Beach Island
Newman's Thorofare
Great Bay
Grassy Channel
Shooting Thorofare
39 30' N
Little Egg Inlet
Main Marsh Thorofare
Little Beach
LEO-15
Atlantic Ocean
1
2
3
4
5
6
7
8
9
10
11
13

Figure 1

Mullica River–Great Bay study site and important localities (**A**) and location of fish tagging and release sites (**B**) during 2003 and 2004. Hydrophone 12 was not deployed during this period and is not shown.

Hudson River (Secor et al., 2001; Zlokovitz et al., 2003) or Chesapeake Bay (Secor, 2000a, 2000b). Relatively little attention has been directed to small coastal bay and estuarine systems that, owing to scale, may have very different dynamics.

The purpose of this study was to determine the annual, seasonal, and episodic patterns of residency and movements for large juvenile and adult striped bass along an estuarine gradient in a small drowned-river-valley estuary. Although most previous telemetry and tracking studies focused on one fish at a time, the estuarine system used in the present study allowed for synoptic observations of numerous individuals. Throughout this study there was an emphasis on individual behavior, an approach that has provided important insight into the stock structure of other fishes (Sutherland, 1996; Slotte and Fiksen, 2000).

Materials and methods

Study site

The Mullica River–Great Bay estuary (Fig. 1) is one of the few remaining relatively undisturbed estuaries in the northeastern United States because there is little agricultural or industrial development in the watershed and human population density is relatively low (Kennish, 2004). This relatively small watershed (1474 km^2; Kennish, 2004) that comprises several tributaries (Batsto, Wading, and Bass Rivers) is part of the Jacques Cousteau National Estuarine Research Reserve (JCNERR) and drains the Pinelands National Reserve at a mean monthly stream flow of approximately 1.7 to 4.2×10^8 L/d (Rhodehamel, 1998) (Fig. 1). Much of the 280 km of shoreline in this watershed consists of cordgrass (*Spartina alterniflora*) dominated salt marsh, and has a tidal range between 0.7 m (in Little Egg Harbor) and 1.1 m (near the mouth of Great Bay). Mean salinity of 29 at the entrance to the bay drops sharply to about 8 within 30 linear km upriver; the inflection point corresponds to a steep decrease in pH from 8.0 to 6.0 owing to tannins leached from the pine-forested watershed (Kennish, 2004). The majority of water exits into the ocean through the narrow but deep (20 m) Little Egg Inlet and to a lesser extent through the Main Marsh Thorofare, an intra-estuarine connection that is part of the Intra-Coastal Waterway (ICW) (Chant et al., 1996).

Estuarine observatory

Wireless hydrophones were deployed at a series of gates in order to enhance detection of tagged striped bass while in residence or moving along the estuarine gradient (Fig. 1). At the entrance to the estuary (Little Egg Inlet) hydrophones 2, 3, and 4 (recorded as positioned

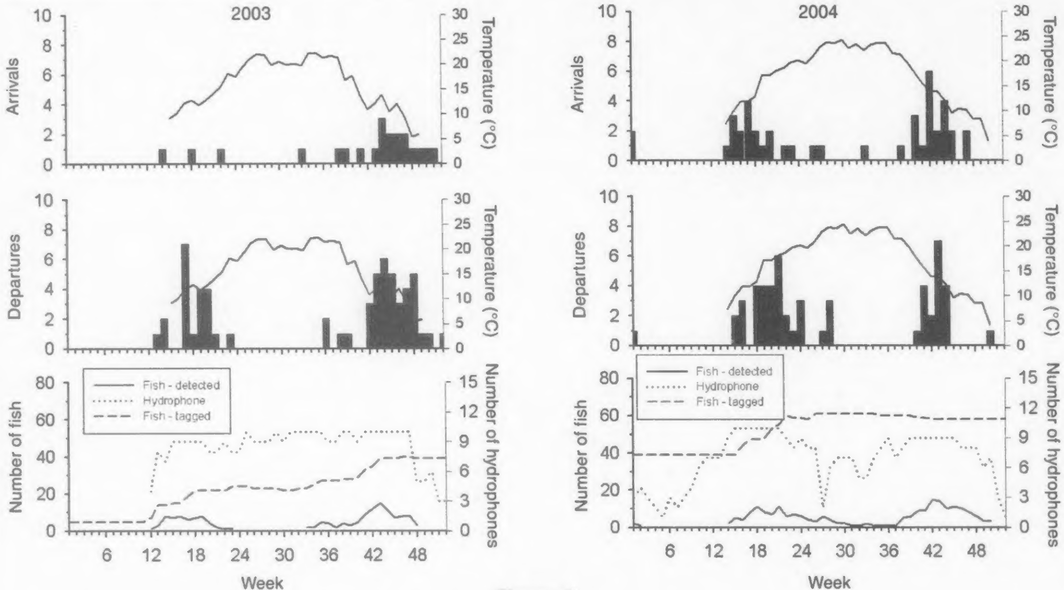

Figure 2

Arrivals and departures of tagged striped bass (*Morone saxatilis*), number of active hydrophones, and number of fish tagged (available) and detected in the system during 2003 and 2004. Number of fish detected in the system and number of active hydrophones included all data combined within each week. Temperature data were collected at a Jacques Cousteau National Estuarine Research Reserve data logger in lower Great Bay (Fig. 1).

at 0 km) were arranged to take advantage of local topography, such as at sand bars, channels, etc. to detect fish moving along several passages. The entrance to Little Egg Harbor was monitored by hydrophone 1 (considered to be 0 km from the inlet for the purposes of this study). This same hydrophone, along with no. 5, also served to identify fish moving through a deep (to 7 m) channel (Little Sheepshead Creek) between Little Egg Harbor and Great Bay. The channel exiting Great Bay to the south (Main Marsh Thorofare) was monitored by hydrophone 13 (4.5 km from the inlet), although this hydrophone was deployed later than the others. Hydrophone 5 (4.5 km from the inlet) also served to monitor fish passing through the deepest channel in Great Bay (Newmans Thorofare). The next gate upstream was located in the Mullica River (hydrophones 6, 7, 8, 9; approximately 18 km from the inlet). Hydrophones 6 and 8 were removed after a test period because they were largely redundant. Farther upstream the next gate consisted of a single hydrophone (no. 10; 28.3 km from the inlet) just above the saltwater-freshwater interface. On occasion, another hydrophone (no. 11; 38.1 km from the inlet) was deployed farther upstream in tidal freshwater. The total number of hydrophones deployed over the period of the study is indicated in Figure 2. Additional details of this estuarine system (referred to as an "observatory") are provided in Grothues et al. (2005). Our ability to detect tagged fish in certain portions of the estuary was affected by the times of hydrophone deployment and, occasionally, by aperiodic retrieval of the hydrophones because of poor weather conditions (ice formation in the winter of 2003–04) or equipment malfunction (Fig. 2).

Striped bass bearing surgically implanted acoustic transmitters (76.8 KHz) with an individual identification code were detected when they came within range (approximately 500 m; Grothues et al., 2005) of moored wireless hydrophones (WHS-1100, Lotek Wireless, Inc., St. Johns, Newfoundland, Canada), which were suspended at a depth of 3.2 m where surrounding total water depth reached a depth of 10 m. Wireless hydrophones transmitted received sound in the 76.8 KHz band by a VHF radio frequency unique to the unit (between 148 and 152 MHz) to shore-based receivers for the interpretation and logging of the data in real time (see Grothues et al., 2005, for additional details). The JCNERR study area also provided useful infrastructure for routine environmental monitoring. Permanent instrumentation included data loggers used to record salinity, temperature, pH, and water depth (Kennish and O'Donnell, 2002) along the estuarine gradient (Fig. 1).

Tagging technique

Fish were collected by hook and line from 2 November 2002 to 2 November 2004 in the study area. Immediately after capture, each individual was anesthetized in a cooler containing 0.4–0.6 g/liter of MS-222 (Sigma-Aldrich Corporation, St. Louis, MO). A transmitter (CAFT 16-3, Lotek Wireless Inc., St. Johns, Newfoundland, Canada) was then surgically implanted in the body cavity. The incision was closed with absorbable ethalon monofilament sutures and treated with antibiotic ointment. An external tag (Floy Tag, Inc., Seattle, WA), with printed contact information, was anchored into the flesh to allow fishermen to report capture later to the study crew. While still anesthetized, the fish was measured (mm total length, TL), injected with Liquamyacin®Pfizer at 0.1 mg/kg fish weight as a prophylactic against latent infection. Each fish was then placed in clean, ambient water until it showed normal swimming ability at which time it was released at the capture site. On occasion, fish were held for short periods of time (two hours) before release. However, one fish was held for four days at Rutgers University Marine Field Station (RUMFS) before surgery and then taken to the site of capture and released.

Data analyses

The sampling unit (n) used in the analyses of telemetry data was an individual tagged fish because this approach places equal importance on the movements of each fish (Rogers and White, in press). For the purpose of this study, immigration of a tagged fish occurred when the first detection of a fish tagged in 2002 was recorded after January 2003 at or near an entrance to the estuary. Emigration was determined by detection at one of the entrances to the estuary followed by no detections of that individual for two consecutive weeks, presumably because it left the estuary for the ocean or an adjacent bay. In order to measure swimming speed, we used the last detection at a hydrophone at one gate and the first detection at the next gate to determine time of travel and distance between hydrophones.

Results

Environmental parameters

Pronounced seasonal changes in temperature and dissolved oxygen occurred consistently throughout the estuary, and salinity and pH decreased in the river (Fig. 3). Temperatures approached, and probably reached, 0°C during both winters but reached maximum temperatures of approximately 25°C farther up the estuary during summer. Temperatures near Little Egg Inlet were consistently cooler than elsewhere in the estuary during both years. Dissolved oxygen values followed the same seasonal trend, except that values were highest in the winter, near 14 mg/L, and lowest in the summer, at 4–6 mg/L, but in both years values at Little Egg Inlet were higher than farther up the estuary. The salinity varied distinctly with distance up the estuary. The values at Little Egg Inlet averaged 28.6 (16.8–32.7) during both years, whereas those upstream at Chestnut Neck (mean=13.8, range 0.9–24.4) and Lower Bank (mean=2.1, range 0–13.4) were much lower. Although there were no data collected at Sweetwater during the 2005 study period, the salinity values averaged 0.1 (range: 0.02–5.1). The estuary differs from many others in the Middle Atlantic Bight in that pH values in the upper portions of the study area are naturally low (Lower Bank, mean 5.9, range=4–7.4). These values tended to be lowest in the spring and winter, presumably because of higher runoff associated with more precipitation and because of lower salinities at that time of the year.

General characteristics of ultrasonically tagged fish

During the study period, 68 striped bass (range 483–978 mm TL) were tagged and tracked through the Mullica River–Great Bay study area. Most of these fish were tagged in Great Bay (n=61), especially in the lower bay near Little Egg Inlet and Shooting Thorofare, although a number were also tagged at Graveling Point and Pebble Beach (Fig. 1B). Most fish were tagged in the fall and spring of 2003 and spring of 2004. The duration of detection of these tagged fish varied greatly among individuals. Some individuals (n=3) were detected only immediately after tagging and not again. Some were detected only during one season or one year (n=3), others (n=5) were detected in both years, and two individuals were detected for almost the entire duration of this study. The mean duration in the study area for fish tagged in 2003 was 43.5 days and in 2004 was 20.0 days. Several fish were captured by anglers within the estuary (n=4), outside the estuary elsewhere in New Jersey (n=5), on the south shore of Long Island (n=1), coastal New Hampshire (n=1) and one was detected by similar hydrophones in the Saco River, Maine (Carter[1]).

The overlap in time between hydrophone deployment and the time of initial tagging of each fish and their exit and re-entry into the estuary determined the frequency and duration of tag detections (Fig. 2). Overall the rate of detection was high; over 97% of all tagged fish were detected after tagging. The number of detections for each individual varied markedly and ranged from 22 to 75,603 contacts; the total number of contacts for all fish was 501,760 over the course of the study. Of the fish tagged and subsequently detected, duration at liberty varied from 15 to 731 days. Most fish were detected by more than one hydrophone and numerous individuals were detected by 2–10 hydrophones.

Annual and seasonal visits to the estuary

The patterns of estuarine use by tagged striped bass were diverse and varied by individual, season, and year. We characterized individual tagged fish by their use of the estuary, either as resident fish (never detected

---

[1] Carter, J. 2005. Personal observ. Department of Life Sciences, Univ. New England, 11 Hills Beach Road, Biddeford, ME 04005.

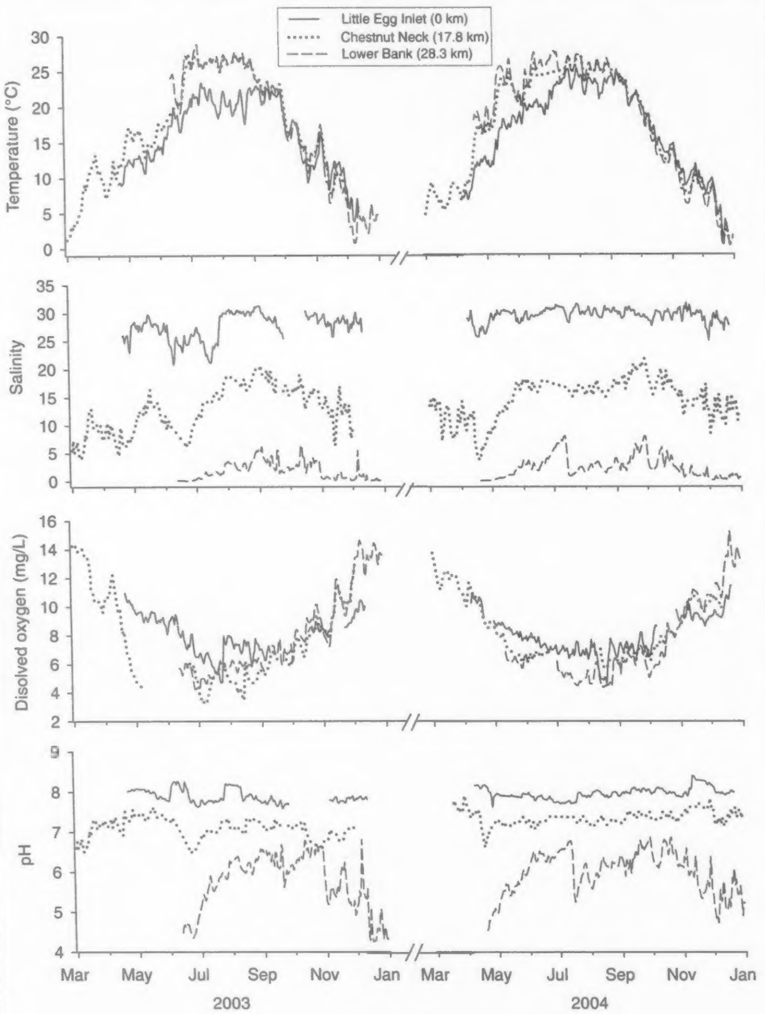

Figure 3

Monthly and annual variation in environmental parameters of the water column during 2003 and 2004 based on Jacques Cousteau National Estuarine Research Reserve data loggers. See Figure 1 for location of data loggers. Some values are missing because of ice cover and because we were unable to download data during winter.

leaving the estuary), seasonal inlet visitors (detected only at the inlet gate by hydrophones 1–4), seasonal estuarine visitors, (within the estuary gate at hydrophones 13, 5–9), or as seasonal river visitors (within the river gate at hydrophones 10, 11) (Fig. 1). The consistency of these four patterns varied with individual fish. Of the total number of tagged fish that could be classified (n=64), 67.1% displayed a single pattern, 31.2% displayed two patterns, and 1.5% exhibited three of the above patterns. Of these patterns there were 105 total classifications. The residents made up 2.8% of all estuarine use patterns. The seasonal inlet visitors made up 36.1%, seasonal estuarine visitors made up 49.5% , and seasonal river visitors made up 11.4% of all estuarine-use patterns. Of these, 58% of all tagged fish (n=67) that left the system returned in later seasons(42%) and years (16%) (proportions were standardized to two-year tags at large for one year).

Seasonal occurrence in the estuary was the result of departure and re-entry of individual fish (Fig. 2). The number of departures for individuals ranged from 0 to 7, whereas arrivals ranged from 0 to 6. In both years most departures and arrivals occurred in the spring and during the fall and early winter and not during mid-winter or summer. In 2003, most departures (n=27) from the estuary occurred between weeks 12 and 21 (late March–May) and again between weeks 39 and 48 (late September–mid November), whereas in 2004 departures (n=14) occurred later, during weeks 17–23 (mid May–mid June) and later (n=4) in weeks 27 and 45 (mid July and early November (Fig. 2). In 2003, most arrivals (n=4) were detected during weeks 40–46 (beginning October and early November) and earlier (n=2) during weeks 16–20 (mid May–beginning June), whereas in 2004 most arrivals (n=7) occurred during weeks 12–20 (mid March–beginning June) and later (n=17) during weeks 37–46 (mid September–mid November).

The departure and arrival times (Fig. 2) corresponded with the seasonal increase and decrease, respectively, of estuarine inlet temperatures (Fig. 3). In both years the number of departures (21% of total fish) and arrivals (21%) was low at temperatures <10°C and >20°C, respectively. During the period between these temperatures (when 79% of both departures and arrivals occurred), departures occurred at a mean of 13.9°C and arrivals occurred at a mean of 14.0°C. These temperatures typically occurred during the spring and fall (Fig. 3).

Patterns of arrival and departure were especially interesting for several individuals that revisited the study area during 2003 and 2004. The best evidence for frequent, seasonal re-entry and departure from the study estuary comes from the redetection of six striped bass tagged on 2 April 2003 at Graveling Point (Fig. 4). Of these, four returned and departed on several occasions. For three of these individuals (tags 95, 97, 99) the pattern of the timing of return and departure was nearly the same over several seasons (winter 2003, spring and winter 2004). Another individual (with tag 96) was redetected only once, but it reappeared (spring 2004) at the same time as the other individuals. Even those fish that were not redetected during a later season or year typically departed the estuary at the same approximate time (spring 2003 and spring 2004) as the other fish (Fig. 2). The close agreement in seasonal arrival to and departure from the estuary is probably the result of seasonal migrations during which fish enter this estuary, and probably other estuaries, on their migration south in the winter and north in the spring.

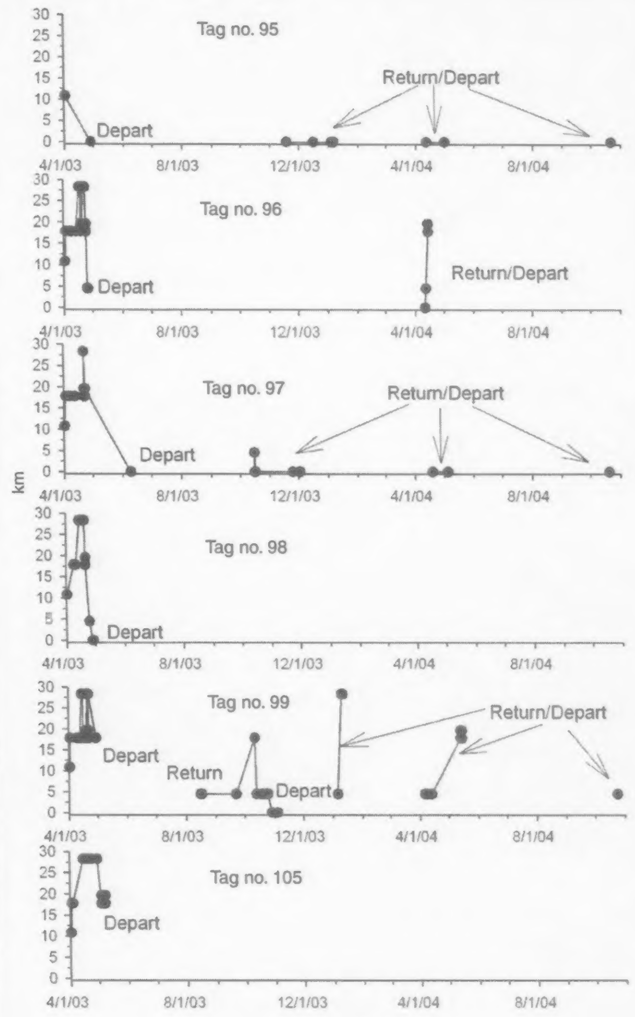

Figure 4

Occurrence and distribution of selected individual striped bass (*Morone saxatilis*) tagged on 2 April 2003 at Graveling Point. Filled circles indicate when there were detections by hydrophones. Distance upstream is from Little Egg Inlet gate (hydrophones 1–4, 13, reported as 0 km from the inlet) to Chestnut Neck gate (hydrophones 6–8, 18 km from the inlet), Lower Bank gate (hydrophone 10, 28 km from the inlet), and Sweetwater gate (hydrophone 12, 38 km from the inlet).

For fish that left the estuary, the last detection was most frequent in the vicinity of Little Egg Inlet where most detections occurred at hydrophones 2 (33%), 1 (23 %), and 4 (20%). Other final detections also occurred within the estuary at hydrophones 6 (9%), 7 (6%), 13 (3%), 5 (3%), and 8 (<1%). The last detection at relatively long distances from the inlet (hydrophones 6, 7, 8) may have resulted from departures during periods before hydrophone 13 was deployed.

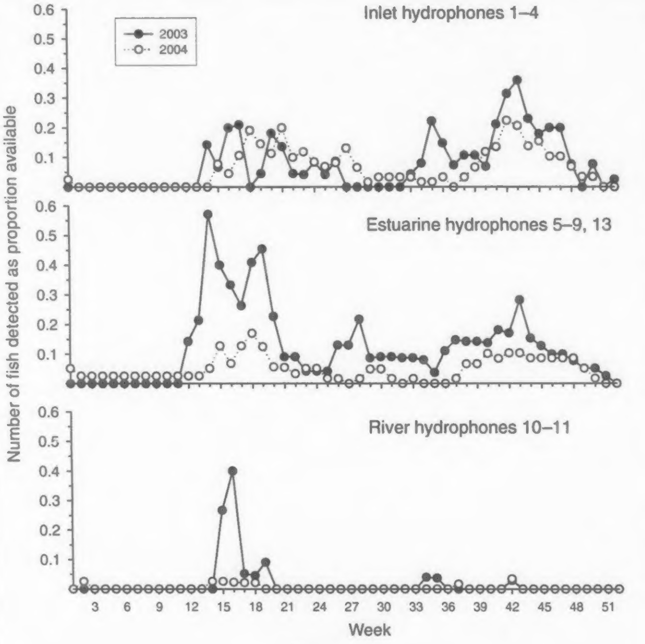

Figure 5

Annual variation in number of fish detected, by week in the inlet, by estuary, and at river gates. See Figure 1 for locations of gates.

Spatial and temporal patterns of striped bass within the estuary

Fish moved, as evidenced by hydrophone detections at selected gates, in a variable manner with respect to areas in the study site, seasons, and years (Figs. 4 and 5). Fish were frequently detected in the polyhaline portions near the inlet and in the estuary and less consistently in the river. The distribution of fish in the estuary varied by season; fish were detected at the inlet gate (hydrophones 1–4) during all seasons, whereas fish detected in spring were more frequently found farther up at the estuary gate (hydrophones 5–9, 13) or farther upstream at the river gate (hydrophones 10–11). However, few fish were detected during the winter at any gate. These general patterns of estuarine use varied between years. A strong peak in estuarine users occurred in the spring (weeks 14–21) of 2003, but there were fewer users in 2004. Modest peaks in inlet and estuarine users occurred in the fall (weeks 34–48) in both years. The sole peak in river use occurred in spring (weeks 14–20) of 2003.

The degree of residency and movements within the estuary varied among individuals over time for a given individual. Some individuals were resident in one portion of the estuary for long periods of time. This finding was substantiated by the long duration of detections for some individuals in the vicinity of the inlet. For example, two fish (n=1273 contacts and 280 cumulative hours of detection) spent 91% and 58% of their time, respectively, at the inlet, even though they were detected at two other gates. Together these types of patterns account for the preponderance of detections in the vicinity of the inlet and for the somewhat lower detections upstream. Another fish, with one of the longer time records (n=1190 hours of detection) was detected at all gates in the study area. Alternatively, some fish were consistently detected farther up the estuary. For example, one fish (n=154.5 hours detected) was detected frequently in the vicinity of Chestnut Neck (75% of the time).

Other individuals, although not detected as frequently, appeared to be resident for relatively long periods. For example, two fish were consistently found farther up the estuary over several months and we interpreted this period as residency. The lack of frequent detections implies that this residency occurred in areas between hydrophone gates. Active telemetry of individual fish confirms this interpretation (Ng, 2006; Ng et al., in press). Movements in the study area were often dynamic; individual fish moved large distances over short periods. Several individuals moved quickly upstream after being tagged lower in the estuary during the spring. Of six individuals tagged on 2 April 2003, five moved upstream 7–10 km into the area of the freshwater-saltwater interface (near Lower Bank, approximately 28.3 km from Little Egg Inlet) or farther into completely freshwater in the vicinity of Sweetwater (approximately 38.1 km from Little Egg Inlet) (Fig. 4). These same upstream movements occurred for 3 of 4 fish tagged at Graveling Point on 2 May 2003. More extensive movements were detected for all 3 fish tagged on 22 April 2004 at Little Egg Inlet. All of these fish moved 17–19 km upstream and were detected at the same locations as those of the previous fish.

Upstream movements were relatively quick. The speed of fish passing upstream from Little Egg Inlet to Chestnut Neck ranged from 0.3 to 2.4 km/h (n=10 fish) and from Chestnut Neck to Lower Bank ranged from 0.09 to 0.5 km/h (n=11 fish). The subsequent movement downstream followed quickly (within a few days) for most fish, but the range of speeds during these movements overlapped with the speed of upstream movements from Lower Bank to Chestnut Neck (0.1–0.3 km/h, n=11 fish) and from Chestnut Neck to Little Egg Inlet (0.1–2.2 km/h, n=12). Perhaps the slower movements between Chestnut Neck and Lower Bank reflect the steeper gradients in salinity, temperature, and especially pH in this region (Fig. 3). Although most of these movements occurred during the spring, others of similar magnitude occurred at other times of the year, as was the case for one fish during the winter of 2004 (Tag no. 99, Fig. 4).

Discussion

Annual and seasonal visits to the estuary

The seasonal visits of many tagged striped bass to this estuary reflect their seasonal migrations up and down the east coast of the United States. This seasonal migration to the south in the fall and winter and to the north in the spring and summer has been observed from prior tag-recapture studies (e.g., Boreman and Lewis, 1987; Waldman et al., 1990). The coastal ocean migrations of larger juvenile and adult striped bass must influence the timing and duration of their occurrence in estuaries. These patterns differ along the east coast of the United States and thus have to be taken into consideration when evaluating occurrences in the study area. In general, populations from North Carolina and southward are considered riverine and do not make coastal migrations, whereas those from Chesapeake Bay to the Bay of Fundy are generally considered to be anadromous and highly migratory (see Rulifson and Dadswell, 1995; Haeseker et al., 1996; Bjorgo et al., 2000 for reviews of the relevant literature), with the exception of the population of the St. Lawrence estuary which is believed to be resident (Coutant, 1985). Thus, it is not surprising that large juvenile and adult striped bass from the Mullica River–Great Bay estuary frequently left the estuary for extended periods. This interpretation is supported by the recapture by hook and line of fish we tagged in the study area at a variety of locations along the coast (northern New Jersey, south shore of Long Island, New Hampshire) and implies the same seasonal migration pattern. Further support is based on the detection of one striped bass tagged in the Mullica River–Great Bay and later detected in the Saco River, Maine, in a similar observation site (Carter[2]) and fish tagged at Saco River, Maine, that have been detected in the southern New Jersey study estuary (n=3) (Able and Grothues, pers. observ.). Earlier tag-recapture studies found striped bass in the Mullica River–Great Bay estuarine system that had been tagged on the south shore of Long Island and northern New Jersey (Clark, 1968).

This study is one of the few that presents data on the high (58%) and seasonal rate of return to an estuary. Most of these returns occurred in the spring and fall when water temperatures were 10–20°C. Annual returns to the same estuary have also been reported in Chesapeake Bay tributaries for a few individuals (n=9) where the returns were assumed to be related to spawning (Hocutt et al., 1990). Many of the instances of fidelity of tagged striped bass to the Mullica River–Great Bay system were the result of detections at the inlet and not farther up the estuary. One possible interpretation is that these fish enter numerous inlets during the north and south coastal ocean migrations, thus providing the relatively high frequency of detections at the study site. This idea could be tested at observation sites in other estuaries.

Spatial and temporal patterns within the estuary

Movements within the estuary were frequently dynamic and were most likely to occur in the spring and fall. The spring movements of several fish tagged near Little Egg Inlet and near Chestnut Neck were commonly upstream to the vicinity of the freshwater-saltwater interface (Fig. 4). These were typically quick movements followed by similarly rapid movements downstream and into the ocean. The short duration in the riverine portion of the study area may reflect the avoidance of the low pH that typically occurs in this system (Fig. 3). These brief visits in the study area were very different from those found in a pilot study (n=4 males, 5 females) in upper Chesapeake Bay tributaries, which indicated a long residence time in the spawning areas (30 days) at least for males (Hocutt et al., 1990). Similarly, in the Roanoke River in North Carolina males remained on the spawning grounds for 21–22 days and females for 8–11 days in different years (Carmichael et al., 1998). The timing and types of movement in the study area, although consistent with an upstream movement for spawning, do not appear to be consistently successful. Some spawning does occur in the upstream portion of the estuary (see Hoff[3] for accounts of egg and larvae collections). However, numerous collections in this estuary with a variety of gears, such as otter trawls (Martino and Able, 2003), seines (Able et al., 1996), traps (Able et al., 2006), and weirs (Able et al., 1996), have yielded less than 20 young-of-the-year (YOY) (<100 mm FL) striped bass. Over the same period, we have frequently collected numerous YOY striped bass in similar sampling programs in Delaware Bay (Nemerson and Able, 2003) and in the New York–New Jersey Harbor Estuary (Able and Duffy-Anderson, 2006). The short period of residency in upstream portions of the Mullica River may indicate the testing and then rejection of the area as a spawning site.

---

[2] Carter, J. 2005. Unpubl. data. Department of Life Sciences, Univ. New England, 11 Hills Beach Road, Biddeford, ME 04005.

[3] Hoff, H. K. 1976. The life history of striped bass, *Morone saxatilis* (Walbaum), in the Great Bay-Mullica River estuary and in the vicinity of Little Egg Inlet. *In* Ecological studies in the bays and other waterways near Little Egg Inlet and in the ocean in the vicinity of the proposed site for the Atlantic Generating Sation, New Jersey (C. D. Milstein, and D. L. Thomas, eds.), p. 43–53. Progress Report for the period January–December 1975. Public Service Electric and Gas Company, 80 Park Plaza T-17-A, Newark, NJ 07101.

This study confirms that there are multiple ways in which striped bass use small estuaries, such as that of the study area, as there are multiple ways in which striped bass use larger systems such as the Hudson River (e.g., Secor et al. 2001). Further, the movement patterns observed in this study may be more diverse and variable than previously reported because the same fish can exhibit different patterns in different seasons and years. This diversity implies that the behavior at the individual level may be as, or more important (Sutherland, 1996; Slotte and Fikson, 2000) than, that at the level of the stock, contingent, or population level and thus is necessary to understand how striped bass use estuarine ecosystems and how biologists can manage natural populations.

Acknowledgments

Numerous technicians from the Rutgers University Marine Field Station assisted in the deployment and maintenance of hydrophone moorings, tagging of fish, and data compilation, especially R. Nichols and M. Greaney. Several recreational fishermen shared their local knowledge and helped extensively with tagging including D. Messerschmid and G. Delaporte. Personnel of the Jacques Cousteau National Estuarine Research Reserve, especially G. Sakowicz, provided access to environmental data. Several anonymous reviews provided helpful comments on an earlier draft. Financial support for the development and deployment of the hydrophones came from the Rutgers University/National Marine Fisheries Service Bluefish/Striped Bass program. This research was conducted under Rutgers University Animal Use Protocol no. 88-042. This paper is Rutgers University Institute of Marine and Coastal Sciences Contribution no. 2006-16.

Literature cited

Able, K. W., and J. T. Duffy-Anderson.
2006. Impacts of piers on juvenile fishes in the lower Hudson River. *In* The Hudson River Estuary (J. S. Levinton, and J. R. Waldman, eds.), p. 428–440. Cambridge Univ. Press, New York, NY.

Able, K. W., M. P. Fahay, D. A. Witting, R. S. McBride, and S. M. Hagan.
2006. Fish settlement in the ocean vs. estuary: comparison of pelagic larval and settled juvenile composition and abundance from southern New Jersey, USA. Estuar. Coast. Shelf Sci. 66:280–290.

Able, K. W., D. A. Witting, R. S. McBride, R. A. Rountree, and K. J. Smith.
1996. Fishes of polyhaline estuarine shores in Great Bay-Little Egg Harbor, New Jersey: a case study of seasonal and habitat influences. *In* Estuarine shores: evolution, environments and human alternations (K. F. Nordstrom, and C. T. Roman, eds.), p. 335–353. John Wiley and Sons, Ltd., Chichester, England.

Arnold, G. P., and H. Dewar.
2001. Electronic tags in marine fisheries research: a 30 year perspective. *In* Electronic tagging and tracking in marine fisheries (J. R. Siebert, and J. L. Nielsen, eds), p. 7–64. Kluwer Academic Publ., Dordrecht, The Netherlands.

Begg, G. A., and J .R. Waldman.
1999. An holistic approach to fish stock identification. Fish. Res. 43: 35–44.

Bjorgo, K. A., J. J. Isley, and C. S. Thomason.
2000. Seasonal movement and habitat use by striped bass in the Combahee River, South Carolina. Trans. Am. Fish. Soc. 129:1281–1287.

Boreman, J., and R. R. Lewis.
1987. Atlantic coastal migration of striped bass. Am. Fish. Soc. Symp. 1:331–339.

Carmichael, J. T., S. L. Haeseker, and J. E. Hightower.
1998. Spawning migration of telemetered striped bass in the Roanoke River, North Carolina. Trans. Am. Fish. Soc. 127:286–297.

Chant, R., M. C. Curran, K. W. Able, and S. M. Glenn.
1996. Delivery of winter flounder (*Pseudopleuronectes americanus*) larvae to settling habitats in coves near tidal inlets. Estuar. Coast. Shelf Sci. 51:529–541.

Clark, J.
1968. Seasonal movements of striped bass contingents of Long Island Sound and the New York Bight. Trans. Am. Fish. Soc. 97(4):320–343.

Cooke, S. J., S. G. Hinch, M. Wikelski, R. D. Andrews, L. J. Kuchel, T. G. Wolcott, and P. J. Butler.
2004. Biotelemetry: a mechanistic approach to ecology. Trends Ecol. Evol. 19(6):334–343.

Coutant, C. C.
1985. Striped bass, temperature, and dissolved oxygen: a speculative hypothesis for environmental risk. Trans. Am. Fish. Soc. 114:31–61.

Gillanders, B. M.
2005. Using elemental chemistry of fish otoliths to determine connectivity between estuarine and coastal habitats. Est. Coast. Shelf Sci. 64:47–57.

Grothues, T. M, K. W. Able, J. McDonnell, and M. M. Sisak.
2005. An estuarine observatory for real-time telemetry of migrant macrofauna: design, performance, and constraints. Limnol. Oceangr. Methods 3:275–289.

Haeseker, S. L., J. T. Carmichael, and J. E. Hightower.
1996. Summer distribution and condition of striped bass within Albemarle Sound, North Carolina. Trans. Am. Fish. Soc. 125:690–704.

Heupel, M. R., J. M. Semmes, and A. J. Hobday.
2006. Automated acoustic tracking of aquatic animals: scales, design and deployment of listening station arrays. Mar. Freshw. Res. 57:1–13.

Hocutt, C. H., S. E. Seibold, R. M. Harrell, R. V. Jesien, and W. H. Bason.
1990. Behavioral observations of striped bass (*Morone saxatilis*) on the spawning grounds of the Choptank and Nanticoke Rivers, Maryland, USA. J. Appl. Ichthyol. 6:211–222.

Jackson, J. R., and J. E. Hightower.
2001. Reservoir striped bass movements and site fidelity

in relation to seasonal patterns in habitat quality. N. Am. J. Fish. Manag. 21:34–45.

Kennish, M. J.
2004. Jacques Cousteau National Estuarine Research Reserve. *In* Estuarine research monitoring, and resource protection (M. J. Kennish, ed.), p. 59–115. CRC Press, Baton Raton, FL.

Kennish, M. J., and S. O'Donnell.
2002. Water quality monitoring in the Jacques Cousteau National Estuarine Research Reserve System. Bull. New Jersey Acad. Sci. 47(2):1–14.

Klein-MacPhee, G.
2002. Striped bass (*Morone saxatilis*, Walbaum 1792). *In* Bigelow and Schroeder's Fishes of the Gulf of Maine (B. B. Collette, and G. Klein-MacPhee, eds.), p 377–389. Smithsonian Institution Press, Washington, DC.

Martino, E., and K. W. Able.
2003. Fish assemblages across the marine to low salinity transition zone of a temperate estuary. Est. Coast. Shelf Sci. 56(5–6):967–985.

Morris, J. A., R. A. Rulifson, and L. H. Toburen.
2003. Life history strategies of striped bass, *Morone saxatilis*, populations inferred from otolith microchemistry. Fish. Res. 62: 53–63.

Nemerson, D. M., and K. W. Able.
2003. Spatial and temporal patterns in the distribution and feeding habits of *Morone saxatilis*, in marsh creeks of Delaware Bay, USA. Fish. Manag. Ecol. 20: 337–348.

Ng, C.
2006. Habitat utilization and movement patterns of adult striped bass, *Morone saxatilis*, in a southern New Jersey estuary using acoustic telemetry. M.S. thesis. 91 p. Rutgers, the State University of New Jersey, New Brunswick, NJ.

Ng, C., K. W. Able, and T. M. Grothues.
In press. Habitat use, site fidelity and movement of adult striped bass in a southern New Jersey estuary based on acoustic telemetry. Trans. Am. Fish. Soc.

Rhodehamel, E. C.
1998. Hydrology of the New Jersey Pine Barrens. *In* Pine Barrens: ecosystem and landscape (R. T. T. Forman, ed.), p. 147–167. Rutgers Univ. Press, New Brunswick, NJ.

Richards, R. A., and P. J. Rago.
1999. A case history of effective fishery management: Chesapeake Bay striped bass. N. Am. J. Fish. Manag. 19:356–375.

Rogers, K. B., and G. C. White.
In press. Analysis of movement and habitat use from telemetry data. *In* Analysis and interpretation of freshwater fisheries data (M. L. Brown, and C. S. Guy, eds.). American Fisheries Society, Bethesda, MD.

Rulifson, R. A., and M. J. Dadswell.
1995. Life history and population characteristics of striped bass in Atlantic Canada. Trans. Am. Fish. Soc. 124:477–507.

Secor, D. H.
1999. Specifying divergent migrations in the concept of stock: the contingent hypothesis. Fish. Res. 43: 13–34.
2000a. Longevity and resilience of Chesapeake Bay striped bass. J. Mar. Sci. 57:808–815.
2000b. Spawning in the nick of time? Effect of adult demographics on spawning behavior and recruitment of Chesapeake Bay striped bass. ICES J. Mar. Sci. 57:403–411.

Secor, D. H., J. R. Rooker, E. Zlokovitz, and V. S. Zdanowicz.
2001. Identification of the riverine, estuarine, and coastal contingents of Hudson River striped bass based upon elemental fingerprints. Mar. Ecol. Prog. Ser. 211:245–253.

Slotte, A., and O. Fiksen.
2000. State-dependent spawning migration in Norwegian spring-spawning herring. J. Fish Biol. 56: 138–162.

Sibert, J. R., and J. L. Nielsen (eds).
2001. Electronic tagging and tracking in marine fisheries, 484 p. Kluwer Academic Publishers, Dordrecht, The Netherlands.

Sutherland, W. J.
1996. From individual behavior to population biology, 224 p. Oxford Univ. Press, New York, NY.

Thorrold, S. R., C. Latkoczy, P. K. Swart, and C. M. Jones.
2001. Natal homing in a marine fish metapopulation. Science 291:297–299.

Tupper, M., and K. W. Able.
2000. Movements and food habits of striped bass (*Morone saxatilis*) in Delaware Bay (USA) salt marshes: comparison of a restored and a reference marsh. Mar. Biol. 137:1049–1058.

Waldman, J. R., D. J. Dunning, Q. E. Ross, and M. T. Mattson.
1990. Range dynamics of Hudson River striped bass along the Atlantic coast. Trans. Am. Fish. Soc. 119: 910–919.

Wooley, C. M., N. C. Parker, B. M. Florence, and R. W. Miller.
1990. Striped bass restoration along the Atlantic coast: a multistate and federal cooperative hatchery and tagging program. Am. Fish. Soc. Symp. 7:775–781.

Young, S. P., and J. J. Isley.
2002. Striped bass annual site fidelity and habitat utilization in J. Strom Thurmond Reservoir, South Carolina-Georgia. Trans. Am. Fish. Soc. 131:828–837.

Zlokovitz, E. R., D. H. Secor, and P. M. Piccoli.
2003. Patterns of migration in Hudson River striped bass as determined by otolith microchemistry. Fish. Res. 63: 245–259.

Microsatellite multiplex panels for genetic studies of gray snapper (*Lutjanus griseus*) and lane snapper (*Lutjanus synagris*)

Mark A. Renshaw
Eric Saillant
Siya Lem
Philip Berry
John R. Gold
Email address for M. A. Renshaw: mrenshaw@ag.tamu.edu
Center for Biosystematics and Biodiversity
Texas A&M University, TAMU–2258
College Station, Texas 77843–2258

Microsatellites are codominantly inherited nuclear-DNA markers (Wright and Bentzen, 1994) that are now commonly used to assess both stock structure and the effective population size of exploited fishes (Turner et al., 2002; Chistiakov et al., 2006; Saillant and Gold, 2006). Multiplexing is the combination of polymerase chain reaction (PCR) amplification products from multiple loci into a single lane of an electrophoretic gel (Olsen et al., 1996; Neff et al., 2000) and is accomplished either by co-amplification of multiple loci in a single reaction (Chamberlain et al., 1988) or by combination of products from multiple single-locus PCR amplifications (Olsen et al., 1996). The advantage of multiplexing microsatellites lies in the significant reduction in both personnel time (labor) and consumable supplies generally required for large genotyping projects (Neff et al., 2000; Renshaw et al., 2006).

In this note, we report the development of multiplex panels of microsatellites that will facilitate population-level genetic studies of both gray (*Lutjanus griseus*) and lane (*L. synagris*) snappers. The overexploitation of Gulf red snapper (*L. campechanus*) in U.S. waters and the increasing restrictions on both commercial and recreational red snapper catches (Gillig et al., 2001) have led to increased fishing pressure on other snapper species (Fischer et al., 2005), including both gray (Burton, 2001; Fischer et al., 2005) and lane snappers (GMFMC[1]). Although neither species has yet been classified as "overfished" or subject to "overfishing," the increased exploitation of the two species could jeopardize these snapper resources in the future. In this study, we optimized multiplex panels for gray and lane snappers from among microsatellite markers designed originally for red snapper by Gold et al. (2001) and vermillion snapper (*Rhomboplites aurorubens*) by Bagley and Geller (1998).

Materials and methods

Samples of gray and lane snappers were obtained off the west coast of Florida during April of 2004. Fin clips and pieces of liver were preserved in 95% ethanol, brought to the laboratory, and stored at room temperature. Genomic DNA was extracted by using an alkaline-lysis method (Saillant et al., 2002) and stored at –20°C.

Microsatellites were first evaluated in single-locus (simplex) reactions in order to determine the size range and ease of scoring of PCR products in each species. PCR amplifications were performed in 11.5-μL volumes comprising 1.5 μL of DNA (approximately 50 ng), 1 μL of 10× reaction buffer [50 mm KCl, 10 mm Tris, 1% Triton-X 100], 0.75 U *Taq* DNA polymerase (Invitrogen, Carlsbad, CA), 200 μm of each dNTP, 1 mm $MgCl_2$, and various quantities of PCR primers. One PCR primer of each pair was labeled with one of three fluorescent dyes from set D (Applied Biosystems, Foster City, CA): FAM, HEX, or NED. Fragment analysis was carried out on an ABI PRISM 377 automated DNA sequencer (Applied Biosystems, Foster City, CA). Allele size was estimated by using the GENESCAN-400HD [ROX] size standard (Applied Biosystems, Foster City, CA); allele size estimation was performed with GENESCAN 3.1.2 (Applied Biosystems, Foster City, CA) and allele calling was performed in GENOTYPER, version 2.5 (Applied Biosystems, Foster City, CA). Multiplex tests were performed only on those microsatellites that amplified successfully and yielded PCR products that were easy to score; loci not meeting these criteria were eliminated from subsequent analyses.

Initial multiplex PCR amplifications were performed by using the three multiplex panels designed to amplify 20 microsatellite loci in red snapper (Renshaw et al., 2006). At first, PCR primer concentrations followed those outlined in Renshaw et al. (2006), and changes were made according to the relative success of amplifications at each microsatellite within a particular multiplex. Microsatellites that failed to amplify in multiplex reactions were optimized in simplex reactions. Additional PCR

---

[1] GMFMC (Gulf of Mexico Fishery Management Council). 2005. Final amendment to the FMPs for: reef fish (Amendment 25) and coastal migratory pelagics (Amendment 17) for extending the charter vessel/headboat permit moratorium (including SEIS/RIR/IRFA), 111 p. Gulf of Mexico Fishery Management Council, 3018 North U.S. Highway 301, Suite 1000, Tampa, FL 33619–2272.

Manuscript submitted 14 September 2006 to the Scientific Editor's Office.

Manuscript approved for publication 9 November 2006 by the Scientific Editor.

Fish. Bull. 105:436-439 (2007).

Table 1

Technical details on amplification of microsatellite loci in gray snapper (*Lutjanus griseus*) and lane snapper (*L. synagris*). Included in the table are the multiplex polymerase chain reaction (PCR) panel, primer quantities, and fluorescent dye labels (Set D; Applied Biosystems, Foster City, CA). PCR protocols, including appropriate annealing temperatures, correspond to those outlined in Renshaw et al. (2006). Primer sequences for *Lca* and *Prs* microsatellites are given in Gold et al. (2001); those for *Ra* microsatellites are given in Bagley and Geller (1998).

Species	Panel	Microsatellite	Quantity (pmol)	ABI dye	PCR protocol
Lutjanus griseus	1	*Lca* 20	5	FAM	Touchdown II
		Lca 43	4	FAM	56°
		Prs 260	1.5	FAM	53°
		Ra 1	3.5	HEX	50°
	2	*Prs* 137	7	FAM	Touchdown II
		Prs 275	6	FAM	54°
		Prs 328	0.8	FAM	52°
		Ra 6	2	NED	50°
	3	*Lca* 22	2.5	FAM	Touchdown I
		Lca 91	8	FAM	56°–50.5°
		Lca 107	6.5	HEX	50°
	simplex	*Prs* 221	5	HEX	Same as panel 2
	simplex	*Prs* 240	5	HEX	Same as panel 3
	simplex	*Ra* 7	5	NED	Same as panel 3
Lutjanus synagris	1	*Lca* 20	5	FAM	Touchdown II
		Prs 248	5	NED	52°
		Prs 260	1.5	FAM	50°
		Prs 303	1.5	NED	48°
		Ra 1	7.5	NED	
		Ra 4	5	HEX	
	2	*Prs* 275	4	FAM	Touchdown II
		Prs 328	1	FAM	52°
		Ra 2	3.5	FAM	50°
		Ra 6	3	NED	48°
	3	*Lca* 22	1	FAM	Touchdown II
		Lca 91	8	FAM	52°
		Prs 240	9	HEX	50°
		Prs 333	3	HEX	48°
		Ra 7	5	NED	

primers (*Ra* 1, *Ra* 2, and *Ra* 4) designed by Bagley and Geller (1998) for vermillion snapper microsatellites were tested in simplex reactions as described above and labeled with one fluorescent dye to allow integration into one of the three multiplex panels.

Multiplex PCR amplifications initially followed the Touchdown I and II protocols outlined in Renshaw et al. (2006). Touchdown PCR protocols enable the amplification of multiple loci with different optimal annealing temperatures. The former (Touchdown I) protocol involved a one-half degree drop in annealing temperature with each subsequent cycle, for a total of 12 cycles, followed by 30 cycles at a bottom annealing temperature that was 6°C below the initial annealing temperature; the latter (Touchdown II) protocol featured a three-step drop in annealing temperature with seven cycles at an initial annealing temperature, followed by seven cycles at a lower annealing temperature, followed by 28 cycles at a bottom annealing temperature that was 4–6°C below the initial annealing temperature. Changes were made to optimize multiplex panels individually for each species. These changes included 1) removal of various primers and addition of others, and 2) modification of annealing temperatures and species-specific differences in primer concentrations.

Once multiplex or simplex protocols were developed for the two species, DNA from 28 individuals of each species was assayed across all optimized loci. Genetic variability of microsatellites in each species was measured by the number of alleles, expected heterozygosity (gene diversity), and observed heterozygosity. Fisher's exact test was used to evaluate loci for significant departures from Hardy-Weinberg equilibrium expectations. Three common causes for genotyping errors—null alleles, large allele dropout, and stuttering—were assessed with MICRO-CHECKER (Van Oosterhout et al., 2004).

Table 2

Summary data for microsatellites amplified from 28 gray snapper (*Lutjanus griseus*) and 28 lane snapper (*L. synagris*). Data for each microsatellite include number of alleles (N_A), size range (in base pairs) of detected alleles, expected (H_E) and observed (H_O) heterozygosity, and probability (P_{HW}) of conformity to Hardy-Weinberg equilibrium expectations. *Lca* and *Prs* microsatellites were developed initially for red snapper (*L. campechanus*) (Gold et al., 2001), and *Ra* microsatellites were developed initially for vermillion snapper (*Rhomboplites aurorubens*) (Bagley and Geller, 1998).

Species	Microsatellite	N_A	Size range	H_E/H_O	P_{HW}
Lutjanus griseus	*Lca* 20	4	216–222	0.707/0.643	0.721
	Lca 22	5	242–252	0.593/0.500	0.050
	Lca 43	2	176–188	0.195/0.214	1.000
	Lca 91	2	134–136	0.036/0.036	1.000
	Lca 107	6	112–144	0.771/0.750	0.266
	Prs 137	7	127–141	0.794/0.679	0.075
	Prs 221	4	235–245	0.566/0.714	0.448
	Prs 240	4	210–220	0.642/0.679	0.963
	Prs 260	9	105–129	0.847/1.000	0.060
	Prs 275	5	156–168	0.548/0.571	0.343
	Prs 328	3	202–206	0.527/0.464	0.842
	Ra 1	7	149–171	0.594/0.571	0.081
	Ra 6	15	113–155	0.926/0.679	0.000
	Ra 7	3	154–158	0.200/0.143	0.127
Lutjanus synagris	*Lca* 20	12	234–262	0.810/0.571	0.009
	Lca 22	8	234–256	0.712/0.679	0.257
	Lca 91	7	139–153	0.601/0.679	0.263
	Prs 240	5	192–202	0.592/0.538	0.484
	Prs 248	17	224–260	0.938/0.893	0.402
	Prs 260	4	92–120	0.292/0.321	1.000
	Prs 275	2	154–156	0.036/0.036	1.000
	Prs 303	4	135–141	0.690/0.643	0.724
	Prs 328	5	198–214	0.631/0.571	0.499
	Prs 333	12	152–180	0.870/0.821	0.327
	Ra 1	9	141–163	0.806/0.893	0.587
	Ra 2	6	82–100	0.704/0.821	0.972
	Ra 4	9	59–99	0.787/0.821	0.660
	Ra 6	4	118–124	0.384/0.464	0.770
	Ra 7	4	177–187	0.612/0.536	0.578

Results and discussion

A total of 14 microsatellites (11 in three multiplex panels and 3 in simplex reactions) were optimized for gray snappers, and 15 microsatellites (in three multiplex panels) were optimized for lane snappers. The multiplex and simplex formats are presented in Table 1 and include for each microsatellite the fluorescent label (Applied Biosystems, Foster City, CA), primer quantity, PCR protocol, and optimized annealing temperatures. Genotype summary data from 28 individuals (in both species) are given in Table 2; data for each microsatellite include number of alleles, size range of alleles detected, expected and observed heterozygosity, and probability of conformity to Hardy-Weinberg equilibrium expectations.

For gray snappers, the number of alleles per microsatellite ranged from two (*Lca* 43 and *Lca* 91) to 15 (*Ra* 6), and expected and observed heterozygosity per microsatellite ranged from 0.036 (*Lca* 91) to 0.926 (*Ra* 6) and from 0.036 (*Lca* 91) to 1.000 (*Prs* 260), respectively. Only one microsatellite (*Ra* 6) deviated significantly ($P<0.05$) from Hardy-Weinberg equilibrium expectations after sequential Bonferroni correction (Rice, 1989). Analysis with MICRO-CHECKER (Van Oosterhout et al., 2004) indicated the possible occurrence of null alleles at *Ra* 6.

For lane snappers, the number of alleles per microsatellite ranged from two (*Prs* 275) to 17 (*Prs* 248), and expected and observed heterozygosity per microsatellite ranged from 0.036 (*Prs* 275) to 0.938 (*Prs* 248) and from 0.036 (*Prs* 275) to 0.893 (*Prs* 248 and *Ra* 1), respectively. None of the 15 microsatellites deviated significantly from Hardy-Weinberg equilibrium expectations after sequential Bonferroni correction (Rice, 1989). Analysis with MICRO-CHECKER indicated the possibility of null alleles at one microsatellite (*Lca* 20) where the probability of deviation from Hardy-Weinberg equilibrium expectations was significant (P=0.009) before Bonferroni correction. One locus, *Lca* 91, exhibited a one base-pair shift (rather than the two base-pair shifts expected from dinucleotide repeats) in samples of lane snapper; this difference in shift could generate scoring problems in future genotyping efforts.

The costs of large genotyping projects can be substantially reduced through the combination of multiple loci in single PCR amplifications (Renshaw et al., 2006). The reduction in costs could enable researchers to increase sample sizes, possibly allowing for the inclusion of additional year classes for temporal studies or could extend a proposed sampling range to include more of the geographic distribution of a species. The multiplex panels and simplex reactions developed in the present study will provide critical tools for future population-level genetic studies designed to identify fishery management units and to monitor changes in genetic effective population size for both gray and lane snappers.

Acknowledgments

We thank the crew of the RV *Tommy Munro* (Florida Fish and Wildlife Research Institute) and M. Murphy, B. Mahmoudi, and R. Lehnert for assistance in sampling, and C. Bradfield and D. Ebelt for assistance in the laboratory. Work was supported by the Marfin Program of the U.S. Department of Commerce (Grant NA04-NMF-4330074), and by the Texas Agricultural Experiment Station (Project H-6703). This article is number 54 in the series "Genetic Studies in Marine Fishes" and is contribution number 147 of the Center for Biosystematics and Biodiversity at Texas A&M University.

Literature cited

Bagley, M. J., and J. B. Geller.
1998. Characterization of microsatellite loci in the vermillion snapper *Rhomboplites aurorubens* (Percoidei: Lutjanidae). Mol. Ecol. 7:1089–1090.

Burton, M. L.
2001. Age, growth, and mortality of gray snapper, *Lutjanus griseus*, from the east coast of Florida. Fish. Bull. 99:254–265.

Chamberlain, J. S., R. A. Gibbs, J. E. Ranier, P. N. Nguyen, and C. T. Caskey.
1988. Deletion screening of the Duchenne muscular dystrophy locus via multiplex DNA amplification. Nucleic Acids Res. 16:11141–11156.

Chistiakov, D. A., B. Hellemans, and F. A. M. Volckaert.
2006. Microsatellites and their genomic distribution, evolution, function and applications: a review with special reference to fish genetics. Aquaculture 255:1–29.

Fischer, A. J., M. S. Baker Jr., C. A. Wilson, and D. L. Nieland.
2005. Age, growth, mortality, and radiometric age validation of gray snapper (*Lutjanus griseus*) from Louisiana. Fish. Bull. 103:307–319.

Gillig, D., W. L. Griffin, and T. Ozuna Jr.
2001. A bioeconomic assessment of Gulf of Mexico red snapper management policies. Trans. Am. Fish. Soc. 130:117–129.

Gold, J. R., E. Pak, and L. R. Richardson.
2001. Microsatellite variation among red snapper (*Lutjanus campechanus*) from the Gulf of Mexico. Mar. Biotechnol. 3:293–304.

Neff, B. D., P. Fu, and M. R. Gross.
2000. Microsatellite multiplexing in fish. Trans. Am. Fish. Soc. 129:584–593.

Olsen, J. B., J. K. Wenburg, and P. Bentzen.
1996. Semiautomated multilocus genotyping of Pacific salmon (*Oncorhynchus* spp.) using microsatellites. Mol. Mar. Biol. Biotechnol. 5:259–72.

Renshaw, M. A., E. Saillant, S. C. Bradfield, and J. R. Gold.
2006. Microsatellite multiplex panels for genetic studies of three species of marine fishes: red drum (*Sciaenops ocellatus*), red snapper (*Lutjanus campechanus*), and cobia (*Rachycentron canadum*). Aquaculture 253:731–735.

Rice, W. R.
1989. Analyzing tables of statistical tests. Evolution 43:223–225.

Saillant, E., A. Fostier, P. Haffrey, B. Menu, J. Thimonier, and B. Chatain.
2002. Temperature effects and genotype-temperature interactions on sex determination in the European sea bass (*Dicentrarchus labrax L.*). J. Exp. Zool. 292:494–505.

Saillant, E., and J. R. Gold.
2006. Population structure and variance effective size of red snapper (*Lutjanus campechanus*) in the northern Gulf of Mexico. Fish. Bull. 104:136–148.

Turner, T. F., J. P. Wares, and J. R. Gold.
2002. Genetic effective size is three orders of magnitude smaller than adult census size in an abundant, estuarine-dependent marine fish (*Sciaenops ocellatus*). Genetics 162:1329–1339.

Van Oosterhout, C., W. F. Hutchinson, D. P. M. Willis, and P. Shipley.
2004. MICRO-CHECKER: software for identifying and correcting genotyping errors in microsatellite data. Mol. Ecol. Notes 4:535–538.

Wright, A. J., and P. Bentzen.
1994. Microsatellites: genetic markers for the future. Rev. Fish Biol. Fish. 4:384–388.

Effect of towing speed on retention of zooplankton in bongo nets

Joseph Kane (contact author)

Jacquelyn L. Anderson

Email address for J. Kane: jkane@whsun1.wh.whoi.edu

National Oceanic and Atmospheric Administration
National Marine Fisheries Service
Northeast Fisheries Science Center
28 Tarzwell Drive
Narragansett, Rhode Island 02882-1152

Long-term time series of zooplankton data provide invaluable information about the fluctuations of species abundance and the stability of marine community structure. These data have demonstrated that environmental variability have a profound effect on zooplankton communities across the Atlantic basin (Beaugrand et al., 2002; Frank et al., 2005; Pershing et al., 2005). The value of these time series increases as they lengthen, but so does the likelihood of changes in sampling or processing methods. Sampling zooplankton with nylon nets is highly selective and biased because of mesh selectivity, net avoidance, and damage to fragile organisms. One sampling parameter that must be standardized and closely monitored is the speed of the net through the water column. Tow speed should be as fast as possible to minimize net avoidance by the organisms, but not so fast as to damage soft bodied zooplankters or extrude them through the mesh (Tranter et al., 1968; Anderson and Warren, 1991).

The bongo plankton sampler (Posgay and Marak, 1980) has been used by many investigators to monitor plankton populations throughout the world's oceans (e.g., Lough et al., 1985; Kane, 1993; Licandro et al., 2001). Tow speed on bongo surveys has ranged from approximately 1 to 4 knots, depending on the target population of the survey program. With the growing interest in long-term time series, the purpose of our study was to evaluate differences in catches with bongo nets towed at two of the common speeds: 1.5 and 3.5 knots. If the differences can be quantified, zooplankton data collected at the two towing speeds could be used to compare or extend time series at the regional level. We made replicate collections at the two different tow speeds and compared species composition, community structure, and overall biomass.

Materials and methods

Plankton samples were collected aboard the RV *Delaware II* from March 29 to April 9 1999 in northeastern U.S. continental shelf waters (Fig. 1). Initially a cross-shelf transect of 10 stations was surveyed, extending from the island of Martha's Vineyard out to just beyond the 200-m isobath. For the remainder of the cruise, samples were collected at 29 stations in a saw tooth pattern throughout the Georges Bank region, most within the 200-m isobath.

At each sampling location two consecutive hauls were conducted with a 61-cm bongo frame fitted with a white colored 0.333-mm mesh net towed obliquely to a maximum depth of 200 m or to within 5 m from the bottom and back to the surface. Wire was payed out at 50 m/min and retrieved at 20 m/min during both tows and a conductivity-temperature-depth (CTD) probe was attached above the bongo to measure sampling depth. A flowmeter was suspended in the center of the bongo frame to measure the volume of water filtered during each tow. The first tow was performed at a ship speed of 1.5 knots, which varyied slightly at times to maintain an approximately 45º wire angle. The sampler was depressed with a simple 45-kg lead ball. After the first tow had been completed, the vessel returned to the exact location where the tow was initiated. The gear was redeployed with a wedge-shaped 1.2-m 108-kg vfin depressor and towed at 3.5 knots without regard to the wire angle. Specimens from all samples were preserved in 5% formalin.

In the laboratory, biomass was measured by displacement volume. The plankton sample, with preserving liquid, was measured in a graduated cylinder, poured through a mesh cone into a second cylinder, and drained until the interval between drops was 15 seconds. The liquid in the second cylinder was measured and the displacement volume of the sample was the difference between readings. Samples were then reduced to approximately 500 organisms by subsampling with a modified box splitter. Zooplankton were sorted, counted, and identified to the lowest possible taxa. Abundance and biomass were expressed as number/100 m^3 and cubic centimeters/100 m^3, respectively.

Abundance of dominant taxa, defined as those contributing on average >1% to the total abundance, were compared between tow speeds. Survey mean abundance values were tested for significant differences by using the conventional paired *t*-test, and its nonparametric counterpart, the Wilcoxon test, was used to compare median abundance levels. The stage distribution of the five most abundant copepods was also examined for significant differences by using the same statistical methods.

Zooplankton community structures from the two tow speeds were compared by using multivariate statisti-

Manuscript submitted 12 Decembber 2006 to the Scientific Editor's Office.

Manuscript approved for publication 14 March 2007 by the Scientific Editor.

Fish. Bull. 105:440–444 (2007).

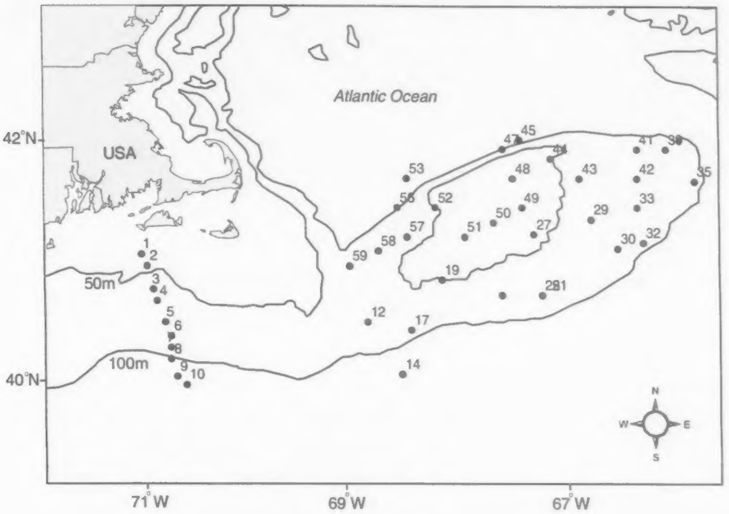

Figure 1

Locations surveyed with the RV *Delaware II* for effect of towing speed on retention of zooplankton in bongo nets. Sampling was conducted from March 29 to April 1999 at two tow speeds: 1.5 and 3.5 knots. Locations are labeled with the station number.

cal and ordination techniques from the PRIMER 6.1.5 software package (PRIMER-E Ltd, Plymouth, UK). Initially, data were log transformed and the biotic relationship between any two samples was represented by the Bray-Curtis index (Bray and Curtis, 1957), which measures the similarity (or dissimilarity) in species composition. The triangular matrix of similarity between each sample was then classified into groups by using two techniques: 1) hierarchical agglomerative cluster analysis, and 2) nonmetric multidimensional scaling (MDS). Clusters of samples that were found to be statistically significant ($P<0.05$) by the similarity profile test (SIMPROF) and also to be isolated by low stress (<0.20) MDS ordinations, were judged to be samples with similar zooplankton community structure. The significance of the resultant groupings was tested by using the nonparametric permutation procedure ANOSIM (analysis of similarity).

Results

Nine taxa dominated the zooplankton community captured during the survey (Table 1). All dominant taxa were common to both tow speeds and their mean abundance ranked in nearly the same order. The only difference was found for the copepods *Temora longicornis* and *Oithona* spp., which were the seventh and eighth most abundant taxa in the 1.5-knot tows, and eighth and seventh most abundant in the 3.5-knot tows (Table 1). The mean and median abundance levels of the dominant species were not significantly different ($P>0.05$) between tow speeds.

The copepodite stage distributions of the dominant copepods were equally represented at the two tow speeds. Mean abundance levels of all *Calanus finmarchicus* life stages and *Pseudocalanus* spp. stage-V copepodites were nearly identical from both hauls (Fig. 2) and not significantly different ($P>0.05$). Slightly higher mean numbers of late-stage copepodites of *Metridia lucens*, *Centropages typicus*, and *Centropages hamatus,* and adults of *Pseudocalanus* spp. were captured at the higher tow speed (Fig. 2), but the values also were not significantly different ($P>0.05$). These similar mean numbers for the various life-stages indicate that there was no substantial difference in the size of particles retained or extruded by the nets at the two tow speeds.

Ordinations of zooplankton community structures from the two speeds were very similar. Cluster analysis of data from both tow speeds produced five significant ($P<0.05$) groupings that were also evident in the low-stress MDS plots (Fig. 3). These station clusters for the two tow speeds were nearly identical, both reflecting the different depth strata and areas sampled during the survey. The two large clusters were essentially inshore and offshore station groupings, and the remaining three were different deepwater (>200 m) sites (Figs. 1 and 3). The community composition of the samples collected at the two speeds was not significantly different (ANOSIM procedure, $P=0.40$).

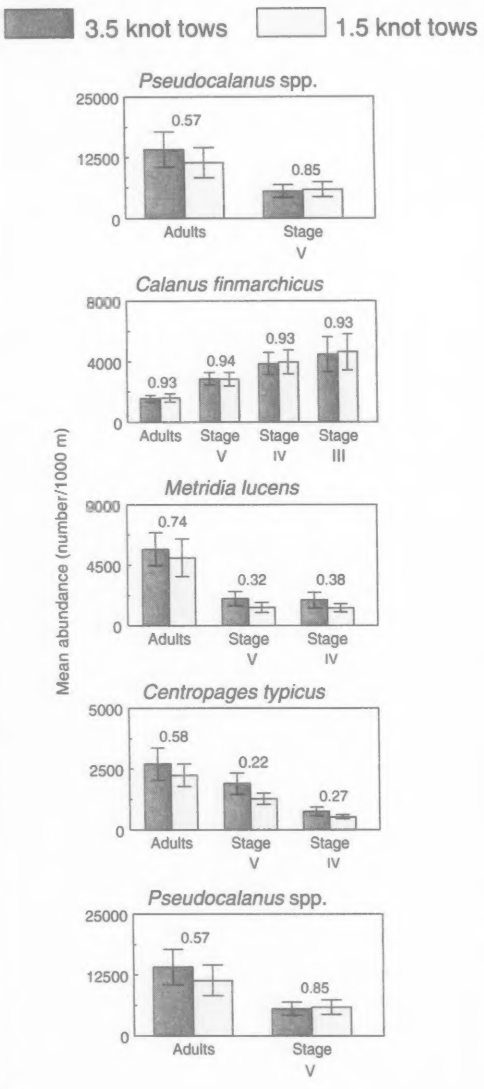

Figure 2

Comparison of mean abundance at 3.5 and 1.5 knot tow speeds for different life stages of the five dominant copepods sampled during the cruise. Only the mean abundance of adults and copepodite stages (denoted as stage III, IV, or V) that were captured quantitatively with the 0.333-mm mesh nets are shown. Mean values for the two tow speeds were not significantly different (*P* values from *t*-test results are given above each tested pair). Error bars represent one standard error. Please note that *y*-axis scales are different.

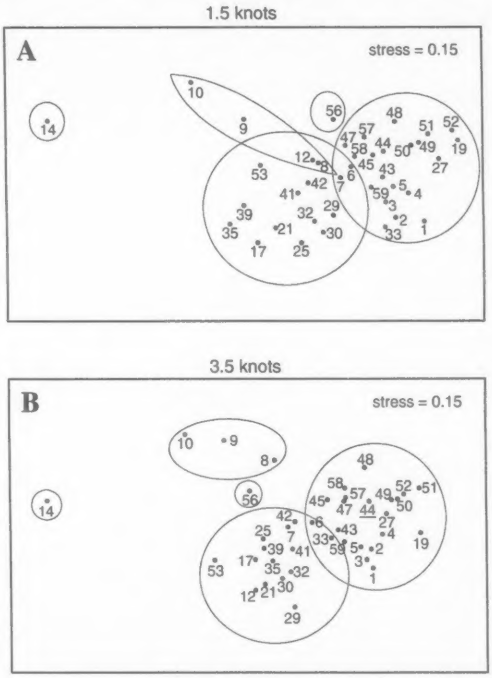

Figure 3

Nonmetric multidimensional scaling (MDS) plots produced after calculation of Bray-Curtis similarity index on log-transformed zooplankton station abundance data obtained with the bongo sampler towed at (**A**) 1.5 knots and (**B**) 3.5 knots. Encircled groups are stations strongly grouped by cluster analysis. The stress value is a measure of the strength of the MDS plot and is considered meaningful if <2.0.

In contrast to species abundance, mean and median displacement volume values from the 1.5-knot tows were significantly different ($P<0.05$) from the faster tows, averaging 40% higher (Table 1). Because mean and median total zooplankton counts at the two speeds were not significantly different ($P>0.05$), the increased biomass could be caused by items not counted in slower tows. These could include phytoplankton, Cnidaria fragments, and general detritus that would have been extruded through the nets at higher speed tows.

Discussion

The degree of similarity between the overall catches at the two speeds was remarkable given the variation normally associated with replicate plankton tows (Wiebe and Holland, 1968). None of the survey mean and median abundance values of dominant taxa were significantly

Table 1

Average abundances (no./100 m^3) and proportions of the dominant taxa (arranged in order of mean abundance in the tow) collected from tows traveled at 1.5 and 3.5 knots. Placed below them are the mean and median abundance values for total zooplankton and displacement volume values (cc/100 m^3) for each tow speed.

Abundance rank	Taxa	Frequency of occurrence	Mean abundance	Median abundance	Mean proportion	Cumulative %
1.5 knots						
1	*Pseudocalanus* spp.	100.0	18,696	10,956	28.6	28.6
2	*Calanus finmarchicus*	100.0	17,478	9929	26.7	55.3
3	*Metridia lucens*	97.4	8812	6417	13.4	68.8
4	*Centropages typicus*	97.4	4067	2149	6.2	75.0
5	*Centropages hamatus*	76.9	3775	3327	5.7	80.8
6	Balanidae	66.7	3424	873	5.2	86.1
7	*Oithona* spp.	89.7	2971	1496	4.6	90.6
8	*Temora longicornis*	92.3	2352	1888	3.6	94.2
9	*Sagitta elegans*	79.5	719	567	1.1	95.3
	Total zooplankton		65,367	49,230		
	Displacement volume		53	49		
3.5 knots						
1	*Pseudocalanus* spp.	100	20,653	14,210	28.9	28.9
2	*Calanus finmarchicus*	100	17,023	8601	23.8	52.8
3	*Metridia lucens*	94.9	10,867	7401	15.2	68.0
4	*Centropages typicus*	97.4	5354	2001	7.5	75.5
5	*Centropages hamatus*	82.1	5199	2357	7.3	82.8
6	Balanidae	64.1	3823	846	5.4	88.1
7	*Temora longicornis*	94.9	2704	1606	3.8	91.9
8	*Oithona* spp.	89.7	2053	1830	2.9	94.8
9	*Sagitta elegans*	64.1	895	1034	1.3	96.1
	Total zooplankton		71,388	65,815		
	Displacement volume		38	35		

different and the rank abundances were nearly identical. Furthermore, nearly identical life-stage distributions were derived for the dominant copepod species at the two tow speeds. There was no significant effect of tow speed on zooplankton community structure.

Catches in most tows at a single location showed good agreement between the catches of taxa at the two speeds, although occasionally there were large differences between species abundance. One reason for this discrepancy may be sampling error attributed to water movement. Although the vessel returned to the exact location where the 1.5-knot tows began, the same specific water parcel was not precisely sampled by the faster tow. Furthermore, the patchiness of zooplankton also makes it difficult to sample exactly the same community with duplicate tows. Nonetheless, these differences were averaged out when several stations were pooled and mean or median abundances were calculated.

Direct comparison between displacement volume measurements made at the two speeds is not recommended. It appears that at the slower tow speed unaccounted material is collected that is extruded through the net meshes at higher speed tows. Filtration pressure across the mesh varies with the square of the approach velocity; thus, 3.5-knot tows will exert a pressure approximately 5.4 times higher than the 1.5-knot tows (Tranter and Smith, 1968). Because this study was conducted at or near the height of the spring phytoplankton bloom in the region, sample biomass in the slower tow was likely elevated by the retention of larger diatom species that dominate the spring bloom on Georges Bank (O'Reilly and Zetlin, 1998). The results indicate that sample displacement volumes for the 3.5-knot tows conducted during early spring should be increased by 40% before comparison to levels for the 1.5-knot tows. Owing to the widespread seasonal and spatial variability of plankton populations, caution should be exercised in applying this conversion factor to other data sets. Colton et al. (1980) also reported that displacement volumes for replicate 3.5-knot tows were lower than those for 1.5-knot tows, but they found the difference was only 20.8%. Their study was conducted in the same region as ours, but samples were collected at one location in early November over a five-day period. Further comparative studies in other seasons and regions would be needed to precisely convert the displacement volumes measured for the two tow speeds.

For projects focusing on zooplankton studies, there may be a need to consider the higher tow speed as the preferred sampling procedure. The escape reaction of the dominant species to the approaching net or loss of dominant species by extrusion through the net does not appear to change substantially between 1.5 and 3.5 knots. At higher tow speeds cleaner samples are collected—samples that are easier to process because more phytoplankton and detritus are extruded from the nets. Although the slower speed has been found to be less damaging to ichthyoplankton specimens (Colton et al., 1980), the condition of the zooplankton specimens captured at the two tow speeds in this study was similar.

This study demonstrates that mean and median counts of common zooplankton taxa collected during 3.5-knot bongo tows are not significantly different from those collected during 1.5-knot tows. On the basis of these findings, we feel that zooplankton data collected at these two tow speeds can be used to compare or extend time series data at the regional level.

Acknowledgments

The authors are grateful to the Narragansett laboratory facility support staff that restored the vfin depressor to its original specifications.

Literature cited

Anderson, J. T., and W. G. Warren.
1991. Comparison of catch rates among small and large bongo samplers for *Calanus finmarchicus* copepodite stages. Can. J. Fish. Aquat. Sci. 48:303–308.

Beaugrand, G., P. C. Reid, F. Ibanez, J. A. Lindley, and M. Edwards.
2002. Reorganization of North Atlantic marine copepod biodiversity and climate. Science 296:1692–1694.

Bray, J. R., and J. T. Curtis.
1957. An ordination of the upland forest communities of southern Wisconsin. Ecol. Mono. 27:325–349.

Colton, J. B., J. R. Green, R. R. Byron, and J. L. Frisella.
1980. Bongo net retention rates as effected by towing speed and mesh size. Can. J. Fish. Aquat. Sci. 37: 606–623.

Frank, K. T., B. Petrie, J. S. Choi, and W. C. Leggett.
2005. Trophic cascades in a formerly cod-dominated ecosystem. Science 308:1621–1623.

Kane, J.
1993. Variability of zooplankton biomass and dominant species abundance on Georges Bank, 1977–1986. Fish. Bull. 91: 464–474.

Licandro, P., F. Ibanez, and T. S. Zunini.
2001. Long term variations of zooplankton in the Ligurian Sea (Western Mediterranean). Archo. Oceanogr. Limnol. 22:159–166.

Lough, R. G., G. R. Bolz, M. Pennington, and M. D. Grosslein.
1985. Larval abundance and mortality of Atlantic Herring (*Clupea harengus* L) spawned in the Georges Bank and Nantucket Shoals areas, 1971–78 seasons, in relation to spawning stock size. J. Northw. Atl. Fish. Sci. 6:21–35.

O'Reilly, J. E., and C. Zetlin.
1998. Seasonal, horizontal, and vertical distribution of phytoplankton chlorophyll *a* in the Northeast U.S. continental shelf ecosystem. NOAA Tech. Rep. NMFS 139, 120 p.

Pershing, A. J., C. H. Greene, J. W. Jossi, L. O'Brien, J. Brodziak., and B. Bailey.
2005. Interdecadal variability in the Gulf of Maine zooplankton community, with potential impacts on fish recruitment. ICES J. Mar. Sci. 62:1511–1523.

Posgay, J. A., and R. R. Marak.
1980. The MARMAP bongo zooplankton samplers. J. Northw. Atl. Fish. Sci. 1:91–99.

Tranter, D. J., and P. E. Smith.
1968. Filtration performance. *In* Reviews on zooplankton sampling methods, Part I (D. J. Tranter, ed.), p. 27–56. Monogr. Oceanogr. Methodol. 2, Zooplankton Sampling. UNESCO (United Nations Educational, Scientific, and Cultural Organzition) Press, Paris.

Wiebe, P. H., and W. R. Holland.
1968. Plankton patchiness: effects of repeated net tows. Limnol. Oceanog. 13: 315–321.

Fishery Bulletin

Guidelines for authors

Content of manuscripts

Contributions published in Fishery Bulletin describe original research in marine fishery science, fishery engineering and economics, as well as the areas of marine environmental and ecological sciences (including modeling). Although all contributions are subject to peer review, responsibility for the contents of papers rests upon the authors and not upon the editor or publisher. *Submission of an article implies that the article is original and is not being considered for publication elsewhere.* Manuscripts must be written in English. Authors whose native language is not English are strongly advised to have their manuscripts checked by English-speaking colleagues prior to submission. **Articles** may range from relatively short contributions (10–15 typed, double-spaced pages, tables and figures not included) to extensive contributions (20–30 typed pages). **Notes** are reports of 5 to 10 pages without an abstract and describe methods or results not supported by a large body of data.

Manuscript preparation

Title page should include authors' full names and mailing addresses and the senior author's telephone, fax number, and e-mail address, and a list of key words to describe the contents of the manuscript. **Abstract** should be limited to 150 words (one-half typed page), state the main scope of the research, and emphasize the author's conclusions and relevant findings. Do not review the methods of the study or list the contents of the paper. Because abstracts are circulated by abstracting agencies, it is important that they represent the research clearly and concisely. **Text** must be typed in 12 point Times New Roman font throughout. A brief introduction should convey the broad significance of the paper; the remainder of the paper should be divided into the following sections: **Materials and methods, Results, Discussion (or Conclusions),** and **Acknowledgments**. Headings within each section must be short, reflect a logical sequence, and follow the rules of multiple subdivision (i.e., there can be no subdivision without at least two items). The entire text should be intelligible to interdisciplinary readers; therefore, all acronyms, abbreviations, and technical terms should be written out in full the first time they are used. Include FAO common names for species in the list of keywords and in the introduction. Regional common names may be used throughout the rest of the text if they are different from FAO common names which can be found at http://www.fishbase.org/search.html. Follow the U.S. Government Printing Office Style Manual (1984 ed.) and the CBE Style Manual (6th ed.) for editorial style; for fish nomenclature follow the most current issue of the American Fisheries Society's Common and Scientific Names of Fishes from the United States and Canada. Dates should be written as follows: 11 November 2000. Measurements should be expressed in metric units, e.g., 58 metric tons (t); if other units of measurement are used, please make this fact explicit to the reader. Write out the numbers zero through nine unless they form part of measurement units (e.g., nine fish but 9 mm).

Text footnotes should be inserted in 9-point font at the bottom of the page that displays the first citation of the footnote. Footnotes should be formatted in the same manner as citations. Footnote all personal communications, unpublished data, and unpublished manuscripts with full address of the communicator or author, or, as in the case of unpublished data, where the data are on file. Authors are advised to avoid references to nonstandard (gray) literature (such as internal, project, processed, or administrative reports, ICES Council Minutes, IWC Minutes or Working Papers, any "research" or "working" documents, laboratory or contract reports, Management Council reports, and manuscripts in review) wherever possible. If these references are used, present them as footnotes and list whether they are available at NTIS (National Technical Information Service) or at some other public depository. Cite all software and special equipment or chemical solutions used in the study, not in a footnote but within parentheses in the text (e.g., SAS, vers. 6.03, SAS Inst., Inc., Cary, NC).

Literature cited comprises published works and those accepted for publication in peer-reviewed literature (in press). Follow the name and year system for citation format in the "Literature cited" section. If there is a sequence of citations in the text, list chronologically: (Smith, 1932; Green, 1947; Smith and Jones, 1985). Abbreviations of serials should conform to abbreviations given in the Serial Sources for the BIOSIS Previews Database. Authors are responsible for the accuracy and completeness of all citations. Literature citation format: Author (last name, followed by first-name initials). Year. Title of report or manuscript. Abbreviated title of the series to which it belongs. Always include number of pages. If the authorship for a sequence of citations is identical, list works chronologically.

Tables and figures—general format

- Zeros should precede all decimal points for values less than one.
- Sample size, *n*, should be italicized.
- Capitalize the first letter of the first word in all labels within figures.
- Do not use overly large font sizes in maps and for units of measurements along axes in figures.
- Do not use bold fonts or bold lines in figures.
- Do not place outline rules around graphs.
- Do not use horizontal lines in graphs to indicate measurement units on axes.
- Use a comma in numbers of five digits or more (e.g. 13,000 but 3000).
- Maps should have a North arrow (or compass sign) and degrees latitude-longitude (e.g., 170°E)

Tables are often overused in scientific papers; it is seldom necessary or even desirable to present all the data associated with a study. Tables should not be excessive in size and must be cited in numerical order in the text. Headings should be short but ample enough to allow the table to be intelligible on its own. All unusual symbols must be explained in the table legend. Other incidental comments may be footnoted with italic footnote markers. Use asterisks to indicate probability in statistical data. Do not type table legends on a separate page; place them on the same page as the table data. *Do not submit tables in photo mode.*

Figures include line illustrations, photographs (or slides), and computer-generated graphs and must be cited in numerical order in the text. Graphics will aid in the comprehension of the text, but they should be limited to presenting patterns rather than raw data. Figures are costly to print and should be limited to six. Figures must be labeled with author's name and number of figure. Avoid placing labels vertically (except on y-axis). Figure legends should explain all symbols and abbreviations and should be double-spaced on a separate page at the end of the manuscript. Please note that we do not print graphs in color.

Failure to follow these guidelines and
to respond to editorial questions
in a timely manner will delay
publication of a manuscript.

Copyright law does not apply to *Fishery Bulletin*, which falls within the public domain. However, if an author reproduces any part of an article from *Fishery Bulletin* in his or her work, reference to source is considered correct form (e.g., Source: Fish. Bull 97:105).

Reprints are available free of charge to the senior author (50 copies) and to his or her laboratory (50 copies).

Submission

The Scientific Editorial Office encourages authors to submit their manuscripts as a *single* PDF (preferred), or Word (zipped) document by e-mail to Fishery.Bulletin@noaa.gov. Please use the subject heading "Fishery Bulletin manuscript submission." *Do not* send encrypted files. For further details on electronic submission, please contact the Scientific Editorial Office directly (see address below). Or you may send your manuscript on compact disc in one of the above formats along with four printed copies (one original plus three copies [stapled]) to the Scientific Editor, at the address shown below.

Dr. Adam Moles
Scientific Editor, *Fishery Bulletin*
Auke Bay Laboratories, Alaska Fisheries Science Center
17109 Pt. Lena Loop Rd.
Juneau, AK 99801

Once the manuscript has been accepted for publication, you will be asked to submit a final software copy of your manuscript. When requested, the text and tables should be submitted in Word or Word Rich Text Format. Figures should be sent as PDF files, Windows metafiles, tiff files, or as EPS files. Send a copy of figures in original software if conversion to any of these formats yields a degraded version.

Fishery Bulletin

Subscription form

Superintendent of Documents **Publications** Order Form

*5178

☐ YES, please send me the following publications:

____ Subscriptions to *Fishery Bulletin*
for $36.00 per year ($50.40 foreign)

The total cost of my order is $ ________ . Prices include regular domestic postage and handling and are subject to change.

(Company or Personal Name) (Please type or print)

(Additional address/attention line)

(Street address)

(City, State, ZIP Code)

(Daytime phone including area code)

(Purchase Order No.)

Charge your order. IT'S EASY!

VISA

MasterCard

Please Choose Method of Payment:

☐ Check Payable to the Superintendent of Documents
☐ GPO Deposit Account ☐☐☐☐☐☐☐—☐
☐ VISA or MasterCard Account
☐☐☐☐☐☐☐☐☐☐☐☐☐☐☐☐☐☐☐☐
☐☐☐☐ (Credit card expiration date)

To fax your orders (202) 512-2250

(Authorizing Signature)

Mail To: Superintendent of Documents
P.O. Box 371954, Pittsburgh, PA 15250-7954

Thank you for your order!

Also available online at http://bookstore.gpo.gov/collections/fishery-bulletin